



PhD course in
“Food and Human Health”

XXXV cycle

Dissertation title

**“Optimization of rapid analytical protocols for
monitoring the contamination with hydrocarbons of
petrogenic origin in the olive oil supply chain”**

PhD candidate

Luca Menegoz Ursol

Supervisor

Prof. Sabrina Moret

2023

TABLE OF CONTENTS

LIST OF FIGURES	1
LIST OF TABLES	5
LIST OF ABBREVIATIONS	7
SUMMARY	11
INTRODUCTION	15
1 Olive oil	17
1.1 Definition, regulation and classification	17
1.2 Extra virgin olive oil supply chain	19
1.2.1 Harvesting	20
1.2.2 Transportation and storage.....	23
1.2.3 Cleaning.....	24
1.2.4 Crushing	25
1.2.5 Malaxation.....	27
1.2.6 Separation between solids and liquids	28
1.2.7 Separation of liquid phases	30
1.2.8 Decanting and filtration	32
1.2.9 Pumping, storage and transportation.....	33
1.2.10 Bottling	34
1.3 Lampante olive oil refining.....	36
1.3.1 Neutralization.....	38
1.3.2 Bleaching	40
1.3.3 Deodorization.....	42
2 Mineral oil hydrocarbons	43
2.1 Origin, definition and chemical structure	43
2.2 Toxicological assessment	46
2.3 Acceptable Daily Intake	48
2.4 Legislation	50
2.5 Sources of contamination	53
2.5.1 Environment.....	55
2.5.2 Pesticides	56
2.5.3 Harvesting	57
2.5.4 Transportation	58
2.5.5 Pre-treatment	58
2.5.6 Extraction	59
2.5.7 Refining	60

2.5.8	Storage and transportation.....	61
2.5.9	Fraudulent admixture.....	61
2.5.10	Packaging.....	62
2.6	Occurrence of MOH in vegetable oils	62
2.7	Analytical methods	67
2.7.1	Sampling	68
2.7.2	Extraction	69
2.7.3	Sample clean-up	70
2.7.3.1	Enrichment	71
2.7.3.2	Interference removal	76
2.7.3.2.1	MOSH: endogenous <i>n</i> -alkanes.....	76
2.7.3.2.2	MOAH: endogenous olefins.....	80
2.7.4	MOSH/MOAH separation.....	85
2.7.4.1	On-line methods	87
2.7.4.2	Off-line methods	89
2.7.5	HPLC-GC interfacing.....	92
2.7.5.1	On-column interface.....	94
2.7.5.2	Y-interface.....	96
2.7.5.3	Wire interface.....	97
2.7.5.4	Programmed-temperature vaporizer interface	99
2.7.6	Gas chromatography and flame ionization detection	100
2.7.7	Integration, quantification and verification of method performance	101
2.7.8	Confirmation techniques: mass spectrometry and comprehensive two-dimensional gas chromatography.....	104
2.7.9	Official reference methods	111
2.7.10	Uncertainty of results: limit of quantification and law limits	112
AIM OF THE WORK.....		117
EXPERIMENTAL WORK.....		121
3	Optimization and validation of microwave assisted saponification (MAS) followed by epoxidation for high-sensitivity determination of mineral oil aromatic hydrocarbons (MOAH) in extra virgin olive oil	123
3.1	Introduction.....	123
3.2	Materials and methods.....	125
3.2.1	Samples.....	125
3.2.2	Reagents and chemicals.....	125
3.2.3	Standard solutions.....	125
3.2.4	Instrumentation.....	126

3.2.5	Oil extraction from olives.....	127
3.2.6	Microwave assisted saponification (MAS).....	127
3.2.7	Epoxidation	128
3.2.8	Quality control and MOH quantification.....	128
3.2.9	Method validation	129
3.2.10	Linearity.....	129
3.2.11	Recovery and repeatability.....	129
3.2.12	Limit of quantification	130
3.3	Results and discussion	130
3.3.1	Optimization of microwave assisted saponification (MAS)	130
3.3.2	Epoxidation	131
3.3.3	Method validation	132
3.3.3.1	Linearity.....	132
3.3.3.2	Recovery and repeatability.....	132
3.3.3.3	Limit of quantification.....	138
3.3.4	MOSH quantification	138
3.3.5	MOH content in EVOO samples	139
3.4	Conclusions	145
4	A study on the impact of harvesting operations on the mineral oil contamination of olive oils	147
4.1	Introduction	147
4.2	Materials and methods	149
4.2.1	Samples	149
4.2.2	Chemicals and standards	151
4.2.3	Instrumentation and chromatographic conditions	152
4.2.3.1	HPLC-GC-FID	152
4.2.3.2	GC×GC-FID/QTOF	153
4.2.4	Oil extraction from the olives.....	154
4.2.5	MOH analysis	154
4.3	Results and discussion	155
4.3.1	Olives sampled from the olive trees (before harvesting).....	155
4.3.2	Harvesting operations and lubricants used.....	157
4.3.3	Olives sampled after harvesting.....	158
4.3.4	Examples of source identification.....	160
4.4	Conclusions	169

5	Evaluation of the impact of olive milling on the mineral oil contamination of extra virgin olive oils	171
5.1	Introduction.....	171
5.2	Materials and methods.....	173
5.2.1	Samples	173
5.2.2	Reagents and chemicals.....	175
5.2.3	Standard solutions.....	176
5.2.4	Equipment, instrumentation and chromatographic conditions.....	176
5.2.5	Oil extraction	177
5.2.5.1	Physical extraction	178
5.2.5.2	Chemical extraction	178
5.2.6	Saponification and epoxidation.....	178
5.2.7	Removal of endogenous <i>n</i> -alkanes.....	179
5.2.8	Olive washing in the laboratory.....	179
5.2.9	MOH quantification and analytical sensitivity	180
5.3	Results and discussion	180
5.3.1	Optimization of MOH extraction from olive paste	180
5.3.2	Optimization of the Alox protocol.....	181
5.3.3	MOH variations along the processing chain in the mill	184
5.3.3.1	Focus on the washing step.....	192
5.3.3.2	Focus on the olives stones	196
5.3.3.3	The impact of olive leaves.....	197
5.3.4	Extra virgin olive oils from the market	199
5.4	Conclusions.....	202
6	The impact of the refining process on the mineral oil contamination of olive oils and olive pomace oils	204
6.1	Introduction.....	204
6.2	Materials and methods.....	205
6.2.1	Samples	205
6.2.2	Chemicals and standards.....	206
6.2.3	Equipments and instrumentation	207
6.2.3.1	HPLC-GC-FID.....	207
6.2.3.2	GC×GC-MS	208
6.2.4	Sample preparation	209
6.2.5	Analytical determination.....	209
6.3	Results and discussion	210

6.3.1	Removal of mineral oil contamination	210
6.3.2	<i>n</i> -Alkane removal	219
6.3.3	Evaluation of the MOAH fraction by GC×GC.....	222
6.3.4	Refined olive oils and refined olive pomace oils from the market	225
6.4	Conclusions	227
CONCLUSIONS AND FUTURE PERSPECTIVES		229
REFERENCES		233
LIST OF PUBLICATIONS.....		265
CONTRIBUTIONS TO NATIONAL AND INTERNATIONAL CONFERENCES AND SEMINARS.....		269
POSTERS		273
AWARDS.....		277

LIST OF FIGURES

Figure 1.1. Flow chart of the operations making up the olive oil supply chain, from the field to the finished product.	20
Figure 1.2. Harvesting of the olives carried out with hand-held combs (A), trunk shaker equipped with the collection umbrella (B), vibrating comb mounted on a tractor (C) and straddle harvester (D).....	22
Figure 1.3. Collection of olives exploiting nets placed on the ground under the trees and their accumulation in plastic bins (A) or in bulk on tractor trailer (B). Plastic bins loaded on covered trucks (C) and stacked at the mill, which is the most common storage (D). ..	24
Figure 1.4. Olive washing machine (A) comprising the washing tank (B) and the conveyor belt with water jets for the final rinse (C).....	25
Figure 1.5. Stone mill (A), knife mill (B), hammer mill (C) and disc mill (D) [adapted from www.oliveoilsource.com (A), www.amenduni.it (B, C) and www.alfalaval.it (D)]. ..	26
Figure 1.6. Battery of malaxers feeded by the crusher (A) and detail of the olive paste under mixing by the rotating blades (B).	28
Figure 1.7. Extraction of olive oil from olive paste by pressing (A), by percolation using a Sinolea system (B) and by centrifugation using a three-phase decanter, with detail of vegetation water and oil outlets (C) [adapted from www.oliveoil.com (A) and www.frantoionline.it (B)].	30
Figure 1.8. Disc centrifuge, with detail of the oil outlet.	31
Figure 1.9. Oil filtration system with horizontally stacked filters (A). Filter before (B) and after (C) filtration.	33
Figure 1.10. Stainless-steel tanks for oil storage.....	34
Figure 1.11. Containers for the sale of EVOO made of glass (A), metal (B) and plastic (C) [adapted from www.olioappo.it (A,B) and www.teatronaturale.it (C)]......	35
Figure 1.12. Closures for oil containers: screw cap (A), roll-on cap (B) and screw cap with interlocking element (C, D), together with typical drip catcher (E) [adapted from www.polsinelli.it]......	36
Figure 1.13. Flow chart of the operations related to the refining process of lampante olive oils.	37
Figure 1.14. Centrifuges used for the separation of soaps from oil in chemical neutralization (A) and distillation column used for physical neutralization (B).	40
Figure 1.15. Mixer for mixing bleaching earths/activated carbon with oil (A, on the right), bleacher (A, on the left) and filtration system for oil/exhausted adsorbents separation (B).	41
Figure 1.16. Distillation column for oil deodorization.	42
Figure 1.17. Generic diagram of a petroleum refining plant, with reference to the distillation temperatures of the various fractions and the range carbon atoms of the hydrocarbons belonging to them [adapted from https://uret.com.tr © FES TANKS]. ..	43
Figure 1.18. Examples of typical chemical structures characterizing MOSH and MOAH fractions [adapted from (EFSA, 2012a)]......	45
Figure 1.19. Range of accumulation of MOSH in human body and distribution of molecular weights of some types of mineral oil products.....	47
Figure 1.20. Overlay of chromatograms of different mineral oil products highlighting their different profiles and distribution of molecular weights.	54
Figure 1.21. General flow chart of the steps that make up an analytical method.....	68

Figure 1.22. Microwave digestion system and related accessories exploited for (MAS).	72
Figure 1.23. <i>n</i> -Alkanes removal from rapeseed oil sample, showing the advantage of elution through Alox to evaluate MOSH contamination in case of signal overload by these endogenous interferents.	78
Figure 1.24. Squalene removal from an EVOO sample by epoxidation, showing the advantage of this treatment in detecting MOAH contamination possibly covered by the signals related to endogenous olefins.	81
Figure 1.25. Order of elution of the various MOH and the related internal standards used to verify the performance of HPLC instrumentation.	87
Figure 1.26. Schematic representation of the on-column interface equipped with SVE.	94
Figure 1.27. Schematic representation of the principles on which the retention gap technique is based.	95
Figure 1.28. Schematic representation of the Y-interface.	96
Figure 1.29. Schematic representation of the wire interface.	97
Figure 1.30. Schematic representation of the PTV interface.	99
Figure 1.31. Example of integration of the MOSH and MOAH fractions, discarding the interferences and carrying out the division of the total hump into C-fractions.	103
Figure 1.32. Schematic representation of a GC×GC-FID/MS with thermal modulation.	109
Figure 1.33. Examples of HPLC-GC-FID chromatograms and GC×GC-FID plots of the MOSH and MOAH fractions of an olive pomace oil, showing the difference in the analytical response obtainable with both techniques. Greater characterization was obtained with the GC×GC where residual olefins, assumed from the HPLC-GC chromatogram, were confirmed and highlighted with red circles [adapted from Biedermann et al. (2020) with permission of Elsevier].	110
Figure 1.34. Schematic representation of the incidence of the distribution of contamination in the definition of the LOQ.	115
Figure 3.1. LC-GC-FID traces of the MOAH fractions of EVOO1 (A) and EVOO2 (B). The overlay of chromatograms starts from the unspiked matrix and the humps with increasing area refer to the different fortification levels reported in Table 3.2.	133
Figure 3.2. Behaviour of the internal standards of the MOAH fraction in different steps of the MAS procedure.	135
Figure 3.3. Overlay of LC-GC-FID chromatograms of the MOSH fraction of an extra virgin olive oil from the market (EVOO_M1) injected at 30 µL (blue line) and 100 µL (black line).	139
Figure 4.1. Olive harvesting carried out by hand-held comb (A), trunk shaker (B), mechanized vibrating comb (C) and straddle harvester (D).	151
Figure 4.2. MOSH and MOAH concentrations of EVOOs from olives sampled before (hand-picked from the trees) and after harvesting operations. Absence of data labels indicates levels below the LOQ (1.0 mg/kg for MOSH and 0.5 mg/kg for MOAH).	160
Figure 4.3. Overlay of MOSH and MOAH HPLC-GC-FID chromatograms of samples TB1: EVOO from olives sampled before (blue line) and after harvesting (black line), hydraulic oil of the vibrating comb (green line) (A). Below, from top to bottom: GC×GC-FID plots of the MOSH (left side) and MOAH (right side) fractions of the hydraulic oil of the mechanized vibrating comb (B) and EVOOs from the olives harvested with different equipment (C). Presence of erucamide and oleamide is highlighted (B, C) together with	

their chemical structure. The red line in B evidences the boundary between MOSH and MOAH areas.	162
Figure 4.4. MS spectra resulting from an identification attempt performed in a generic point of the MOAH cloud.	163
Figure 4.5. Overlay of MOSH and MOAH HPLC-GC-FID chromatograms of samples IB4: EVOO from olives sampled before (blue line) and after harvesting (black line), hydraulic oil (green line) and grease (purple line) of the straddle harvester (A). Below, from top to bottom: GC×GC plots of MOSH and MOAH of the grease (B), MOSH of the hydraulic oil (C), including on the right SIC plots at m/z 71 (alkanes/iso-alkanes) and at m/z 82 (naphthenes) (C') and EVOO from olives after harvesting with the straddle harvester (D). In B the presence of oxygenated compounds in the MOAH fraction of the grease is highlighted.	165
Figure 4.6. Presence of oxygenated compounds in the MOAH fraction of the grease highlighted using SIC mode at m/z 257.2475 (upper figure), together with spectra and hypothesized chemical structure (lower figure). The spectra in red is the experimental one, while the one in blue is the most similar to it from NIST library.	166
Figure 4.7. Overlay of MOSH HPLC-GC-FID chromatograms of samples TB6: EVOO from olives sampled before (blue line) and after harvesting (black line), hydraulic oil (green line) and grease (purple line) of the trunk shaker (A), as well as EVOO from olives after the harvesting (black line) and a PAO-based lubricant (orange line) (D). Below, GC×GC plots of the MOSH fraction of: hydraulic oil (B), grease (C) and EVOO from olives after harvesting with the trunk shaker (E).	167
Figure 4.8. HPLC-GC-FID chromatograms of the MOSH fraction of samples IB2 before (blue line) and after harvesting (black line).	169
Figure 5.1. Examples of chromatograms relating to different types of vegetable oils before and after Alox applied on the saponified/epoxidized samples.	183
Figure 5.2. Overlay of chromatograms of samples TB6 (A), I2 (B) and IB1 (C) relating to the oil extracted from olives sampled from different processing steps to highlight the effect of transportation.	188
Figure 5.3. Overlay of chromatograms of samples IB4 (A) and F1B (C) relating to the oil extracted from olives sampled from different processing steps to highlight the effect of crushing/malaxation.	190
Figure 5.4. Bar plots relating to the variations (in mg/kg) occurring in the various samples in relation to the overall milling process (A), the washing step (B) and the oil extraction step (C). Mean MOSH concentrations of the samples before and after the considered processing step are also reported, together with the average variation.	191
Figure 5.5. Overlay of chromatograms of the <i>n</i> -hexane extracts from liquid-liquid extraction of water and ethanol used for washings (A) and of olive oils extracted from the olives before and after these washings (B).	195
Figure 5.6. Average concentrations of MOSH in two different oil varieties following addition of different percentages of leaves during olive milling.	198
Figure 5.7. Overlay of all 22 MOSH chromatograms of the EVOOs sampled from the market, where the presence of two main molecular weight distributions is highlighted. For better comparison, the scale of the signals has been changed to make them overlap.	200
Figure 5.8. Quantifications relating to EVOOs taken from the centrifuge at the milling plant and bought at the supermarket. EVOOs encoded from M1 to M12 were taken from Menegoz Ursol et al. (2022) and derived from traditional agriculture, while from M13 to	

M22 derived from organic agriculture. Oils were sorted in ascending order based on MOSH content, and concentrations below the LOQ (0.5 mg/kg) were reported with this value. Green and red lines indicate the threshold of 13 mg/kg of MOSH and 2 mg/kg of MOAH respectively, in accordance with the benchmark levels of LAV & BLL (2022) and the limit imposed by the SCoPAFF (EC, 2022)..... 201

Figure 6.1. Overlay of chromatograms related to the MOSH fractions of samples LOO3 and LOO4, highlighting the loss of the most volatile fraction ($<n-C_{35}$) in the deodorization step of oil refining. 212

Figure 6.2. Overlay of the chromatograms of LOO5 (A), LOO6 (B) and LOO2 (C' and C''), related to samples coming from different refining steps. In A, B and C, different profiles probably due to cross- contamination occurred during sampling are visible. In C'', removal of the most volatile compounds is already visible during deacidification, and further improved during deodorization. 216

Figure 6.3. Overlay of chromatograms of LOO2 in the different refining steps (A), and example of integration discarding residual olefins for sample LOO2 and LOO3 (A and B). Although the MOAH profile of LOO3 (B) resembles that of its MOSH fraction (C), the retention times of the apexes of the two humps are shifted, and it matches better to that of the residual olefins. 218

Figure 6.4. Overlay of chromatograms referring to the crude, bleached and deodorized lampante oil of the refining line LOO3, not subjected to epoxidation. Endogenous compounds, interfering with the MOAH fraction, are highlighted. 219

Figure 6.5. HPLC-GC-FID chromatogram of crude pomace oil COPO2, where the MOAH hump and the series of unresolved peaks and signals for which an identification was attempted are boxed in yellow and red respectively (A). PAH and low alkylated MOAH are encircled in red in the GC×GC plot, while highly alkylated MOAH are encircled in yellow (B). The latter, always encircled in yellow, are better highlighted in the SIC plot (B''). 223

Figure 6.6. (B) shows the GC×GC plot of olive pomace oil COPO2 after bleaching. Most of the signals referable to low alkylated MOAH and PAH, previously present in the area inside the dotted red circle, were removed or reduced in concentration, Their position is highlighted by small red circles. Location of the MOAH cloud, as well as the presence of amides, justified as artifacts or interferences, are highlighted. In (A), MS spectra related to the identification of neophytadiene..... 225

LIST OF TABLES

Table 1.1. Physical, chemical and organoleptic characteristics of the different olive oil categories [adapted from IOC Standard COI/T.15/NC No 3/Rev.18 June 2022].	19
Table 1.2. Classification of mineral oils [adapted from JEFCA (1995)]......	49
Table 1.3. Chronological progression of legislation relating to mineral oils in food.	53
Table 1.4. Occurrence data relating to the presence of mineral oils in vegetable oils from various works in the literature.	64
Table 1.5. Sample enrichment methods for the analysis of mineral oils in vegetable oils.	75
Table 1.6. Sample purification methods for the analysis of MOSH in vegetable oils. ..	80
Table 1.7. Sample purification methods for the analysis of MOAH in vegetable oils. ..	85
Table 1.8. MOSH/MOAH separation methods, aimed at MOSH recovery, applied to vegetable oils.....	90
Table 1.9. MOSH/MOAH separation methods, aimed at recovery of both fractions, applied to vegetable oils.	91
Table 10. Main HPLC-GC coupling interfaces exploited for mineral oils applications.	93
Table 1.11. Ranges related to the C-fractions and the total hump expressed as elution times of n-alkanes [adapted from (Bratinova & Hoekstra, 2019)]......	102
Table 1.12. Performance requirements for MOSH and MOAH analysis in fats and oils [adapted from (Bratinova & Hoekstra, 2019)]......	104
Table 3.1. Linearity.....	132
Table 3.2. Recovery and RSD at different fortification levels (with Gravex and motor oil).	134
Table 3.3. Repeatability of C-fractions.	137
Table 3.4. MOSH and MOAH data of the oils sampled from the market.	141
Table 3.5. MOSH and MOAH data of the oils obtained from olives picked from the trees and sampled at the mill.	145
Table 4.1. Characteristics of the sampling sites.....	150
Table 4.2. Sampled lubricants and their characteristics. The % of MOAH in brackets (when available), refers to data obtained from the integration of the 2D plot deriving from GC×GC-FID analysis.	158
Table 5.1. Characteristics of samples related to the monitoring of the MOH contamination at the mill.	174
Table 5.2. Recovery and RSD (3 replicates) of solvent and oil fortified with Gravex and motor oil and data comparison of oils with and without added mineral oils with expected values from a collaborative study.....	182
Table 5.3. MOSH and MOAH concentrations (mg/kg oil) of the samples from the different processing steps, together with the percentage of MOAH, where assessable (values above the LOQ). Arrows indicate significant increase (red arrow) or decrease (green arrow) between one step and the other (in accordance with the established criteria).	185
Table 5.4. MOSH concentration, expressed on the oil extracted from the olives, following their washing under different conditions.	193
Table 5.5. MOSH concentration in the oil extracted from olives before and after pitting.	197

Table 6.1. Information relating to the samples of lampante and pomace oils in terms of distribution of the MOH contamination, together with the process conditions capable of having an influence in the removal of the most volatile fractions.	206
Table 6.2. MOSH distribution in lampante olive oils and crude olive pomace oils.	211
Table 6.3. MOSH and MOAH concentrations for each refining step, expressed for single C-fractions and as total contamination, and related percentage of removal (%) for fractions $n\text{-C}_{10-25}$, $n\text{-C}_{10-35}$ and $n\text{-C}_{10-50}$ due to deodorization.	213
Table 6.4. Concentrations of endogenous n -alkanes in the different steps of the refining process for some selected samples. Significantly different concentrations due to deodorization, with respect to data from the previous steps, are highlighted in blue. .	220
Table 6.5. Percentage removal of n -alkanes which underwent a significant change in deodorization. Where the removal was not significant, a dash is present.....	222
Table 6.6. MOSH and MOAH data of olive oils and olive pomace oils from the market. Dash indicates that no signal was detectable.	226

LIST OF ABBREVIATIONS

1-MN	1-Methylnaphtalene
2-MN	2-Methylnaphtalene
2D	Two-dimensional
5B	<i>n</i> -Pentylbenzene
actSi	Activated silica gel
ADI	Acceptable Daily Intake
AFSCA	Federal Agency for the Safety of the Food Chain
Alox	Activated aluminium oxide
BLL	Food Federation Germany
BMEL	German Ministry for Nutrition, Agriculture and Consumer Protection
BfR	German Federal Institute for Risk Assessment
bw	Body weight
CEN	European Committee for Standardization
COPO	Crude olive pomace oil
Cho	Cholestane
CyCy	Cyclohexylcyclohexane
DBTS	Dibenzothiophenes
DCM	Dichloromethane
DEHB	1,4-di(2-ethylhexyl)benzene
DGF	German Society for Fat Science
DIPN	2,6-diisopropylnaphthalene
DNA	Deoxyribonucleic acid
EC	European Commission
EEC	European Economic Community
EFSA	European Food Safety Authority
EI	Electron impact
EU	European Union
EtOH	Ethanol
EVOO	Extra virgin olive oil
F344	Female Fisher 344 rats
FAO	Food and Agriculture Organization of the United Nations
FBO	Food business operator
FEDIOL	Federation of the European Vegetable Oil and Proteinmean Industry
FFA	Free fatty acids

FID	Flame ionization detector
FT-MIR	Fourier transform mid-infrared spectroscopy
FT-NIR	Fourier transform near-infrared spectroscopy
FVG	Friuli-Venezia Giulia
GC	Gas chromatography
GC×GC	Comprehensive two-dimensional gas chromatography
Hex	<i>n</i> -Hexane
HDPE	High-density polyethylene
HPLC	High performance liquid chromatography
HPO	Hand-picked olives
ID	Internal diameter
IJO	International Jute Organization
IOC	International Olive Council
ITERG	Institut des Corps Gras
JECFA	Joint FAO/WHO Expert Committee of Food Additives
JRC	Joint Research Centre
LAV	Consumer Protection Consortium of the Federal States
LB	Lower bound
LC	Liquid chromatography
LLE	Liquid-liquid extraction
LOD	Limit of detection
LOQ	Limit of quantification
LPG	Liquefied petroleum gas
LVI	Large volume injection
LVOO	Lampante virgin olive oil
<i>m/z</i>	Mass to charge ratio
MAE	Microwave assisted extraction
MAS	Microwave assisted saponification
<i>m</i> CPBA	<i>meta</i> -Chloroperoxybenzoic acid
MLN	Mesenteric lymph nodes
MOH	Mineral oil hydrocarbons
MOAH	Mineral oil aromatic hydrocarbons
MOE	Margin of exposure
MOSH	Mineral oil saturated hydrocarbons
MS	Mass spectrometry

MU	Measurement uncertainty
NOAEL	No Observed Adverse Effect Level
NPLC	Normal phase liquid chromatography
OC	On-column
OO	Olive oil
OPO	Olive pomace oil
OVOO	Ordinary virgin olive oil
PAH	Polycyclic aromatic hydrocarbons
PAO	Poly-alpha-olefins
PCEE	Partially concurrent eluent evaporation
PDMS	Polydimethylsiloxane
PE	Polyethylene
PET	Polyethylene terephthalate
PLE	Pressurized liquid extraction
POSH	Polyolefin oligomeric saturated hydrocarbons
PP	Polypropylene
pSPE	Planar solid phase extraction
PT	Proficiency test
PTV	Programmed temperature vaporizer
PVC	Polyvinylchloride
QIVN	Quasi-imaging visible near-infrared
RG	Retention gap
ROO	Refined olive oil
ROPO	Refined olive pomace oil
ROAH	Resin oligomeric aromatic hydrocarbons
ROSH	Resin oligomeric saturated hydrocarbons
rpm	Rounds per minute
RSD%	Relative standard deviation
SCoPAFF	Standing Committee of Plants, Animals, Food and Feed
SCF	Scientific Committee of Food
SE	Solvent evaporator
SiAg	Silver silica
SIC	Selected ion chromatogram
SPE	Solid phase extraction
SVE	Solvent vapor exit

TAG	Tryglicerides
TBB	1,3,5-Tri- <i>tert</i> -butylbenzene
TDI	Tolerable Daily Intake
TIC	Total ion chromatogram
TOF	Time-of-flight
VOO	Virgin olive oil
WHO	World Health Organization

SUMMARY

The present PhD project was born from the need of various stakeholders, in particular the associations of the Italian olive oil supply chain, to investigate the problem of the presence of mineral oils in olive oils, in order to implement policies aimed at its minimization. This problem, which emerged in 2008 following the importation of heavily contaminated sunflower oil from Ukraine, began to capture the attention of the scientific world becoming, in few years, a hot topic.

Mineral oils are a class of hydrocarbon contaminants, saturated (MOSH) and aromatic (MOAH), that originate from petroleum. Due to the wide use of products deriving from its distillation and refining in any sector, private and industrial, these contaminants are ubiquitous and are the most present contaminants within our body. We come into contact with these compounds every day, even if the main way of absorption is linked to food, as the result of three main different contributions: environmental contamination, process contamination and migration from packaging. Unlike many known contaminants, however, their toxicity has not yet been clearly defined. Despite this, it has been demonstrated that MOSH are able to accumulate in different organs of our body, a behaviour for which information about consequences on health are lacking, but those of greater concern are MOAH. These share part of their chemical structure with the well-known PAH, and thus are suspected to possibly comprise carcinogenic, mutagenic and genotoxic compounds, for which occurrence in food should be completely eliminated. However, this uncertainty about toxicology, together with the lack of validated methods for their analysis at low levels, meant that a legal limit was never introduced. Nonetheless, the legislative world has not stood idly by, and several draft laws have been proposed over the years, providing an idea of the goal to be achieved, which have caused the large-scale retail trade to move accordingly, starting to require food producers to respect these limits. However, these limits are very stringent for oil producers, as this matrix is one of the most contaminated due to its chemical affinity with mineral oils. Hence this PhD project was born, or rather from the need of the associations of the olive oil supply chain to precisely identify the sources of contamination, in order to try to implement prevention strategies. For this purpose, a sampling was organized, which involved all stages of the supply chain, from the olives from the tree to the finished oil.

The first part of the project concerned the implementation and optimization, and when possible validation, of methods to be used for the analysis of these matrices, since no suitable method was present in the literature. This involved the optimization of methods for the extraction of oil from the matrices by chemical means, as well as for the analysis of these contaminants with high sensitivity (evaluation of background contamination),

solving the problem of interference by endogenous compounds of the matrix for both the MOSH and MOAH fractions prior to HPLC-GC-FID analysis (reference instrumentation). Performance of these methods, based on microwave assisted saponification, epoxidation and elution through aluminum oxide, resulted well in line with the JRC guidelines. Thus, these methods could be applied for the analysis of the samples deriving from the sampling along the supply chain.

Indeed, the second part of the work therefore concerned the monitoring. For practicality, the work was divided into two main parts. The attention was firstly focused on the evaluation of the impact of the operations carried out in the field, with particular reference to the harvesting phase, and was later moved to the milling operations at the mill plant. The harvesting was found to be the main source of contamination in the extra virgin olive oil supply chain, due to leaks of lubricants and hydraulic oils, as well as contact of the olives with greased mechanical parts. A qualitative confirmation of the identity of the contamination was obtained, for these samples, also with the GC×GC technique with double detection, FID and MS. Transportation and operations at the milling plant, on the other hand, did not report any major criticalities, even if the use of machinery that requires lubrication never completely excludes the possibility of contamination. Rather, the washing phase, which was the subject of a specific focus, if correctly applied can partially decrease the contamination found in the finished oil. Indeed, the contamination seems to be localized mainly on the surface of the olive, even if some of it can penetrate into the pulp. Unexpectedly, the oils sampled at the mill were on average less contaminated than the oils purchased at the supermarket, underlining the importance of future developments aimed at also verifying the processes performed between the extraction of the oil and its marketing (storage, filtration and transport).

Finally, the third part regarded the monitoring of the refining process of lampante olive oil and crude olive pomace oil. Also in this case, no critical issues were highlighted. Rather, the refining process has a decontamination role. Indeed, it is able to remove the most volatile fraction of MOH contamination during the deodorization process, as well as to adsorb part of the aromatic contamination, also referable to PAH, during the decolorization.

INTRODUCTION

1 Olive oil

1.1 Definition, regulation and classification

Olive oils are oils obtained from the solely mechanical or physical extraction of olives, the fruit of the olive tree "*Olea europaea* L.", under specific conditions not leading to its alterations, and excluding oils obtained with the use of solvents, re-esterification processes or by mixing with oils of other nature. Beside the extraction per se, other treatments like washing, decantation, centrifugation and filtration, are allowed in order to still be able to define olive oils as such. Actually, a more correct nomenclature, when oils are extracted following these methods, provides for the use of the designation of virgin olive oils. Virgin olive oils can in turn be classified according to their suitability for direct human consumption or not (if they need further processing before being considered edible) and, going further into detail, based on their chemical, physical and organoleptic characteristics. Who defines them, and therefore the product designation of the various types of olive oils in Europe, is the European Union (EU) through the issuing of regulations. However, other standards may be applied elsewhere, based on where olive oils are traded.

More than 50 years ago, Regulation (EEC) 136/66 posed for the first time the basis for the definition of the various types of olive oils and for harmonization of the edible oils and fats market within the EU and towards foreign countries. However, this regulation, which is no longer in force, did not report any analytical parameter beside free acidity (and the related analytical methods for its verification), and has more recently given way to Regulation (EEC) 2568/91, whose last amendment dates back to 2019. The latter laid down the foundation of olive oil EU Legislation, becoming in effect a cornerstone, and establishing specifically:

- the parameters to be used to verify olive oils quality and purity, as a reference also in case of official control;
- the limits for each parameter, which contribute to the definition of the commercial category of olive oils;
- the analytical methods to be used to evaluate the parameters of olive oils and verify if they fit with its commercial category.

However, these regulations have legal value only for Member States, and are not applicable to non-EU states in the context of international trade. Thus, outside the EU borders, harmonization for the olive oil market is based on the standards of the

International Olive Council (IOC), at least for the countries which are its members, among which the EU itself is present. This is also the reason why the European legislation is aligned, since its joining, with the IOC Trade Standard, which for olive oils is the standard COI/T.15/NC No 3/Rev.18 June 2022. In an even broader vision, and therefore considering OOs in a worldwide scenario, reference is also made to the standards of the Codex Alimentarius. In particular, the specific standard relating to olive oil is the CODEX STAN 33–1981, last revised in 2017.

Unlike the European legislation, the other two standards just mentioned are not mandatory, but adopted based on a consensus, and therefore even though the countries who adhere are expected to respect them, in case of transgression no penalty can be provided.

Therefore, putting together these standards, the classification of olive oils provides for the distinction of:

- extra virgin olive oil (EVOO): physically extracted olive oil, of higher quality and fit for consumption;
- virgin olive oil (VOO): physically extracted olive oil, of medium quality and fit for consumption;
- ordinary virgin olive oil (OVOO): physically extracted olive oil, of lower quality and fit for consumption (this category is nowadays present within the IOC trade standard and the Codex Alimentarius, while the UE deleted it);
- lampante olive oil (LOO): physically extracted olive oil, not edible and thus intended for refining before consumption or for technical use;
- refined olive oil (ROO): LOO subjected to refining treatment;
- olive oil (composed of refined and virgin olive oils) (OO): ROO blended with any virgin olive oil suitable for consumption (EVOO, VOO, etc.).

In addition, oil can also be obtained from further physical or solvent extraction of the pomace, the solid residue of the physical extraction of olives, excluding oils obtained by re-esterification or mixtures with other type of oils. Olive pomace oil is divided into:

- crude olive pomace oil (COPO): chemically or physically extracted pomace oil, not edible and thus intended for refining before consumption or for technical use;
- refined olive pomace oil (ROPO): COPO subjected to refining treatment;

- olive pomace oil (composed of refined olive pomace oil and virgin olive oils) (OPO): ROPO blended with any virgin olive oil suitable for consumption (EVOO, VOO, etc.).

The main parameters (physical, chemical and organoleptic), with their relative limit values, which contribute to the definition of the various categories of oil, are shown in Table 1.1.

Table 1.1. Physical, chemical and organoleptic characteristics of the different olive oil categories [adapted from IOC Standard COI/T.15/NC No 3/Rev.18 June 2022].

Oil category	Free acidity (%/m oleic acid)	Peroxide value (mEq O ₂ /kg oil)	UV absorption			Organoleptic characteristics				
			K270 or K268	K232	ΔK	Odour/taste	Colour	Aspect 20°C x 24h	Median of defect	Median of fruity attribute
EVOO	≤0.80	≤20.0	≤0.22	≤2.50	≤0.01	-	-	-	Me=0.0	Me>0.0
VOO	≤2.0	≤20.0	≤0.25	≤2.60	≤0.01	-	-	-	0.0<Me≤3.5	Me>0.0
OVOO	≤3.3	≤20.0	≤0.30	-	≤0.01	-	-	-	3.5<Me≤6.0	-
LOO	>3.3	-	-	-	-	-	-	-	Me>6.0	-
ROO	≤0.30	≤5.0	≤1.25	-	≤0.16	acceptable	light yellow	limpid	-	-
OO (ROO +VOO)	≤1.00	≤15.0	≤1.15	-	≤0.15	good	light, yellow to green	limpid	-	-
COPO	-	-	-	-	-	-	-	-	-	-
ROPO	≤0.30	≤5.0	≤2.00	-	≤0.20	acceptable	light, yellow to brown/ yellow	limpid	-	-
OPO (ROPO +VOO)	≤1.00	≤15.0	≤1.70	-	≤0.18	good	light, yellow to green	limpid	-	-

1.2 Extra virgin olive oil supply chain

To facilitate the reader in understanding the results reported in this thesis, the purpose of this chapter and of the following one is to provide an *excursus* of the different phases that are part of the olive oil supply chain (Figure 1.1), discussing the most commonly used

methods and machinery. The different steps will be treated in a synthetic way, without discussing in detail the technological choices or their influence on the quality of the finished oil, unless it is necessary to better highlight the differences among different processing methods.

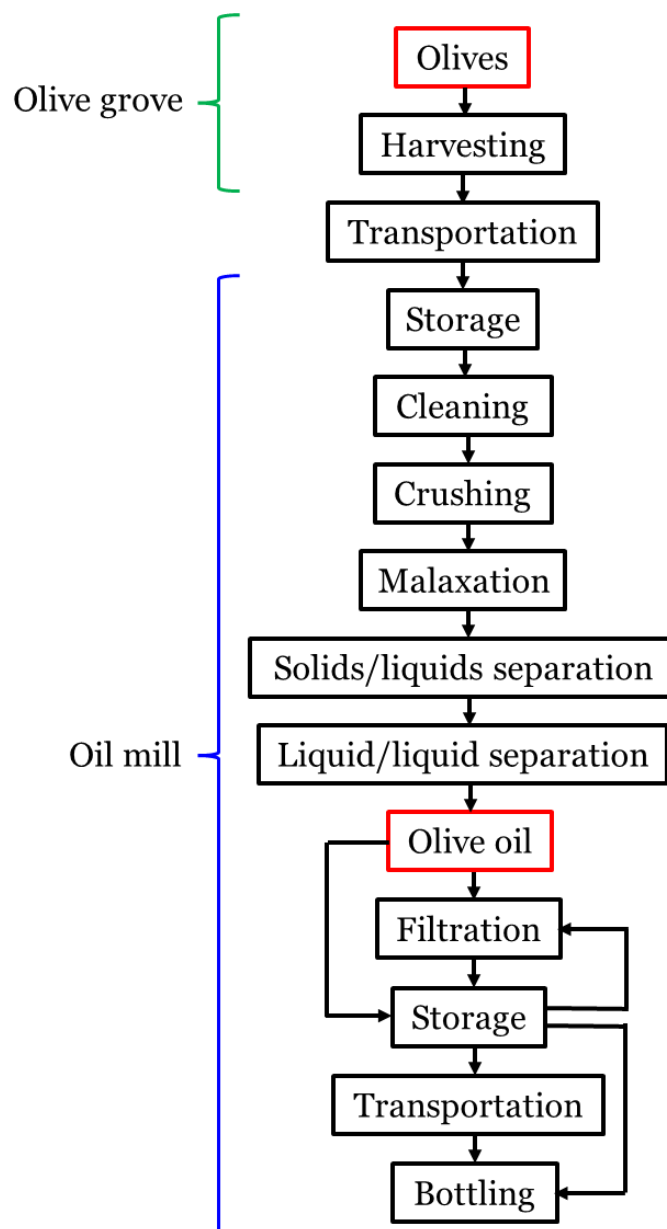


Figure 1.1. Flow chart of the operations making up the olive oil supply chain, from the field to the finished product.

1.2.1 Harvesting

The first step relating to the olive oil supply chain is undoubtedly the olive harvest, which operations include the detachment of the olives from the trees and their collection (Nasini & Proietti, 2014). Methods to perform the harvesting depend on different factors, like the age, the size and the shape of the trees, their arrangement within the olive grove, the type

of soil and the cultural techniques (Petraakis, 2006). Harvesting methods have indeed evolved over the years to meet the need to increase the productivity, the collection efficiency and, at the same time, to reduce costs. Towards this direction, technological changes in olive cultivation have mainly involved the increase of the density of plantation and the improvement of the cultural techniques, which are also the consequence of the evolution of the harvesting machinery.

Starting from the simplest option, the harvesting can be done by hand, i.e. by means of rakes that are run through the branches to pluck the olives. This method has the advantage that it can be easily carried out in any type of olive grove and requires minimal investments in terms of equipment, but on the other hand it is the most expensive methodology due to the labor required, which nevertheless results in the lowest productivity. For this reason, it is now disappearing in favor of collection with hand-held combs or more complex machinery (Nasini & Proietti, 2014).

Harvesting with hand-held combs (Figure 1.2A), or similarly with shaking hooks, is suitable for all types of tree training systems like for the previous method, and therefore it is his worthy replacement. This method is very common, even if it is preferentially exploited in olive groves where the age of the trees, their arrangement or the terrain are not suitable for the use of bigger harvesting machinery. These equipments have a telescopic pole, allowing the operator to reach the highest branches, which at the top has a mobile element. Its motion is provided by electric or endothermic engines, or by pneumatic force, i.e. driven by air put under pressure by means of a compressor. Hand-held combs are of different types, having either oscillating, vibrating or rotating teeth, which are used to hit the olives and branches and facilitate their detachment by a beating action. Shaking hooks are slightly different as they have a hook that provides for their connection to the branches of the tree in order to vibrate them and make the olives fall. For both methods, the olives fall on nets previously positioned under the tree, which are then emptied into containers suitable for their transport to the mill. About nets, they can be completely moved by hand or connected to reel systems which, once they are manually unrolled and placed under the tree by the operators, after the olives fall they are automatically rewound and the olives are conveyed directly into the collection containers. About mechanized harvesting, one of the methods involves trunk shakers. Trunk shakers are similar to shaking hooks and are also based on the use of vibrations, generated by large masses in eccentric or orbital motion, which are transmitted to the trunk of the tree, or to the branches if the latter is too large, through a mechanical arm (possibly telescopic) equipped with a jaw. This machinery can be either mounted on tractors or self-propelled,

and it may or not be equipped with a collection umbrella (Figure 1.2B). When the umbrella is present, it is wrapped around the trunk to automatically collect the olives falling during the vibration cycle into a hopper, which is subsequently emptied. When not, olives fall onto the nets and are handled as previously described.

Always referring to mechanical arms, other equipments, generally mounted on tractors, have a big comb at their end which causes the olives to fall according to the same principle as hand-held combs, of which they can be considered an evolution on a larger scale (Figure 1.2C).

Finally, more and more used now are the straddle harvesters (Figure 1.2D), which are determining the increase in the spread of high-density olive groves, where trees are grown in such a way that machinery, similar to those used in the vineyards for grape harvesting, can be exploited. These machines are made to pass astride the trees arranged in vineyard style and, similarly to the grape harvesters, have shaking bars that determine the detachment of the olives from the trees, which are then intercepted and collected by the machine into its containers. The latter are subsequently emptied by tipping them or by means of an auger (like combine harvesters) onto trailers (Nasini & Proietti, 2014).



Figure 1.2. Harvesting of the olives carried out with hand-held combs (A), trunk shaker equipped with the collection umbrella (B), vibrating comb mounted on a tractor (C) and straddle harvester (D).

1.2.2 Transportation and storage

About transportation of the olives from the olive grove to the mill, this must be carried out promptly and following appropriate criteria, in order to avoid the deterioration of the olives consequently affecting the olive oil quality. For example, the use of sacks should be completely avoided. Olives are commonly transported to and stored at the mill inside plastic bins having holes to allow the circulation of the air avoiding fermentative process and heating due to their catabolic activity (Figure 1.3A) (Petraakis, 2006). Overloading of the containers should also be avoided as it would cause the crushing and breaking of the olives in the lower layers determining unwanted enzymatic phenomena and growth of molds and bacteria. However, for some harvesting methods unloading into bins is not feasible, and therefore the olives can be unloaded directly into tractor or truck trailers to be moved in bulk (Figure 1.3B). In the last case, for the above reasons, the period of stay inside the trailer must be short and the olives must be processed within a few hours from harvesting. Regardless of the method used, the olives are sometimes covered with waterproof canvas during transport, or transported in covered trucks, to preserve and protect them until they arrive at the mill (Figure 1.3C). As said, after transportation, olives should be milled as soon as possible, according to the stage of maturation. However, for less ripe olives, but mainly in case of need, storage can last up to a few days. Olives can be conveniently stored inside plastic bins until processing, also given the possibility of stacking and moving them easily with a forklift (Figure 1.3D), while the other option, applicable for example for olives arriving in bulk, is to store them on the ground in dedicated areas, indoor or outdoor under canopies (Di Giovacchino, 2013; Leone, 2022). This may also depend on the policy applied by the mill and the agreements put in place with the suppliers, which sometimes could require the separate processing of the olives.



Figure 1.3. Collection of olives exploiting nets placed on the ground under the trees and their accumulation in plastic bins (A) or in bulk on tractor trailer (B). Plastic bins loaded on covered trucks (C) and stacked at the mill, which is the most common storage (D).

1.2.3 Cleaning

According to the harvesting method, and therefore of the possible contact with the ground and the presence of unwanted material, olives may need to be subjected to a cleaning treatment prior to milling, in order to preserve the machinery and the quality of olive oil. The cleaning consists of two specific operations: separation and washing (Peri, 2014a). With the separation, foreign materials such as leaves, branches, pieces of wood or metal and stones are removed using sieves and/or aspirators/blowers (Leone, 2022). This first step is important to avoid breakages or abrasions of machinery with mechanical parts moving at high speed, such as the crusher or the decanter, and to exclude the leaves and wood from the grinding process, whose presence would modify the sensory characteristics of the oil (Di Giovacchino, 2013). After these operations, olives are weighed before entering the actual milling flow.

Instead, the washing step takes place simply using water in dedicated washing machines (Figure 1.4A), which is also partly recycled from previous washes after decanting, and

whose purpose is to remove mineral material, soil, dust and residues of pesticide products (Petrakis, 2006; Di Giovacchino, 2013). At first the olives are immersed in a tank where a coarse washing takes place (Figure 1.4B), possibly with the introduction of air to create turbulence and increase cleaning efficiency, and subsequently they are moved by means of a conveyor belt under water jets for a final rinse (Figure 1.4C) (Peri, 2014a; Leone, 2022). At this point, either a conveyor belt or a screw elevator transfers the olives to the entrance of the crusher.



Figure 1.4. Olive washing machine (A) comprising the washing tank (B) and the conveyor belt with water jets for the final rinse (C).

1.2.4 Crushing

Crushing has the purpose of breaking up the cellular structures of the olives to allow the release of oil from their vacuoles, which constitutes about 15-25% of the weight of the olive (Petrakis, 2006; Leone, 2014). Olive oil is subsequently separated from water and solid components in the following steps. Crushing is carried out subjecting olives to pressure, impact or shear forces with the aim of creating a fine and homogeneous paste, and it is performed mainly with two types of machinery: the stone mills and the metal crushers, the latter comprising hammer, knife and disc mills (Leone, 2014).

The stone mill is the oldest type of machinery, and it consists of two to four round millstones, of considerable weight, which are rotated over a granite base crushing the olives present along their path (Figure 1.5A). The effect is both pressure and shearing, which allows the breaking of both the stones and the pulp. The disadvantages of this type of milling are the discontinuity, as a new olives batch cannot be introduced until the previous is unloaded (20-30 minutes to obtain the paste), and the exposure to air, which generates oxidative phenomena and the risk of contamination. On the other hand, the

milling takes place slowly and this allows to avoid overheating phenomena and to reduce the possibility of emulsions formation, facilitating the subsequent malaxation (Di Giovacchino, 2013). This type of technology is now disappearing from modern oil mills. Differently, the other three systems are lately the most widespread, as they have a continuous functioning.

In the knife mill the olives are introduced centrally to the machinery and collide violently against a series of metal plates rotating at high speed inside a perforated cylinder (Figure 1.5B). The olive paste by centrifugal force tends to be thrown outwards and, when it reaches the right size as the result of the shearing action, it passes through the holes and is discharged. The hammer mill works similarly, where spokes with steel plates (hammers) impact with the olives and determine the exit of the pasta through the perforated grid (Figure 1.5C) (Leone, 2022). Instead, in disc mills the olives are always loaded from the center of the machinery and, by centrifugal force, are pushed outwards radially and are forced to pass between two toothed metal discs, placed opposite each other. These discs are designed so that during rotation the teeth of one occupy the empty spaces of the other, forcing the olives to pass in narrow spaces and inevitably be reduced to a finely paste (Figure 1.5D) (Leone, 2014). In these last three systems the rotation speed is very high and this generates very emulsified olive pastes, which may require a longer and more complex malaxation. However, they have the advantage of having high throughput, processing continuity and an easy coupling with malaxing systems (Figure 1.6A) (Petrakis, 2006).

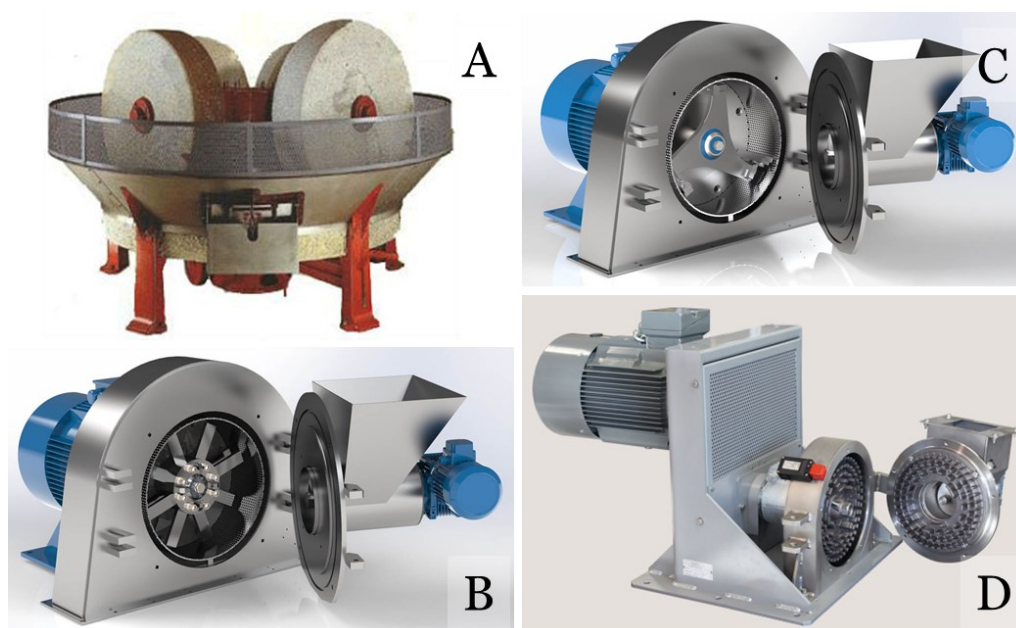


Figure 1.5. Stone mill (A), knife mill (B), hammer mill (C) and disc mill (D) [adapted from www.oliveoilsource.com (A), www.amenduni.it (B, C) and www.alfalaval.it (D)].

1.2.5 Malaxation

Malaxation is the operation having the purpose of favoring the subsequent separation of the oil from the rest of the mass by centrifugation, breaking the emulsion formed during crushing (Petrakis, 2006). Indeed, from the crushing a semifluid mass is obtained, composed of solid components, which are the fragments of stones, pulp and peels of the olives, and a liquid fraction, represented by water, oil and their emulsion (Leone, 2022). Malaxation helps the droplets of dispersed oil to merge into larger drops, a process called coalescence. This step is carried out inside the malaxer, a stainless-steel heated chamber (Figure 1.6A), thanks to the slow (max 20 rpm, rotations per minute) and continuous mixing of the olive paste performed by rotating blades (Figure 1.6B), which allow the meeting of water molecules and the formation of hydrogen bonds between them. As a consequence of that, the oil is expelled out of the aqueous medium generating a lipid phase containing, at the end of the process, more than 80% of the total oil present. The rest remains trapped at cellular level or engaged in stable emulsion. The walls of the malaxer are heated thanks to a jacket for hot water circulation, as the extraction yield is strongly dependent on the time and temperature employed in the process. Higher temperatures and longer times of malaxation increase yield, but can cause deterioration of the quality of the oil, giving way to oxidative phenomena. For this reason, the compromise between yield and quality is found for 20-50 minutes processing at temperatures between 25 °C and 30 °C (Tamborrino, 2014), which can sometimes also be carried out in an atmosphere saturated with inert gas to counteract oxidation. Another advantage of temperature is to make the mass less viscous, and therefore more easily centrifugable in the following step (Petrakis, 2006).



Figure 1.6. Battery of malaxers fed by the crusher (A) and detail of the olive paste under mixing by the rotating blades (B).

1.2.6 Separation between solids and liquids

The olive paste at this point of the process is made up of solid and semi-solid components for 25-30% by weight, water for 50-60%, and finally oil for 10-20%. This step therefore involves the separation of olive oil from the rest of the mass, which however is never complete due to a partial retention of the oil into the solids. Oil recovery is considered optimal when it reaches 80-85% (Baccioni & Peri, 2014). The physical separation of the oil from the malaxed pulp can be carried out in three different ways, as also this step has seen the evolution and application of various methods over the years. These, to report them, are: pressing, percolation and centrifugation (Firestone, 2005; Di Giovacchino, 2013).

Pressing is the oldest method, though not so widespread anymore, based on the principle that by applying pressure on a solid mass containing liquids it is possible to obtain the leakage of the latter (as when squeezing a sponge). Different mats of polypropylene are spread with the malaxed olive paste, operation generally carried out automatically by paste distributors, and are placed one over the other by threading them around a central drainpipe to create a pile (Figure 1.7A). Steel discs are interspersed every 5 of them, to allow the homogeneous application of pressure on the pile. Indeed, once completely loaded, the latter is placed under a hydraulic press and subjected to pressure up to 400 atm. Under this pressure, the liquid part (oil and vegetation water) is drained and discharged through the central pipe to be later subjected to the following steps. High yields and cheapness of the machinery are strengths of this technique, even though the

amount of work required, the low working capability and the discontinuity of the operation almost favored its disappearance and the spread of different systems (Petrakis, 2006; Di Giovacchino, 2013; Servili et al., 2022).

The percolation method is instead based on the different surface tension of water and oil. This difference allows thousands of steel blades, once inserted into the olive paste inside a dedicated machine called Sinolea (Figure 1.7B), to "get wet" preferably with oil, which creates a coating layer over them. Thus, when these are retracted from the mass, the oil drips off from them and is recovered. The movement of the blades must be slow. Compared to the previous one, this method is completely automated, continuous (even if the process takes some time) and relatively cheap, but it gives the lower oil yield. For these reasons it has recently been coupled to centrifugation systems, allowing to recover part of the residual oil in the paste. Even this system is no longer widely used (Petrakis, 2006; Di Giovacchino, 2013; Servili et al., 2022).

The most used system to date applies the centrifugation, allowing to work continuously and with high throughput. With this system the water is removed from the solid phase thanks to the action of centrifugal force, with the aim of speeding up a spontaneous process which is the separation of different phases based on their different density (Petrakis, 2006). The machines involved in the process are horizontal centrifuges called decanters (or separators), consisting of a cylindrical case with a truncated conical end and a screw conveyor, also having a cylindrical truncated cone shape mounted concentrically to it (Figure 1.7C). Due to the rotating speed up to 5000 rpm, the denser solid parts of the paste, which is centrally fed to the centrifuge along its rotation axis, are thrown against the walls of the machine and gradually removed by means of the screw conveyor, which push them towards the conical part allowing in the meantime the removal of liquids. The liquid phase, on the other hand, forms two concentric inner layer, in contact with each other, that moves in the opposite direction. Thus water and oil are pushed through defined paths, generated by barrier plates, and leave the decanter from their respective unloading ports (Leone, 2022). Decanter can be two or three-phases according to the separation carried out. In two-phases decanter the separation of olive oil from water and pomace is obtained, even though the latter two come out together. Differently, in three-phase system (which was developed previously and is considered the traditional one), the decanter is also capable to perform an additional separation between water and pomace, which then come out separately. Even if the oil is already obtained in this step, it often still contains 2-5% of water in emulsion and of dispersed solids, due to the relatively low rotating speed, not allowing to achieve a complete separation. The addition of water to

the malaxed paste to be subjected to centrifugation can help in this purpose (mostly for three-phase systems) even if, inevitably, oil must undergo a further and final centrifugation step, discussed in the next paragraph. Two-phase systems are preferred because they require little or no amount of water to be added for their operation, which simplifies the disposal of vegetation waters. Nevertheless, regardless of the system used, the extraction yields are slightly lower than those obtainable by pressing, but the reduction in working times, combined with the other advantages reported above, have made it the most widely used system (Petrakis, 2006).



Figure 1.7. Extraction of olive oil from olive paste by pressing (A), by percolation using a Sinolea system (B) and by centrifugation using a three-phase decanter, with detail of vegetation water and oil outlets (C) [adapted from www.oliveoil.com (A) and www.frantoionline.it (B)].

1.2.7 Separation of liquid phases

As already mentioned, from the centrifugation performed with the decanter, an olive oil that may still contain impurities (particles of water and dispersed solids) is obtained. Their separation could also take place spontaneously, for example in a settling tank, but the need to reduce processing times has led to the use of centrifugal systems (Petrakis, 2006). In particular, the disc centrifuge, which is a vertical centrifuge with a high rotating speed (up to 12000 rpm), is the machine in charge to carry out this operation of oil finishing and clarification (Figure 1.8). From the operational point of view, the turbid oil

coming from the decanter is added with 3-10% of water and fed from the top of the machinery, centrally reaching the bottom of the centrifuge by gravity. The latter is composed of a bowl containing conical discs, stacked and spaced apart, to allow the passage of liquids. Due to the high-speed rotation, the liquid is accelerated by centrifugal force and the solids contained are immediately pushed externally onto the walls, at the periphery of the bowl, while the vegetation water is positioned immediately above them. The oil, having a lower density, finds itself in a more central position and moves upwards and towards the rotation axis, pushed by the water beneath it, until it flows out through a central outlet located at the top. On the other hand, the vegetation water is discharged a little further down, from a concentric outlet to that of the oil, while the solids are removed either manually, requesting the machine to be stopped, or automatically, by means of a mechanism that allows the opening of the bottom of the bowl for a few tenths of a second and their expulsion to the outside during rotation. At this point the oil is ready to be stored and bottled, although it may still contain finely dispersed solid residues and water which could impair oil stability, due to enzymatic (hydrolysis and oxidation) or microbiological (fermentation) spoilage, or not be visually appreciated by the consumers (formation of deposits at the base of the bottle). For this purpose, it is possible to carry out decanting and/or filtration steps (Baccioni & Peri, 2014; Leone, 2022).



Figure 1.8. Disc centrifuge, with detail of the oil outlet.

1.2.8 Decanting and filtration

A first approach to remove the impurities present in the oil involves decanting. With decanting, impurities are left to settle on the bottom of particular storage tanks, and subsequently the oil above is transferred to another tank where the process can be repeated until the required degree of purification is achieved (Leone, 2022). The time between one pouring and the other is approximately of 20-30 days (Di Giovacchino, 2013).

As an alternative, or in support of it, the oil can be filtered, and this becomes particularly important for oils with a certain relatively long shelf-life, which therefore require greater stability. Filtration can be performed directly on the freshly extracted oil, but more often it is carried out at the end of the storage period, therefore just before packaging, by passing the oil through filters of suitable porosity. The operating mechanism provides for the retention of the larger solids on the surface of the filters (surface filtration), as they are not able to enter the pores, and of the smaller solids inside the latter (depth filtration) (Figure 1.9C). The most commonly used filter media are cellulose sheet filters (Figure 1.9B) and diatomaceous earth filters, even if in some realities cotton wool filters are also used.

Cotton wool filters are the most basic and less used, as they are less effective in retaining smaller components, as the oil is simply filtered by gravity through a layer of cotton wool placed on metal vats with a perforated bottom for oil collection.

For the other two systems, filters are stacked horizontally, tightly packed (Figure 1.9A), and filter plates are positioned between them, which in this way alternate areas for turbid oil loading and filtered oil unloading. The turbid oil is pushed into the feeding plates, forced under pressure to pass through the filters and then discharged from the collecting plates on the other side. The difference between them lies in the material constituting the filter, which in the first case includes cellulose sheets, while in the other steel grids on which diatomaceous earths are stratified. In the latter the filtration is more intense and determines the unwanted retention also of valuable compounds contained in the oil, and for this reason it is not the one preferably used (Peri, 2014b; Leone, 2022; Servili et al., 2022).



Figure 1.9. Oil filtration system with horizontally stacked filters (A). Filter before (B) and after (C) filtration.

1.2.9 Pumping, storage and transportation

After filtration, the oil is stored until bottling. However, this last step, as well as the previous ones, require the movement of the oil, or of the other matrices derived from the milling of the olives, between different areas and machinery within the milling plant. For this purpose, pumps are used. The pumps that are most suited to handle viscous and dense material, such as oil or olive paste, are rotary (or volumetric) pumps, which can provide a continuous flow and avoid shear forces. These are gear pumps, lobe pumps, single rotor screws pumps and peristaltic pumps (Peri, 2014c).

About oil storage, the best and most common way (if not the only one nowadays) involves the use of metallic tanks made of stainless-steel kept inside buildings, having a vertical distribution and a cylindrical shape (Figure 1.10). Their bottom can be either flat or sloped/cone shaped, the latter to allow periodic removal of any sediment (Petraakis, 2006). Even large underground vats with walls covered with inert material can be conveniently used (Di Giovacchino, 2013). Tank dimensions, and therefore the respective storage volumes, can be variable, they can have fixed or floating roofs, be smaller to allow their stacking in order to manage in the easiest way different production batches, and so on. These differences depend on the specific needs of the mill.

Similarly to storage, if the oil has to be transported in bulk, e.g. to be bottled elsewhere, this process is carried out using tank trucks with stainless-steel walls. Trucks that make

these transfers have to be used exclusively for the transport of virgin olive oil (Servili et al., 2022).



Figure 1.10. Stainless-steel tanks for oil storage.

1.2.10 Bottling

Bottling of the oil can be performed directly at the oil mill or at packaging companies, and the final containers can be made of glass (Figure 1.11A), metal (Figure 1.11B) or plastic (Figure 1.11C), and can be of variable volumes, from 50 mL to 5 L (Servili et al., 2022). Metal containers are usually made of tin, tin-free steel based on chromium, aluminium or aluminium alloys, while plastic ones exploit polymers like polyethylene terephthalate (PET), high-density polyethylene (HDPE) and polyvinylchloride (PVC) (Limbo et al., 2014). Plastic-coated cardboard and ceramic are other types of available containers, but are less widespread (Boskou, 2006b). Among the plastic containers, apart from the classic bottles, bag-in-box are also exploited. Except for plastic bottles which can be formed directly in situ, the containers usually arrive at the milling plant packed in several layers over pallets wrapped in a plastic sheet, with cardboard or plastic panels placed between one layer and the other.



Figure 1.11. Containers for the sale of EVOO made of glass (A), metal (B) and plastic (C) [adapted from www.olioappo.it (A,B) and www.teatronaturale.it (C)].

As regards the sequence of operations, which are carried out semi-manually, but also automatically, they are the depalletization of the containers, their external and internal cleaning (due to the possible presence of foreign materials, particulates or dust, containers can be blown with compressed air to clean them before being filled), their filling, their closing and their palletization for transport to the store.

The filling can be performed by means of filling machines that work by gravity or exploiting vacuum. Both systems are equipped with two flow lines, one for introducing the oil and one for air removal. When the bottle is put in contact and sealed with the filling valve, in the first system the oil flows into the bottle by gravity through one of the two lines, while the other allows the air present in the bottle to be expelled. In the other system, the second line is connected to vacuum creating a depression inside the bottle which draws oil from the storage tank towards it (Limbo et al., 2014).

Finally, the closure provides hermetic sealing of the containers, which generally takes place by means of screw caps and roll-on caps. In screw caps the thread of the cap is screwed either on the thread of the bottle neck, and this commonly occurs for glass and plastic bottles (Figure 1.12A), or on a threaded element that is inserted by pressure (interlocking) into the opening of the container. The latter usually applies to metal containers (usually retractable), but also to glass bottles (Figure 1.12C and 1.12D). Roll-on caps are similar, and are used in glass bottles, where the difference is that the aluminium cylinder is rotated by pressure on the screw of the bottle neck, thus acquiring in this way its final shape (Figure 1.12B).

Caps can be made of plastic, tinplate, tin-free steel or aluminium, and usually contain an elastic and soft plastic element which acts as a seal between the cap and the mouth of the

bottle. In addition, inside the mouth of the bottle, there is usually a plastic element called drip catcher, positioned by interlocking, which also allows a better seal, but also makes easier for the consumer to pour the oil (Figure 1.12E) (Limbo et al., 2014).



Figure 1.12. Closures for oil containers: screw cap (A), roll-on cap (B) and screw cap with interlocking element (C, D), together with typical drip catcher (E) [adapted from www.polsinelli.it].

1.3 Lampante olive oil refining

Not all olive oils have the characteristics to be sold as extra virgin. In fact, as previously reported, olive oils that do not meet the limits relating to chemical-physical indexes set by the legislation (the main one being a free acidity higher than 3.3% *m/m* of oleic acid), and having certain sensory defects, are not considered edible and are consequently classified as lampante oils. This is usually the consequence of olives that are in a bad state of conservation, which results in obtaining low quality oils. Therefore, the latter are intended either for technical use, or must undergo refining to lower the acidity below 0.3%, remove other defects (bad smell and taste), impurities and foreign substances, thus being finally suitable for human consumption (Morchio, 2022). Acidity is usually the reference parameter, as it turns out to be the most frequently associated with olives of poor quality, but it is not the only one to consider, as refining becomes necessary also when other parameters are exceeded, e.g. the peroxide value and the UV absorption, not allowing the oil to be classified within the other categories reserved for olive oils of higher value. Refined oils, once the process is completed, are odorless, colorless and tasteless, and are therefore rarely sold as such to be consumed. For this reason, they are often blended with small percentages of extra virgin and virgin oils, which give them back a

certain flavor and sensory profile, provided however that a free acidity value less than 1% is reached (Peri, 2014d). A flow chart of the operations related to the refining of lampante olive oil is provided in Figure 1.13.

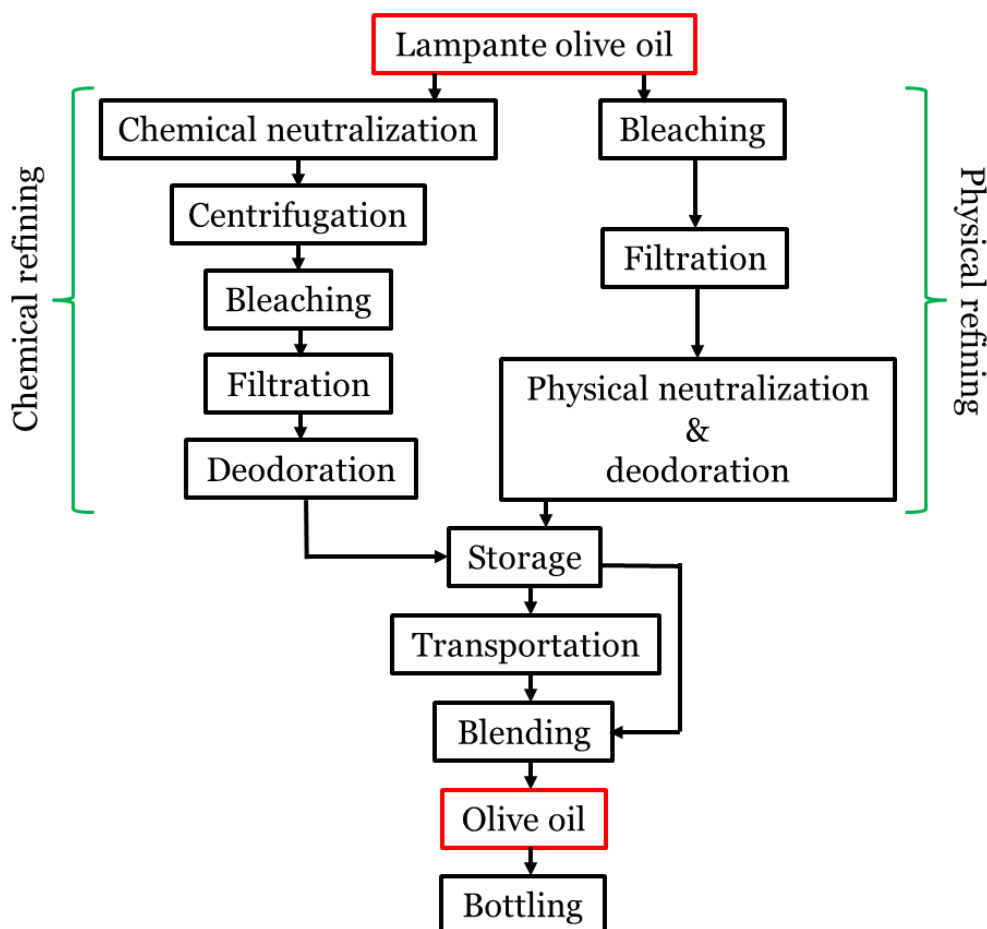


Figure 1.13. Flow chart of the operations related to the refining process of lampante olive oils.

In addition to lampante olive oil, also olive pomace oil needs to be refined before being marketed and, although this chapter is particularly focused on the former, the steps that make up their refining process are very similar. What mainly changes are just the operating conditions under which certain phases are carried out and therefore, at least from an operational point of view, what is described below is valid for both of them.

Unlike lampante oil, which is basically obtained in the same way as a virgin or extra virgin olive oil, even though it does not share the same quality, the extraction of pomace oil involves some additional steps. In particular, in some cases the fresh pomace, derived from the first physical extraction, is subjected to a second malaxation at higher temperature followed by three-phase centrifugation, recovering about 50% of the residual oil, which then enters the refining process, and obtaining a yield of about 1% referred to the olives (Peri, 2014d; Morchio, 2022). This mainly occurs when two-phase decanters

are used for the first extraction, as they provide a very moist pomace, so that this is also an opportunity to remove a significant portion of water. The pomace, at this point, still contains an average 2.5% of oil. Hence, after this first step, as well as in all the other cases where the pomace is directly processed (where the residual oil is still between 2.5% and 5%), solvent extraction is applied after few pre-treatments (Morchio, 2022). The pomace undergoes a first step of pitting, carried out in a rotating cylinder having a sieving action, thanks to the presence of a grid, and subsequently a drying step, which has the purpose of obtaining a pomace with a residual humidity of 6-8% to allow efficient solvent extraction of the oil, which is generally carried out with *n*-hexane or technical hexane (Peri, 2014d). Too much water would act as a barrier and the solvent could not penetrate the matrix. The drying process takes place by loading the pomace into a rotating cylinder containing diaphragms, which allow for a large contact surface with a counter-current air flow at 300-400 °C, carrying away humidity. At this point solvent extraction takes place, in continuous (in counter-current mode) or discontinuous mode (Morchio, 2022). The pomace is mixed with hexane, which penetrates the solid matrix and solubilizes the oil contained therein, and then the exhausted solid residue is separated from the liquid medium by gravity or by mechanical means (e.g. filtration). From both the pomace impregnated with solvent and the solvent-oil mixture, the hexane is evaporated, recondensed and recycled for subsequent extractions. The solvent-oil mixture is desolventized in a multiple-effect evaporator under vacuum (Peri, 2014d), after which the oil obtained enters the refining process that, as for lampante oil, begins with the neutralization step.

Finally, unlike lampante oil, a further step envisaged for pomace oils is the winterization (also called de-waxing), which can be carried out at different points of the process, and involves cooling the oil between 5-8°C to allow the solid fraction, made up of waxes and saturated triglycerides and fatty acids, to crystallize and precipitate. After that, the definitive separation of the solid phase takes place by filtration or centrifugation. This process is performed to avoid the final product to have sediments and appear cloudy (Ruiz-Méndez & Aguirre-González, 2013).

1.3.1 Neutralization

The neutralization is the first step of the refining process and has the purpose of reducing the acidity of lampante oil, linked to the presence of free fatty acids (FFAs), by means of their saponification with alkali and thus their conversion to soaps, which are insoluble into the oil (Ruiz-Méndez & Aguirre-González, 2013). This step can also be preceded by

decanting, centrifugation or, more rarely, by filtration of the oily mass, to remove any suspended materials, but also moisture, which could cause the presence of cloudiness and sediments in the finished product. Also degumming can be performed, which is an acidification step with phosphoric or citric acid to promote precipitation of mucilages and organic impurities (mainly phospholipids, called gums), subsequently removed by settling or centrifugation (Firestone, 2005). However, this mainly concerns seed oils and olive pomace oil, and only more rarely lampante olive oils, which are preferentially subjected to a simple washing (Ruiz-Méndez & Aguirre-González, 2013). The acids used must then be neutralized, before proceeding with a physical refining, or are neutralized directly by the alkalis used in the chemical refining (Peri, 2014d; Morchio, 2022).

For chemical neutralization, an aqueous solution of sodium hydroxide is added to LVOO in slight excess with respect to the calculated amount (10-20%) and is kept under slow and continuous agitation, at the temperature of 70-80 °C. Once the soaps have formed, they are hydratable and therefore easily separable from the oil either by sedimentation or centrifugation. Sedimentation is mainly linked to refining plants that use batch saponification, and therefore where the process is discontinuous, while alternatively and for continuous processing the separation is accelerated by the use of centrifuges (Morchio, 2022). Operationally, the oil stored in suitable tanks is fed into a heat exchanger, to reach the required temperature, and then into a mixer, where the lye is fed and the neutralization process starts. Oil can alternatively be sent directly to the mixer if this it is equipped with a heating jacket. After the process, water is added to help phase separation and the mixture obtained is temporarily stored (always in slow mixing to avoid formation of emulsions) in a buffer tank for 20 minutes, before being sent to the first centrifuge. The oil that comes out of the latter still contains a high amount of residual soaps, which could poison bleaching earths and clog any filters placed in the oil path. Therefore, the oil mass is heated again to 70-80 °C by means of a further heat exchanger and added with hot water (90-95 °C), before being sent to the second and last centrifuge. Summarizing, the first centrifuge carries out the first massive removal of soaps, while the second aims to remove the residual ones (Figure 1.14A). At this point, the oil contains little amounts of water, which can deactivate bleaching earths, and thus need to be dried either into a deaerator under vacuum and heating conditions (80 °C) or by distillation, to be ready for bleaching (Ruiz-Méndez & Aguirre-González, 2013; Morchio, 2022).

Alternatively to chemical neutralization, or in support of it for oils with marked acidity, neutralization can also take place physically, and therefore by steam distillation (Firestone, 2005). This usually takes place in a distillation column similar to the one used

for the final deodorization step (Figure 1.14B) and, when used in place of chemical neutralization, is commonly performed after the bleaching step. Indeed, the high temperatures used can fix the color, due to artifacts formation, which are then difficult to eliminate. Operationally, crude oil is introduced into a deaerator under vacuum for the removal of water and air present and then it is heated up to 225-240 °C by different heat exchangers and fed into the upper part of the distillation column, the latter containing packed material and working under vacuum. The oil then flows downwards by gravity and meets the counter-current steam flow injected from the bottom of the column, which strips away the free fatty acids and any other extraneous and unpleasant volatile substances. The oil is then cooled and sent either to chemical neutralization, if still necessary, or directly to bleaching, if not performed before (Morchio, 2022). Finally, in other cases, the deacidification step is instead carried out at the same time as the deodorization, applying more extreme temperature and vacuum conditions (Peri, 2014d).

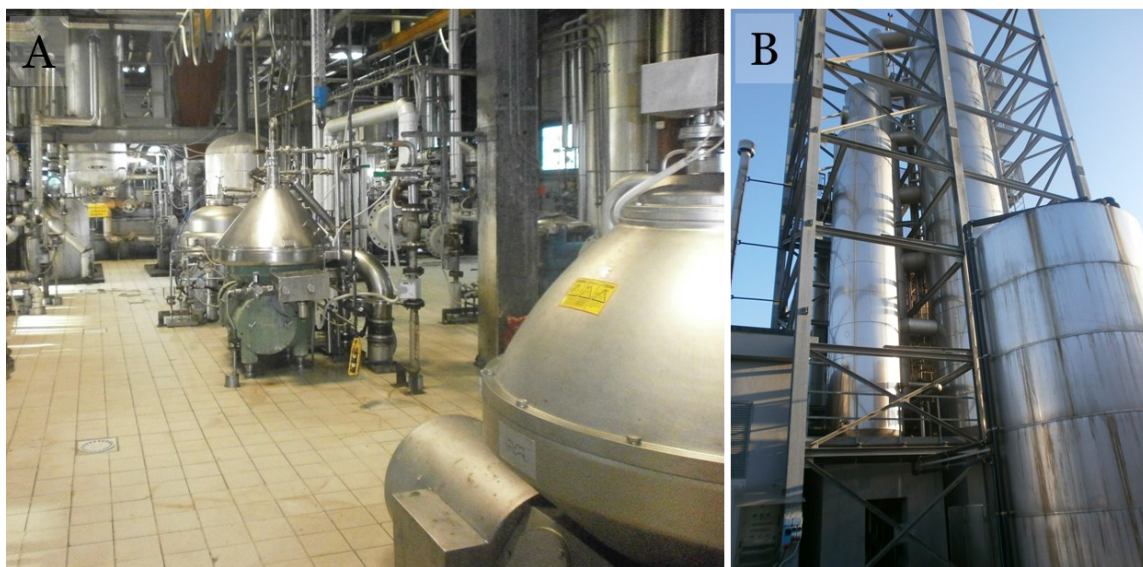


Figure 1.14. Centrifuges used for the separation of soaps from oil in chemical neutralization (A) and distillation column used for physical neutralization (B).

1.3.2 Bleaching

Following the neutralization phase, the oil is bleached thanks to the removal of colored endogenous compounds such as chlorophylls, carotenes and xanthophylls, together with compounds generated during the previous steps performed at high temperature, which give a brown color to the oil. For this purpose, the oil is added with bleaching earths (mineral clay based on bentonite, kaolinite and montmorillonite, which are aluminum-magnesium silicates, activated with sulfuric or chloridric acid) inside a first mixer by means of screw hoppers for 0-5-1.5% by weight, and possibly also with activated carbon

up to 0.5%. Then, the mixture is slowly stirred under vacuum inside the bleacher at a temperature of 90-110 °C, for times ranging from 20 minutes up to 1 hour (Figure 1.15A). During the process, unwanted endogenous components adhere to the surface of bleaching earths or are absorbed by activated carbon inside its distinctly porous structure. Polycyclic aromatic hydrocarbons (PAH) are also efficiently abated when activated carbon is used, as well as pesticide residues and some odorous compounds. When the bleaching cycle is over, and after cooling, solids are removed from the oil by filtration using filter-plates or leaf filters, made up of a series of stainless-steel mesh nets (Figure 1.15B). After that, the adsorbents used still contain a quantity of oil around 30%, and are thus treated with air and steam in an attempt to recover most of it (Peri, 2014d; Morchio, 2022). Bleaching is a discontinuous process, but can also be carried out in a continuous mode. In the first case it is performed in cylindrical containers equipped with mixing and heating systems, where the bulk of oil remains for the entire time of the process until it is discharged. In the second case the oil is pumped through filters composed of partially exhausted earths for a first reduction of coloring compounds and then it is sent to the mixer, where it remains only for the time necessary for the addition and dispersion of the bleaching earths. After that, the mass is sent to a retention tank where it remains the time necessary for bleaching, leaving the mixer available for subsequent lots (Ruiz-Méndez & Aguirre-González, 2013).

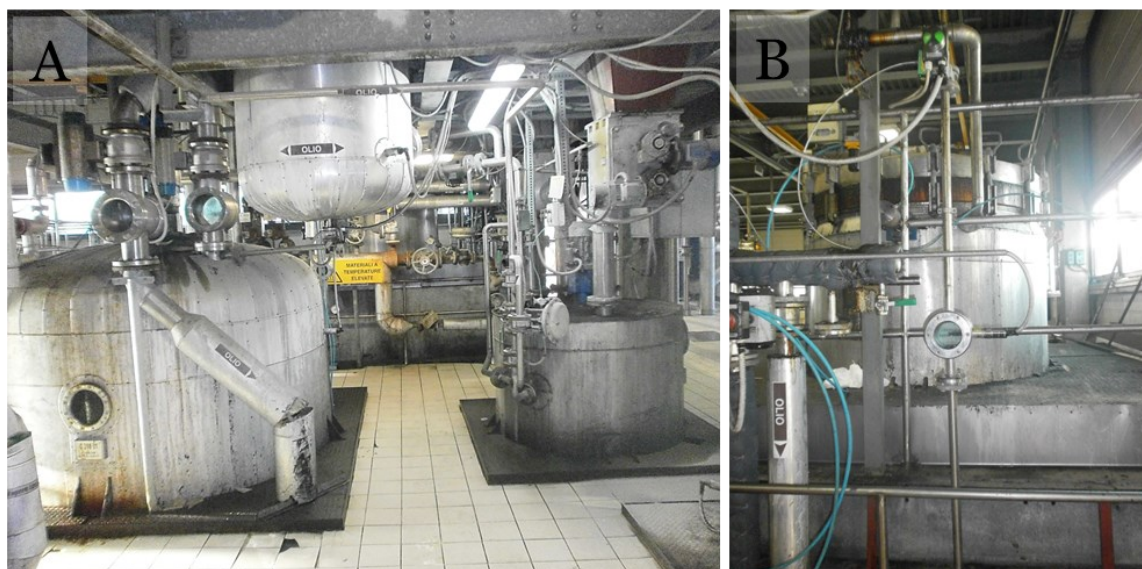


Figure 1.15. Mixer for mixing bleaching earths/activated carbon with oil (A, on the right), bleacher (A, on the left) and filtration system for oil/exhausted adsorbents separation (B).

1.3.3 Deodorization

The last step of LVOO refining is the deodorization, which is carried out in continuous, semi-continuous or discontinuous deodorizers (distillation columns) (Figure 1.16) operating under strong vacuum (around 1 mbar), and exploiting stripping gas (usually nitrogen) or steam stream to remove undesirable odors (Firestone, 2005; Morchio, 2022). As previously reported, in addition to deodorization, this step also allows to remove residual FFA not eliminated in the previous phases, finally achieving neutralization of the oil. To some extent, deodorization is also capable to cause further decoloration of the oil and to remove the most volatile fraction of mineral oils, as reported later.

As for physical deacidification, the deaerated oil meets the stripping flow of gas or steam at the level of the distillation column, which determine the removal of the most volatile components. Processing times and temperatures depend on the characteristics of the plant, even though in general the temperature ranges from 180 to 270 °C (the most common temperature is about 235-240 °C) and times are of the order of 2-3 hours (Ruiz-Méndez & Aguirre-González, 2013; Morchio, 2022). At this point the oil is cooled down and placed into storage tanks, waiting to be bottled or shipped to packaging companies, as it happens (and already described) for extra virgin olive oil. Bottling takes place after blending of the refined oil with variable percentages of virgin or extra virgin olive oils.



Figure 1.16. Distillation column for oil deodorization.

2 Mineral oil hydrocarbons

2.1 Origin, definition and chemical structure

Mineral oil hydrocarbons (MOH) are a class of ubiquitous environmental and processing contaminants, which are commonly found in different food matrices in concentrations in the order of tens of mg/kg. Although they may also derive from coal, natural gas and biomass, their main origin is petrogenic, and therefore attributable to crude oil (EFSA, 2012a). Indeed, they are hugely present in a great variety of products obtainable from petroleum distillation and subsequent refining/purification (Figure 1.17).

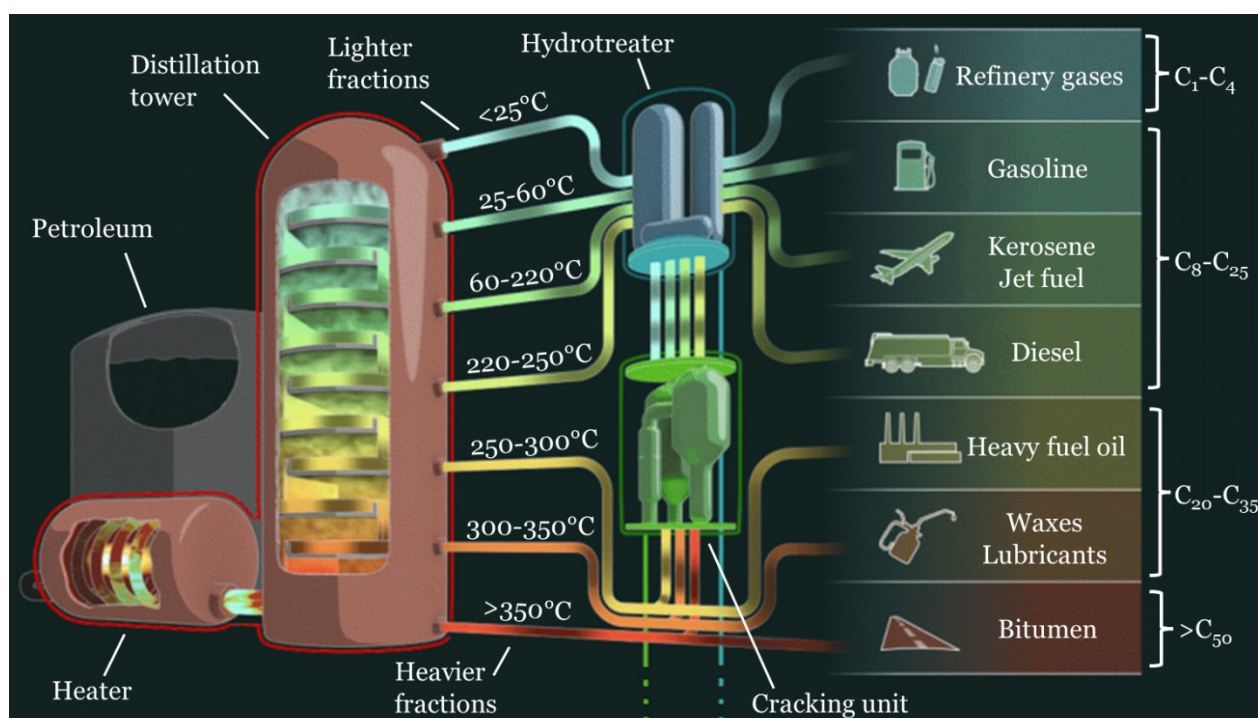


Figure 1.17. Generic diagram of a petroleum refining plant, with reference to the distillation temperatures of the various fractions and the range carbon atoms of the hydrocarbons belonging to them [adapted from <https://uret.com.tr> © FES TANKS].

These products are widely exploited by the industry in a multitude of sectors, private or commercial, including the food supply chain and its different stages (Weber et al., 2018), consequently increasing MOH spread as contaminants at different levels. Products from petroleum distillation can be used in their original form, after blending with other intermediate fractions or as additives for other types of products, based on the desired use. Thus, because of this great variety, they are generally identified on the basis of their physical characteristics, e.g. boiling point, density, viscosity etc., which are closely related to the distillation process (Eneh, 2011), rather than on their composition. For this reason, it follows that their classification depends on the distillation cut from which they derive. In particular, they can be grouped into:

- light distillates: liquefied petroleum gas (LPG), gasoline, naphtha;
- middle distillates: kerosene, diesel, solvents;
- heavy distillates and residues: heavy fuel oil, lubricating oils, wax, asphaltic material.

Regardless of the origin and the final use, all these products are generically classified under the name of mineral oils.

From the chemical point of view, mineral oils are complex mixtures of thousands of hydrocarbons (MOH), with a very high degree of isomerization, and consist of chains from 10 to over 50 carbon atoms. For this reason, for their identification it is not possible to refer to single compounds, but rather to classes of compounds sharing a common chemical structure. Based on this approach, MOH can be classified as:

- paraffins: linear (*n*-alkanes) and branched (isoalkanes) saturated aliphatic hydrocarbons;
- naphthenes: cyclic saturated aliphatic hydrocarbons (mainly rings with 5-6 carbon atoms), alkyl-substituted or not, even present as multi-ring systems;
- aromatics: single or multiple ring aromatic systems (generally with a maximum of 5 rings), alkylated at different degrees to more than 98%, and possibly containing heteroatoms (mainly nitrogen and sulfur) (Bratinova & Hoekstra, 2019).

Although this is the pure chemical classification, according to the analytical approach, and also of the impact of these compounds on human health, they are commonly grouped into two main classes, which are the mineral oil saturated hydrocarbons (MOSH) and mineral oil aromatic hydrocarbons (MOAH) (Biedermann et al., 2009). The first one includes paraffins and naphthenes, while the other, as the name implies, the aromatics (Figure 1.18).

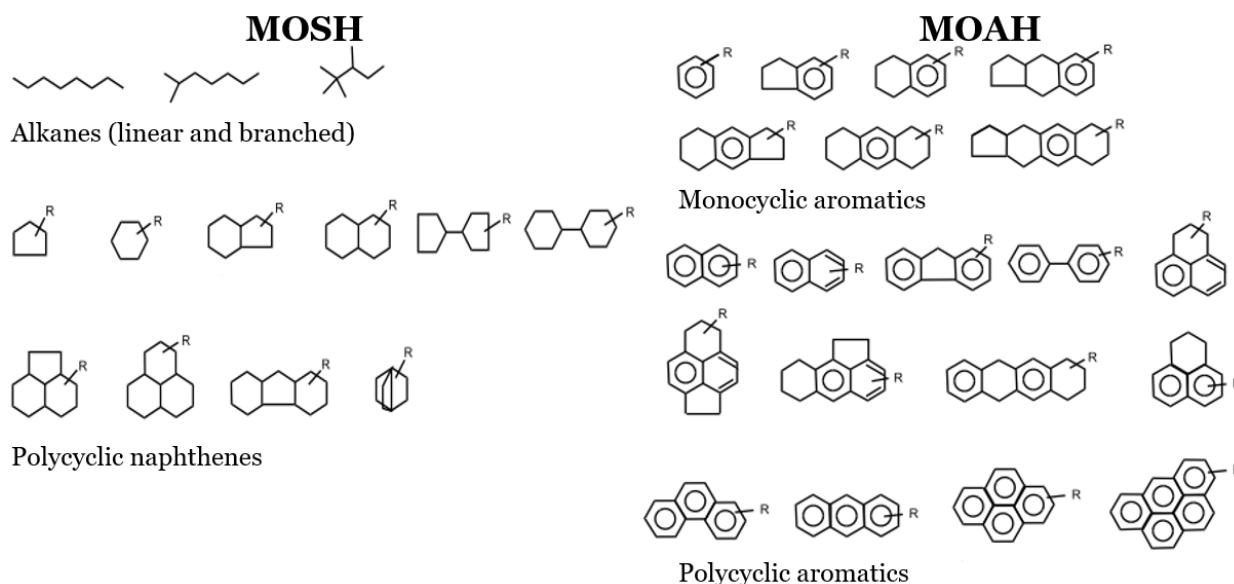


Figure 1.18. Examples of typical chemical structures characterizing MOSH and MOAH fractions [adapted from (EFSA, 2012a)].

MOAH in technical grade mineral oils typically make up 15-35% of total MOH, while they are absent or at least minimized in food grade ones, as they are subjected to refining and purification treatments for their removal (Grob et al., 1991a; Moret et al., 1997). For this reason, in presence of MOAH contamination, MOSH are certainly present, while the same may not be true for the opposite. In the past, this often resulted in the development of methods focused on the MOSH fraction, used as a marker for the contamination by mineral oils (Wagner et al., 2001b; Moret et al., 2009). In addition, MOSH and MOAH deriving from the same source share the same range of molecular weights, which are typical of the mineral oil from which the contamination originated, obtained from the same distillation cut. However, even though the source of contamination can be hypothesized based on the molecular weight distribution (Wagner et al., 2001a), the presence of a large number of similar petroleum distillation products determines in most cases that the source remains doubtful (Moret et al., 2003, 2010).

Finally, MOAH should not be confused with polycyclic aromatic hydrocarbons (PAH), which albeit chemically similar, are not alkylated and, although they can be found in crude oil, are mainly formed by incomplete pyrogenic processes (Moret & Conte, 2000; Bertoz et al., 2021), and with resin oligomeric aromatic hydrocarbons (ROAH) (Updated EN 16995:2017). Another clarification to make concerns MOSH, which do not comprise hydrocarbons naturally present in food matrices, e.i. endogenous *n*-alkanes from *n*-C₂₁ to *n*-C₃₅, (with the prevalence of odd terms) and terpene hydrocarbons (Srbinovska et al., 2020b), as well as resin oligomeric saturated hydrocarbons (ROSH), poly- α -olefins

(PAO), and oligomers consisting of saturated hydrocarbons from synthetic polyolefins, known as polyolefin oligomeric saturated hydrocarbons (POSH) (Biedermann-Brem et al., 2012; Biedermann & Grob, 2015; Updated EN 16995:2017).

2.2 Toxicological assessment

The toxicity of mineral oils is controversial, and although studied for years, no firm conclusions have been reached so far, thus further investigations are underway. Indeed, the latest official evaluation is dated back in 2012, when the European Food Safety Authority (EFSA) published its opinion (EFSA, 2012a), but an updated version is expected by the beginning of 2023.

The main problem for MOH evaluation is related to the lack of data on accumulation and exposure, which is also a consequence of the nature of these contaminants. Thousands of variable complex mixtures consisting of thousands of different compounds are impossible to evaluate individually using a “compound-by-compound” approach. Thus, for toxicological purposes, these substances are preferentially divided into groups according to common characteristics. In general terms, based on the most current knowledge, the danger to human health deriving from mineral oils depends fundamentally on the distribution of the molecular weights of the hydrocarbons involved and on the refining degree, which means presence/absence of aromatic hydrocarbons.

Starting from the latter, toxicity is mainly linked to their carcinogenic, genotoxic and mutagenic potential (IARC, 1987; Henry, 1998), which however appears to be mainly referred to MOAH showing polycyclic structures with 3-7 rings, not or slightly alkylated, that actually seem hardly to be detected in food (Grob, 2018a). Some highly alkylated ones act as tumour promoters, but are not carcinogens themselves, as bulky alkylations seem to prevent their direct intercalation into deoxyribonucleic acid (DNA). Simpler MOAH, i.e. mono- and di-aromatics, are more likely to be found in food and seem to show little toxicological relevance, even though some of them, such as naphthalene, are carcinogenic being cytotoxic and promoters of proliferative regeneration (EFSA, 2012a). Aromatic hydrocarbons appear to be well absorbed and rapidly distributed throughout all the body, but no trace of them is present in human tissues as they are extensively metabolized and not bioaccumulated (EFSA, 2012a; Barp et al., 2014).

Conclusions about MOSH toxicity are equally uncertain, but their tendency to accumulate in tissues throughout lifetime, as exposure data suggest, is clear. Several studies demonstrated the presence of MOSH in human milk and tissues, such as adipose tissue, liver and mesenteric lymph nodes (MLN) (Noti et al., 2003; Concini et al., 2008; Concini

et al., 2011; Barp et al. 2014), drawing the conclusion that they are by far the most present contaminants within the human body. Accumulation in human tissues concerns hydrocarbons having 15 to 45 carbon atoms, even though the critical range is slightly narrower and goes from 20 to 40 (Barp et al., 2017b), covering the distribution of a wide range of mineral oil products (Figure 1.19).

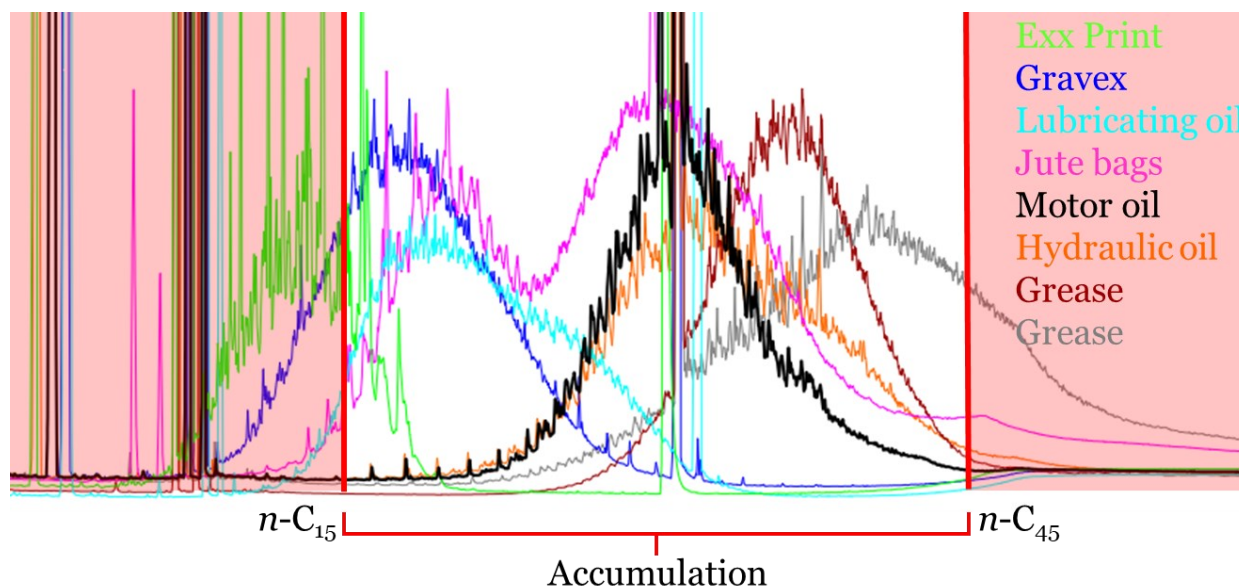


Figure 1.19. Range of accumulation of MOSH in human body and distribution of molecular weights of some types of mineral oil products.

MOSH composition found in human lymph nodes and adipose tissue was similar, with a maximum presence of C_{23-24} hydrocarbons, while was slightly shifted to higher molecular weights (C_{25-28}) for liver and spleen. The degree of accumulation appeared to be inversely proportional to the chain length of the hydrocarbon involved, and to be greater for branched and cyclic hydrocarbons (Low et al., 1992; Scotter et al., 2003; Barp et al., 2017a, b; Cravedi et al., 2017). As can be understood, accumulation therefore concerns only certain hydrocarbons. Indeed, from a deeper characterization, MOSH composition in human bodies resulted different from that of MOH human are exposed to, with differences also in relation to the body parts under examination (Biedermann et al., 2015). This is probably the result of selective uptake, elimination by evaporation, metabolic degradation, or even non-absorption of certain classes of hydrocarbons. Moreover, a significant proportion of MOSH that humans ingest is already pre-metabolized by plants and animals, and thus the contamination range is the result of an upstream selection which is consequence of the food chain (Grob, 2018b). The result of MOSH accumulation is the increase of organ weight, mainly affecting MLN, spleen and liver, which seems to be a permanent condition. To this aspect has been given little consideration, as the main

criticality linked to MOSH seemed to be the formation of granulomas in liver and spleen, generating inflammatory response, and histiocytosis in MLN, highlighted in Fisher F344 rats (F344) (Nash et al., 1996; Shoda et al., 1997). Granuloma formation was considered the reference negative effect on which to base the risk assessment (EFSA, 2012a), even if this is now questioned as weight increase seems to be more critical (Grob, 2018a). It is now hypothesized that granuloma formation was instead related to the ingestion of *n*-alkanes rather than mineral oils, and that this was a response specific to F344. In fact, Barp et al. (2017b) found that regardless of the molecular weight of MOSH administered to F344, the presence of granulomas was not detected as long as *n*-alkanes over *n*-C₂₅ were not present. F344 seemed able to eliminate them, but to strongly accumulate those above this threshold up to *n*-C₃₅, due to crystallization. This kind of effect was not also attributable to humans. Only little concentrations of *n*-alkanes were found in human liver and spleen (Barp et al., 2014; Biedermann et al., 2015), and unexpectedly also in other rat species (Griffis et al., 2010), suggesting that they were either not adsorbed or efficiently metabolized. Moreover, the prevalence of liver granulomas in the population is low, and they are not even associated with inflammation, further questioning the validity of considering them as the relevant critical effect for MOSH toxicity on which to base future Acceptable Daily Intake (ADI) thresholds (Grob, 2018a). Finally, also about accumulation, animal tests appeared to be unreliable. In particular, the latter lasted for far less time than human lives, thus comparison between chronic (humans) and subchronic (animals) exposure could not be reliable. Moreover, weight of these animals was very different from that of humans. Not by chance, discrepancies were found between recent data, about concentrations and distribution of MOSH in the different rats tissues, compared to previous results in humans (Barp et al., 2017a, b; Cravedi et al., 2017). For this reason, transfer of knowledge from rats to humans remains questionable and more in-depth investigations will be needed.

2.3 Acceptable Daily Intake

The accumulation on organs such as spleen, liver and lymph nodes, with related histological and haematological abnormalities, was already highlighted in 1989, by the European Scientific Committee on Food (SCF) (SCF, 1989). Based on studies carried out on Fisher 344 rats, a temporary ADI of 0.005 mg/kg body weight (bw) was set for oleum-treated MOH and 0-0.05 mg/kg bw for hydrogenated products, even though reference to the need for better assessments to be carried out in short-term (by the end of 1990), as well as long-term studies (within 5 years from the publication of this opinion), was made.

These further studies were carried out considering mineral oil products used in food at that time, meaning products ranging from low viscosity oils to waxes. Among others, the main consequences of their ingestion evaluated on F344, as previously described, were granulomas in liver and histiocytosis in lymph nodes. From all these evidences, a Group ADI of 0-20 mg/kg of body weight (bw) was established for highly refined waxes and synthetic hydrocarbon oils used as additives in food and food packaging materials, having average molecular weight not less than 500 Da (corresponding to n -C₃₅), maximum of 5% components below n -C₂₅ and minimum viscosity at 100 °C of 11 mm²/s, and a temporary Group ADI (due to the need of further evaluations) of 0-4 mg/kg bw for white paraffinic oils with medium and high viscosity, with average molecular weight not less than 480 Da (corresponding to n -C₃₄), minimum carbon number as above and minimum viscosity at 100 °C of 8.5 mm²/s (SCF, 1995). These criteria were established to help characterization and classification of the different types of mineral oils, given the high heterogeneity of products. On the other hand, the same year and based on the same data, the Joint FAO/WHO (Food and Agriculture Organization of the United Nations/World Health Organization) Expert Committee on Food Additives (JEFCA) established a different classification of mineral oils distinguishing waxes with high, intermediate and low-melting-point, as well as paraffin oils with high and medium/low viscosity, with the latter further classified in classes I, II and III, always according to the average molecular weight, carbon number at 5% distillation point and the viscosity at 100°C. Readers are referred to Table 1.2 for a better understanding of the classification.

Table 1.2. Classification of mineral oils [adapted from JEFCA (1995)].

Classification	Viscosity at 100 °C (mm²/s)	Average molecular mass (Da)	Carbon number at 5% distillation point
Microcrystalline wax (high melting point)	≥ 11	≥ 500	≥ 25
Microcrystalline wax (low melting point)	3.3	380	22
Mineral oil (high viscosity)	> 11	≥ 500	≥ 28
Mineral oil class I (medium/low viscosity)	8.5 - 11	480 - 500	≥ 25
Mineral oil class II (medium/low viscosity)	7.0 - 8.5	400 - 480	≥ 22
Mineral oil class III (medium/low viscosity)	3.0 - 7.0	300 - 400	≥ 17

The resulting ADI were a Group ADI of 0-20 mg/kg bw for microcrystalline waxes (high melting point) and high viscosity mineral oils, a temporary ADI of 0-10 mg/kg bw for class I and a temporary Group ADI of 0-0.01 mg/kg bw for class II and III mineral paraffins. No ADI was instead set for low melting point waxes (JECFA, 1995). In 2002 further studies were available, but JECFA opinion only reconfirmed the ADI values set in the previous evaluation (JEFCFA, 2002). In 2006 EFSA, due to lack of toxicity data, set a restriction of 0.05 mg/kg food for waxes, paraffinic, refined, derived from petroleum-based or synthetic hydrocarbon feedstock, meeting the specifications of an average molecular weight not less than 350 Da (about C₃₂), a minimum viscosity at 100 °C of 2.5 mm²/s and a content of not more than 40% *w/w* of hydrocarbons with a carbon number less than 25 (EFSA, 2006), and in 2009 established an ADI value of 12 mg/kg bw for high viscosity white mineral oils used as food additives, with average molecular weight over 500 Da (carbon chain length C₂₂₋₆₀), minimum viscosity at 100 °C of 11 mm²/s and carbon number more than 25 at 5% distillation point (EFSA, 2009a). This ADI was based on a No Observed Adverse Effect Level (NOAEL) of 1200 mg/kg bw per day and replaced the value of 0-4 mg/kg bw set by SCF in 1995. Contextually, a statement was made regarding the application of this ADI also to medium/low viscosity mineral oils of class I. In fact, this ADI was later extended also to this category (EFSA, 2013). Finally, in 2012 EFSA published an opinion about MOH in food, and about MOSH stated that they can be accumulated in human tissues and form microgranulomas, but due to insufficient data on accumulation no new ADI could be specified, and those set by SCF in 1989 and JEFCFA in 2002 were confirmed as valid. For MOAH, on the other hand, the Margin of Exposure (MOE) for absorption through food was not evaluable, as no safe dose can be determined for genotoxic compounds, so the need for their absence from food was expressed (EFSA, 2012a). After this opinion JECFA, based on a re-evaluation, withdrew the temporary Group ADI of 0.01 mg/kg bw for class II and III mineral oils established in 2002, since data supporting their maintenance were not available, and modified that of class I (JECFA, 2012; JEFCFA, 2013).

2.4 Legislation

The presence of MOH contaminants in foodstuffs is still not regulated with a legal limit. About intentional use, some requirements regard the use of white mineral oils, meaning oils refined for the removal of the MOAH fraction, as additives in plastic food contact materials (Regulation (EU) No 10/2011), in food (Regulation (EC) No 1333/2008; Regulation (EU) No 231/2012) or in pesticides (Regulation (EC) No 1107/2009;

Regulation (EU) No 540/2011; Regulation (EU) No 2015/1608). Their use is allowed with limitations to their minimum molecular weight, minimum number of carbon atoms and viscosity.

Regarding accidental contamination, the only limit ever entered into force was that imposed by the European Commission (EC) in 2009, after EFSA risk assessment, following the importation into the European Union of thousands of tons of Ukrainian sunflower oil heavily contaminated with mineral oils (levels up to 2000 mg/kg), defined in the measure of 50 mg/kg by Regulation (EC) No 1151/2009. This limit was based on an estimate of the average daily consumption of 60 g of vegetable oil, at 2000 mg/kg of mineral paraffins, by 60 kg consumers, as well as on the distribution of molecular weights of the hydrocarbons making up the fractions, which based on the available toxicological evidences from the Joint FAO/WHO Expert Committee on Food Additives (JEFCA, 2002), reported above for mineral oil class I, were considered not of concern for human health (EFSA, 2008). However, this evaluation did not take into account the presence of the much more toxic MOAH up to 1800 mg/kg, as later verified (Biedermann and Grob, 2009a). This limit was subsequently withdrawn in 2014 as non-compliant samples were not found in those years (Regulation (EU) No 853/2014). In the following years, except in rare cases, various attempts at legislation concerned foods in general, without specific references to vegetable oils.

In 2011, based on further toxicological studies, the German Federal Institute for Risk Assessment (BfR) recommended a limit of 12 mg/kg of food for MOSH with hydrocarbons from n -C₁₀ to n -C₁₆, justifying it with the non-accumulation of this fraction in tissues, while a limit of 4 mg/kg was specified for hydrocarbons distributed in the adjacent fraction, from n -C₁₇ to n -C₂₀ (BfR, 2011).

Taking into account these recommendations, some attempted legislation was issued by European countries, which however just ended up in draft ordinances never entered into force, hence no limits have been imposed to date. An example are the draft ordinances published by the German Ministry for Nutrition, Agriculture and Consumer Protection (BMEL). In the I ordinance of 2011, specific migration limits for mineral oils from packaging made up of recycled fibres in food of 0.6 mg/kg for MOSH and of 0.15 mg/kg for MOAH, both from n -C₁₀ to n -C₂₅ were proposed, but never applied. In the following ordinance of 2013, no MOAH migration (for hydrocarbons made up of 10 to 25 carbon atoms) was considered acceptable (MOAH < 0.15 mg/kg food). In the III ordinance of 2014 new limits were set related to packaging and food. For the latter, food could be placed on the market if the contamination found after migration from packaging made of recycled

cardboard was below of 2 mg/kg for MOSH $n\text{-C}_{20-35}$ and 0.5 mg/kg for MOAH $n\text{-C}_{16-35}$ (Purcaro et al., 2016b). Finally, in 2017 BMEL removed specific migration limit for MOSH, while maintaining that for MOAH (BMEL, 2017), which was also further reconfirmed in 2020 (BMEL, 2020). This limit of 0.5 mg/kg for MOAH, which often returned in the various legislative attempts, although it had no legal value, became a reference for the large-scale retail trade of food products, which in turn required the food producers to respect it.

Meanwhile, the Scientific Committee of the Federal Agency for the Safety of the Food Chain (AFSCA) published an advice on action thresholds for various food types, proposing a level of 100 mg/kg for MOSH $n\text{-C}_{16-35}$ in animal and vegetable fats and oils and, following the approach by BMEL, of 0.5 mg/kg for MOAH in the same range of molecular weights. An action threshold corresponds to “the maximum content of a contaminant that a food can contain when it is consumed in large quantities, without exceeding the acceptable daily intake” (AFSCA, 2017). In 2019, a slightly different approach, based on the use of benchmark levels, was proposed by the representatives of the Consumer Protection Consortium of the Federal States (LAV) and Food Federation Germany (BLL), whose food list was also expanded by one food category a year later. Benchmark levels are levels that “can be expected with high statistical probability as the result of a good technical manufacturing practice”. According to that, in both publications they were set at 13 mg/kg for MOSH for vegetable oils, while MOAH should be not present at concentration higher than the limit of quantification (LOQ). Such LOQ corresponded to the LOQ_{max} reported for this food category by the guidance of the Joint Research Centre (JRC) (Bratinova & Hoekstra, 2019), but referred to the total hump (LAV & BLL, 2020). In 2021 and 2022, new product categories were added to the list, but without modifications to MOSH and MOAH benchmark levels for vegetable oils (LAV & BLL, 2021, 2022).

Finally, as published in the summary report of early 2022, EU Member States in a meeting of the Standing Committee on Plants, Animals, Food and Feed (ScoPAFF) agreed on a common approach of a limit of 2 mg/kg for MOAH (again equal to the LOQ established by JRC) for fats and oils, with immediate effect. Even though this limit is not yet legally binding *stricto sensu*, and it is left up to the Member States to enforce the change, the food business operators (FBO) are required to withdraw or recall the food products from the market if they are at or above the limit, according to articles 14 and 19 of Regulation No (EC) 178/2002 concerning the general principles of food safety (European

Commission, 2022). All these documents, with a specific reference to limits related to vegetable oils when present, are summarized in Table 1.3.

Table 1.3. Chronological progression of legislation relating to mineral oils in food.

Year	Authority/document	Proposed limit (mg/kg)
2008	European Commission/Regulation 1151/2009	MOSH <50*
2011	BfR/opinion	MOSH $n\text{-C}_{10-16}$ <12 MOSH $n\text{-C}_{17-20}$ <4
2011	BMEL/I draft ordinance	MOSH $n\text{-C}_{10-25}$ <0.6 MOAH $n\text{-C}_{10-25}$ <0.15
2013	BMEL/II draft ordinance	MOAH <0.15
2014	BMEL/III draft ordinance	MOSH $n\text{-C}_{20-35}$ <2 MOAH $n\text{-C}_{16-35}$ <0.5
2017	BMEL/IV draft ordinance	MOAH <0.5
2017	AFSCA/action threshold	MOSH $n\text{-C}_{26-35}$ <100 MOAH $n\text{-C}_{16-35}$ <0.5
2019	LAV & BLL/benchmark levels	MOSH <13 MOAH <2
2020	LAV & BLL/benchmark levels	MOSH <13 MOAH <2
2020	BMEL/V draft ordinance	MOAH <0.5
2021	LAV & BLL/benchmark levels	MOSH <13 MOAH <2
2022	SCoPAFF (EC)/statement	MOAH <2
2022	LAV & BLL/benchmark levels	MOSH <13 MOAH <2

*The only legal limit that came into force, subsequently withdrawn in 2014.

2.5 Sources of contamination

Mineral oils can contaminate food at any point of the supply chain, from the field to the packaged product. Based on that, the extent of the contamination can depend on the source of contamination, as well as on food composition. Indeed, some food matrices like edible oils and fats are more likely to be contaminated by MOH due to their non-polar nature and hence their chemical affinity for fatty matrices. Not surprisingly, vegetable oils have often proven to be one of the most contaminated foodstuffs (EFSA, 2012a). This is further compounded by their extensive use in people diets, mainly in the Mediterranean area, which significantly contributes to increasing human exposure to these compounds.

The main reason for the ubiquitous presence of these contaminants is the widespread use of petroleum-derived products in a multitude of sectors. Since they cover a wide range of molecular weights (Figure 1.20), their final uses are manifold.

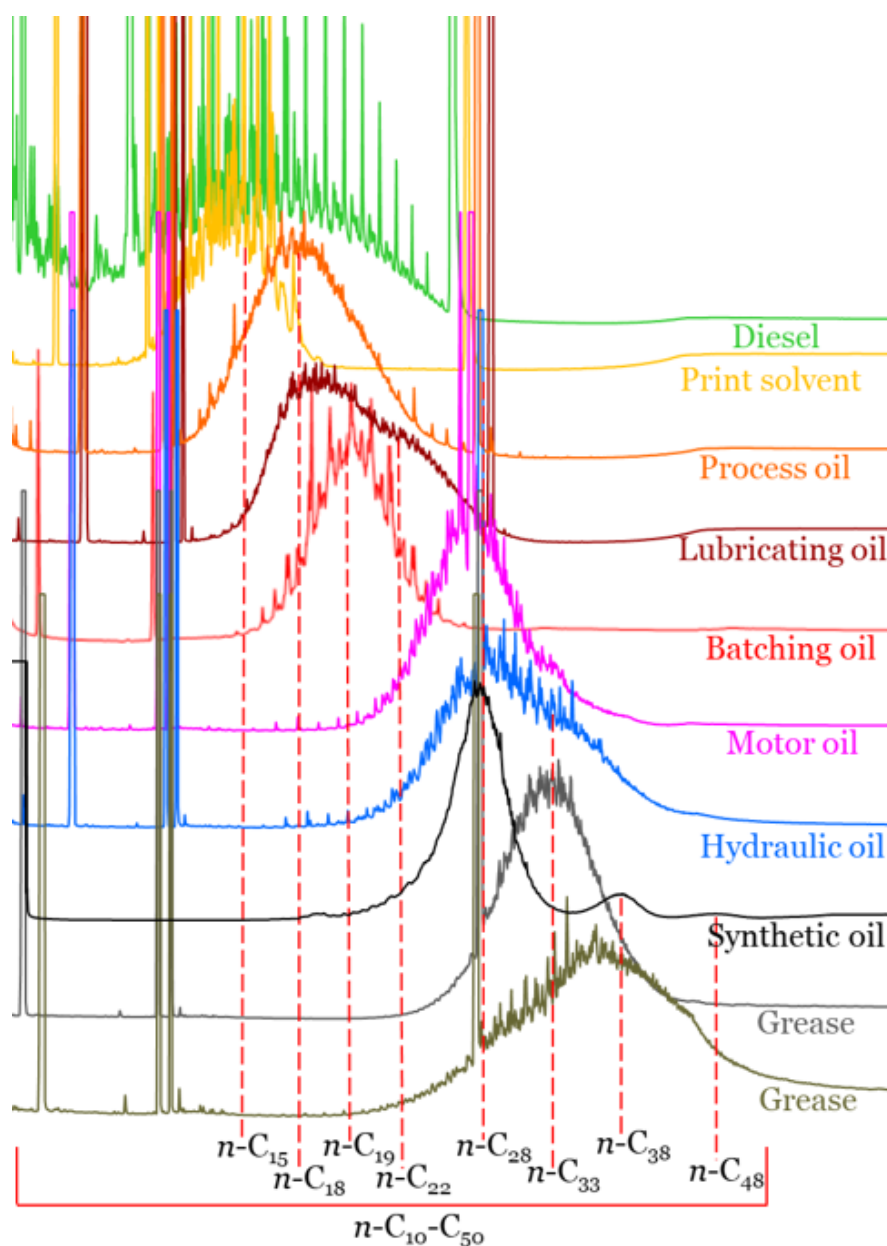


Figure 1.20. Overlay of chromatograms of different mineral oil products highlighting their different profiles and distribution of molecular weights.

Lighter fractions are those of refinery gases ($n\text{-C}_{1-4}$), immediately followed by fuels like gasoline, diesel and heating oils, which generally contain hydrocarbons from $n\text{-C}_8$ to $n\text{-C}_{25}$ and a high proportion of n -alkanes. Within this range fall also paraffin oils which, as already reported, can be used for plant protection purposes. The intermediate ones include lubricating (e.g. motor oils) and hydraulic oils, centered around $n\text{-C}_{23-30}$ and distributed in the range $n\text{-C}_{20-40}$. These, as well as heavier products, are all generally

deparaffinated over $n\text{-C}_{22}$ to avoid crystallization of waxes (Biedermann et al., 2015; Grob, 2018a). Heavier fractions are those of greases, centered around $n\text{-C}_{30-35}$, as well as those found in synthetic oils (e.g. used as fuel additives for certain types of motors or as food-compatible lubricating oils) which range from $n\text{-C}_{25}$ to beyond $n\text{-C}_{45}$. Finally, reaching over $n\text{-C}_{50}$, are those of tar used for asphalt production, derived from crude oil distillation residues (Grob et al., 2001; Neukom et al., 2002; Moret et al., 2009). It is therefore evident that, according to these petroleum products, the sources can be manifold either of voluntary or accidental nature, and for this reason contamination can occur almost in all the different stages of vegetable oils production. However, sources of contamination (detailed in the next paragraphs) have often only been hypothesized (Moret et al., 2009), since not much can be found in the literature about the correlation and the incidence on the final contamination of each single step of food processing, from raw material to the finished product.

2.5.1 Environment

Regarding vegetable oils supply chain, the first possible source of contamination in chronological order is represented by the environment, and in particular air pollution. This is responsible for the background levels found in edible oils. The presence of unburnt engine oil or diesel oil in the air, due to the discharges of the means of transport (Brandenberger et al., 2005), heating oil from domestic or industrial heating systems, discharges from power plants or tar particles released following the wear of the asphalt, are only some of the sources of MOH that determine their deposition on plants. Deposition can take place directly through the gas phase, for the lighter ones, i.e. hydrocarbon chain up to $n\text{-C}_{25}$, or conveyed by the atmospheric particulate matter, to which they are adhered, for heavier fractions. Neukom et al. (2002) highlighted the presence of mineral paraffins in the air, both in city and countryside areas, as well as the correspondence between their composition and that found in soil and crops, and attributable to the sources just reported. Analogously, Grundböck et al. (2010) found 2.4 mg/kg of MOSH in sunflower oil extracted from seeds hand-picked near the city, with a distribution typical for lubricating oils, while four-fold lower levels were found moving away from it. Thus, all the sources listed above seem to be the main contributors to the environmental contamination, which becomes more significant in urban areas. Contamination from air pollution is facilitated by the presence of waxes on the surface of the seeds and fruits, which due to chemical affinity, act as absorbents towards the surrounding environment. Not surprisingly, the contamination is mainly located in the

cuticle or shell of the latter (Moret et al., 2003; Fiorini et al., 2008; Fiselier & Grob, 2009; Gómez-Coca et al. 2016b; Pineda et al., 2017; Grob, 2018b).

In some cases, presence of MOH was also attributed to biogenic mechanisms (Gómez-Coca et al., 2016b; Pineda et al., 2017), while according to other authors the involvement of enzymatic processes seems unlikely (Moret et al., 2003; Grob, 2018b). Thus, considering that the proof of the petrogenic origin of MOH has been ascertained by identifying specific markers, such as steranes and hopanes, formed under geological conditions (Populin et al., 2004; Gagni & Cam, 2007), accumulation during the life of the plant or radical absorption was also hypothesized (Pineda et al., 2017), taking into account the accumulation of these hydrocarbons in the soil and their resistance to degradation (Neukom et al., 2002). This also would explain the constancy of the levels of contamination, found in these last two works cited, in leaves sampled at significant time distance.

Despite this, based on data already present in the literature, the environmental contribution seems to be not very significant, and sometimes MOH are not even detectable. Gharbi et al. (2017) could find no correlation between the position of the olive grove, with respect to possible sources of contamination, and the levels of MOH found. Various olive samples, exposed to different atmospheric conditions, showed similar MOSH profiles. For example, of 27 olive samples manually picked from the trees of Italian olive groves, both near roads with heavy traffic or away from traffic and industrial plants, and extracted with solvent (i.e. MOH are extracted almost quantitatively differently from the physical extraction), none showed detectable MOSH contamination with a LOQ of 1-2 mg/kg (Moret et al., 2003). Similarly, the mean concentrations found in sunflower oil extracted with solvent from 14 seed samples, collected manually from fields and gardens, were 0.4 and 0.7 mg/kg respectively, with a maximum recorded value of 2.5 mg/kg near the city (Fiselier & Grob, 2009; Grundböck et al., 2010). Again, a mean concentration of 2.6 mg/kg was found by Gharbi et al. (2017) in the oils extracted from 9 olive samples collected by hand from the trees. In all these cases, MOAH were either not present (<LOQ) or not considered in the analysis.

2.5.2 Pesticides

For higher contamination associated to olives at tree level, the contribution due to the use of mineral oil-based pesticides can not be excluded, since paraffins showing a distribution between n -C₁₁ and n -C₃₀ are authorized as additives and active substances in plant protection products (Regulation (EC) No 1107/2009; Regulation (EU) No 540/2011;

Regulation (EU) No 2015/1608; Brühl, 2016), whose limits and specifications are not established. Refined paraffines and micro crystalline waxes are used as insecticides for mites, mealybugs, spiders and scale insects, as well as against fungi (Helmy et al., 2012). Besides having acaricidal, insecticidal and fungicidal properties per se, also thanks to the ability to suffocate pests by forming a thin layer impermeable to gases on the crops, they are used as formulation aids in phytosanitary products together with other active compounds, to allow a better vehiculation and persistence of the active principles on the plants. For example, pesticides were hypothesized as an important source of mineral oils in grapeseed oil (Fiorini et al., 2008), but also in olive oils (Nartea, 2017). However, these are food grade mineral oils, also known as white oils, which are refined to remove the more toxic MOAH, differently from the technical grade ones containing them around 15-35% (Biedermann et al., 2009; EFSA, 2012a; Spack et al., 2017; Pirow et al., 2019). For this reason, more worrying are uses outside the law, where the illicit practice of admixing mineral oils with phytosanitary products, always to achieve a better adhesion of the active principles to crops, could lead to the indiscriminate use of non-food grade oils.

2.5.3 Harvesting

Contribution to the presence of mineral oils in the raw material can also be associated with harvesting operations. The increase in production volumes, combined with the need to contain costs, promoted the spread of mechanized cultivation and harvesting systems (Lavee, 2010). These include e.g. tractors, trunk shakers, harvesters, as well as manual instruments equipped with pneumatic, electric or thermal engine for harvesting, pruning and other agronomic practices. Exhaust gases, as well as leaks of lubricants from mechanical parts, engines and hydraulic circuits, can be associated with mineral oil presence in the finished product. For example, sunflower seeds collected at the outlet of a combine harvester reported MOSH contaminations centered on *n*-C₁₇ and *n*-C₂₇, typical of diesel oil and lubricating oil, with an average level of 5.6 mg/kg in the extracted oil, but even reaching 13.7 mg/kg (Grundböck et al., 2010). Nartea (2017) found high levels of MOSH (reaching 69.2 mg/kg) in olive oils, accompanied by MOAH, as the result of contamination occurring during pruning operations using chainsaws at the same time as olive harvest, and evaluated the incidence of the type of machinery used for olive collection as well. A minor impact in terms of MOH contamination was indeed present when electric or vegetable oil-lubricated harvesting machinery were used, confirming the potential criticality of this step.

2.5.4 Transportation

Importance must be given both to containers for the collection and to the subsequent transport of the food product to the following processing step. MOH concentration in sunflower seeds, analyzed before and after delivery to the extraction plant, remained practically constant, demonstrating a negligible impact of transportation (Grundböck et al., 2010). However, the use of containers or wagons which are not properly washed, or which are dedicated to other non-food uses, can lead to a cross contamination ending on raw materials.

Moret et al. (1997) and Grob et al. (1991c, 1992a) found contamination of several hundreds of mg/kg of MOH in rice, cocoa beans, coffee, nuts etc., transported inside jute or sisal bags. Jute and sisal fibers are treated with batching oil, a mineral oil containing 20-30% of MOAH and distributed from $n\text{-C}_{14}$ to $n\text{-C}_{22}$ (Bonvehí & Ventura-Coll, 2014), to soften them and facilitate their weaving. As still used in some countries, this practice resulted in a contribution of contamination also onto olives (Nartea, 2017). The situation has improved over the years, also thanks to the criteria adopted by the International Jute Organization (IJO) in 1998, and subsequent updates (IJO Standard 98/01, 2005), for their manufacture. Some alternatives for fibers spinning using vegetable oils were provided (EFSA, 2004), but the matter is not completely solved and this type of contamination is still found in various foods.

2.5.5 Pre-treatment

For some types of oil products, some preliminary steps to which the raw material is subject before oil extraction can be critical, e.g. sunflower seeds are dried with heated air that is aspirated from areas adjacent to the processing plant, where the presence of trucks and tractors in motion can determine their exhaust gases to end up in the product. In fact, contamination by mineral paraffins with distributions attributable to fuels up to 41 mg/kg have been found in oil from seeds which contained 1.5 mg/kg before this step (Grundböck et al., 2010). Similarly, before being separated and destined to the oil industry, grape seeds, which are one of the by-products of the wine and spirits industry, stay in contact with the marc during fermentation, determining their enrichment by contact with mineral oils initially present in peels and stems. Average MOSH concentrations of 34.3 mg/kg were found in the resulting oils, decreasing to 26.4 mg/kg if any residues of marc were carefully removed from the seeds before extraction, and to 7.2 mg/kg for grape seeds taken from the intact grape (Fiorini et al., 2008). In the olive oil industry, olive pomace

is usually stored for weeks in areas outside the plants before extraction, in direct contact with asphalt and atmospheric agents, and later handled with bulldozers or other machinery. Therefore, exhaust gases, lubricating or hydraulic oils can end up on it, as contaminations centered between $n\text{-C}_{27}$ and $n\text{-C}_{29}$, as well as contamination levels increasing more than ten times during pomace storage, confirmed (Moret et al., 2003, 2009).

2.5.6 Extraction

Another substantial contamination can occur during the extraction process at the oil mill (Fiselier & Grob, 2009) and can be attributed to accidental contact with mineral oil products, like lubricating and hydraulic oils from mechanical parts of machinery where losses are always possible (Moret et al., 2009), and to the use of extraction aids. This last point was investigated by Gómez-Coca et al. in 2016b, which verified the presence of paraffins in talc, used in the measure of 1-3% of olive paste to increase oil extraction yield. Unfortunately, the relatively high limit of quantification (15 mg/kg) did not allow to notice differences directly on olive oil, but the analysis of the talc itself and of pomace oil, derived from olive paste with (49 mg/kg) and without its addition (27 mg/kg), provided confirmation. Also leaking from a malfunctioning press pump determined extra virgin olive oil to be contaminated with technical grade oil (Moret et al., 2003).

In addition to these criticalities, also the extraction method can play a role. In fact, in physically extracted oils, a significant portion of MOH remains adsorbed in the solid structures (exocarp, endocarp, shells) as the oil has a limited extraction power (Moret et al., 2003; Gómez-Coca et al., 2016b; Pineda et al., 2017). On the contrary, if solvent extraction is involved, mineral oil concentrations are 2-10 times higher, as extraction occurs almost quantitatively (Wagner et al., 2001b; Lacoste, 2014; Gharbi et al., 2017). Higher levels of contamination were also reported when a second centrifugation was applied on the pomace (Gómez-Coca et al., 2016b). This happened because of the re-concentration of the residual contamination, present in the entire bulk of solids, into the small volume of oil left. Not surprisingly, contamination in pomace oil, obtained by solvent extraction of the solid olive residue, reaches levels up to hundreds of mg/kg (Moret et al., 2003, 2009, 2010). The residual amount of oil in the pomace stands at 1-2% of the weight of the olives, and the re-concentration effect becomes preponderant, even for relatively clean olives. In fact, in olive pomace oils, background levels are already higher than in extra virgin olive oils, as the oil extracted from fresh pomace reported average MOSH level of 18.3 mg/kg. Similarly, pomace obtained with a pilot plant and

from hand-picked olives, which therefore didn't have contact with the various sources of contamination reported so far, already contained from 20 to 40 mg/kg (Moret et al., 2003; Gómez-Coca et al., 2016b). However, the way of storing and handling the pomace, as described before, its high contact surface, which allows high absorption from the surrounding environment, together with its degradation during relatively long storage, which favors MOH release, result in levels of hundreds of mg/kg (Moret et al., 2010).

2.5.7 Refining

Following the extraction phase, in case they are not directly marketable due to poor quality characteristics (e.g. lampante and pomace olive oil), vegetable oils are subjected to refining. This process, requiring a heat input, may use mineral oils inside serpentines as heat exchange fluids which, in case of leakage, can be responsible of additional contamination. Heat is also used in vegetable oil supply chains to bring back to their liquid state masses of oil that condense at ambient temperature, while they are kept inside storage or transport tanks (Moret et al., 2009).

However, refining process is not always responsible for a contribution to the contamination, but it can also lead to its reduction. Indeed, this process includes a deodorization step, which can determine a more or less marked decrease in MOH concentrations, depending on the composition of the contamination, where the more volatile components (generally hydrocarbons up to n -C₂₅) are stripped away due to volatility during vacuum steam distillation. This behaviour was verified in lampante olive oil by Moret et al. (2003). However, depending on the type of oil and deodorization conditions, hydrocarbons can be further removed up to n -C₃₀ (Fiorini et al., 2008). In fact, the latter registered an average decrease in MOSH content from 120 to 90 mg/kg during the refining process of grape seed oil. Wagner et al. (2001b) highlighted a decrease in contamination from 55 to 14 mg/kg in peanut oil, involving the removal of paraffins up to n -C₂₃₋₂₅ and, similarly, reductions up to 75% were witnessed for hydrocarbons $\leq n$ -C₂₄ in cocoa butter and coconut oil by Stauff et al. (2020), with the incidence of removal decreasing moving towards n -C₃₅. As a confirmation, high levels of MOH up to slightly beyond n -C₃₀, and with a profile often matching with that of the mineral oil fraction removed from vegetable oils, was found in the relative steam distillation condensates (Wagner et al., 2001b; Stauff et al., 2020).

2.5.8 Storage and transportation

Also storage or transportation of edible oils from the extraction plant to the refining plant, or to the bottling plant, can be critical points of the supply chain. Moret et al. (2003) compared contamination present in lampante oil sampled at the extraction plant and subsequently transported to the refining plant, finding an average level of 18 mg/kg of MOSH into the latter when, in the same oil before this step, MOH were not detectable. This happens for example when tank trucks or tankers, used for the transport of edible oils, are previously used for the transport of technical grade mineral oils or fuels, as well as of different edible oils having different contaminations levels. Analogously, this can occur pumping various edible oils through common valves and pipelines.

Moh et al. (2001) reported that up to 85,000 metric tons of crude palm oil shipped to Europe from Indonesia were contaminated with diesel oil. Although the actual cause remained uncertain, it was speculated that the contamination could have occurred during storage and/or transportation in tanks previously used to transport this mineral oil product. Since it is difficult to completely empty and properly clean these tanks between transports, this practice should be avoided. Regarding this problem, EFSA has adopted several scientific opinions on the evaluation of the substances on their acceptability as previous cargoes for edible fats and oils, which have been consolidated in Commission Regulation (EU) No 579/2014, as regards the transport of liquid oils and fats by sea. Due to insufficient information on their toxicity and low exposure through this way, white mineral oils and paraffin waxes would still be provisionally accepted for previous cargo, (EFSA, 2009b; EFSA, 2011, 2012b, 2012c; Regulation (EU) No 579/2014). However, FEDIOL (the Federation representing the European Vegetable Oil and Proteinmeal Industry) removed also paraffin waxes and white mineral oil from its acceptability list, and indicated specific code of practice for edible oil transportation (FEDIOL, 2014, 2018).

2.5.9 Fraudulent admixture

References to MOH contamination occurring in this way are fortunately rare to find in the literature. Nevertheless, according to Biedermann & Grob (2009a), an example of fraudulent admixture involved huge amounts of Ukrainian sunflower oil in 2008, found to be contaminated with concentrations of MOSH often above 1000 mg/kg (EFSA, 2008), which later proved to actually contain also MOAH (even up to 1800 mg/kg). This sunflower oil was assumed to be added with mineral oils as the result of a fraud. Other frauds can be the results of the blending of quality oils (EVOOs, VOOs) with cheaper, but more contaminated ones, like e.g. pomace oil (Moret et al., 2010).

2.5.10 Packaging

Finally, the last phase of the chain from which contamination can originate is the bottling, and therefore migration from packaging. Olive oil is generally packaged in glass bottles, which are generally unaffected by mineral oil presence, but plastic and metal packaging (aluminium or tin cans) are also quite common, especially outside Italy. Oil contained in metal containers already resulted in MOH contamination, even around 100 mg/kg (Grob et al., 1997). In fact, white mineral oils are used in can forming process, to protect the metal surface from staining and to lubricate the molds where the metal container body is formed. MOH can also become part of the composition of the plastic materials used in contact with food (Regulation (EU) No 10/2011), for which limitations on the composition and generic migration limits are defined, but this does not exclude they could be a possible source. Mineral waxes or mineral oils can be used to treat bottle caps (Moret et al., 2009; Brühl, 2016), becoming a critical point also for the “practically inert” glass packaging. Finally, migration from plastic materials can also include POSH, which are eluted together with MOSH in high performance liquid chromatography (HPLC) coupled to gas chromatography (GC) equipped with flame ionization detection (FID), and can be exchanged for them in the absence of confirmation methods (Biedermann-Brem et al., 2012; Biedermann & Grob, 2015; Gharbi et al., 2017).

2.6 Occurrence of MOH in vegetable oils

Occurrence data related to MOH in olive oils found in the literature are shown in Table 1.4. Extra virgin olive oils and olive oils generally reported fairly aligned levels of contamination, on average around 10-15 mg/kg and 2-3 mg/kg of MOSH and MOAH respectively. Pomace oil was significantly more contaminated, even with several hundred of mg/kg of MOSH, along with the related MOAH. Data reported are not many, and do not always agree with each other, as evidenced also from the wide range of values reported. This is probably due to different sources of contamination. However, it must be emphasized that data from different time periods may be difficult to compare, due to the different sensitivity of the analytical methods. Since they have been improved over the years, now it is possible to evaluate contaminations that a few years ago would have been considered even absent, determining inconsistency in results. Despite this, uncertainty also derives from the approach used to express the analytical data (e.g. lower or upper bound) which, especially for quite high LOQ, can significantly influence the results. Finally, some data presented were obtained with manual off-line methods, not allowing

MOAH evaluation, translating into a reduced amount of information about the presence of aromatic hydrocarbons, which from a toxicological point of view are instead those of greatest interest. Nevertheless, it has to be considered that in the last 10 years attention to the mineral oil topic has increased, and this might have led to the implementation of minimization strategies, with the consequent general decrease in the average levels of contamination.

Table 1.4. Occurrence data relating to the presence of mineral oils in vegetable oils from various works in the literature.

Matrix	N. of samples	Analytes	Analytical determination	LOQ	MOSH mg/kg (min-max; mean)	MOAH mg/kg (min-max; mean)	References
EVOO (mill)	12	MOSH	Direct injection LC-GC-FID	1	<LOQ	-	Moret et al., 2003
EVOO	10	MOSH	Direct injection LC-GC-FID	1	<LOQ	-	Moret et al., 2003
EVOO	73	MOSH	Direct injection LC-GC-FID	1	<LOQ-120.0; 4.0	-	Moret et al., 2010
EVOO	4	MOSH	Direct injection LC-GC-FID	2	7.6-19.5; 13.0	-	Tranchida et al., 2011b
EVOO	1	MOSH	Direct injection LC-GC-FID	0.7	<LOQ	-	Purcaro et al., 2013c
EVOO	6	MOSH/MOAH	Direct injection LC-GC-FID	0.4	4.0-21.8; 12.9	<LOQ	Zoccali et al., 2016
EVOO	559	MOSH/MOAH	Alox, epoxidation, purification SPE-GC-FID	1	<LOQ-85.5; 14.4 (<i>n</i> -C ₁₀₋₃₅)	<LOQ-16.5; 2.1 (<i>n</i> -C ₁₀₋₃₅)	Luisi, 2016
EVOO	40	MOSH/MOAH	Epoxidation, LC-GC-FID	2	<LOQ-46.0; 8.0	<LOQ	Moret, 2016
EVOO	5	MOSH/MOAH	Epoxidation, LC-GC-FID	2	10.3-38.0; 19.1	<LOQ	Gharbi et al., 2017
EVOO	6	MOSH	SPE-LVI-GC-FID	2.5	3.6-30.3; 11.4	-	Liu et al., 2017
EVOO	7	MOSH	SPE-GC-FID	2.5	<LOQ-2.7; 0.4	-	Li et al., 2017
EVOO	2284	MOSH/MOAH	Alox, epoxidation, purification SPE-GC-FID	1	<LOQ-193.8; 10.3 (<i>n</i> -C ₁₀₋₃₅)	<LOQ-30.9; 2.7 (<i>n</i> -C ₁₀₋₃₅)	Luisi, 2019
EVOO	22	MOSH	Direct injection LC-GC-FID	1.3	<LOQ	-	Zoccali, 2020
EVOO	5	MOSH/MOAH	Direct injection LC-GC-FID	2	<LOQ	<LOQ	Zoccali, 2021
EVOO	7	MOSH/MOAH	Epoxidation, SPE-GC-FID	0.5	<LOQ	<LOQ	Ruiz et al., 2021
EVOO	1	MOSH/MOAH	Epoxidation, LC-GC-FID	1	14.9	2.1	Nestola, 2022
LOO	6	MOSH	Direct injection LC-GC-FID	1	<LOQ	-	Moret et al., 2003

Table 1.4. *Continued.*

Matrix	N. of samples	Analytes	Analytical determination	LOQ	MOSH mg/kg (min-max; mean)	MOAH mg/kg (min-max; mean)	References
OO	13	MOSH	Direct injection LC-GC-FID	1	6.0-30.0; 14.0	-	Moret et al., 2003
OO	1	MOSH/MOAH	Alox, enrichment, epoxidation, LC-GC-FID	1	21.0	4.0	Biedermann et al., 2009
OO	4	MOSH	Direct injection LC-GC-FID	2	17.7-159.4; 64.0	-	Tranchida et al., 2011b
OO	2	MOSH/MOAH	Direct injection LC-GC-FID	0.4	11.5-205.6; 108.6	<LOQ-8.0; 4.0	Zoccali et al., 2016
OO	16	MOSH	Epoxidation, LC-GC-FID	2	18.0	-	Moret, 2016
OO	4	MOSH/MOAH	Alox, epoxidation, LC-GC-FID	0.5	min-9.1; 6.5	min-1.3; 1.1	Van Heyst et al., 2018
OO	97	MOSH/MOAH	Alox, epoxidation, purification SPE-GC-FID	1	3.7-191.6; 16.2 (<i>n</i> -C ₁₀₋₃₅)	<LOQ-28.6; 2.3 (<i>n</i> -C ₁₀₋₃₅)	Luisi, 2019
OO	2	MOSH/MOAH	Direct injection LC-GC-FID	2	<LOQ	<LOQ	Zoccali, 2021
OO	7	MOSH/MOAH	Epoxidation, SPE-GC-FID	0.5	1.1-24.2; 8.2	<LOQ-12.9; 3.5	Ruiz et al., 2021
COPO	3	MOSH	Bromination, LC-GC-FID	20	100.0-300.0; 230.0	-	Moret et al., 2003
OPO	7	MOSH	Bromination, LC-GC-FID	20	121.0-250.0; 145.0	-	Moret et al., 2003
OPO	1	MOSH/MOAH	Alox, enrichment, epoxidation LC-GC-FID	1	320.0	55.0	Biedermann et al., 2009
OPO	2	MOSH	Direct injection LC (Alox)-GC-FID	1	50.0-160.0; 105.0	-	Fiselier et al., 2009b
OPO	1	MOSH	Direct injection LC-GC-FID	2	180.6	-	Tranchida et al., 2011b

Table 1.4. Continued.

Matrix	N. of samples	Analytes	Analytical determination	LOQ	MOSH mg/kg (min-max; mean)	MOAH mg/kg (min-max; mean)	References
OPO	2	MOSH/MOAH	Direct injection LC-GC-FID	0.4	229.8-444.8; 337.3	32.1-66.1; 49.1	Zoccali et al., 2016
OPO	11	MOSH	Epoxidation, LC-GC-FID	2	174.0	-	Moret, 2016
COPO	77	MOSH	SPE-GC-FID	15	62.0-967.0	-	Gómez-Coca et al., 2016b
OPO	47	MOSH	SPE-GC-FID	15	257.0-433.0	-	Gómez-Coca et al., 2016b
OPO	5	MOSH/MOAH	Epoxidation, SPE-GC-FID	0.5	22.4-79.2; 51.0	7.7-22.4; 17.9	Ruiz et al., 2021

n.d. not defined; - not available

2.7 Analytical methods

As for any analyte, the analytical method is the set of those procedures that allow, starting from a sample usually taken from a larger set of elements, to obtain a final result that is as faithful and representative as possible of the latter. Among these procedures, sample preparation is perhaps the most complex, as it is aimed at extracting the analytes of interest from the matrix in which they are found, preferentially quantitatively, and at eliminating or mitigating any interference. The ultimate goal is to selectively concentrate the analyte under investigation in order to achieve the greatest sensitivity obtainable for the purpose, and the greatest reliability of the results. This is the most important phase of the whole analytical process, which requires the greatest manipulation by the analyst, and for this reason it is the one for which data may be subjected to a higher variability, especially when dealing with specific matrix/analyte combinations.

In this regard, vegetable oils are one of the most complex matrices to deal with in the analysis of mineral oils. The presence of interferents, i.e. compounds naturally present in the matrix and eluting with the compounds of interest, together with the need to reach lower and lower limits of quantification, require an adequate sample preparation. As just highlighted, sample preparation is a major aspect of the entire analytical process, which consists of several steps. Indeed, the latter also includes the final steps of the analytical determination and the interpretation and elaboration of the results, which are equally important, especially in relation to the analysis of mineral oils, as discussed below. The scheme of a generic analytical process is shown by means of a flowchart in Figure 1.21.

Main aspects of sample preparation and analytical techniques related to mineral oils will be discussed below, focusing mainly on the most widespread applications, with a particular reference to vegetable oils and, when available, the official reference methods specific for this matrix. For further information, it is possible to refer to some published reviews (Biedermann & Grob, 2012a, b; Moret et al., 2012; Purcaro et al., 2012, 2016a; Brühl, 2016; Biedermann et al., 2017b; Weber et al., 2018).

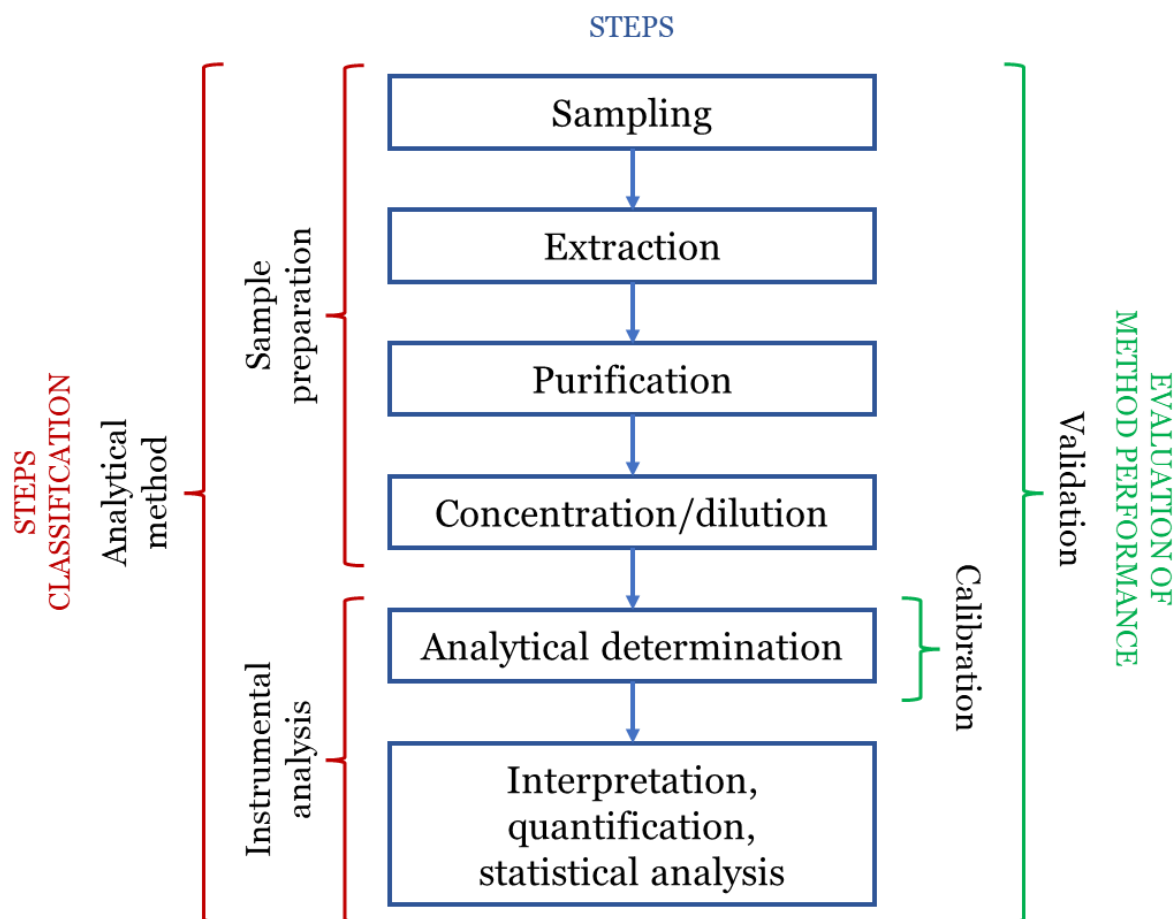


Figure 1.21. General flow chart of the steps that make up an analytical method.

2.7.1 Sampling

Sampling is the first stage of the entire analytical protocol. Its importance lies in the assumption that an error at this point is not amendable afterwards, leading to incorrect results. This is the consequence of the fact that the sample considered for the analysis consists only of a small aliquot of a larger set of elements, and it is therefore important that it could assure the representativeness of the overall mass from which it was taken. After that, specific methods for sample handling and storage may be required in order to avoid distorted results.

In 2017, the European Commission published the Recommendation (EU) No 2017/84 on the monitoring of mineral oil hydrocarbons in food and in materials and articles intended to come into contact with food, without providing information about the sampling procedures, but referring to the Regulation (EC) No 333/2007 for such indications. Regulation 333/2007 lays down the sampling methods for the analysis of trace elements and processing contaminants in foodstuff, with particular reference to lead, cadmium, mercury, inorganic tin, inorganic arsenic, 3-MCPD and polycyclic aromatic

hydrocarbons. Nevertheless, its requirements, also given the chemical similarity with PAH, can be applied also for mineral oils. Also in the official method EN 16995:2017 some indications were provided in this regard, in particular referring to the ISO 5555:2001 standard, about the sampling of animal and vegetable fats and oils, which was reviewed and reconfirmed in 2017, as well as to the standard methods from the German Society for Fat Science (DGF), namely DGF-C-I 1 (08) to DGF-C-I 5 (08). Other specific requirements, related to sampling in the context of the analysis of MOH (e.g. material of samples containers, sample identification, sample manipulation etc.), were outlined in the guidelines published by the JRC (Batinova & Hoekstra, 2019). These guidelines arose precisely from the need to standardize, in addition to analysis and data reporting, the sampling methodologies in the context of mineral oils, to enable Member States to provide EFSA with mineral oil monitoring data as specified in the Recommendation (EU) No 2017/84. Nevertheless, they can also be applied outside the specific context.

2.7.2 Extraction

Contamination by MOH can have different sources and can be found in a wide range of foodstuffs and materials. Food matrices are among the most complex and differentiated and consequently the extraction procedures of contaminants are matrix-specific and can vary from one sample to another. As a consequence, these procedures need to be chosen wisely to assure a quantitative recovery of mineral oils from the matrix. Therefore, parameters like e.g. type of solvent, solvent volumes, type of contact, contact times etc. become fundamental. About solvents, given their apolar character, these contaminants need to be extracted with non-polar organic solvents, commonly *n*-hexane (Hex). Extraction is strongly matrix dependent.

For example, for liquid samples, i.e. water, wine etc., a liquid-liquid extraction (LLE) is often the best and fastest alternative, since migration of these compounds towards a more chemically similar phase is favored. Extraction is also rapid when evaluating superficial contamination in dry foods, or in certain food packaging, where only contact with *n*-hexane is required (Vollmer et al., 2011). On the contrary, for the evaluation of the internal contamination of solid matrices, matrices insoluble in organic solvents, or containing water, the extraction step may consist of several passages, having the purpose of allowing the permeation of the solvent and the intimate contact with analytes. Indeed, in wet solid matrices, water act as a barrier to the extraction of mineral oils, creating a layer that does not allow the permeation of the solvent. In this case, sample needs to be dried before extraction (Biedermann & Grob, 2012a) or a two steps extraction, first with

ethanol (EtOH) and then with *n*-hexane is needed. The same, possibly preceded by soaking in hot water, is required for quantitative extraction from some dry foods, i.e. semolina pasta, bread, etc. (Purcaro et al., 2016a). The permanence in contact with ethanol and *n*-hexane allows the swelling of the fibers and a better release of MOH from paper and board (Lorenzini et al., 2010). Even more efficient extractions on these matrices could also be obtained using specific equipments exploiting high temperature under pressure (to maintain liquid the solvent), as for pressurized liquid extraction (PLE) (Moret et al., 2013, 2014b) and microwave assisted extraction (MAE) (Purcaro et al., 2009; Moret et al., 2019).

On the other hand, vegetable oils would not require any extraction step defined as such, since they are completely soluble in non-polar solvents and can be directly dissolved and injected into the instrument for the analysis. Indeed, the separation (or in better words “extraction”) of MOH from oil is obtained simply by elution of the sample through a silica column for liquid chromatography (LC) (Purcaro et al., 2016a), where the triglycerides (TAG) are retained, while MOSH and MOAH are instead eluted. However, the amount of oil that the column can withstand is limited (Biedermann et al., 2009). For this reason, when working on fats and oils, any pre-treatment of the sample usually does not aim to extract the contaminants per se, but rather to increase the sensitivity of the analytical method as well as to purify the sample from matrix interference.

2.7.3 Sample clean-up

As just mentioned, direct analysis of vegetable oils is not always able to provide satisfactory results in terms of sensitivity, and therefore of the achievable limit of quantification. Even though for some matrices an extraction with *n*-hexane is sufficient, and the samples is already injectable, for oils and fats a sample clean-up prior the analytical determination is almost mandatory. Indeed, the most common instrumental configuration for mineral oil analysis involves the use of a HPLC column containing a stationary phase of silica having dimension of 25 cm x 2 mm of internal diameter (ID), which can retain a maximum of 20 mg of fat (Biedermann et al., 2009). Beyond this amount, the active sites of the column becomes saturated, determining a loss in the separative power towards MOSH and MOAH and, in case of excessive overload, the elution of triglycerides through the entire column and their transfer to the GC, fouling the transfer line and compromising the analytical column. However, under these conditions, a LOQ lower than 2 mg/kg is hardly achievable and this, as better specified later, runs counter the required levels of sensitivity. In addition, direct analysis provides

chromatograms difficult to interpret and to integrate due to the presence of interfering signals related to compounds naturally occurring in the oil matrix, having the same elution time of MOH. These are mainly endogenous *n*-alkanes for the MOSH fraction, and olefins and related isomerization products for the MOAH fraction. This occurrence often does not allow a correct quantification of the MOH present, or does not allow it at all. Therefore, sample preparation protocols to overcome these problems were implemented.

2.7.3.1 Enrichment

In order to avoid exceeding the HPLC column loading capacity towards the fat, different approaches aimed at eliminating triglycerides and extracting unsaponifiable components, category to which mineral oils belong, were proposed.

The first of these approaches is the saponification, that allows the extraction of mineral oils with organic solvent from the alkaline aqueous/alcoholic environment in which the saponification takes place. The solution obtained can either be directly analyzed or evaporated to a more concentrated solution, since the injection in LC is now not limited by the initial fat amount. At present, this procedure can be performed in different ways, which differ in terms of instrumentation, time, volume of solvents and need for heating (De Medina et al., 2013). First saponification protocols, involving both mineral oils or other analytes, date back to the 90s and some of them are based on standard methods (IUPAC Commission on Oils, 1992; Castle et al., 1993; Guinda et al., 1996; Koprivnjak et al., 1997; ISO 3596:2000). Even though they are still applied in some cases, they are often disadvantageous precisely in the aspects just listed, and therefore little used by now. Indeed, over the years methods have undergone several changes and improvements, and more convenient ones are now available.

For example, ultrasound assisted saponification makes use of relatively cheap instrumentation and allows to work at room temperature, reducing the time to few minutes (De Medina et al., 2013). These authors could isolate the unsaponifiable fraction of VOO, but this method was also applied to mineral oil analysis in EVOO by Quisillo (2021). Microwave assisted saponification (MAS) represents a good alternative, successfully applied in different food matrices for the determination of various lipophilic contaminants (Paré et al., 1994; Carro et al., 2002; Fujita et al., 2009) (Figure 1.22). MAS allows to saponify the sample in short time, using reduced solvent volumes and with little sample handling, thanks to the severe conditions of temperature and pressure that take

place inside the MAS vessels during the reaction, which increase its efficiency without affecting the unsaponifiable fraction (De Medina et al., 2013). The only disadvantage of using MAS, compared to traditional methods, is that it requires expensive specific equipment that not all laboratories can afford to buy. Even though this protocol was initially applied to the extraction of mineral oil contamination from cereal-based products (Moret et al., 2016) and of the unsaponifiable fraction from fats (Mascrez et al., 2021), a validated protocol for mineral oil determination in vegetable oils was lacking, and represented one of the goal of this thesis work.

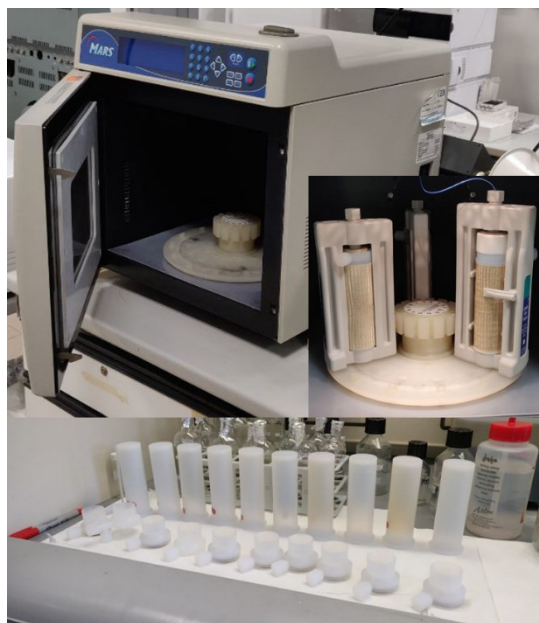


Figure 1.22. Microwave digestion system and related accessories exploited for (MAS).

Using basic laboratory equipment, a rapid saponification protocol was recently proposed in the DGF C-VI 22 (20) method (Albert et al., 2022) and in the recent revision of the EN 16995:2017 method (from here on, for more detailed information about methods, refer to Table 1.5). With these protocols complete saponification is achieved in 30 minutes at 60 °C under agitation, followed by recovery of the *n*-hexane extract. While in the DGF method the saponification stops here, in the EN 16995:2017 method additional *n*-hexane is added to the aqueous/ethanolic phase to perform a second extraction, which is subsequently combined with the first one. Very similar to both is the saponification approach used by Nestola (2022), including also in this case a re-extraction of the aqueous phase, even though this author delegated part of operations, related to this sample preparation, to the autosampler.

A second extraction was introduced to solve a problem common to these saponification methods, which often emerged and was subject of debate during the meetings related to

the collaborative study for updating the EN 16995:2017 method (in which the Food Chemistry laboratory of the University of Udine participated), related to a slight partition of MOH between alcoholic and *n*-hexane phases. However, also in this way, the problem was not completely solved. 1,3,5-Tri-*tert*-butylbenzene (TBB) was chosen as reference internal standard, by virtue of the easier integration of its signal and its higher degree of alkylation compared to the other standards, which makes it more comparable to the main compounds found in the MOAH fraction of edible oils, and thus for which a similar behavior is assumed.

This problem does not arise when using a completely different approach, based on the use of adsorbents with fat-retention properties. As the sample is only passed through a cartridge for solid phase extraction (SPE), and the analytes are easily eluted with the appropriate eluent mixture, there is no possibility for partition, and the standards remain aligned with each other. However, with this approach, to be able to retain the bulk of triglycerides related to e.g. 1 g of oil, it is necessary to use significant amounts of solid phase, which inevitably require high volumes of solvent to elute, and quantitatively recover, the compounds of interest. In fact, as evaluated by Moret et al. (2011), 1 g of activated silica gel (actSi) can only retain, based on the type of oil, 125-150 mg of sample. In 2009, Biedermann et al. published a method exploiting a large column filled with activated silica gel (12g) on which 1 g of oil, dissolved in *n*-hexane, was loaded. Appropriate optimization of the eluent mixture, which was Hex/dichloromethane (DCM) 20:80, allowed the elution of both MOSH and MOAH without the risk of witnessing triglyceride breakthrough. Limit of detection (LOD) was lowered more than three times with respect to direct injection. A completely different approach was instead used by Wrona et al. (2013), where the activated silica in the column was just the support for a solution of sulfuric acid, which determined the chemical combustion of fat, without affecting the mineral oil fraction. In this way, 5 g of oil could be processed to counterbalance the small injection volume, with the recovery of only the MOSH fraction (this method was not tested on MOAH).

While in both cases the purpose was only to retain/decompose the triglycerides, in order to extract MOH and reach an adequate level of sensitivity, other methods exploited combinations of different adsorbents for both MOH enrichment and sample purification or MOSH/MOAH separation. For this reason, they deserve to be briefly reported also in this section.

For example, activated aluminum oxide (Alox) is exploited to retain *n*-alkanes, which are interferences for the MOSH fraction. However, the presence of excessive amounts of

triglycerides would deactivate the phase causing this effect to collapse (Fiselier et al., 2009a). Thus, the presence of fat greatly limits the amount of oil that can be loaded onto the Alox column, requiring a previous enrichment step. The solution found by Fiselier & Grob (2009) was to sourmount the Alox with a layer of actSi (6 g) to not allow triglycerides, coming from 1 g of oil, to reach the underlying phase. Similar was the method proposed a few years later by Zurfluh et al. (2014), where a double bed cartridge, whit 8 g of actSi, was used to retain the same amount of oil.

Another adsorbent widely used in the field of mineral oils is silver silica (SiAg). As reported in many works, silver silica has the main purpose of improving separation between MOSH and MOAH, but it can also be used for obtaining a simultaneous sample enrichment. Indeed, retention of unsaturated lipids by silver silica was already studied (Cert & Moreda, 1998; Mander & Williams, 2016), and no difference in this property could be observed with respect to activated silica, when this comparison was made (Moret et al., 2011). Thus, some works reported the use of a single phase of SiAg to achieve both effects. This was for example the subject of the work by Li et al. (2017), using 10 g of SiAg to retain 1 g of oil.

The LOQ of these methods (as well as those in the following paragraphs), although shown in the tables, are not taken into consideration in the discussion if not necessary, as they depend on the analytical instrumentation, the injection volume, the intra- or inter-laboratory evaluation etc., but also on the approach used to express them (lower or upper bound), which it is rarely specified. This therefore would not allow objective comparisons. Anyway, all these methods require the use of high volumes of solvent, both for the elution and for the conditioning step, thus more recent protocols based on saponification are more advantageous in these terms. This is important for the environment and the health of operators, but also for the reliability of the analytical results. Working with high volumes, which often need to be reconcentrated before instrumental analysis, enhance the level of impurities in the final solution, if reagents and solvents are not of high purity grade or become contaminated during sample preparation.

Table 1.5. Sample enrichment methods for the analysis of mineral oils in vegetable oils.

Analytes	Sample preparation	Instrumental analysis/detection	LOD/LOQ [mg/kg]	Reference
MOSH	1 g oil loaded on double bed SPE AloX + 6 g actSi, 25 mL Hex elution	<ul style="list-style-type: none"> • LC-LC-GC-FID on-column interface • LVI-GC-FID on-column injector 	LOD=0.1	Fiselier & Grob, 2009
MOSH/MOAH	1 g oil loaded on SPE 12 g actSi, 35 mL DCM/Hex 20:80 <i>v/v</i> elution	<ul style="list-style-type: none"> • LC-GC-FID Y-piece interface • LC(off-line)-GCxGC-FID/MS 	LOD=1	Biedermann et al., 2009
MOSH	5 g oil loaded on SPE 40 g 100:30 <i>w/v</i> actSi-98% H ₂ SO ₄ , 20 mL Hex elution	GC-FID on-column splitless injector	LOQ=1	Wrona et al., 2013
MOSH/MOAH	1 g oil loaded on double bed SPE (mixture 10 g actAlox + 7 g 0.3% SiAg) + 8 g actSi, MOSH 23 mL Hex and MOAH 50 mL 25:0.25:74.75 DCM/toluene/Hex elution	LC-GC-FID Y-piece interface	LOQ=0.3	Zurfluh et al., 2014
MOSH	1 g oil loaded on SPE 10 g 1% SiAg, 14 mL Hex elution	GC-FID on column splitless injector	LOQ=2.5	Li et al., 2017
MOSH/MOAH	<ul style="list-style-type: none"> • 1 g oil + 10 mL Hex/EtOH 50:50 <i>v/v</i> • Saponification with 3 mL aqueous KOH 33% <i>m/m</i> at 60 °C x 30 min + 5 mL Hex and 5 mL water/EtOH 1:1 <i>v/v</i> 	<ul style="list-style-type: none"> • LC-GC-FID Y-piece interface • LC-GCxGC-MS 	LOQ=1	DGF C-VI 22 (20) Albert et al., 2022
MOSH/MOAH	<ul style="list-style-type: none"> • 1 g oil + 10 mL Hex/EtOH 50:50 <i>v/v</i> • Saponification with 2 mL KOH 1 g/mL at 65 °C x 20 min + 4 mL of water + re-extraction aqueous phase with 5 mL Hex 	<ul style="list-style-type: none"> • LC-GC-FID Y-piece interface • LC (off-line)-GC-MS 	LOQ=1	Nestola, 2022
MOSH/MOAH	Sample preparation as in DGF C-VI 22 (20) + re-extraction aqueous phase with 5 mL of Hex	<ul style="list-style-type: none"> • LC-GC-FID Y-piece interface • LC (off-line)-GCxGC-MS 	LOQ=3 (MOSH) LOQ=2 (MOAH)	Update of EN 16995:2017

2.7.3.2 Interference removal

The integration of MOH chromatograms is complicated, and often hampered, by the presence of compounds naturally present in the matrix, which have a similar affinity to MOH in the chromatographic separation and thus co-elute with them causing signals overlap. This occurrence can either disturb the integration, introducing variability or overestimations on the final result, or not allow it all. The latter occurs when the concentration of the interfering compounds is significantly preponderant with respect to that of mineral oils, or even when it is so high as to determine overload of the detector, compromising the quality of the chromatographic trace.

In particular, in olive oils, this is due to the presence of endogenous *n*-alkanes for MOSH (Fiselier & Grob, 2009), instead to olefins, mainly squalene and its isomers, for MOAH (Biedermann et al., 2009). For their removal, several solutions were proposed over the years.

2.7.3.2.1 MOSH: endogenous *n*-alkanes

Endogenous *n*-alkanes are naturally occurring long chain hydrocarbons present at high concentration in vegetable oils, representing one of the main classes of compounds of the unsaponifiable fraction. Although they are distributed in various parts of the plant, a significant amount is present in the external cuticle of the plant epidermis (Srbinovska et al., 2020b). *n*-Alkanes are also present in petroleum, as components of the MOSH fraction, but they are easy distinguishable from those of petrogenic origin for the prevalence of odd-numbered terms, having a number of carbon atoms typically ranging from *n*-C₂₁ to *n*-C₃₅ (Fiselier et al., 2009a; Srbinovska et al., 2020b). This specific distribution is a consequence of their biosynthetic mechanism. In fact, while petrogenic *n*-alkanes derive from randomized geological processes that occurred over millions of years, natural *n*-alkanes seem to derive from a specific reaction passing through the elongation of preformed fatty acids, followed by the loss of their carboxyl carbon. Since in this mechanism the elongation goes through the addition of two carbon atoms at a time, the loss of the carboxyl group determines the preferential formation of species with an odd number of carbon atoms (Bognar et al., 1984; Samuels et al., 2008).

In GC-FID analysis, *n*-alkanes appear as sharp and isolated peaks. However, this very much depends on the amount of sample injected and its *n*-alkane content. Indeed, when the amount of *n*-alkanes is too high, the GC column is not able to separate them completely due to overload, and therefore the peaks begin to partially overlap, with a loss

in resolution. The chromatographic signal can also get worse as the result of the saturation of the incoming signal from the detector. As *n*-alkanes signal adds up to that of MOH, this occurrence can make it difficult to draw the upper contour of the hump during the integration, as the lack of resolution between peaks itself generates a profile similar to a hump (Figure 1.23), determining uncertainty in the interpretation of the chromatogram (Fiselier et al., 2009a). Thus, depending on the amount of these compounds, either their signal can be discarded during the integration of chromatograms, simply not considering the areas of the sharp peaks above the MOSH hump from *n*-C₂₁ onwards or, if they are present in such concentration that their signal is not well resolved, not allowing to distinguish the MOH hump, the sample needs to be adequately treated before the analysis for their removal. It must be taken into account that, even in the case they are in low quantities and can be easily discarded during the integration phase, it is possible that the contamination is, at least minimally, overestimated. This is particularly evident on samples with low levels of contamination, where the difference in the magnitude of the signals between *n*-alkanes and MOSH becomes comparable.

When *n*-alkanes show overload problems, there are two solutions: either less sample is injected, to restore balance with the phase available in the GC column for optimal separation, or these endogenous compounds are removed by means of an appropriate sample preparation step. The first solution is applicable only to those samples having MOSH contamination for which a loss in sensitivity, due to the injection of a smaller amount of sample, still allows to quantify the contamination in a reliable way. Therefore, this approach is not suitable for assessing background levels of contamination. In this context, as well as for vegetable oils particularly rich in these compounds, *n*-alkanes removal represents the best choice, and allows considerable gain in sensitivity. So far, the only technique available for the removal of these endogenous interferences involves the elution of the sample through a SPE cartridge of Alox, activated at approximately 400 °C, which proved to have a strong retention towards *n*-alkanes beyond *n*-C₂₀ (Fiselier et al., 2009a) (Figure 1.23). The retention is also towards MOAH, which in almost all the protocols proposed are not recovered. However, much attention must be paid to the conditions under which this step is performed, as the mobile phase used (*n*-hexane provide the best retention of *n*-alkanes), the column temperature (temperature above 25-30 °C decreases the retention), the presence of polar components (retention power collapses) and the amount of *n*-alkanes loaded into the column (to avoid phase overloading) can influence the success of this purification step (Fiselier et al., 2009a). The

protocols present in the literature will now be treated without going into detail. For more detailed information, the reader is referred to Table 1.6.

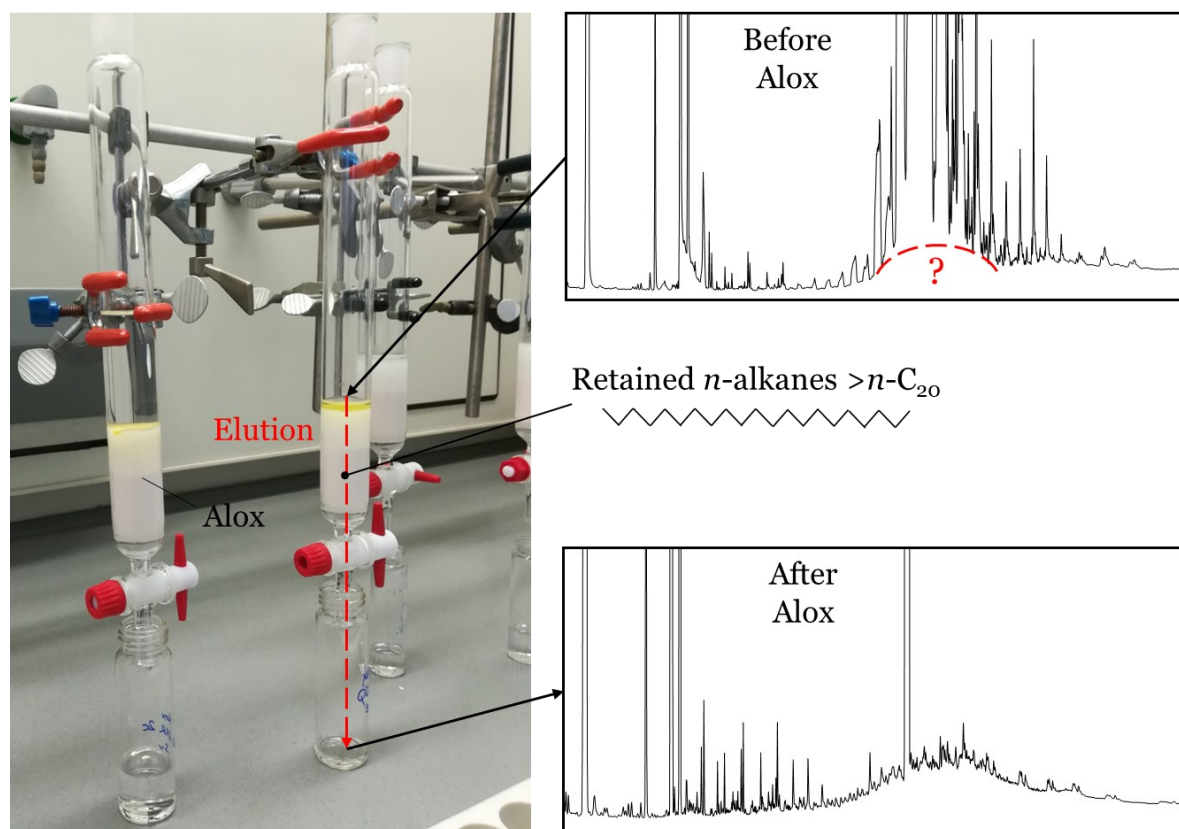


Figure 1.23. *n*-Alkanes removal from rapeseed oil sample, showing the advantage of elution through Alox to evaluate MOSH contamination in case of signal overload by these endogenous interferents.

The first protocol available in the literature, and the only one involving a small scale SPE of Alox (100 mg of oil onto 3.5 g of phase), which was really advantageous in terms of the amount of consumables needed, was proposed by Wagner et al. (2001a), although it was initially aimed at the removal of brominated olefins from the MOAH fraction. During its application the ability to retain *n*-alkanes above *n*-C₂₂ was discovered. The use of low volumes of solvent was also achievable with the on-line implementation of this step, which moreover reduced sample handling and standardized the procedure, as for the method developed by Fiselier et al. (2009b). The sample injected (max 20 mg), after elution through a silica column which retained triglycerides and polar compounds that would bind and deactivate the active sites of Alox, was sent through an Alox column, which bed size depended on the amount of sample loaded. However, both methods started from low amounts of oil and did not allow the achievement of particularly low LOQ. Based on the same principle, i.e. by exploiting a first elution through activated silica, the methods from Fiselier & Grob (2009) and Zurfluh et al. (2014) exploited an off-line approach based on the use of a double phase cartridge (20 g and 10 g of Alox respectively).

The off-line approach allowed for a greater flexibility in the choice of bed volume, resulting in a greater sample loading (1 g of oil), beneficial for sensitivity, even though this came together with a significant increase in solvent volumes. The latter were instead lower in the EN 16995:2017 reference method, published a few years later. However, the LOQ that resulted from an inter-laboratory comparison, was quite high. The solution was then found with the DGF C-VI 22 method (20). Using the same protocol (same sorbents and solvent volumes) as for the EN 16995:2017 method, the sample was loaded after enrichment by saponification, thus loading an amount of sample corresponding to three times more than before, obtaining significant improvements in terms of LOQ. Another little difference, not related to sensitivity, regarded the addition of a little layer of sodium sulphate on the top of the column to protect the activated phases from any residual traces of humidity coming from the previous saponification step, important to avoid Alox deactivation. In the updated version of the EN16995:2017, which was subjected to inter-laboratory validation and will be published early next year as new reference method, the Alox step provides for the application of the same protocol.

Although the removal of endogenous *n*-alkanes can be beneficial, it must be also taken into account that even its indiscriminate application can lead to unreliable results. According to Albert et al. (2022), for oils like e.g. cocoa butter, palm oil etc. containing limited amounts of *n*-alkanes, as thus for oils where the integration of the chromatogram is still possible also without sample pre-treatment, their removal is not recommended, as discrimination of high boiling MOSH due to the Alox step, also in relation to their composition, was reported. Indeed, an underestimation of 20-40% was ascertained for certain mineral oils also by previous works (Fiselier et al., 2009a, b; Albert et al., 2022), probably as the result of the retention of some MOSH which are structurally similar to *n*-alkanes, due to linear sections of their molecules. This more likely occur for molecules of higher molecular mass, also as the result of their competition against the few *n*-alkanes present towards Alox binding sites. Thus, to introduce less error as possible in MOSH analysis, the use of Alox must be prudent and come from an actual need. This, as said, can depend on the type of oil subjected to analysis, as well as on the purpose of the latter, e.g. Alox may be required to evaluate low levels of contamination, for which it is necessary to inject high sample amount to reach the required sensitivity, while avoiding signal overload and the problems associated with it.

Table 1.6. Sample purification methods for the analysis of MOSH in vegetable oils.

Sample preparation	Instrumental analysis/detection	LOD/LOQ [mg/kg]	Reference
0.1 g oil loaded on SPE 3.5 g AloX, 2 mL Hex eluate	LVI-GC-FID on-column injector	LOD=5-20	Wagner et al., 2001a
Direct injection	LC-LC(Alox)-GC-FID on-column interface	LOD=3	Fiselier et al., 2009a, b
1 g oil loaded on double bed SPE 20 g AloX + 6 g actSi, 25 mL Hex elution	<ul style="list-style-type: none"> • LC-LC-GC-FID on-column interface • LVI-GC-FID on-column injector 	LOD=0.1	Fiselier & Grob, 2009
1 g oil loaded on double bed SPE (mixture 10 g AloX + 7 g 0.3% SiAg) + 8 g actSi, MOSH 23 mL Hex and MOAH 50 mL 25:0.25:74.75 DCM/toluene/Hex elution	LC-GC-FID Y-piece interface	LOQ=0.3	Zurfluh et al., 2014
0.3 g oil loaded on double bed SPE 10 g AloX + 3 g actSi, 25 mL Hex elution	LC-GC-FID Y-piece interface	LOQ=10	EN16995:2017
Saponified extract (1 g oil) loaded on double bed SPE 10 g AloX + 3 g actSi + 1 g Na ₂ SO ₄ , 25 mL Hex elution	<ul style="list-style-type: none"> • LC-GC-FID Y-piece interface • LC-GC×GC-MS 	LOQ=1	DGF C-VI 22 (20) Albert et al., 2022

2.7.3.2.2 MOAH: endogenous olefins

MOAH analysis in vegetable fats and oils is mainly complicated by the presence of high amounts of natural olefins such as squalene, isomerization products of squalene, sterenes, carotenes and their derivatives, present natively or formed during oil refining processes (Biedermann et al., 2009; Bratinova & Hoekstra, 2019). Even though some mono/low unsaturated compounds can also elute together with MOSH (Lommatzsch et al., 2015; Sdrigotti et al., 2021), olefins present in vegetable oils co-elute preferentially with MOAH and, differently from *n*-alkanes for MOSH, their signal in the chromatogram is hardly discarded in the integration phase, since they are usually present at high amount, covering that related to mineral oils. Only MOH with low molecular mass can possibly not be affected by the presence of their presence since the latter are heavier and come out later in the chromatogram. However, since olefins are often present in such amounts as to saturate the analytical column, they tend to invalidate the quality of the entire chromatographic trace, even in the internal standards area, thus completely

hindering the analysis of MOAH (Nestola, 2022). To solve this problem different protocols have been proposed. Among them, chemical derivatization, passing through an epoxidation reaction, is generally the preferred route, although some alternative protocols based on the use of adsorbents (e.g. SiAg) have been proposed (Mattara, 2013). Epoxidation is a reaction that affects the double bonds of olefins which are broken by oxidation leading to the formation of an epoxide (Figure 1.24). This derivatization makes olefins more polar, shifting their retention time on the silica HPLC column beyond that of MOAH (Biedermann et al., 2009). The existing methods, reported in detail, can be found in Table 1.7.

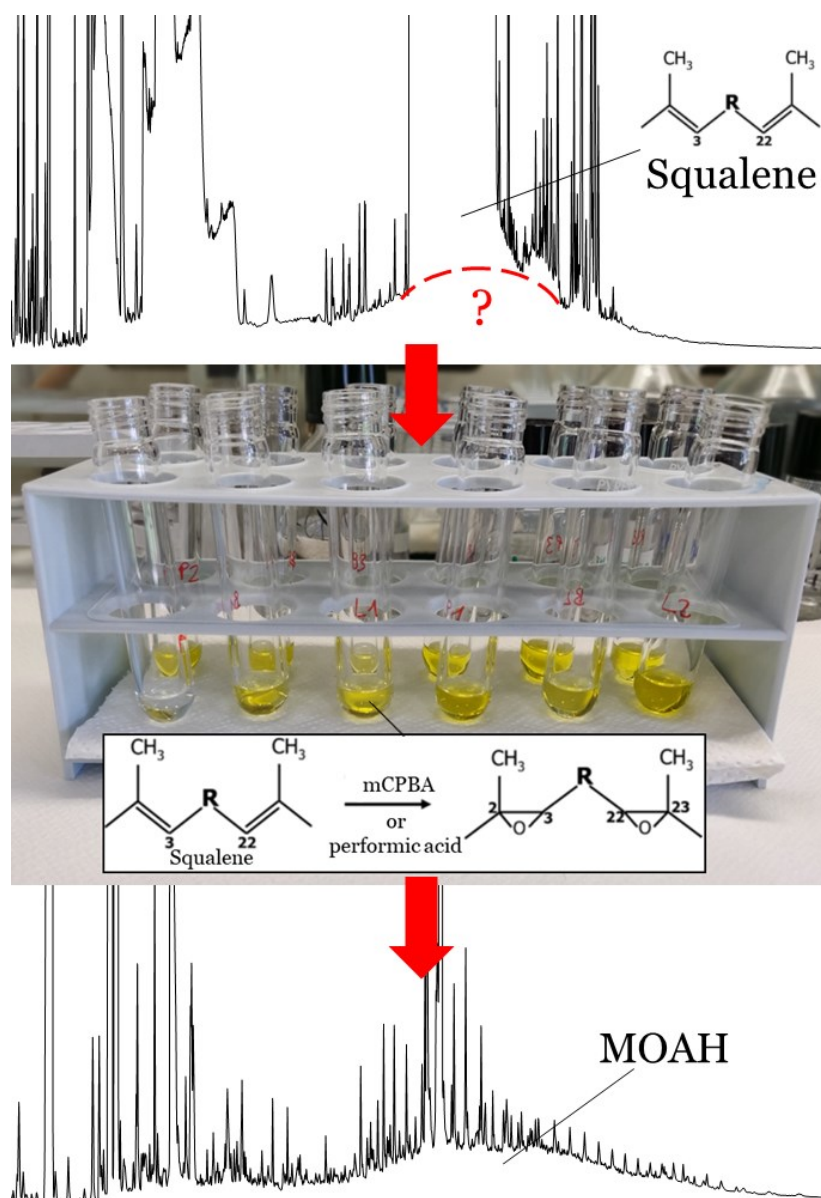


Figure 1.24. Squalene removal from an EVOO sample by epoxidation, showing the advantage of this treatment in detecting MOAH contamination possibly covered by the signals related to endogenous olefins.

The first method proposed involving derivatization was the bromination, using bromine as derivatization agent (Wagner et al., 2001a). Bromine in chloroform was used to derivatize olefins co-eluting in the MOSH fraction, since no controlled MOSH/MOAH separation was achievable at that time and this co-elution often occurred. This method was later discarded because of the toxicity of bromine and because it affected MOAH, causing an underestimation of the aromatic contamination.

Later in 2009 another method, aimed at the evaluation of the MOAH fraction and this time involving the use of *m*CPBA (*meta*-chloroperoxybenzoic acid), was proposed, giving better results in terms of selectivity, but still struggling with some issues (Biedermann et al., 2009). Unless the reaction conditions were perfectly kept under control, the method proved to be not very robust and to lead to losses of aromatic compounds (20-40%), especially the more susceptible ones such as thiophenes. Indeed, some method drawback were later highlighted by Nestola & Schmidt (2017). In particular, the use of DCM was disadvantageous due to the sub-ambient cooling necessary to slow down the reaction, hence to avoid MOAH losses, and to the need of the presence of edible oil in the reaction environment, as it contains polyunsaturated fatty acids which are preferentially oxidized, acting as a buffering agent and thus preserving the aromatics (Biedermann et al., 2009). Moreover, sodium carbonate used to stop the reaction was unable to stop it completely, allowing the reaction to continue also within the autosampler vial, with the risk for MOAH to be oxidized before sample injection. Given the presence of fat, as can be guessed, the amount of sample injectable was limited, with negative consequences on the sensitivity of the method. A similar method was recently reported also by Stauff et al. (2020). In 2017, the method proposed by Nestola & Schmidt involved the use of *m*CPBA too, but brought some modifications that aimed to solve some of these critical issues. For example, the reaction was carried out in ethanolic reaction environment at room temperature, slowing down the kinetics of the oxidation, thus no buffer oil was needed anymore. This could be exploited later to improve sensitivity, as epoxidation on saponified samples was feasible. Furthermore, the reaction was stopped definitively with sodium thiosulfate, avoiding the risk of affecting MOAH in the sample waiting for injection. Compared to the method of Biedermann et al. (2009), it also had the advantage of not requiring solvent exchange by evaporation prior to injection into the HPLC-GC-FID system, which was necessary in the previous case because DCM injection would have resulted in a time shift of the transfer windows of the fractions of interest from LC to GC. These conditions simplified laboratory operations, increased the control of the reaction and therefore allowed automated sample preparation (Nestola & Schmidt, 2017; Biedermann et al.,

2020). As anticipated, epoxidation was applied also on the oil sample after enrichment by saponification. In particular, albeit with some modification (the main one being the execution of the reaction at 40°C), this was introduced in the DGF C-VI 22 (20) and the update of the EN16995:2017 methods.

Despite the continuous evolution of methods in the last years, increasingly optimized in search of achieving lower LOQ and greater robustness, in some cases inter-laboratory comparisons still show poor alignment between results. Dwelling on the MOAH fraction and the epoxidation by *m*CPBA, this is often a consequence of the presence of olefinic residues that persist to varying degrees after the sample preparation, and significantly increase the data variability due to the integration (difficulty in discriminating between MOAH-related and olefin-related signals). This happens either more often for vegetable oil samples that were subjected to refining treatment or for certain type of oils, e.g. palm oil, where biogenic interferences are more persistent, perhaps due to isolated or terminal double bonds, poorly accessible during epoxidation (Biedermann et al., 2020). For these reasons, with the aim to increase the efficiency of this reaction, Nestola recently published a new epoxidation method relying on the use of performic acid, synthesized *in-situ*, as epoxidizing agent, including also chloroform in the reaction environment to increase the reaction rate (Nestola, 2022). In this way, epoxidation proved to be effective in removing π -electron-deficient olefins, typical of refined oils, if compared to the previously reported methods. The method proved to be an excellent tool, even though, losses of some classes of aromatics could not be prevented (mainly aromatics with three or more rings).

Finally, as mentioned above, the use of adsorbents to remove olefins, particularly silver silica, was investigated. The potential of SiAg towards olefins is not new. Different methods already exploited impregnation of sorbents with AgNO₃ to improve the separation of lipids based on their degree of unsaturation (Momchilova & Nikolova-Damyanova, 2003; Fuchs et al., 2011) or to separate polycyclic aromatic compounds according to the ring number (Nocun & Andersson, 2012). Silver ions act as electron acceptors and therefore the double bonds of aliphatic or aromatic compounds, which have high electronic density, can bind forming reversible complexes, possibly broken by a solvent of suitable polarity. Compounds containing double bonds also include olefins, which are therefore retained or at least slowed down in the elution (Mander & Williams, 2016). For MOAH, however, the issue is complicated by their affinity for the stationary phase, which is very similar to that of olefins, and thus a co-elution is difficult to avoid. For this reason, some olefins can be removed, while part of them often remain, even when using this quite selective adsorbent. A possible solution would be the increase of the

dimension of the SPE columns, thus increasing the number of theoretical plates, even though this would be associated with an inevitable increase in eluent volumes. In this regard, Mattara (2013) tried to exploit the potentiality of automated SPE using a modified pressurized liquid extraction (PLE) system (SpeedExtractor), already used for the extraction of the mineral oil contamination from different matrices (Moret et al., 2013, 2014b), to use a bigger sorbent bed without increasing elution times and solvent volumes. This method provided excellent purification results for different classes of olive oil towards squalene and its isomerization products, e.g. optimal retention when applied to olive oil and olive pomace oil, while the application on other fatty matrices resulted to be less efficient, with the worst results for palm oil (Mattara, 2013; Moret, 2016). Optimal separation was instead obtained when using planar solid phase extraction (pSPE), which was firstly applied for MOSH/MOAH separation (Wagner & Oellig, 2018), and then adapted employing silver ions to achieve the separation between MOAH and native terpenes (olefins) in vegetable oils, i.e. Ag-pSPE (Wagner & Oellig, 2022), even if only for screening purposes due to the high detection limits not in line with the current MOH requirements (for this reason it is not shown in the table). Good results were also obtained for on-line applications, where a SiAg column was placed in the eluent path, after a silica column used to retain triglycerides, for the purification of the MOAH fraction (Zoccali et al., 2016). However, a drawback of this last method regarded the recovery of MOAH without olefins, which is optimal only up to anthracene, as for aromatics of higher molecular mass there are still problem of co-elutions, mainly when sterenes and carotenes are present. This could be a relative problem if MOAH in food were indeed mono- or diaromatic species (Grob, 2018a). Moreover, the low stability of the silver-ion column in withstanding multiple elutions makes the off-line approach more feasible.

Finally, in one case, the coupling of epoxidation, based on a slightly modified version of the method by Biedermann et al. (2009), with subsequent elution through silver silica brought some benefits. In particular, the epoxidation was carried out by exploiting a more diluted sample extract and *m*CPBA solution, with the aim to eliminate most of the interfering olefins, but deliberately maintaining a residue that allowed to be sure that MOAH were preserved. The residual olefins, significantly reduced, were then eliminated by sample elution through a mixed bed of silver silica and activated silica (Menegoz, 2019).

To conclude, although the use of adsorbents is sometimes exploitable, epoxidation is the fastest, most effective, user-friendly and solvent-saving method to be applied in routine analysis. Nonetheless, the epoxidation protocol is the one most commonly found in all the

recent works available in the literature, including reference methods that also carried out inter-laboratory validation (for example the DGF C-VI 22 (20) and the update of the EN 16995:2017 methods). Therefore, to date, it is commonly considered by the scientific community, in the field of mineral oils, the reference protocol to be applied for MOAH purification.

Table 1.7. Sample purification methods for the analysis of MOAH in vegetable oils.

Sample preparation	Instrumental analysis/detection	LOD/LOQ [mg/kg]	Reference
0.3 g oil + 10% <i>m</i> CPBA in DCM cooled in ice + reaction stopped with 10% aqueous Na ₂ CO ₃	<ul style="list-style-type: none"> • LC-GC-FID Y-piece interface • LC (off-line)-GCxGC-FID/MS 	LOD=3 LOQ=8	Biedermann et al., 2009
Direct injection	LC-LC-LC(SiAg)-GC-FID/MS PTV injector	LOD=0.1 LOQ=0.4	Zoccali et al., 2016
0.3 g oil + 20% ethanolic <i>m</i> CPBA + reaction stopped with 10% aqueous Na ₂ S ₂ O ₃	LC-GC-FID Y-piece interface	LOQ=3	Nestola & Schmidt, 2017
Epoxidation at -18 °C x 10 min of 0.3 g oil + 3% <i>m</i> CPBA in DCM + reaction stopped with ascorbic acid + clean-up step	<ul style="list-style-type: none"> • LC-GC-FID Y-piece interface • LC (off-line)-GCxGC-MS 	LOD=1.5 LOQ=2.5	Stauff et al., 2020
Epoxidation of saponified sample with 10% ethanolic <i>m</i> CPBA at 40 °C x 20 min + reaction stopped with 10% aqueous Na ₂ CO ₃ /Na ₂ S ₂ O ₃ .	<ul style="list-style-type: none"> • LC-GC-FID Y-piece interface • LC-GCxGC-MS 	LOQ=1	DGF C-VI 22 (20) Albert et al., 2022
Epoxidation of saponified sample with CH ₂ O ₃ in presence of CHCl ₃ for 20 min at 65 °C + reaction stopped with water	<ul style="list-style-type: none"> • LC-GC-FID Y-piece interface • LC (off-line)-GC-MS 	LOQ=1	Nestola, 2022

2.7.4 MOSH/MOAH separation

MOH are a complex mixture of thousands of hydrocarbons isomers that during the analytical determination, which is performed with capillary gas chromatography coupled with a flame ionization detector, cannot be separated as individual compounds. Not surprisingly, the typical chromatogram of mineral oils is recognizable for the humps resulting from the overlap of thousands of unresolved peaks. In addition, another limiting aspect of GC in this application is its incapability to separate MOSH from MOAH. Indeed, these compounds co-elute from the column despite having different chemical structure, due to the correspondence of their molecular weights, and therefore of their boiling

points. However, the separate evaluation of these two classes is of fundamental importance in the light of their different toxicological relevance (EFSA, 2012a). For this reason, the separation must take place upstream of the GC, and can be performed in two different ways: either using HPLC, which was the first analytical approach applied, or using SPE cartridges, sometimes replaced by larger columns filled with suitable sorbents (Purcaro et al., 2016a). These two methods, besides MOSH/MOAH fractioning, also allow to isolate MOH from fat (if present) prior to the analytical determination, which would be detrimental to the GC column. However, while SPE has the advantage to allow separation to be carried out with basic and cheap equipment, on the other hand HPLC, which is now part of the standard instrumentation of any laboratory, is usually preferred for the more rapid and easier sample preparation, the reduced risk of contamination, the reduced solvent consumption, and a more reproducible separation between the two fractions. Moreover, HPLC allows for easy on-line coupling with GC. On the contrary, protocols based on use of cartridges or columns for solid phase extraction, besides being less robust and more prone to sample contamination, as a consequence of the increased sample handling, only provides for the off-line coupling.

Evaluation of the correct MOSH/MOAH separation is fundamental to avoid problems of over- or underestimation of the contamination. To this purpose, samples are spiked with a mixture of internal standards that determine both the start and the end of MOSH and MOAH fractions. This mixture, which is used also for quantification purposes, contains: *n*-undecane (*n*-C₁₁), *n*-tridecane (*n*-C₁₃), cyclohexylcyclohexane (CyCy) and cholestane (Cho), which co-elute with the MOSH fraction, and *n*-pentylbenzene (5B), 1- and 2-methylnaphthalene (1- and 2-MN), 1,3,5-tri-*tert*-butylbenzene (TBB) and perylene (Per), which co-elute with MOAH. In particular, the peak of Cho marks the end of the MOSH fraction, while TBB and Per mark the beginning and the end of the MOAH fraction, respectively (Biedermann et al., 2009; Bratinova & Hoekstra, 2019). Cho has an alkylated four-rings saturated polycyclic structure, and elutes after the naphthenes due to extra retention by ring number. TBB shows a fairly alkylated monoaromatic structure, thus elutes before the alkylated benzenes, while Per, which consists of five condensed aromatic rings with no alkylations, elutes after the alkylated polycyclic aromatics. In addition to verifying their presence within the fraction to which they belong, it is equally important to check the ratios between their areas, which indicate whether or not the fraction are collected entirely. In 2017, Biedermann et al., (2017) published an update concerning a better and more robust management of collection/transfer windows, in order to withstand more robustly a shift of the elution times of the two fractions. This can happen

either in cases of the analysis of highly refined mineral oil products of high molecular mass (e.g. cosmetics analysis) or, in the specific context of vegetable oil analysis, when using a heavily used HPLC column which has lost efficiency and retention power. To render MOSH/MOAH separation less dependent on the state of the HPLC column, the authors recommended to consider CyCy as the marker for the end of the MOSH fraction, because it is eluted after Cho due to the prevalence of the size exclusion effect, and to add 1,4-di(2-ethylhexyl)benzene (DEHB) as an additional standard for the MOAH fraction. DEHB, having a longer alkyl chain than TBB, elutes before the latter and immediately after MOSH. It was therefore proposed to start MOAH transfer immediately after the MOSH fraction (Figure 1.25).

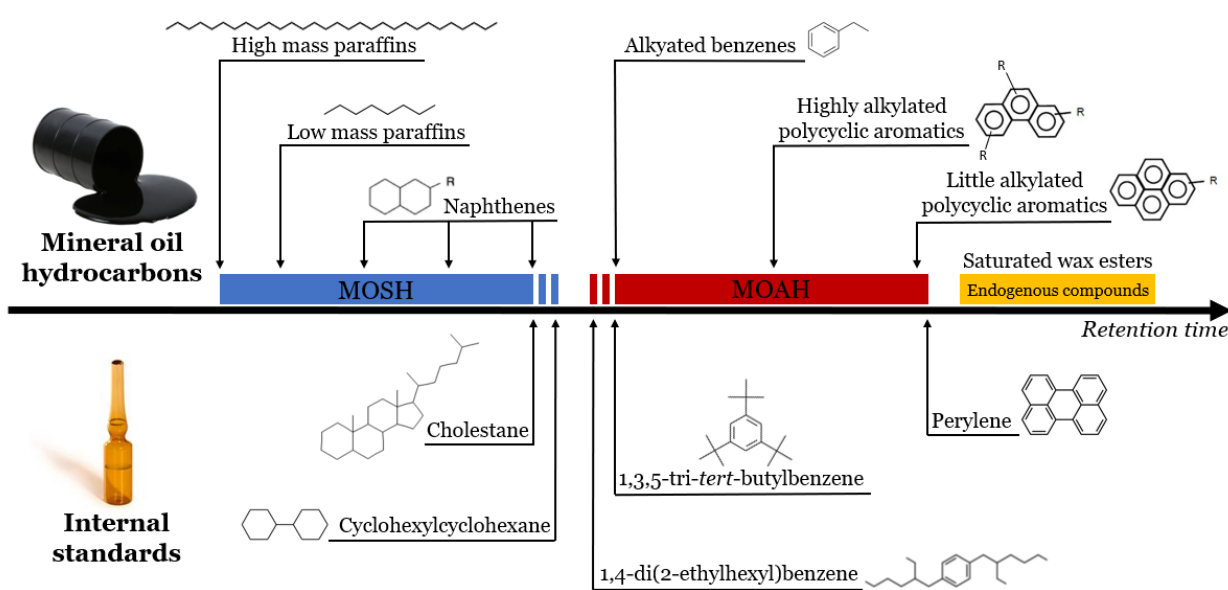


Figure 1.25. Order of elution of the various MOH and the related internal standards used to verify the performance of HPLC instrumentation.

2.7.4.1 On-line methods

The first online methods proposed for the determination of mineral oils in different matrices, food and non-food, date back between 1980 and 1990, and concerned only the determination of mineral paraffins (later called MOSH), due to the difficulty of obtaining a controlled separation of the latter from the aromatic fraction, which was not taken into account at the time (Grob et al., 1991a, b, c; Grob & Bronz, 1995; Droz & Grob, 1997). Sample preparation was in these cases reduced to a simple sample dilution followed by injection into the HPLC-GC system. Nevertheless, in those years LC-GC technique experienced success, and in 1997 a method for separate analysis of MOSH and MOAH in vegetable oils was developed, which also allowed the analysis of the latter grouped by

number of aromatic rings. It made use of a silica column connected on-line to a second amino column by means of a solvent evaporator (SE), necessary for the reconcentration of the fraction eluting from the first column and to remove the DCM not tolerated from the amino column. While the first column isolated the MOH from fat, the second one separated paraffins from aromatics, and the latter into classes based on ring number (Moret et al., 1996, 1997). The SE consisted of a short metal vaporizing chamber (1 mm ID) packed with silica gel and vapour discharge occurred by vapour overflow helped by the applied vacuum. It enabled the evaporation of the MOH fraction (6 mL) eluting from the large silica column loaded with 150-200 mg oil (which resulted in a LOD of 1 mg/kg). Due to its complexity this method was never applied for routine analysis, and the topic of mineral oils had no particular following in the early 2000s, although some works were published.

The topic came up again in 2008, involving the vegetable oil matrix, when the importation from Ukraine of thousands of tons of sunflower oil contaminated with mineral oils was discovered (EFSA, 2008), requiring the development of a suitable method of analysis. Indeed, a simpler instrumental configuration than that previously discussed, and now largely applied since it became the reference one according to the EN 16995:2017 official method (even in its updated version) and the JRC guidance (Bratinova & Hoekstra, 2019), was introduced by Biedermann et al. in 2009. More detailed information and the fundamentals of this method were thoroughly reviewed in 2012 by Biedermann & Grob (2012a, b), while some modifications, for specific applications, were reported in the following years. In particular, in this method MOSH/MOAH separation is obtained by normal-phase liquid chromatography (NPLC) using a silica gel column having dimensions of 25 cm x 2 mm ID. The oil sample, dissolved as it is or after the necessary sample preparation steps previously reported, is injected into the HPLC apparatus and eluted with the appropriate gradient of Hex and DCM that allows the separation of the two fractions of interest. Separation occurs based on size exclusion mechanisms and chemical affinity for the polar stationary phase. The gradient and the eluent flow can vary according to the type of instrumentation and on-line coupling mode. Anyway, as a rule of thumb MOSH, which are totally apolar, are eluted practically unretained with *n*-hexane while MOAH, being slightly polar by virtue of their aromaticity, are retained and eluted only with the application of a more polar gradient, obtained with a mixture of *n*-hexane/dichloromethane, generally with a DCM content around 30%. This, broadly speaking, usually applies also to off-line separations. The two fractions are then subjected

to on-line GC-FID analysis separately (Biedermann et al., 2009; Biedermann & Grob, 2012a). Interfaces used for HPLC-GC coupling will be discussed below.

About deviations from the standard method, for particular applications, Tranchida et al. (2011b) optimised chromatographic conditions to get a faster analysis cycle for MOSH both in LC and GC, and the same did Barp et al. (2013) extending the analysis also to MOAH, gaining a soft improvement in LOQ, together with saving time and solvents. Later, Zoccali et al. (2016), mentioned before, worked to an on-line instrumental setup to obtain MOSH/MOAH separation together with an additional separation from interfering olefins from the MOAH fraction exploiting a SiAg column, to avoid sample preparation. Something similar was carried out before by Fiselier et al. (2009a, b) towards *n*-alkanes in the MOSH fraction, with the use of an Alox column.

2.7.4.2 Off-line methods

Besides on-line methods, also procedures for off-line separation of MOSH and MOAH were developed, starting from procedures able to isolate only the MOSH fraction, due to the difficulty in recovering aromatics without triglyceride breakthrough, and later proposing others for both MOSH and MOAH. In most of the applications, the two fractions are manually separated eluting the sample through an SPE cartridge or larger columns. These alternative methods to the already well-established on-line procedures are useful, since do not oblige a laboratory to own a dedicated and expensive instrumentation. Specifications of methods aimed at the recovery of the MOSH fraction are shown in Table 1.8, while those related to both MOSH and MOAH are shown in Table 1.9.

One of the first off-line methods, aimed at determining MOSH in vegetable oils, was reported by Fiorini et al. (2010), who used a 2 g SPE cartridge of not activated silica gel to process 20-150 mg of oil. The loading amount was based on the expected concentration of MOSH, as loading more would have resulted in a widening of the elution window, not allowing to use small volumes of solvent (5 mL). Always in this regard, not activated silica was preferred, due its less retention power translating in a more rapid elution. A year later, Moret et al. (2011) tested different types of adsorbents, i.e. deactivated and activated silica and silver silica, to evaluate their behaviour. The choice fell on silver silica that enabled improved MOSH/MOAH separation, and allowed for olefin retention, due as seen before to its retention towards compounds having insaturations (Momchilova & Nikolova-Damyanova, 2003; Fuchs et al., 2011; Nocun & Andersson, 2012). This is fundamental in off-line methods involving SPE, where separation efficiency is lower than

HPLC. 100-125 mg of fat (also in this case, based on the type of oil) could be separated on 1 g of SiAg with this method. Later, SiAg was used also in the ISO 17780:2015 method and by Gómez-Coca et al., (2016a), increasing the loading amount to 1 g of vegetable oil to counterbalance the following small injection volume, even though with a considerable increase in the amount of silica (around 15 g and slightly over) and solvents. In this regard, two more advantageous methods were later proposed. The first one, with the aim of improving the ISO method, started from the same amount of oil (1g), but MOSH could be eluted on a 10 g cartridge (Li et al., 2017). In the same year, the protocol was further improved in terms of solvent volumes and amount of adsorbent, also thanks to the introduction of large volume injection (LVI) for the analytical determination, that allowed to start from a lower amount of sample (Liu et al., 2017).

Table 1.8. MOSH/MOAH separation methods, aimed at MOSH recovery, applied to vegetable oils.

Sample preparation	Instrumental analysis/detection	LOD/LOQ [mg/kg]	Reference
0.02-0.15 g oil loaded on SPE 2 g Si, 5 mL Hex elution	GC-FID on-column splitless injector	LOD=5 LOQ=15	Fiorini et al., 2010
0.100-0.125 g loaded on SPE 1 g 10% SiAg, 2.5 mL Hex elution	LVI-GC-FID on-column injector	LOD=5 LOQ=15	Moret et al., 2011
<ul style="list-style-type: none"> • 1 g oil loaded on double bed SPE 18.5 g 10% SiAg + 0.5-1.0 cm Na₂SO₄, 55 mL Hex elution • 0.25 g oil into SPE 2 g actSi, 3.5 mL Hex elution (rapid method for refined and virgin/cold-pressed oils) 	GC-FID on-colum injector, PTV injector or equivalent	LOQ=50	ISO 17780:2015 Lacoste, 2016
1 g oil loaded on double bed SPE 15 g 10% SiAg + 1 cm sea sand, 60 mL Hex elution	GC-FID on-column injector	LOD=5.0 LOQ=15.0	Gómez-Coca et al., 2016a
1 g oil loaded on SPE 10 g 1% actSi-AgNO ₃ , 14 mL Hex elution	GC-FID on column splitless injector	LOQ=2.5	Li et al., 2017
0.2 g oil loaded on SPE 2 g 1% SiAg, 3 mL Hex elution	LVI-GC-FID PTV injector	LOQ=2.5	Liu et al., 2017

Instead, the first off-line protocol for MOSH and MOAH separation, always based on the use of a small SPE (3 g) of SiAg mixed with actSi, was that proposed by Fiselier et al. (2013). After MOSH elution with Hex, MOAH were eluted thanks to a suitable eluting mixture composed of three solvents, namely DCM, toluene and Hex, as well as to SiAg having a lower percentage of AgNO₃ compared to other methods (meaning lower

retention toward MOAH to allow their easier elution). Moreover, toluene was introduced to efficiently deactivate the retention power of silver nitrate for unsaturated hydrocarbons, while maintaining that of actSi towards triglycerides and waxes, avoiding their breakthrough. A similar method was that recently proposed by Ruiz et al. (2021). Almost the same eluent mixture was also exploited by Zurfluh et al. (2014), although in the latter the aim was the recovery of MOAH retained by a larger column packed with Alox and SiAg, used for the simultaneous removal of *n*-alkanes from the MOSH. On the other hand, a slightly different method was instead reported by Luisi (2016) during a round table on mineral oils, who loaded the oil sample on a double phase cartridge, made up of 1 g of SiAg sourmounted by 6.5 g of actSi, and eluted it with a combination of solvents similar to that of HPLC, i.e. MOSH eluted with *n*-hexane, while MOAH with a mixture of DCM/Hex 25:75 *v/v*.

Table 1.9. MOSH/MOAH separation methods, aimed at recovery of both fractions, applied to vegetable oils.

Sample preparation	Instrumental analysis/detection	LOD/LOQ [mg/kg]	Reference
0.2 g oil loaded on SPE 3 g 0.3% SiAg (SiAg 1% + actSi), MOSH 6 mL Hex and MOAH 10 mL 20:5:75 DCM/toluene/Hex <i>v/v/v</i> elution	LVI-GC-FID on-column injector	LOD=0.5 LOQ=0.5	Fiselier et al., 2013
1 g oil loaded on double bed SPE (mixture 10 g actAlox + 7 g 0.3% SiAg) + 8 g actSi, MOSH 23 mL Hex and MOAH 50 mL 2:0.25:74.75 DCM/toluene/Hex elution	LC-GC-FID Y-piece interface	LOQ=0.3	Zurfluh et al., 2014
0.5 g oil loaded on double bed SPE 1 g 10% SiAg + 0.5 g Na ₂ SO ₄ + 6.5 g actSi, MOSH 18 mL Hex and MOAH 25 mL 75:25 Hex/DCM elution	GC-FID on-column injector	LOQ=1	Luisi, 2016
Epoxidized sample into SPE 6 g 1% SiAg, MOSH 8 mL Hex and MOAH 9 mL Hex/toluene/DCM 40:40:20 <i>v/v/v</i> elution	GC-FID on-column injector	LOQ=0.5	Ruiz et al., 2021

Finally, off-line fractionation can also be performed using HPLC, where the outgoing fractions from the HPLC are recovered and injected into GC at a later time. This is suitable for laboratories that do not own coupled instruments, and allows for faster and more robust fractionation than manual methods. If necessary, it is also possible to carry out

further sample treatments on the sample extracts, that may also simply involve a reconcentration before injection into the GC to gain sensitivity.

2.7.5 HPLC-GC interfacing

HPLC and GC can be connected directly, through a transfer line, or indirectly, with the aid of an autosampler. In the first case, the HPLC pump itself pushes the eluent towards the GC, i.e. a switching valve send the eluent either to the waste or to the GC during the HPLC run while, in the second case, the collection is delegated to the autosampler, whose syringe collects the eluate from a flow cell and places it in vials waiting for the following injection into the GC. Transfer/collection occurs only in the elution windows of MOSH and MOAH (Biedermann et al., 2009). Since the fractions of interest may elute in a relatively high solvent volumes (200-1000 μL), it was necessary to find a solution to allow for the transfer of hundreds of microliters. The solution to this need was found in different types of HPLC-GC interfaces that have followed over the years, and whose evolution has already been extensively covered (Grob, 2000; Biedermann & Grob 2012a; Purcaro et al., 2012; Moret et al., 2014a), and mainly concern the use either of a retention gap (RG) or a vaporizing chamber. While the latter is a full-fledged injector, retention gap is a trivial uncoated deactivated fused silica capillary, positioned before the analytical column to which it is connected. Techniques based on the retention gap usually require the use of a solvent vapor exit (SVE) positioned in between the retention gap and the analytical column, which remains open only during the transfer allowing for solvent discharge, thus preserving the detector from contact with huge amounts of solvent vapours (Grob & Biedermann, 1996; Moret et al., 1996). SVE is regulated by a valve, and the transfer line to the valve has an internal diameter greater than the analytical column, so that when the valve is open, the vapours are offered less resistance and preferentially take that path. SVE is instead not necessary when, e.g. in the case of injection with an autosampler, only a small portion of the fractions eluted from the HPLC is injected, generally with a maximum of 50-100 μL . This however leads to a loss of sensitivity, therefore its application is less frequent. Depending on the transfer temperature, the retention gap allows for reconcentration of volatile compound by solvent trapping, while non-volatiles are reconcentrated due to the so-called phase-ratio focusing effect (Moret et al., 2014a). The main coupling interfaces between HPLC and GC for LVI are summarized in Table 1.10, and better explained in the following paragraphs, mainly focusing on those used for mineral oil determination.

Table 1.10. Main HPLC-GC coupling interfaces exploited for mineral oils applications.

Type of interface, name and principle of the transfer technique		HPLC-GC transfer temperature	Retention of volatiles	Optimization required	Advantages	Disadvantages
Techniques based on the retention gap	On-column interface	Conventional (solvent flooding) Below the solvent boiling point	Very good/Solvent trapping	Very easy/Transfer temperature	Allows optimal volatile retention	Requires on-column injector and very long retention gap and doesn't allow transfer of high solvent volumes
		With partially concurrent eluent evaporation (PCEE)	Good/Solvent trapping	Easy/Transfer temperature and HPLC flow rate	Allows volatile retention	Requires on-column injector and 5-10 m long retention gap
	Y-interface	Maily used with PCEE Below the solvent boiling point	Good/Solvent trapping	Easy/transfer temperature and HPLC flow rate	Good retention of volatil/Represents a versatile interface for other applications	Requires 5-10 m long retention gap
Techniques based on the use of a vaporizing chamber	Wire-interface	Above the solvent boiling point in the vaporizing chamber and close to the dew point in the oven	Good/Soaking-effect	Relatively easy/Transfer and oven temperature, and solvent vapor exit (SVE) closure	Allows volatile retention	Requires short coated pre-column/Need for heating source for the vaporizing chamber (e.g. from a second FID block)
	Programmed temperature vaporizer injector (PTV)	Above the solvent boiling point in the vaporizing chamber	Mainly on packed liner	Difficult (several parameters need to be optimized)	Avoids introduction of high-boiling compounds and don't need SVE	Difficult to optimize/ Allows to transfer moderate volumes of solvent

2.7.5.1 On-column interface

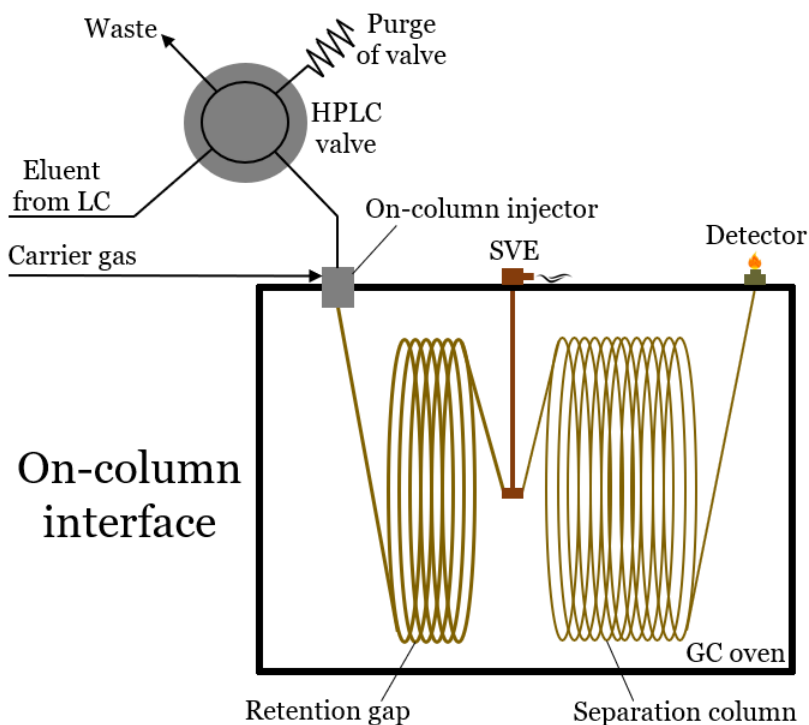


Figure 1.26. Schematic representation of the on-column interface equipped with SVE.

Figure 1.26 displays the configuration of the on-column interface equipped with SVE for large volume injection. The interface is represented by a valve able to send the solvent either to the waste or to the GC, a long retention gap (30-50 m) which connects the valve to the GC column (or more often to the pre-column), and the SVE. During the transfer the eluent is pushed by the LC pump into the retention gap and the carrier gas enters the evaporation zone laterally with respect to the eluent flow, at the on-column injector. The transfer occurs at a temperature lower than the boiling point of the solvent and the carrier gas flow distributes it along the walls of the capillary creating a thin liquid film, a phenomenon called solvent flooding.

RG internal diameter for mineral oil application is usually 0.53 mm, while the length is 5-30 m depending on the volume to be injected. The injection of hundreds of microliters of eluate directly into the analytical column would wet a large part of the stationary phase, preventing it from performing its separative effect and thus broadening and fragmenting the analytes band. The internal lumen of the retention gap gets saturated of solvent vapours quickly, which prevent the liquid film from evaporating simultaneously from the entire surface, thus evaporation occurs exclusively from the rear of the solvent front, from which the carrier gas flow arrives. The more volatile analytes evaporate together with the

solvent and move forward to the point where they meet the solvent in liquid form and recondense. This mechanism, called solvent trapping, continues until the last portion of solvent evaporates, releasing the entire pool of focused analytes into the analytical column (Grolimund et al., 1998; Boselli et al., 1998, 1999). Solvent trapping is very advantageous when samples contain hydrocarbons more volatile than $n\text{-C}_{13}$. On the other hand, higher boiling analytes, when the solvent evaporates, remain condensed where they are, along several meters of retention gap, until the temperature suitable for their release in the gas phase is reached. At this point, they move fast through the retention gap without being minimally slowed down (no phase is present) until they reach the head of the GC column, where they are refocused thanks to the phase-ratio focusing effect, which is enhanced by the phase soaking and the cold trapping effects, and retained until the temperature for their release is reached (higher than that needed in the deactivated capillary) (Grob, 1987, 1991) (Figure 1.27).

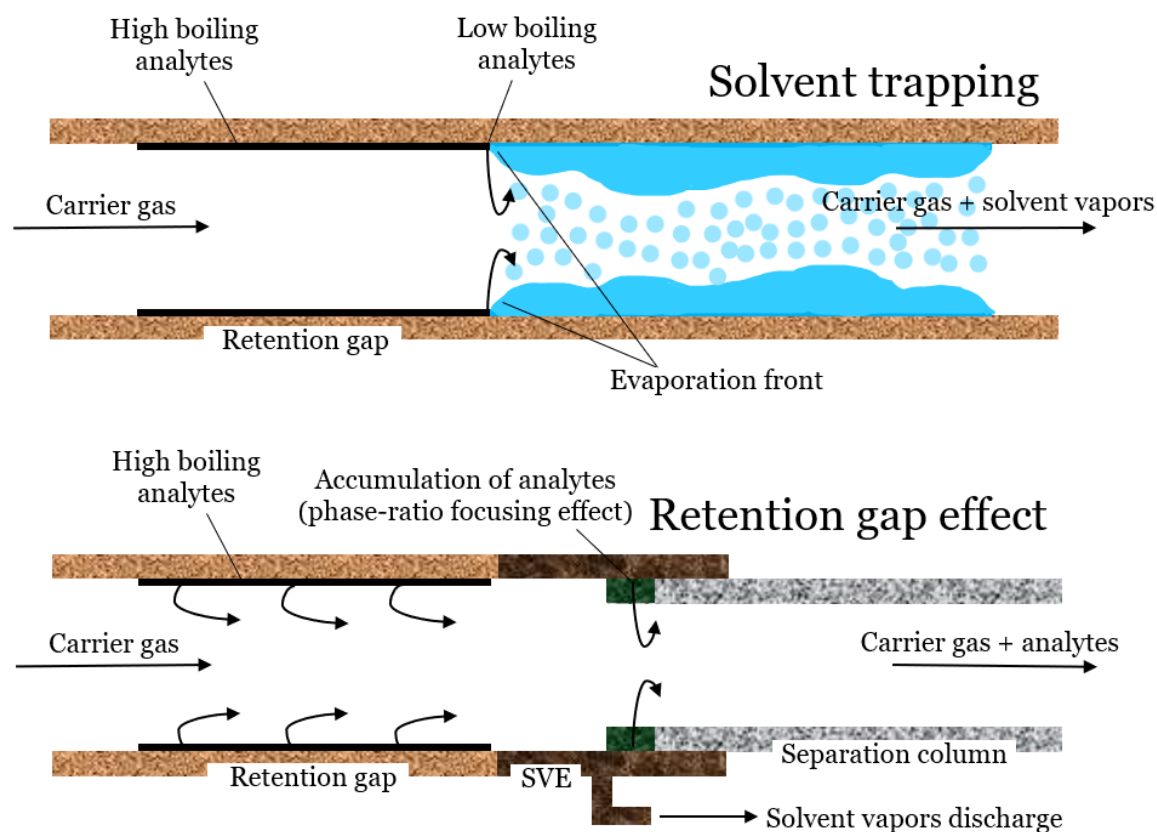


Figure 1.27. Schematic representation of the principles on which the retention gap technique is based. Throughout this process, solvent discharge occurs continuously through the SVE positioned between the retention gap and the analytical column, which has to be closed shortly before all the solvent is removed, to avoid losses of volatile analytes. Continuous solvent discharge is necessary, according to the technique of the partially concurrent

eluent evaporation (PCEE), due to the limited capacity of the retention gap, which otherwise would allow the transfer of only volumes of eluent lower than 100 μL . With PCEE, most of the LC eluent (for example 90%) is evaporated instantaneously during transfer, leaving only a small part of it into the retention gap in liquid form. In this way the length of the retention gap can be reduced, or fractions of greater volume can be introduced. The disadvantage of this technique is that it requires the optimization of some parameters, for example the solvent flow rate and the speed of solvent evaporation (which depends on the settled temperature). The transfer rate must slightly exceed the evaporation speed and the length of the retention gap be adjusted to the volume of the LC fraction to be transferred.

The only problem with this configuration is a memory effect equivalent to 0.5-3% of the previous transfer since, due to the slow transfer of the HPLC eluent, when the transfer stops the last droplets of the fraction go back to the transfer line, due to capillary forces and also driven by the carrier gas, remaining there until the following run (Biedermann & Grob, 2009c). The Y-interface, explained later, was developed to solve this problem.

2.7.5.2 Y-interface

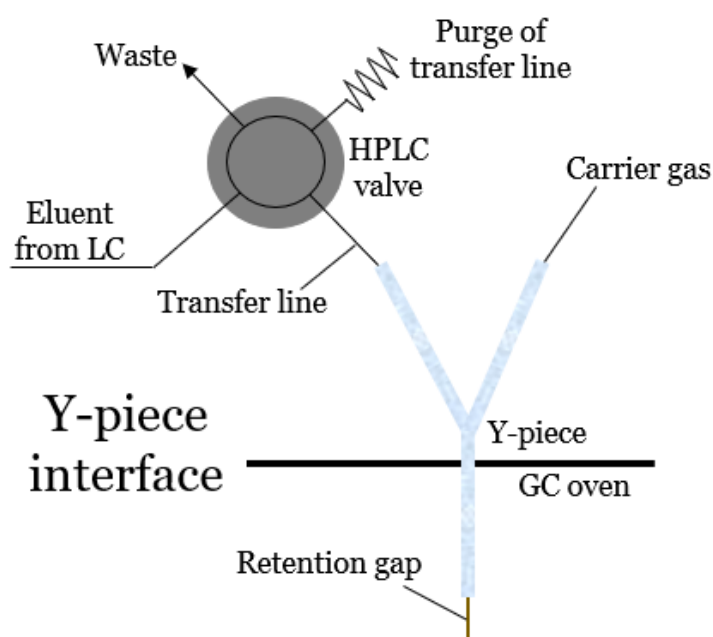


Figure 1.28. Schematic representation of the Y-interface.

In 2009, with the publication of the LC-GC-FID method that became the reference for the analysis of mineral oils (Biedermann et al., 2009), the Y-interface in fact supplanted all other types of interfaces. From the operational point of view, this interface is basically the

same as the on-column interface, with some small constructive differences conceived in order to solve the memory effect problem encountered with the latter, which was thus minimized below 0.02%. Indeed, differently from the on-column configuration, the transfer line of the eluent from the HPLC and the gas carrier line meet at the level of the arms of a glass Y-piece, while the precolumn is connected to its leg, i.e. the Y acts as an injector (Figure 1.28). In this case, the only residue of eluent at the end of the transfer, which is then backflushed in the transfer line by the carrier gas, derives from the end of the fraction where the analytes of interest should not be present, or at least present in concentrations not affecting the subsequent run (Biedermann & Grob, 2009c).

With the Y-interface, based on the need, conditions like HPLC flow rate, GC temperature and the carrier gas flow rate can be adjusted to perform fully or partially concurrent eluent evaporation (making this interface extremely versatile), even if the latter is always preferred for mineral oil application due to its excellent retention towards volatile compounds, giving quantitative recoveries for compounds from $n\text{-C}_{10}$ onwards. In terms of performance, the Y-interface and the programmed-temperature vaporized (PTV) do not show substantial differences, indeed both are widely used for mineral oil determination. However the Y-interface does not require specific components and it is technically simpler (Purcaro et al., 2013c).

2.7.5.3 Wire interface

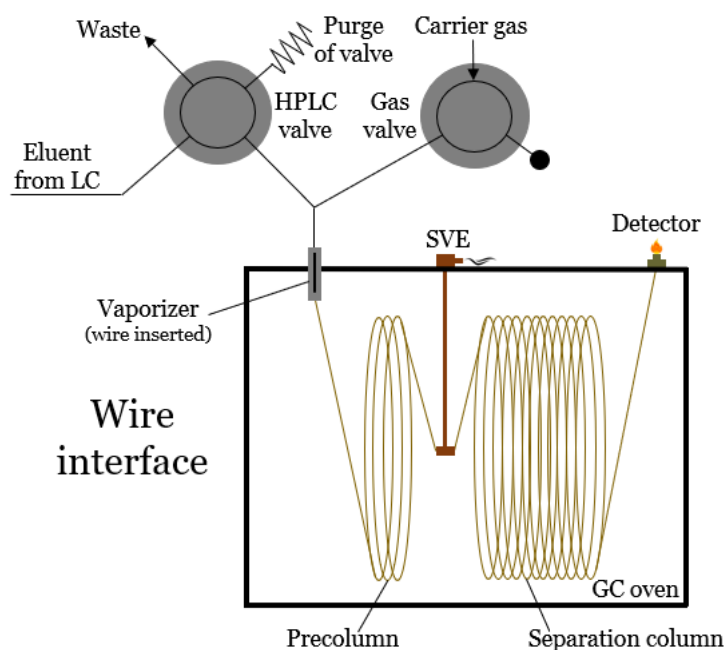


Figure 1.29. Schematic representation of the wire interface.

This interface, which is based on the use of a vaporizing chamber, allows for fully concurrent eluent evaporation, as the LC-GC transfer occurs at temperature by far higher than the solvent boiling point, and was introduced in the field of mineral oil determination to increase the volume of the fraction that can be transferred to the GC by preventing volatile losses. The configuration showed in Figure 1.29 is in a way similar to that of the Y-interface, but the principle is quite different. In particular, it consists of a very short retention gap (less than 10 cm) heated at high temperature (250-350 °C), usually in the heating block of a FID detector, which acts as a vaporizing chamber. During the transfer of the LC fraction, the carrier gas is stopped. To avoid solvent shooting, resulting from violent evaporation, a piece of wire is inserted into the short capillary, from which comes the name of wire-interface (Grob & Bronz, 1995). Solvent vapors are discharged through the SVE due to their expansion (by vapor overflow). A downside to this transfer system is that it does not allow to retain the most volatile components, even though the phase-soaking effect occurring in the retention pre-column mitigate this problem. This effect can be exploited when the stationary phase and the solvent have similar polarity and the column temperature is close to the dew point (temperature limit of recondensation of the vapor phase): under these conditions, the eluent swells the stationary phase, increasing its retention power (the retention power can be increased up to 5 times the normal value). This interface was successfully adopted for the determination of mineral paraffins in vegetable oils (Grob et al., 1997; Wagner et al., 2001b; Moret et al., 2003), and remains a valid alternative with respect to the most commonly used.

2.7.5.4 Programmed-temperature vaporizer interface

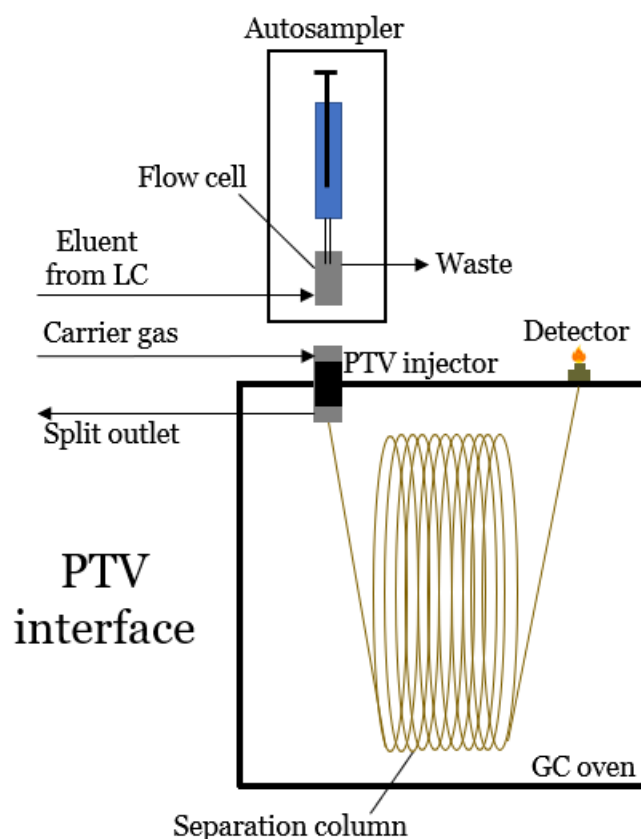


Figure 1.30. Schematic representation of the PTV interface.

PTV is the injector of choice when injecting high solvent volumes, thanks to the possibility to split the solvent and due to the presence of liner packed with adsorbents, which can retain a lot of liquid per unit of internal volume (Hoh & Mastovska, 2008). In addition to that, unlike on-column injection, PTV preserve the system from high-boiling components, whose boiling point is higher than the operating temperature of the GC and would therefore not be expelled remaining in the system. As a disadvantage, given the temperatures necessary to release the analytes adsorbed to the liner, this type of technique is not suitable for thermolabile compounds, as well as for the most volatile ones (below $n\text{-C}_{14}$). On the other hand, with some small modifications, it proved to be able to retain up to $n\text{-C}_9$ (Zoccali et al., 2020).

The common configuration, as reported by Sandra *et al.* (1999), foresees that the eluent from the HPLC flows through a flow cell, from which an autosampler syringe takes out the fraction of interest at the right moment and injects it into the liner of the PTV injector (Figure 1.30). However, the union of the PTV with an on-column interface is possible, and also allows to obtain better performance (Grob, 2000; Biedermann & Grob, 2013). This, in a particular configuration, exploited a modified syringe through which the eluent

continuously flowed, pushed by the HPLC pump. It was therefore the position of the plunger to determine the flow to be directed either to waste or to the PTV injector (Tranchida et al., 2011b). This kind of interface is really common and PTV is popular in many laboratories, therefore it is not surprising that its application also for the analysis of mineral oils in vegetable oils is reported in the literature (De Koning et al., 2004; Tranchida et al., 2011b; Zoccali et al., 2012, 2020).

2.7.6 Gas chromatography and flame ionization detection

The quantification of MOSH and MOAH, previously separated by the HPLC, is obtained with GC equipped with FID detector. Capillary columns with apolar stationary phase of polydimethylpolysiloxanes (PDMS), or slightly polar ones obtained by the addition of 5% of the phenyl phase, are used. Given the high number of compounds, and of structure isomers, this technique is not able to separate every single compound present in the analyzed fraction. This results in chromatograms that show broad, symmetrical and gaussian shaped humps of unresolved peaks. MOSH and MOAH having the same source, i.e. deriving from the same distillation fraction, produce traces distributed over the same retention times, as the result of the corresponding composition of molecular masses. However, MOAH constitute the 15-35% of the total content of hydrocarbons, when present (EFSA, 2012a). FID has a response factor of virtually 1, which is independent of the chemical structure of the compounds eluted, thus providing a signal which is just proportional to the amount of hydrocarbons present, regardless of whether these are paraffins, olefins, aromatics etc. (Weisman, 1998; Wagner et al., 2001a). Actually, the response factor is slightly higher for MOAH than for MOSH, but the approximation is largely acceptable (Biedermann & Grob, 2012a). However, this detector has two main disadvantages, which are the lack of selectivity and sensitivity. Both these problems are partially solved by using sample preparation techniques, such as those previously reported, combined with the presence of a HPLC pre-separation phase, that are intended to ensure that only what needs to be detected reaches the FID. In addition, the experience of the analyst in interpreting the chromatograms, e.g. in case of residual interferences like olefins in refined oils, is of fundamental importance (Biedermann & Grob, 2012b; Biedermann et al., 2020). On the other hand, mass spectrometry (MS) is more sensitive and selective, but quantification is not possible since it can give very different responses even for hydrocarbon compounds of the same mass. This would require to perform a calibration for each individual compound which, given the enormous amount of compounds present, would be not feasible (Biedermann et al., 2009; Biedermann & Grob,

2012a). Anyway, MS can be useful to characterize the contamination and confirm, through specific markers, its petrogenic origin, as discussed below.

2.7.7 Integration, quantification and verification of method performance

As already reported, the chromatographic trace of mineral oils is typical and recognizable by the presence of humps of unresolved peaks in the chromatogram. Thus, MOH are integrated by drawing a straight line from the start to the end of the hump itself. To do so, it is a good practice to overlay the GC run of a procedural blank, i.e. a solvent blank that underwent all the sample preparation steps, to identify and discard background noise due to sample preparation. The presence of a blank also allows to check the trend of the baseline, which could present drifts due to column bleeding.

Signals not related to MOH, such as *n*-alkanes of natural origin or olefin/olefin residues, should not be considered and their area has to be subtracted from the rest of the hump (Figure 1.32). Synthetic hydrocarbons not belonging to MOH, when recognizable, should also be detracted. They comprise POSH, which are oligomers generated during the production of polyethylene, polypropylene and polybutylene, as well as ROSH and ROAH, which are ingredients of hot-melt adhesives. These species are recognizable for their typical pattern, but since the overlap with MOH does not allow their complete separation during integration, their presence must be reported in the final report. About PAO, which are isoparaffins with short main- and long sidechains typical synthetic lubricants, there are conflicting opinions regarding the subtraction of their signal or not.

About data reporting, MOH results can be provided as “total MOSH and MOAH”, considering quantification performed on the total hump, or according to specific molecular mass ranges, expressed by the number of carbon atoms, into which the total area is divided. This convention was based on the fact that, as highlighted by studies on rat and human tissues (Concin et al., 2008; Barp et al., 2014; Biedermann et al., 2015), different molecular mass ranges result in different degrees of accumulation and toxicological relevance. Initially, reference intervals for MOSH and MOAH were extrapolated from the criteria specified by the BfR (BfR, 2011, 2012a), where toxicological data were interpreted setting the first two fractions at *n*-C₁₀₋₁₆ and *n*-C₁₇₋₂₀. The upper limit was set at *n*-C₃₅, based on the range of accumulation evaluated on Fisher rats, and a further cut, on the basis of the molecular weights involved in the migration via the vapor phase, was set at *n*-C₂₅ (BfR, 2012b; Biedermann & Grob, 2012b). Subsequently, with new data available, Biedermann et al. (2017b) suggested to extend the higher fraction up to *n*-

C₄₀, keeping all the other cuts defined up to that point. Finally, the more recent guidelines published by the JRC, in agreement with EFSA, further extended the range up to *n*-C₅₀, in order to reflect the composition of some lubricants distributed on higher molecular weights. With this document, the so-called C-fractions were definitively defined, where cut at *n*-C₂₀ and *n*-C₄₀ were not included for MOAH (Bratinova & Hoekstra, 2019) (Table 1.11).

Table 1.11. Ranges related to the C-fractions and the total hump expressed as elution times of *n*-alkanes [adapted from (Bratinova & Hoekstra, 2019)].

MOSH	MOAH
C-fractions	
≥ <i>n</i> -C ₁₀ to ≤ <i>n</i> -C ₁₆	≥ <i>n</i> -C ₁₀ to ≤ <i>n</i> -C ₁₆
> <i>n</i> -C ₁₆ to ≤ <i>n</i> -C ₂₀	> <i>n</i> -C ₁₆ to ≤ <i>n</i> -C ₂₅
> <i>n</i> -C ₂₀ to ≤ <i>n</i> -C ₂₅	
> <i>n</i> -C ₂₅ to ≤ <i>n</i> -C ₃₅	> <i>n</i> -C ₂₅ to ≤ <i>n</i> -C ₃₅
> <i>n</i> -C ₃₅ to ≤ <i>n</i> -C ₄₀	> <i>n</i> -C ₃₅ to ≤ <i>n</i> -C ₅₀
> <i>n</i> -C ₄₀ to ≤ <i>n</i> -C ₅₀	
Total hump	
≥ <i>n</i> -C ₁₀ to ≤ <i>n</i> -C ₅₀	≥ <i>n</i> -C ₁₀ to ≤ <i>n</i> -C ₅₀

From the practical point of view, the chromatogram of the GC run of either a mixture of *n*-alkanes up to *n*-C₅₀ eluted under the same chromatographic conditions of the sample, or a preconstituted mixture containing only *n*-alkanes relating to the extremes of the C-fractions, is superimposed to the sample, and segmentation of its total area into sub-areas is performed (Figure 1.31). However, as emerged from the summary report of the SCoPAFF (EC, 2022), the intention is to remove the C-fractions for MOAH, returning to the evaluation of their hump in its entirety since, differently from MOSH, no link between certain toxicological effects and their molecular weight could be found. Moreover, there is not always correspondence between the retention of MOSH and that of MOAH (for example, perylene which has 20 carbon atoms elutes together with *n*-C₂₈).

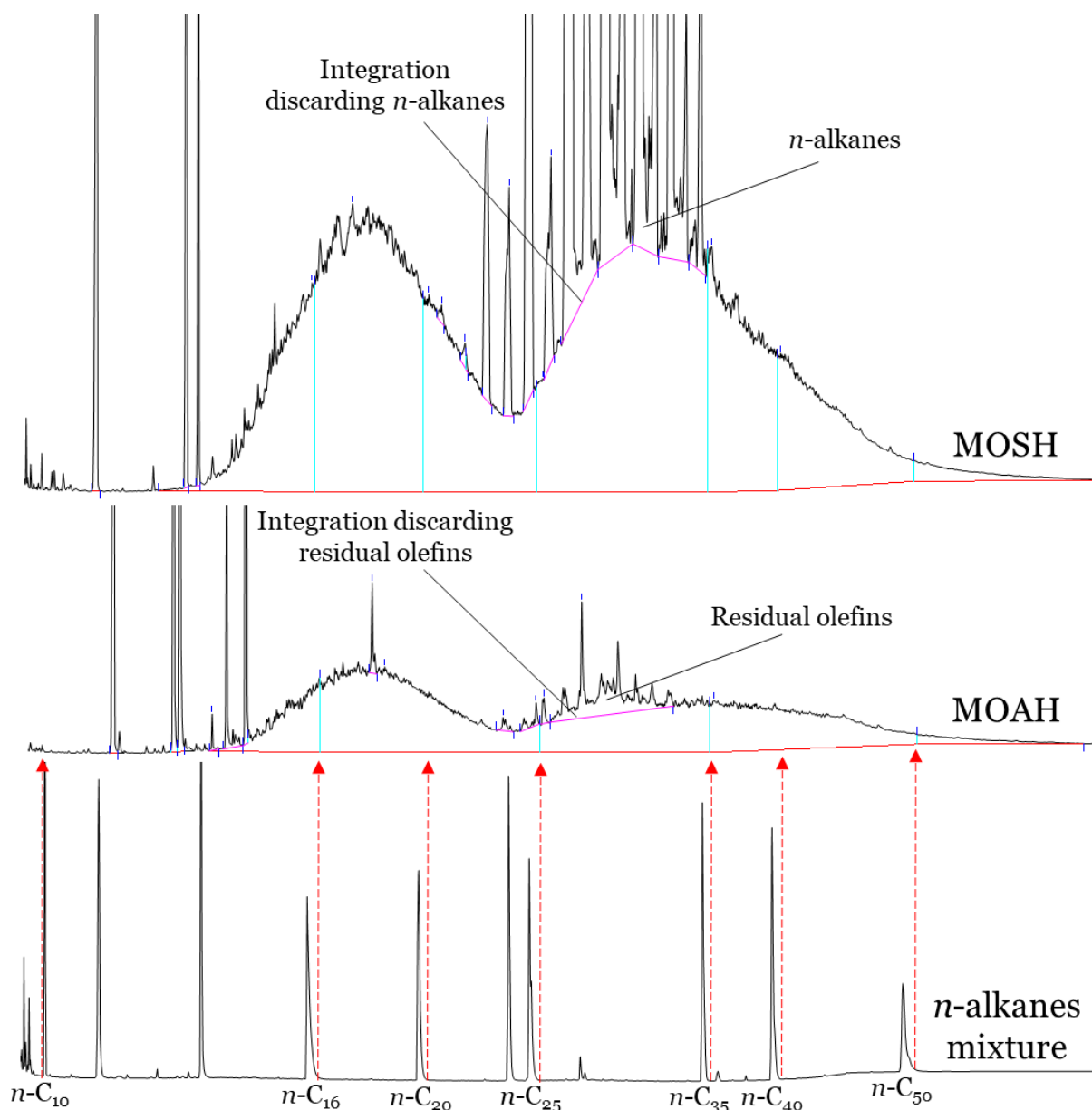


Figure 1.31. Example of integration of the MOSH and MOAH fractions, discarding the interferences and carrying out the division of the total hump into C-fractions. The red baseline comes from a blank run.

Once the areas are obtained, quantification can be performed according to either the internal or external standard method. The former one is usually the method of choice as MOH analysis typically involves several sample preparation steps, not always with specific control of the volumes involved, thus the internal standards added at the beginning of the procedure allow to correct for analyte losses. Nonetheless, if samples are treated exactly the same, with a precise control of the volumes in every single step, also external calibration is feasible. This often makes the analyst lean towards using the internal standard, albeit external calibration may prove useful either as further quality control or when internal standards can not be used due to the presence of sample components co-eluting and interfering with them (Wagner et al., 2001a; Concini et al.,

2008; Tranchida et al., 2011b). Anyway, according to the updated EN16995:2017 method, the internal standards to be used as reference for the quantification of the MOSH and MOAH fraction are CyCy and TBB, respectively. CyCy for MOSH has been chosen as, being not present in nature, the presence of interfering peaks that could distort the results is unlikely, while TBB as, during method validation, provided more quantitative recoveries for MOAH. However, this may depend on the sample preparation procedures, and therefore each method must be evaluated in this respect with recovery tests, as different results can be obtained.

Finally, regardless of the method applied in mineral oil analysis, it must respond to parameters that confirm the reliability of the results. For this evaluation the method has to pass through a validation process. The description for the calculation of these parameters, which are linearity, LOQ, recovery and intermediate precision, is given for example in the Eurachem guide (Magnusson & Örnemark, 2014), while performance requirements for MOSH and MOAH analysis in fats and oils reported in the JRC guidance, related to this parameters, are shown in Table 1.12 (Bratinova & Hoekstra, 2019).

Table 1.12. Performance requirements for MOSH and MOAH analysis in fats and oils [adapted from (Bratinova & Hoekstra, 2019)].

Food category	LOQ-max [mg/kg]	LOQ-t [mg/kg]	Rec [%]	Intermediate precision [%]
Fats/oils	2	0.5	70-120	20

2.7.8 Confirmation techniques: mass spectrometry and comprehensive two-dimensional gas chromatography

Given its high selectivity, MS combined with LC-GC allows the identification of specific components in the mixture of hydrocarbons which are markers of the contamination by mineral oils. These markers are hopanes, steranes and the isoprenoids pristane and phytane. These compounds derive from biological and chemical transformation of organic matter in the subsoil and therefore are specific indicators always present in petroleum derivatives. In some cases, other kind of markers, like 2,6-diisopropylnaphthalene (DIPN) for recycled paperboard and dibenzothiophenes (DBTS) for refined mineral oils, also allow to identify the possible source of contamination (Populin et al., 2004; Biedermann & Grob, 2015; Zoccali et al., 2016; Biedermann et al., 2017a; Spack et al., 2017). More recently, also a pool of 16 markers were proposed as

tracers of possible MOAH contamination (Jaén et al., 2021). The verification of their presence, obtained by extracting the signals related to their specific fragments from the total MS signal, is an important confirmation, since the FID is not able to provide qualitative information, i.e. MS should reduce the possibility of getting false positive results. DIPN shows a peculiar pattern in GC-FID, which is easy recognizable, but confirmation, mainly when it is present at low concentrations, requires the use of MS (Biedermann et al., 2017a). The EN 16995:2017, being to date the last published reference method, also recommended the use of MS in case of suspected interference from natural sources. Moreover, MS can also provide further information unraveling the composition of the mixture, by indentifying specific compounds or classes of compounds selecting specific masses (Koning et al., 2004; Spack et al., 2017; Jaén et al., 2021). For example, Carrillo et al. (2022b) identified mass to charge ratio (m/z) 71 and 82 as typical fragments deriving from *n*-alkanes/isoalkanes and naphthenes, respectively. Similarly, the fragments with m/z 68 and 82 were also referred to naphthenes by Biedermann et al. (2015). However, the main issue related to the use of some ions comes from their lack of specificity, which could lead to false positive results. In fact, Spack et al. (2017) proposed a GC-MS method to confirm the presence of MOSH and MOAH, trying to rule out potentially deceptive interference which are non-discriminable with GC-FID. To do so, the authors exploited fragments with m/z 43, 57, 71 and 85 for MOSH and m/z 91, 105, 119 for MOAH, even though the reliability of these fragments was contested, as they also originate from endogenous interferences present in food, such as squalene, carotenoids, sterenes etc. (Biedermann et al., 2017a).

Although MS detector is able to provide more detailed information on sample composition, it gives its best when associated with separative techniques with a higher resolution power like comprehensive two-dimensional GC (GC×GC) (Biedermann and Grob, 2009c; Tranchida et al., 2013; Biedermann et al., 2017b; Nolvachai et al., 2017). GC×GC is currently the best technique to confirm data from HPLC-GC-FID (Biedermann et al., 2017b) and to achieve an in-depth characterization of MOH (Biedermann & Grob, 2019; Sdrigotti et al., 2021). In fact, GC×GC-MS was indicated also by EFSA and JRC as election technique for confirmation and characterization of the mineral oils fractions (EFSA, 2012a; Bratinova & Hoekstra, 2019) even though, to date, no validated and standardized methods exists (Hochegger et al., 2021).

With GC×GC it is possible to reach higher resolutions as the separation is performed with two GC capillary columns, connected in series, having different stationary phase, apolar and mid-polar, thus exploiting two orthogonal separation mechanisms within a single run

(Liu & Phillips, 1991), allowing in this way a group type separation (Vendeuvre et al., 2007). This becomes of fundamental importance, for example, when dealing with toxicology. In MOH application, the apolar one is usually coated with ~100% PDMS, similarly to the one used in GC-FID analysis with the current reference method (Biedermann et al., 2009), and therefore separates the hydrocarbons predominantly on the basis of the molecular mass, and thus volatility. The medium-polar one is generally coated with about 50% PDMS-50% phenyl, and always involves mechanisms of separation based on the boiling point, but also on polarity and molecular conformation. More polar columns, which could better discriminate the MOAH fraction, are not usable due to their narrower operating range, which would not allow to reach high temperatures for the elution of hydrocarbons up to n -C₅₀. The columns order is not established a priori, as it depends on the type of application and for which of the two fractions, MOSH or MOAH, a more informative characterization is needed. MOAH are better unravelled when using a medium polar column in the 2nd dimension, and this configuration was the first explored (Biedermann & Grob, 2009a). However, according to subsequent investigations (Van der Westhuizen et al., 2011), currently the mid-polar stationary phase is preferably used as the first column (reverse configuration). In this way MOSH are better characterized (Biedermann et al., 2015), achieving separation between paraffins and isoalkanes from the naphthenes and increasing the capability to resolve chemical classes otherwise problematic to separate using the “normal” setup, e.g. MOSH from POSH, while still maintaining an adequate level of characterization for MOAH, resolving the latter into subclasses with respect to aromaticity and alkylation (Sdrigotti et al., 2021). Information about the position of these alkylations and their type, again important for a better understanding of the toxicity of these substances, are however not obtainable with either of the two configurations.

From a technical point of view the first and second columns, nominally 1st and 2nd dimensions, are connected via a modulator, capable of recollecting small portions of carrier gas arriving from the first dimension, possibly containing few analytes, and releasing them every few seconds (generally 4-6 s) to be eluted in the second dimension, resulting in a high resolution power, but also in a sensitivity enhancement thanks to the refocusing effect achieved during modulation (Biedermann & Grob, 2009a; Tranchida et al., 2011a). Resolution is certainly also a direct consequence of the detector, indeed when coupled with GC×GC, MS should have high acquisition rates in the range 10-100 Hz, which is why a time-of-flight (TOF) is often used (Niyonsaba et al., 2019; Polyakova et al., 2022). The modulator can be a thermal modulator, if it uses alternatively a jet of cold and

hot gas to focus and re-mobilize the fraction being modulated respectively, or a flow modulator, if it uses a connection between the first and the second dimension having a storage loop with a particular geometry able to exploit carrier flows to trap and release the fraction of interest (Duhamel et al., 2015; Zoccali et al., 2017). The first one is generally preferred for easier use and optimization (Boswell et al., 2020). The concept behind GC×GC is that if some analytes co-elute from the first column there is hope that, using a different separation mechanism, they are separated by the second one. For this reason, the peak capacity in comprehensive GC is assumed to be the product of the individual peak capacities of the two dimensions (Vendeuvre et al., 2007). However, according to this mechanism, while the length of the column in the 1st dimension can be of the order of magnitude of those used for conventional GC, and therefore between 10 and 20 m, the column of the 2nd dimension must be 1-2 m long, in order to allow the analytes to be eluted within the modulation window. If not, the overlap of two successive modulations is possible. This means that such a short column therefore requires a reduced diameter and stationary phase dimension, to equally allow high resolution. The final result is the obtaining of two-dimensional (2D) plots, where the elution times in the 1st and 2nd dimension are respectively found in the abscissa and ordinate axes (Purcaro et al., 2016a). Despite the high resolving power, the separation between MOSH and MOAH is not completely achievable even with this technique. Therefore, the separation has to be carried out upstream by LC, and then MOSH and MOAH are injected separately. Indeed, four and five ring naphthenes (e.g. steranes, hopanes, bicyclic sesquiterpenes etc.) tend to co-elute with highly alkylated one to three ring aromatics, thus no complete separation is obtainable without pre-fractionation (Biedermann & Grob, 2010, 2015; Purcaro et al., 2013a, b). Pre-separation is also related to the abundance of MOSH with respect to MOAH, the signal of the latter otherwise dominated and covered from that of the other fraction (Biedermann & Grob, 2009a). LC separation can either be performed off-line or on-line, with the first approach being the most applied due to the additional complexity related to a direct connection between the two instruments which requires the removal of large amounts of solvent. Indeed, only few works can be found in the literature exploiting on-line coupling (Zoccali et al., 2015b; Bauwens et al., 2021).

Apart from that, the possibility to characterize the degree of refinement of MOH and to distinguish them from synthetic hydrocarbons such as POSH, which in HPLC-GC-FID is not possible, turns out to be a big plus (Biedermann & Grob, 2015; Lommatzsch et al., 2016). On the other hand, for certain applications, the potential of this technique in the field of mineral oils still remains limited, and this happens mainly when dealing with

contaminations in complex food matrices (like vegetable oils), as well as when dealing with highly alkylated or partially hydrogenated mineral oils. These situations generate 2D plots with poorly resolved clouds, showing little structure, from which it becomes difficult to extrapolate qualitative information. MOAH of this type, with chemical characteristics attributable to more saturated compounds, are eluted in areas of the plot that are not consistent with those relating to compounds with a comparable number of aromatic rings, distorting the results and fooling the analyst. In these situations not even the use of MS is of great support as the extensive fragmentation, which is typically experienced with hydrocarbons when using an electron impact (EI) source at 70 eV, the lack or little abundance of the molecular ion, together with the lack of references in the NIST database, often do not allow a unique identification of single compounds (Polyakova et al., 2022). About detection, besides MS, GC×GC can be equipped also with FID. In this case, the instrument foresees either the existence of two separate channels connected with the two different detectors (Bauwens et al., 2022), or the carrier flow from the 2nd dimension to be splitted to be sent simultaneously to both detectors (Boswell et al., 2020), with priority to the FID which is less sensitive (Figure 1.32). In this way, based on the specific need, as has already underlined, the MS allows to obtain qualitative information, while the FID allows for quantification, even though its use for this last purpose has rarely been reported. Some quantification attempts have been made, even with good agreement with the HPLC-GC-FID data (Biedermann & Grob, 2009c; Purcaro et al., 2013b; Bauwens et al., 2022), but the main source of variability derives from the impossibility, in the 2D plot, to discard the peaks that are above the hump of mineral oils without including in the subtraction also useful area relating to the latter, as operations of this type are not included in most of the softwares (Sdrigotti et al., 2021). Only recently some steps have been taken in this direction, with the development of a prototype software able to carry out these subtractions and to quantify the hump of mineral oils automatically (Bauwens et al., 2021), which was recently used with good results for the analysis of mineral oil contamination in fish feed (Bauwens et al., 2022), and later also validated on different food matrices (Bauwens et al., 2023). The representation of a generic GC×GC system is reported in Figure 1.32.

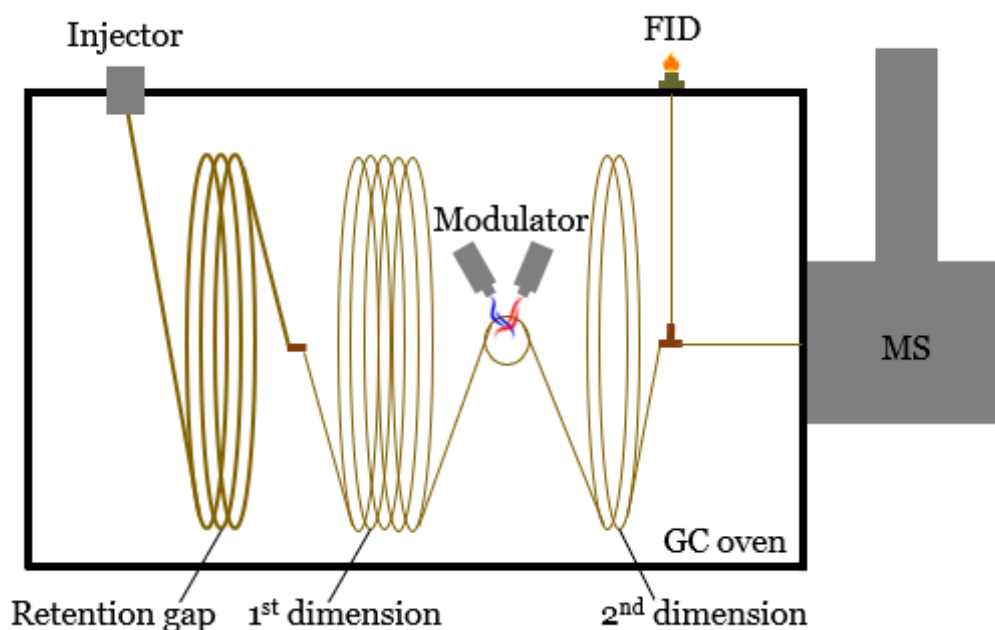


Figure 1.32. Schematic representation of a GC×GC-FID/MS with thermal modulation.

Specifically talking about applications of MS detection and GC×GC separation in the context of vegetable oils, only few works can be found. One of the first was that of Populin et al. (2004) which, as anticipated before, using a LC-LC (off-line)-GC-MS could verify the occurrence of a fixed ratio of $\sim 3.4\%$ between the area of the hopanes and that of MOSH able to confirm the petrogenic origin of the contamination. This findings were then exploited by Zoccali et al. (2016), who used a LC-LC (SiAg)-GC-FID/MS, where the dual detection was intended precisely to verify the presence of hopanes. More recently, GC-MS was used with the different purpose of tracing back interfering signals that persisted in the MOAH fraction after epoxidation, eventually identified as derivatives of phytosterols (Nestola, 2022). About comprehensive GC, a characterization of the aromatic hydrocarbons present in vegetable oils and fats (sunflower oil and margarine) was obtained in 2009 using a LC (off-line)-GCxGC-FID/MS in the normal configuration. Thanks to MS, and the elution of an appropriate pool of standards, it was possible to define with some degree of approximation different sectors in the GC×GC plot to characterize MOAH by ring number and alkylation degree, while the presence of the FID allowed to estimate the relative abundance of each group. MS allowed also to identify olefins like squalene and carotenoids, as well as sterenes derived from edible oil refining (Biedermann & Grob, 2009a). From the same authors again another off-line approach, this time with GC×GC in reverse configuration, was used to recognize and characterize the nature of residual interferences after epoxidation visible in the HPLC-GC-FID chromatogram of different oils being hazelnut oil, olive pomace oil, grapeseed oil and

extra virgin olive oil. Interferences seemed to derive mainly from sterenes and squalene derivatives (isomerized squalene), both as the result of the refining of vegetable oils. Thanks to the separation power of the comprehensive GC, three main different areas of the plot (red circles in Figure 1.33) were identified as the areas in which these interferences were located. The use of MS allowed a first evaluation of the samples and identification of these compounds in the total ion chromatogram (TIC), and then the extraction of specific ions typical to different olefins (squalene, squalene derivatives, sterenes, steradienes) having m/z 137, 158, 253, 380, 396 and 410, to be exploited in selected ion chromatogram (SIC) for a better interpretation of the 2D plot, thanks to the enhanced contrast with the background (Biedermann et al., 2020).

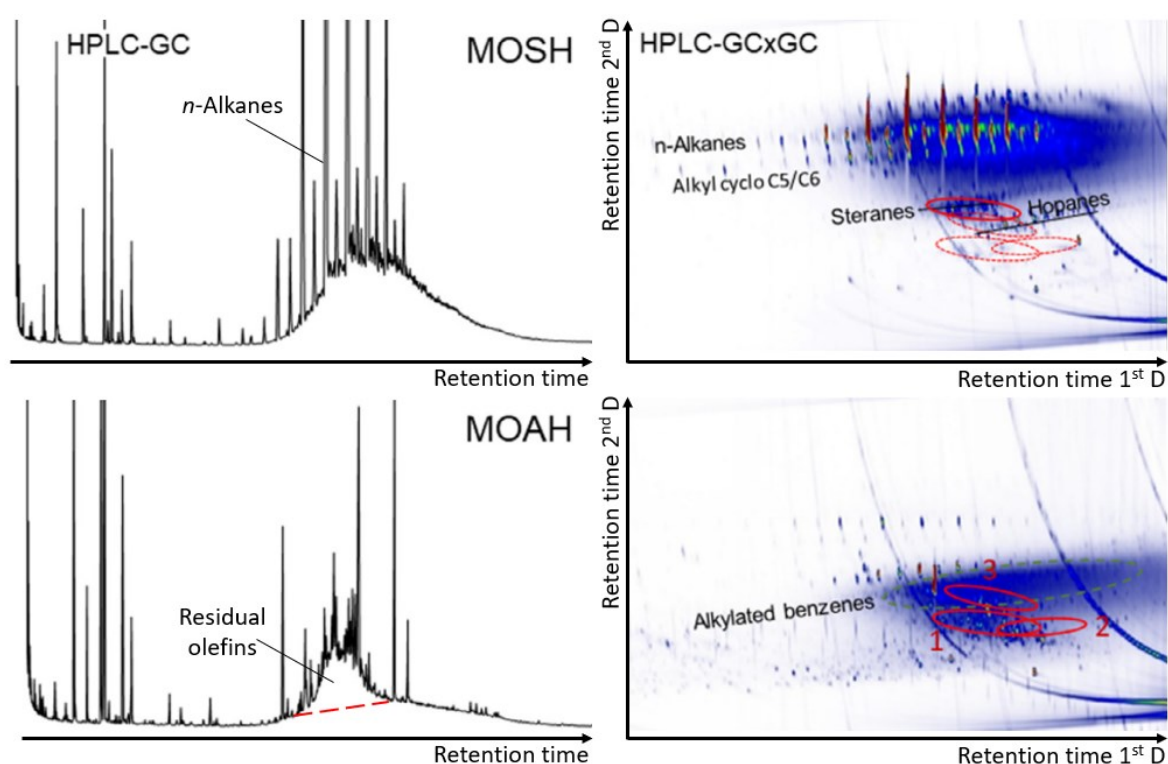


Figure 1.33. Examples of HPLC-GC-FID chromatograms and GC×GC-FID plots of the MOSH and MOAH fractions of an olive pomace oil, showing the difference in the analytical response obtainable with both techniques. Greater characterization was obtained with the GC×GC where residual olefins, assumed from the HPLC-GC chromatogram, were confirmed and highlighted with red circles [adapted from Biedermann et al. (2020) with permission of Elsevier].

Albert *et al.* exploited the same approach for sunflower and palm oil, using the same m/z ratios together with m/z 536, characteristic for carotenes, again to trace olefins residues, while introducing m/z 119, selective to alkylated mono aromatic species (Albert et al., 2022). Finally, GC×GC-MS was also used to identify certain classes of compounds which are preferentially removed from sunflower and palm oil, cocoa butter and coconut fat, in the deodorization step occurring during their refining treatment, both from MOSH and

MOAH fractions. The great separation power of comprehensive GC, together with MS, allowed also in this case to isolate and identify the different classes of compounds subject to removal, and to highlight them using SIC (Stauff et al., 2020).

2.7.9 Official reference methods

Although mineral oils have been studied for decades, only two official methods are available for their determination in vegetable oils. However, in light of the latest updates by JRC (Bratinova & Hoekstra, 2019), BMEL (2020), LAV & BLL (2021) and SCoPAFF (EC, 2022) they are now obsolete as their performance are not aligned with the required LOQ of 2 mg/kg for MOAH.

The first of them is the ISO 17780:2015 method, which has a field of application limited to aliphatic hydrocarbons. Principle of the method is the off-line isolation of the MOSH fraction on a SiAg column and its following analysis by GC-FID with on-column injection (2 μ L). No other sample preparation steps for interferences removal are envisaged. This method, from an international validation, resulted suitable for contamination in the range 50-1000 mg/kg (ISO 17780:2015; Lacoste, 2016).

The other one is the EN 16995:2017, promoted by the Institut des Corps Gras (ITERG), aimed at the analysis of both MOSH and MOAH and based on the use of the on-line HPLC-GC-FID platform coupled via Y-interface for LVI. In this case, the sample is injected just after dissolution (some additional steps are foreseen for insoluble or water-containing fats), adjusting the injection volume according to the amount of endogenous interferences present to avoid overloading of the chromatogram. Clean-up steps involving Alox and epoxidation, as well as enrichment on actSi column, were reported to be optional and so their application is at the analyst's discretion. In this case, from inter-laboratory validation, the method proved to be suitable above 10 mg/kg.

In the last years, the focus was on introducing additional clean-up steps in the EN 16995:2017 method to lower the LOQ, for both MOSH and MOAH, from 10 mg/kg to 1–2 mg/kg. Recently, a further interlaboratory study for the revision of the EN 16995:2017 method, based on the DGF C-VI 22 (20) method that was previously validated among different German laboratories, was carried out. In this case, both the enrichment step by saponification as well as purification steps aimed at the MOSH and MOAH fractions, by elution through Alox and epoxidation respectively, were an integral part of the procedure. The method was successfully validated, resulting in a LOQ of 3 mg/kg for MOSH and 2 mg/kg for MOAH. At present, the method was sent to the International Organization for Standardization (ISO) for approval.

2.7.10 Uncertainty of results: limit of quantification and law limits

One of the main problems related to the analysis of mineral oils in complex matrices such as vegetable oils is the uncertainty related to the results. In this regard, it is not uncommon for different laboratories to provide different results referable to the same sample, even with contamination at relatively high level (which decreases the incidence of interference due to any external factor). An evident example is provided by the results of different proficiency tests (PTs) that have taken place over the years, some of which were reported in the previous paragraphs. One of the first was organized by the JRC in 2008, concerning the analysis of mineral oils in sunflower oil at levels between 100 and 350 mg/kg and involving 55 laboratories, asked to use their in-house method of analysis (Karasek et al., 2010). The range of results provided was very wide, and even after discarding outliers (20% of total), the relative standard deviation (RSD%) was still 26%. The lack of harmonized and validated protocols for sample preparation was surely one of the causes of poor alignment among laboratories, but considering that in those years mineral oils didn't have the attention they have now, also little knowledge of the subject by the analysts, especially when interpreting the chromatograms, could be the cause of wrong quantifications. With the aim of reducing this variability, since 2012 ITERG organized three collaborative trials annually. The purpose was to instruct and subsequently select international expert laboratories about the application of a specific off-line procedure to be validated, which indeed was later proposed as ISO reference method for the analysis of MOSH in vegetable oils (ISO 17780:2015). Considering as acceptable an RSD% of 25%, the laboratories were able to quantify lower concentrations, which allowed to define the applicability of the method above 50 mg/kg of MOSH (Lacoste, 2016), value in accordance with the only legal limit ever applied to food following the Ukrainian sunflower oil scandal (Regulation (EC) 1151/2009). In this case, in addition to the use of a specific procedure for which the laboratories were trained, the achievement of this value was allowed by giving specifications also regarding the way to integrate the *n*-alkanes of natural origin. However, based on the toxicological evidence (EFSA, 2012a), a method with a limit of applicability of 50 mg/kg was not fit for purpose. Furthermore, no reference was present for the determination of the more toxic aromatic fraction. A new reference method, currently the only one available, was then proposed in 2017 for the analysis of MOSH and MOAH in vegetable oils and foodstuff on basis of vegetable oils (EN 16995:2017). In this case, indication was given for optional application of sample purification procedures, aimed at the removal of *n*-alkanes and olefins, as well

as to perform sample enrichment. This method also introduced the concept of using MS as confirmatory analysis for the mineral origin of the contamination. The LOQ, determined through a ring test organized in 2015 by ITERG, and always considering acceptable an RSD of 25%, resulted in 10 mg/kg for both fractions. This LOQ was later reconfirmed in 2018 in another collaborative study by ITERG, regarding MOSH and MOAH determination in additives, pre-mixtures, feed materials and vegetables oils (EN 17517:2021). This level of sensitivity could be considered a positive result, if compared with the previous evaluations, but not when considering the requested limit of 2 mg/kg or lower. Therefore, work was done in the last years to implement the EN 16995:2017 method especially in terms of sensitivity, which seemed to be the missing piece, and a further collaborative study was carried out. In this case, sample enrichment and olefin removal were considered mandatory, and a LOQ of 3 and 2 mg/kg, for MOSH and MOAH respectively, was finally reached.

By improving sample preparation, together with laboratory experience, it was therefore possible to reach lower LOQ. However, sample preparation procedures and the integration remain responsible of high data variability. Instead, instrumental analysis, when properly optimized, has shown to have an irrelevant effect on the final results (Biedermann & Grob, 2012a), even if MOSH and MOAH separation is performed with off-line techniques (Fiselier et al., 2013). As regards the preparation of the sample, often the cause of the variability turns out to be the procedure itself, rather than the sample manipulation (which in any case must be considered). From the previous paragraph it should be clear as the complexity of the oil matrix does not always allow direct analysis of the sample due to the presence of interferences. In those cases, it is almost mandatory its pre-treatment for their removal. However, the cost of obtaining an interpretable chromatogram is often the loss of compounds of interest. For example, the passage on Alox showed to possibly determine also isoalkanes losses from 5% to 20%, based on the degree of activation of the absorbent and the length of their carbon chain (Fiselier & Grob, 2009; Fiselier et al., 2009a). Epoxidation of aromatic compounds determines losses from 20% to 40%, depending on their number of rings and presence of compounds more susceptible to oxidation (e.g. thiophenes), reaction environment (more or less polar), degree and type of unsaturation of the fatty acids present in the matrix, origin and type of olefins present, etc. Sometimes the reaction does not reach completeness leaving olefinic residues, or can bring to artifact formation, which can be exchanged for mineral oils causing an overestimation of the results (Biedermann et al., 2009; Nestola & Schmidt, 2017; Biedermann et al., 2020). Also, the presence of polyolefin from plastics can be

mistaken for mineral oil, distorting the analysis response. Both these cases would call for the need of confirmatory analysis exploiting GC-MS and GC×GC-FID/MS (Biedermann & Grob, 2015; Biedermann et al., 2017b, 2020; Nestola, 2022), but their validation is still missing (Sdrigotti et al., 2021). The saponification step to achieve sensitivity adds variability for the simple fact that the handling of the sample increases significantly. Furthermore, internal standard partition between the different phases involved in this step, affects the quantification (Nestola, 2022).

A significant source of variability is also introduced during the integration of the chromatograms. MOH appear as humps of unresolved peaks which cover a wide range of retention times, unlike isolated compounds that appear as resolved peaks of short amplitude. Thus, the positioning and the inclination of the baseline, trying to consider the blank run as a reference, can determine to obtain results that differ from each other even by 30%, in worst cases. Moreover, a blank run without the presence of the matrix does not generate the same background noise, and still remains an approximation. Things get even more complicated in the presence of baseline drifts due to column bleeding when the GC oven ramp reaches its maximum temperature, especially for hydrocarbon fractions with high molecular weight that elute in that area. For this reason, baseline drift is a parameter to be kept under control in accordance with the updated EN 16995:2017 method. In addition, at low concentrations even closer to the LOQ, the contribution of the background noise begins to become more and more significant (Biedermann & Grob, 2012b). The incidence of the background noise is matrix dependent and mainly affects contaminations distributed over wide ranges of molecular mass, i.e. for the same area, referred to the same amount of analyte, a narrower range creates a signal that deviates more from the baseline and is more easily distinguishable. For the latter, LOQ is lower (Figure 1.34).

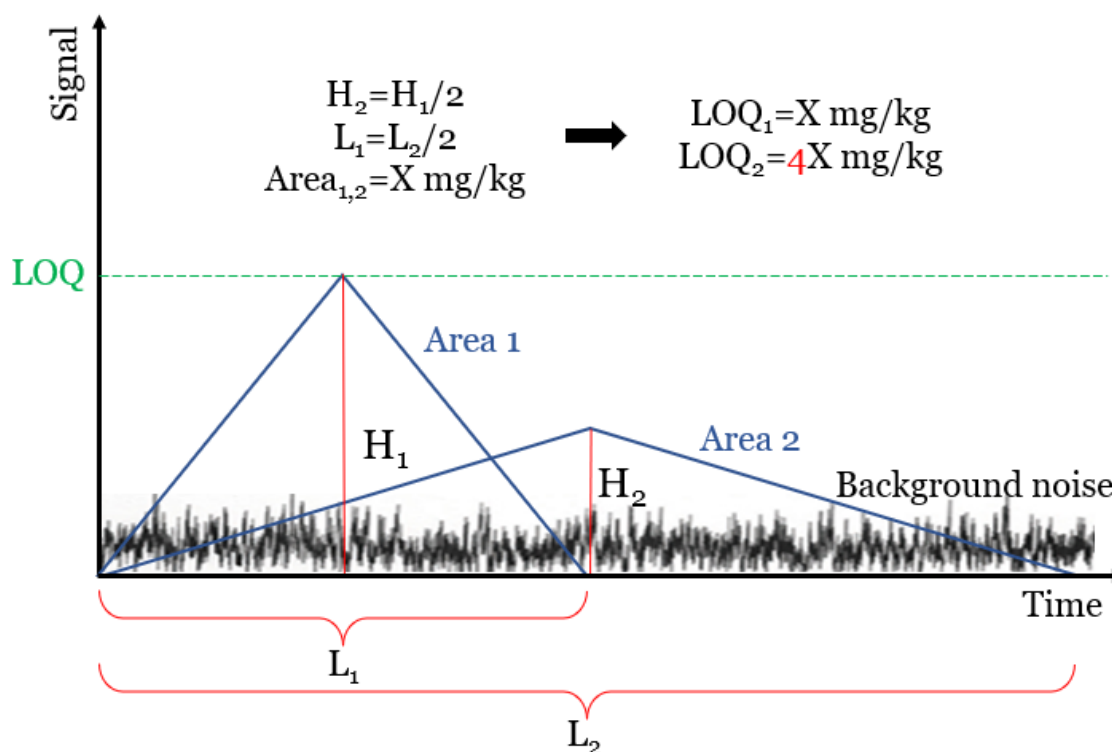


Figure 1.34. Schematic representation of the incidence of the distribution of contamination in the definition of the LOQ.

The definition of standard integration rules, as reported in the updated EN 16995:2017 method, can be of help in reducing the variability related to this step. This is even more important when the analyst decide not to proceed with the chemical removal of the *n*-alkanes and olefins, in case their quantity is limited and it is possible to identify the profile of the MOH hump, therefore discarding their areas during integration, or when facing with other contaminants co-eluting with MOH (POSH, ROSH, ROAH, PAO). Anyway, based on the extent of their presence, also this step can lead to a different degree of approximation of the results (Neukom et al., 2002), which is linked to the analyst subjective interpretation of the chromatogram based on his experience, with consequent addition of uncertainty. Finally, even with a proper integration, some interferences may also fall at the elution time of internal standards used for the quantification, distorting the final results, which often happens in the presence of dirty reagents such as *m*CPBA (Nestola, 2022).

Last but not least, the variability of the data also originates from the definition of LOQ. The definition of a target LOQ, as happened with the publication of the JRC guidance (Bratinova & Hoekstra, 2019), should not leave room for misunderstandings, as it presupposes the existence of a common approach to determine it, and consequently also to report the data, i.e. define the use of a lower, medium or upper bound approach to

express data below the LOQ. Unfortunately, currently a common convention is lacking, and this creates confusion and mismatch between results provided by different laboratories.

To conclude, when setting law limits, all these factors need to be considered. The toxicological aspect is surely the first and most important, however the intrinsic limits of the analytical methods, in a particular application such as that of mineral oils, cannot be ignored. It would be counterproductive to impose certain limits when the latter does not allow their achievement with adequate reliability, giving rise to possible disputes and to unfair treatment from large-scale retail towards vegetable oils producers. The last collaborative study by ITERG was very important to take stock of the situation and evaluate the analytical level reached so far by the laboratories, which has undoubtedly improved over the years. However, although considered acceptable, the uncertainty associated with the results is still significant at the level of the 2 mg/kg, and this must be taken into account before reaching the definitive definition of a legal limit.

AIM OF THE WORK

The first main purpose of this PhD project was the implementation, optimization and, when possible, validation of rapid and solvent saving analytical protocols for the evaluation of mineral oil in vegetable oils, meeting the performance criteria required by the guidelines published by the Joint Research Centre (JRC) of the European Commission (Bratinova & Hoekstra, 2019). In particular, the aim was to implement sample preparation protocols having adequate concentration factors to reach the required quantification limits, while achieving reproducible results. Protocols based on microwave-assisted saponification, subsequent epoxidation and (when necessary) elution through activated Alox, followed by on-line LG-GC-FID analysis, were optimized and possibly validated. Also GC×GC-FID/MS was exploited in certain situations to investigate in more depth, from a qualitative point of view, the composition of the mineral oil contaminations.

These methods were then exploited to analyze samples coming from samplings carried out along the extra virgin olive oil production chain, as well as the lampante olive oil and the olive pomace oil refining chains, considering every single step from the olives to the finished oil, with the aim of identifying the critical ones in the context of mineral oil contamination. This was to collect occurrence data on background contamination levels (useful for the definition of legal limits), to identify the main sources of contamination and to define their impact on the overall contamination, with the ultimate goal to provide information aimed at minimizing the risk of contamination.

EXPERIMENTAL WORK

3 Optimization and validation of microwave assisted saponification (MAS) followed by epoxidation for high-sensitivity determination of mineral oil aromatic hydrocarbons (MOAH) in extra virgin olive oil

This chapter has already been published in: Menegoz Ursol, L., Conchione, C., Srbinovska, A., & Moret, S. (2022). Optimization and validation of microwave assisted saponification (MAS) followed by epoxidation for high-sensitivity determination of mineral oil aromatic hydrocarbons (MOAH) in extra virgin olive oil. *Food Chemistry*, 370, 130966.

3.1 Introduction

Mineral oil hydrocarbons (MOH) are a class of environmental and processing contaminants of petrogenic origin consisting of complex mixtures of thousands of hydrocarbon isomers. Based on their chemical structure, all these compounds can be divided in two subgroups which are the mineral oil saturated hydrocarbons (MOSH) and the mineral oil aromatic hydrocarbons (MOAH). The first group includes paraffins (linear and branched alkanes) and predominantly alkylated naphthenes (cyclic alkanes), while the other includes mono- or polyaromatic compounds with an alkylation degree greater than 98% (Bratinova & Hoekstra, 2019). The different classification of these compounds is also based on their toxicological relevance and, although data are still controversial, the latest evidence confirm MOSH to accumulate in human organs and tissues, and MOAH to carry out carcinogenic, genotoxic and mutagenic actions, with particular reference to polyaromatic species with 3-7 rings (EFSA, 2012a; EFSA, 2019), and therefore being of greater concern for consumer safety. The non-polar character conferred by their chemical structure determines a marked affinity for fatty matrices which translates in their widespread presence in vegetable oils, whose occurrence and possible sources has already been widely described (Moret et al., 2003; EFSA, 2012a; Brühl, 2016; Gómez-Coca et al., 2016b; Purcaro et al., 2016b; Gharbi et al., 2017).

Environmental contamination is believed to be the cause of background levels of MOSH, detectable in almost all vegetable oils (also when extracted directly in the laboratory from the handpicked raw matter). To date there is no strong evidence of the presence of MOAH in samples contaminated by the environment, probably due to the low quantities present and because they may undergo oxidation. Rapid and high sensitivity methods, able to detect very low MOH levels, are needed to better elucidate the impact of background contamination from the environment. High MOSH levels can be found when the contamination comes from the use of food grade lubricating oils (from which MOAH are

removed) in processing plants, but the highest concern arises when unrefined or partially refined mineral oil fractions (containing also MOAH) enter the production chain. For this reason in the last years the attention has been particularly focused on the MOAH, and although their presence in foodstuffs is still not regulated, and it has been highlighted that only a small part of those found in food includes the most dangerous species with 3 or more rings (Grob, 2018a), the large-scale distribution requires producers to respect very low limits in the order of 0.5 mg/kg, a limit reported in different draft ordinances of the BMEL, including the last one (BMEL, 2020).

Based on the recent JRC guidance on sampling and analysis of MOH in food and food contact materials (Bratinova & Hoekstra, 2019), HPLC-GC-FID is currently considered the reference method for MOH analysis (Biedermann et al., 2009; Biedermann & Grob, 2012a).

When analyzing vegetable oils, reaching the required sensitivity with the on-line method not preceded by suitable sample preparation, is critical for two aspects. When using a 2 mm x 250 mm silica gel HPLC column, the amount of sample directly injectable in the instrument is limited to 20 mg by the column capacity towards triglycerides. Moreover, the MOAH fraction is disturbed by the presence of interferences, mainly olefins deriving from the matrix, that cover the signal of interest and need to be removed before the chromatographic determination. For the removal of triglycerides, the proposed approaches include a saponification step (Regulation (EC) No 656/95; Guinda et al., 1996; Koprivnjak et al., 1997) or the passage through glass columns filled with fat retainers such as silica and alumina (Biedermann et al., 2009; Zurfluh et al., 2014). However, these methods have the disadvantage to be time consuming, to consist of several steps and to make use of high volumes of solvents, which translates in the risk to introduce contamination.

A more convenient alternative is MAS, already applied for the determination of mineral oils in cereal-based foods (Moret et al., 2016) and, more recently, on fish products (Srbinovska et al., 2020a). Advantages and major applications of MAS have been recently reviewed by (Moret et al., 2019). On the other side, for the removal of olefins the best available procedure is based on epoxidation (Biedermann et al., 2009; Nestola & Schmidt, 2017), a reaction capable to oxidize olefins, increasing their polarity, and hence their HPLC retention beyond that of the MOAH. The criticality linked to these protocols concerns the optimization of the reaction conditions to avoid the presence of residual olefins or the aromatic compounds are affected by the oxidation, causing respectively to overestimate and underestimate the contamination. As reported by (Biedermann et al.,

2020), given some practical advantages, the Nestola & Schmidt (2017) protocol is to be preferred.

On this basis, the aim of this work was to validate a rapid, highly sensitive and solvent sparing method for MOAH quantification in extra virgin olive oil (EVOO), a cornerstone food of the Mediterranean diet. The method is based on the application of the epoxidation according to a slightly modified Nestola & Schmidt (2017) protocol on a pre-enriched sample obtained by MAS, followed by LC-GC-FID analysis. Moreover, since the MOSH fraction is not affected by the epoxidation, MOSH quantification is still possible, with the sole care of adjusting the injection volume to avoid signal overload by endogenous *n*-alkanes.

The validated method was later used to analyze a number of olive oils extracted with the Abencor system from olives picked directly from the olive trees, for which low background values are expected, and to a number of EVOO taken from the Italian market or directly from the mill.

3.2 Materials and methods

3.2.1 Samples

Twelve EVOOs of different brands, purchased in different supermarkets in the North of Italy, 6 additional EVOO samples taken directly from the extraction plant, and 10 oil samples extracted with an Abencor apparatus from handpicked olives, were analyzed using the validated method here reported.

3.2.2 Reagents and chemicals

m-Chloroperbenzoic acid (*m*CPBA), potassium hydroxide, sodium thiosulfate, sodium sulfate, methanol, toluene, *n*-hexane and dichloromethane (the last two distilled before use) were obtained from Sigma-Aldrich (St. Louis, Missouri, USA). Ethanol was purchased from Supelco (Bellefonte, Pennsylvania, USA). Pure water was obtained with a Milli-Q system from Millipore (Bedford, Massachusetts, USA).

3.2.3 Standard solutions

A commercial motor oil (*n*-C₁₆₋₅₀ range, centered on *n*-C₂₈ and containing 19.5% of MOAH) was purchased on the market and used to prepare a standard solution at 0.86 mg/mL used to fortify an EVOO (hereafter called EVOO₁) free of MOAH, exploited for the validation (to test linearity in the matrix and recovery and repeatability at different

spiking levels). The Gravex (a naphthenic-based process oil, n -C₁₂₋₂₈ range, centered on n -C₁₈ and containing 27.0% of MOAH) was supplied by a manufacturer and used to prepare a standard solution at 1.02 mg/mL used to fortify another EVOO (hereafter called EVOO2), with a pre-existing contamination (n -C₂₄₋₅₀ range, centered on n -C₃₆) and also used for the validation.

The n -C₁₀₋₄₀ n -alkane standard mixture (added with n -C₅₀) used to verify GC performance (containing even-numbered alkanes in the specified range, each at 0.05 mg/mL), as well as the internal standards solution (IS) used to check the transfer windows of the fractions from the HPLC to the GC, and for quantification purposes, were purchased by Restek (Bellefonte, Pennsylvania, USA). The latter included n -C₁₃ at 0.15 mg/mL, 1,3,5-tritert-butylbenzene (TBB), n -C₁₁, cyclohexylcyclohexane (CyCy), pentyl benzene (5B), 1-methyl naphthalene (1-MN), 2-methyl naphthalene (2-MN) at 0.30 mg/mL and 5- α -cholestane (Cho) and perylene (Per) at 0.60 mg/mL. All the solutions were in toluene and stored at -18 °C.

3.2.4 Instrumentation

The Abencor system, purchased from MC2 Ingenieria Y Sistemas (Seville, Spain), consisted of a hammer mill M-100, equipped with the 5.5 mm screen, and a centrifugal machine CF-100. The malaxation unit was replaced with a cooking machine HF807 Companion XL from Moulinex (Ecully, France), and equipped with the mixing shovel.

The Microwave Extraction System MARS, equipped with GreenChem Plus Teflon vessels and able to host 14 samples simultaneously, was purchased by CEM Corporation (Matthews, North Carolina, USA). The LC-GC-FID system, namely LC-GC 9000, was from Brechbühler (Zurich, Switzerland) and consisted of an HPLC Phoenix 9000 and a GC Trace 1310 series by Thermo Fisher Scientific (Waltham, Massachusetts, USA), equipped with a double channels configuration able to perform MOSH and MOAH analysis simultaneously. The connection between the two instruments occurred through a Y-interface (Biedermann and Grob 2009b; Biedermann et al. 2009) managed by a switching transfer valves system. The HPLC was equipped with a Lichrospher Si-60 column by Sepachrom (Milano, Italy) of 25 cm \times 2.1 mm ID, packed with 5 μ m particle size, while both GC channels consisted of an uncoated/deactivated retention gap of 10 m \times 0.53 mm ID to exploit the retention gap technique (Biedermann & Grob, 2012a). The retention gap was connected with a GC column by Mega (Legnano, Milan, Italy) of 10 m \times 0.25 mm ID, coated with a 0.15 μ m film of PS-255 (1% vinyl, 99% methyl polysiloxane) through a steel T-piece, connected in turn with a solvent vapour exit (SVE) to remove the

solvent evaporating during partially concurrent eluent evaporation (Boselli et al., 1999). The LC flow was set at 300 $\mu\text{L}/\text{min}$ and started with 100% *n*-hexane for 0.1 min, reaching a *n*-hexane/dichloromethane ratio of 70:30 after 0.5 min. A backflush at 500 $\mu\text{L}/\text{min}$ (lasting 9 min) was started 6 minutes after the sample introduction. Then the column was reconditioned for 6.5 min with *n*-hexane at 700 $\mu\text{L}/\text{min}$ and at 300 $\mu\text{L}/\text{min}$ for 1.5 min. The GC worked at a constant pressure of 60 kPa, except during the transfer from the LC, when the pressure was raised to 90 kPa. The temperature gradient started 8.5 min after the start of the transfer from 51 $^{\circ}\text{C}$, reaching 350 $^{\circ}\text{C}$ at a rate of 20 $^{\circ}\text{C}/\text{min}$. The FID was held at 360 $^{\circ}\text{C}$, 10 $^{\circ}\text{C}$ above the maximum temperature of the oven to avoid the recondensation of the analytes.

3.2.5 Oil extraction from olives

Olive crushing was performed with the hammer mill on about 800 g of olives, malaxation was carried out in the cooking machine at 40 $^{\circ}\text{C}$ for 45 min, using the mixing program 3 (slow and continuous), and centrifugation occurred at 3500 rpm for 60 s. Since the centrifuge separated only the pomace from the liquid part, the oil was left to separate from the water autonomously overnight. At this point, the oil was transferred to a storage vessel prior to analysis.

3.2.6 Microwave assisted saponification (MAS)

1 g of oil was weighed inside a Teflon vessel, 10 μL of IS were added directly into the oil and finally 10 mL of *n*-hexane and 10 mL of a 1.5 N methanolic KOH solution were added. After inserting a magnetic stir bar to allow sample agitation during the saponification, the tube was closed inside its clamp and positioned into the microwave extractor (Mars, CEM Corporation, Matthews, NC). The microwave saponification program provided 5 minutes of pre-heating to reach the temperature of 120 $^{\circ}\text{C}$, which was held for 20 min, then followed by the cooling phase. Once reached the ambient temperature, the sample was added, directly into the vessel, with 40 mL of water and 3 mL of methanol (both left to flow along the walls of the vessel, in order to avoid emulsion formation), and then it was left to rest for 30 minutes at -18 $^{\circ}\text{C}$. The sample was then allowed to return to room temperature and the organic phase was collected quantitatively, transferred to a test tube and evaporated under mild vacuum to a volume of 4 mL. The latter was then subjected to a further washing with the addition of 3 mL of a 2:1 (*v/v*) $\text{CH}_3\text{OH}/\text{H}_2\text{O}$ mixture, which operationally consisted of 20 s of strong stirring with Vortex, followed by centrifugation

at 5000 rpm for 5 min. The organic phase was then collected again quantitatively and concentrated under mild vacuum to a volume of 700 μL .

3.2.7 Epoxidation

Epoxidation was carried out on the saponified sample according to a slightly modified Nestola & Schmidt (2017) protocol. 500 μL of a 20% (*m/v*) ethanolic solution of mCPBA were added to the 700 μL extract from the previous step. The solution was then stirred at 500 rpm for 15 min at room temperature, after which the reaction was stopped with the addition of 2 mL of a 10% (*m/v*) aqueous solution of sodium thiosulfate and added with 500 μL of ethanol. Three minutes of stirring were required after these additions to allow an intimate contact between the phases. Finally, about 600 μL of the organic phase were taken and transferred into an autosampler vial containing a spatula tip of anhydrous sodium sulphate, to adsorb any residual traces of water.

3.2.8 Quality control and MOAH quantification

The performance of the analytical system was checked periodically by injecting the *n*-C₁₀₋₄₀ *n*-alkane standard mixture (plus *n*-C₅₀) and the IS solution, and by running a procedural blank each batch of sample. The response ratio of *n*-C₅₀ to *n*-C₂₀, which according with the JRC guidance (Bratinova & Hoekstra, 2019) should be comprised between 0.8 and 1.2, as well as the baseline drift, were also checked and taken under control.

After epoxidation, 100 μL of the sample extract, corresponding to a sample amount of approximately 115 mg of the initial sample, were then injected into the LC-GC-FID apparatus for MOAH quantification. The area referable to the MOAH hump was obtained by integrating the entire signal and subtracting all peaks standing on the top of the hump. Concerning the MOSH, the injection volume was adjusted to 30 μL (instead of 100 μL) in order to avoid overloading by endogenous *n*-alkanes, and the signal due to natural *n*-alkanes was subtracted from the total hump. The total hump area was divided into C-fractions, as required by the JRC guidance (Bratinova & Hoekstra, 2019).

Finally, the quantification was performed with the internal standard method using CyCy for the quantification of MOSH, and the average value obtained with 5B, 1-MN, 2-MN and TBB for the MOAH. All data were corrected for the recovery.

3.2.9 Method validation

The adequacy of the performance of the analytical method was assessed referring to the JRC guidance (Bratinova & Hoekstra, 2019). Briefly, for the oil matrix recoveries between 70 and 120% and a maximum RSD of 20% were considered as acceptable.

The two EVOOs used for the validation were free from detectable MOAH in one case (EVOO1), while had a pre-existing MOAH contamination in the other case (EVOO2). In the latter the MOAH contamination was of 0.9 mg/kg, comparable to one of the fortification levels, but located at higher retention times ($> n\text{-C}_{25}$) and therefore in an area of the chromatogram that did not interfere with the added Gravex.

The fortification was carried out by spiking aliquots of 1 g of each of the two oils to be submitted to the analytical protocol, with the mineral oil at the different levels reported in Table 3.2.

3.2.10 Linearity

Following the Eurachem guide (Magnusson & Örnemark, 2014), method linearity was assessed for both MOSH and MOAH constructing a six-point calibration curve in matrix. The range evaluated went from 2.0 to 40.7 mg/kg for the MOSH and from 0.5 to 9.9 mg/kg for the MOAH, in order to cover the range of contaminations usually found in this type of oil. The fortification was carried out by directly spiking 1 g of EVOO1 with the commercial motor oil standard solution at the different MOSH and MOAH levels reported in Table 3.2. The analytical protocol under validation was then applied to the samples thus formed (4-6 replicates for each point of the curve).

The regression curves were then estimated by applying the least squares method and the linearity within the range considered was assessed by the Mandel fitting test ($p < 0.05$) and the residue analysis.

3.2.11 Recovery and repeatability

Method recoveries were calculated on 4-6 replicate analyses (see Table 3.2) carried out over different days (2 replicates per day) on two different EVOOs, spiked with the Gravex or the motor oil, and free of contamination in the respective molecular range of interest. In particular, EVOO2 was spiked with Gravex at 3.1, 5.1 and 10.2 mg/kg of total MOH, while EVOO1 (also used for testing linearity) was fortified with MOH from motor oil at spiking levels comprised between 2.5 and 50.6 mg/kg. The quantified MOH were

compared with the expected contamination (added amounts) and expressed as percentage recovery.

Inter-day repeatability referred to total MOAH (n -C₁₀₋₅₀) and to each C-fraction, was assessed on the same samples used to test recovery and linearity. In case of sample EVOO₂, also the pre-existing contamination (18 replicates) was quantified and used to assess repeatability.

3.2.12 Limit of quantification

The total LOQ (referring to the whole hump present in the sample) was estimated in accordance with the SANTE guidance (2019), i.e. the lowest spiked level of validation capable of meeting the method performance acceptability criteria, which in the specific case are those reported in the JRC guidance (Bratinova & Hoekstra, 2019). In addition, always based on the latter, also the LOQ referred to the individual C-fractions was estimated.

3.3 Results and discussion

3.3.1 Optimization of microwave assisted saponification (MAS)

The starting point for MAS optimization was the protocol developed by Moret et al. (2016) for mineral oil determination in cereal-based foodstuffs. With respect to the cited method, processing time and temperature (120 °C for 20 min), as well solvent volumes (KOH in methanol and n -hexane) remained the same (10 mL each), while important modifications regarded the amount of the sample to process in relation to the concentration of the KOH solution used, and the introduction of an additional washing step. In particular, it was decided to start from 1 g of sample, which was enough to reach the sensitivity required, maintaining low the amount of solvent needed for sample processing. When using saturated KOH in methanol under the described conditions, emulsion formation and, in some cases, the formation of a solid soap was observed during the MAS. These problems disappeared by lowering the concentration of the KOH solution to 1.5 N, which was equally sufficient to quantitatively hydrolyze all the fat present. Complete saponification was verified by weighting the residue of the unsaponifiable components after evaporating to dryness the hexane extract obtained with the MAS procedure.

The presence of n -hexane, placed from the start in the reaction environment, allows the transfer of mineral oils to the organic phase already during the MAS cycle, greatly reducing sample handling compared to classic saponification methods. Indeed, when using microwave energy, the presence of hexane in the reaction tube does not obstacle the

saponification. Furthermore, the reaction, carried out at higher temperature, higher pressure and under magnetic agitation, is more rapid and efficient, and hence takes place quantitatively. After the MAS cycle, the addition of water (40 mL) has the purpose to wash the sample from the residual KOH solution and the soaps formed, while the addition of methanol aims to break up any emulsion formed, promoting phase separation, also with the help of low temperature (-18 °C). After this first wash, the recovered organic phase, concentrated at 4 mL, needs to be further washed in a test tube with a CH₃OH/H₂O mixture 2:1 (*v/v*). After vortexing, a good phase separation was obtained by centrifugation and the organic phase was recovered. When omitting this additional washing step, or when deviating from the optimal CH₃OH/H₂O ratio, a gel was formed during the following concentration step.

By using the procedure described, a 5-fold sensitivity increase was obtained with respect to direct injection. While direct sample injection into the LC-GC-FID system in the presence of triglycerides is limited to 20 mg of fat, by starting from 1 g of sample and injecting 100 µL of the final sample extract, an amount corresponding to around 115 mg of the oil is introduced in the chromatographic system. With this quantity injected it was possible to easily reach a LOQ of 0.5 mg/kg for the total MOAH quantified in real and spiked samples used for recovery tests. Real contaminations generally covered the range over *n*-C₂₀₋₂₅.

3.3.2 Epoxidation

Epoxidation was performed on the saponified sample following the protocol proposed by Nestola & Schmidt (2017) which is more practical to apply, and has the advantage that can be also applied on sample extracts free from fat. In particular, with respect to the protocol proposed by Biedermann et al. (2009), the reaction can be carried out at ambient temperature, no solvent exchange is necessary and the reaction is definitively stopped with the addition of sodium thiosulphate, making the sample more stable over time before injection (Biedermann et al., 2020). Since the method indicated as optimal a *n*-hexane:ethanol ratio of 7:5, the extract of the saponified sample was reconcentrated to 700 µL and 500 µL of the *m*CPBA solution was added for the epoxidation. The chromatographic traces obtained on a large number of samples, together with recovery data, demonstrated that under these conditions it is possible to obtain complete removal of the olefins and negligible MOAH losses.

3.3.3 Method validation

3.3.3.1 Linearity

The calibration curves were constructed, considering each internal standard separately, and linearity of the method was confirmed for both MOSH (range 2.0-40.7 mg/kg) and MOAH (range of 0.5-9.9 mg/kg) by the coefficients of determination (R^2) always above 0.998, the p-values in the order of magnitude of 10^{-30} for the Mandel fitting test and the randomized dispersion of residues. The equations of the different calibration curves are shown in Table 3.1.

Table 3.1. Linearity.

Fraction	Linearity range (mg/kg)	I.S.	Equation	R^2
MOSH	2.0 - 40.7	CyCy	$y = 1.0718x - 0.4915$	0.998
		<i>n</i> -C ₁₃	$y = 1.0168x - 0.3249$	0.999
MOAH	0.5 - 9.9	5B	$y = 1.0413x - 0.0794$	0.999
		1-MN	$y = 1.134x - 0.1181$	0.999
		2-MN	$y = 1.1421x - 0.1176$	0.999
		TBB	$y = 0.8834x - 0.0503$	0.999

3.3.3.2 Recovery and repeatability

Figure 3.1A shows the overlays of the MOAH traces of the two EVOOs used for method validation. Figure 3.1A shows sample EVOO1 added with different amount of motor oil and used to check linearity, as well recovery and repeatability, while Figure 3.1B shows sample EVOO2 (also used to assess recovery and repeatability), added with different amounts of Gravex, and with a pre-existing contamination in the range *n*-C₂₅₋₅₀.

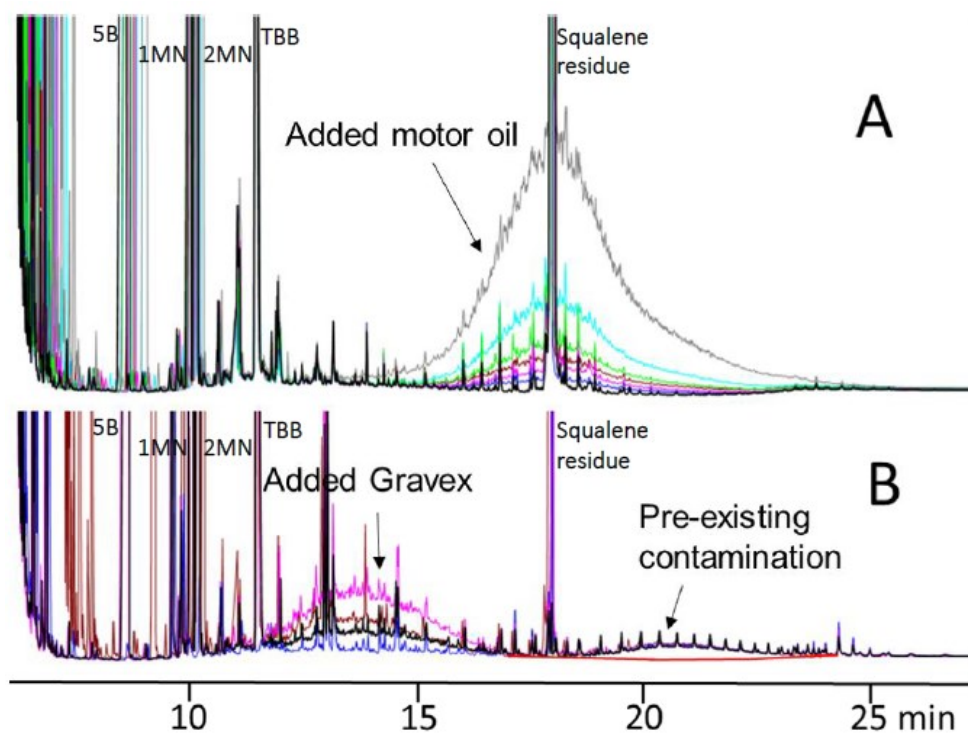


Figure 3.1. LC-GC-FID traces of the MOAH fractions of EVOO1 (A) and EVOO2 (B). The overlay of chromatograms starts from the unspiked matrix and the humps with increasing area refer to the different fortification levels reported in Table 3.2.

Table 3.2 reports percentage recoveries calculated using internal standards $n\text{-C}_{13}$ and CyCy for the MOSH and 5B, 1-MN, 2-MN and TBB for the MOAH. Residual standard deviations (RSD) for the replicate analyses (4-6 replicates for each spiking levels as shown in Table 3.2), are also reported.

Recoveries obtained were well within the range 70-120% requested by the JRC guidance (Bratinova & Hoekstra, 2019) for this matrix, regardless of the type of mineral oil and EVOO considered. More precisely, MOSH recovery was practically quantitative (on average 97.2 for $n\text{-C}_{13}$, and 100.7% for CyCy). Concerning the MOAH, the different standards gave different recoveries, ranging from a minimum average value of 83.5% for TBB to a maximum average value of 105.7% for 2-MN. RSD lower than 10%, well within the JRC reference value, were found for all the spiking levels, demonstrating a good repeatability for both total MOSH and MOAH.

Table 3.2. Recovery and RSD at different fortification levels (with Gravex and motor oil).

Sample	Type of mineral oil	Number of replicates	MOSH added (mg/kg)	Recovery % (mean)		RSD (%)		MOAH added (mg/kg)	Recovery % (mean)				RSD (%)			
				<i>n</i> -C ₁₃	CyCy	<i>n</i> -C ₁₃	CyCy		5B	1-MN	2-MN	TBB	5B	1-MN	2-MN	TBB
EVOO1	motor oil	6	2.0	95.5	98.7	4.0	4.6	0.5	96.4	104.7	105.8	81.9	9.4	9.4	9.2	9.0
		4	4.1	95.2	98.2	8.2	9.3	1.0	99.2	105.2	106.0	84.8	5.1	3.5	3.3	4.4
		4	6.1	94.7	96.6	5.5	7.0	1.5	96.6	102.9	103.8	83.4	8.1	7.0	6.6	7.6
		4	8.2	95.3	97.6	4.8	6.7	2.0	97.3	104.3	105.2	83.8	4.8	2.6	2.2	5.2
		4	20.4	97.9	100.9	3.3	3.9	4.9	100.7	106.7	107.4	87.2	2.4	3.0	3.3	1.8
		4	40.7	103.1	106.6	2.4	3.3	9.9	102.4	109.8	110.4	87.8	2.6	4.7	5.0	1.7
EVOO2	Gravex	6	2.2	99.6	103.1	3.3	2.6	0.8	93.4	99.7	101.7	79.4	5.0	4.2	4.8	5.0
		6	3.7	94.9	100.4	4.9	3.9	1.4	94.6	102.4	102.6	79.8	2.2	2.7	2.9	2.6
		6	7.4	98.1	104.3	4.5	6.3	2.8	100.6	106.0	108.0	83.3	5.8	5.7	6.1	4.4
MEAN RECOVERY*				97.2	100.7				97.9	104.6	105.7	83.5				

*All replicates at different spiking levels.

The reason of the different recoveries observed when using TBB or one of other internal standard was investigated along the different steps of the MAS procedure.

To this purpose 1g of the oil sample was weighted in the MAS tube, added with 10 mL of hexane and the IS, and an aliquot (50 μ L) was injected after stirring (step 1). Soon after, the same sample was added with 10 mL of a KOH solution 1.5 N in methanol, stirred again, and another 50 μ L aliquot of the hexane phase was injected (step 2). Further 50 μ L aliquots were finally injected after the MAS procedure followed by the washing steps (step 3).

By comparing the areas of the IS obtained from these trials, carried out in double (Figure 3.2), it was possible to conclude that the different recoveries observed depended on the different partition of these standards between the aqueous/alcoholic phase and the *n*-hexane phase (already visible in step 2 when adding the KOH solution, before the MAS procedure), and on the fact that part of the *n*-hexane phase remained in the aqueous/alcoholic phase, concentrating the standards in the organic solvent (this effect is well visible in step 3 for TBB). By measuring the *n*-hexane phase after the MAS (step 3) it was found that about 1.8 mL of the *n*-hexane phase remained in the lower phase. This fact, together with the lower solubility of TBB in the aqueous/alcoholic phase (higher partition in the *n*-hexane phase) with respect to 1-MN and 2-MN, explains the different mean recoveries obtained.

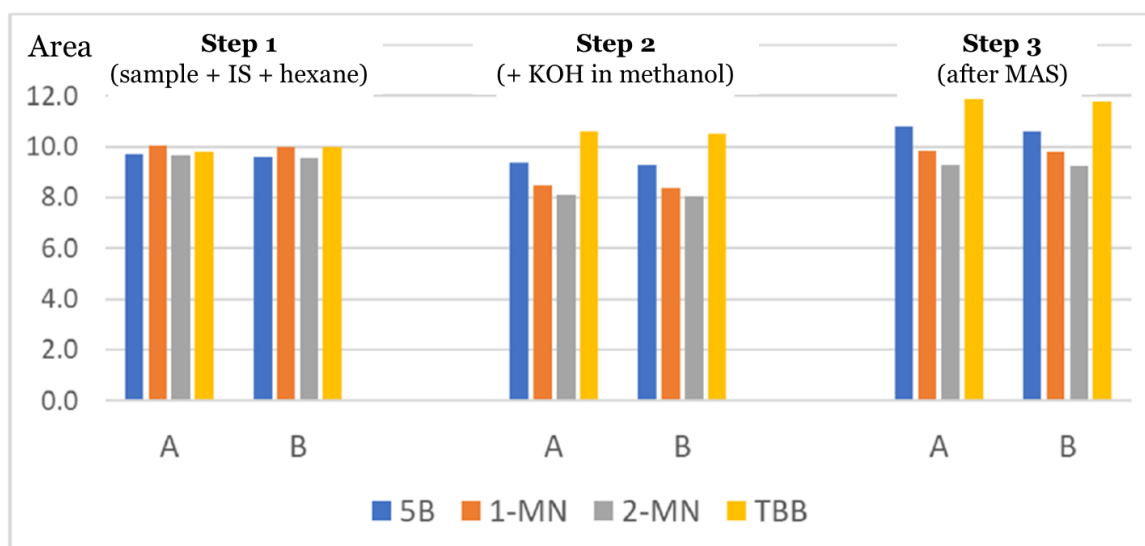


Figure 3.2. Behaviour of the internal standards of the MOAH fraction in different steps of the MAS procedure.

To solve the discrimination problem, the amount of hexane was increased to 15 mL (the maximum amount that can be added in the saponification tube), thus obtaining only little

improvements. An additional hexane extraction gave, instead, the formation of an emulsion difficult to break. Finally, it was decided to maintain the initial conditions which allowed to minimize sample handling and to use a small amount of organic solvent.

Based on previous experience, standard partition also occurs when using classical saponification. Despite this could be considered a weakness of all methods based on saponification, it was proved that validation data support the reliability of the results provided. Indeed, by correcting the data for recovery, a realignment of the quantified contamination, independently on the IS used, was always observed. Furthermore, data obtained on selected samples with relatively high contamination levels were in good agreement with those obtained by direct HPLC-GC following epoxidation (data not reported).

Table 3.3 shows repeatability referred to the C-fractions making up the humps (which are of interest in relation to the performance criteria required by the JRC guidance (Bratinova & Hoekstra, 2019)). Optimal inter-day repeatability was achieved for each level considered, sometimes even at concentrations below 0.1 mg/kg. However, since for some replicates at this level the RSD exceeded the limit of 20%, based on these results the lowest level tested attainable with acceptable repeatability was set at 0.2 mg/kg.

Table 3.3. Repeatability of C-fractions.

Sample	Number of replicates	Type of mineral oil	MOAH added or present (mg/kg)	C-fraction	Mean concentration (mg/kg)*				RSD%				
					5B	1-MN	2-MN	TBB	5B	1-MN	2-MN	TBB	
EVOO 1	6	Motor oil	0.5	<i>n</i> -C ₁₆₋₂₅	0.1	0.1	0.1	0.1	21.0	21.0	20.8	21.0	
				<i>n</i> -C ₂₅₋₃₅	0.3	0.3	0.3	0.3	6.7	6.8	6.6	5.8	
				<i>n</i> -C ₃₅₋₅₀	0.1	0.1	0.1	0.1	16.9	16.6	16.4	17.2	
	4		1.0	<i>n</i> -C ₁₆₋₂₅	0.2	0.2	0.2	0.2	9.3	10.4	10.5	9.8	
				<i>n</i> -C ₂₅₋₃₅	0.7	0.7	0.7	0.7	8.0	6.0	5.8	7.1	
				<i>n</i> -C ₃₅₋₅₀	0.1	0.1	0.1	0.1	13.3	14.4	14.5	13.8	
	4		1.5	<i>n</i> -C ₁₆₋₂₅	0.3	0.3	0.3	0.3	11.0	10.8	10.6	10.2	
				<i>n</i> -C ₂₅₋₃₅	1.0	1.0	1.0	1.0	4.3	3.9	3.7	3.7	
				<i>n</i> -C ₃₅₋₅₀	0.2	0.2	0.2	0.2	19.6	17.6	17.1	19.4	
	4		2.0	<i>n</i> -C ₁₆₋₂₅	0.4	0.4	0.4	0.4	5.3	3.1	2.9	6.0	
				<i>n</i> -C ₂₅₋₃₅	1.3	1.3	1.3	1.3	2.9	2.0	1.9	2.7	
				<i>n</i> -C ₃₅₋₅₀	0.3	0.3	0.3	0.3	15.9	13.5	13.1	16.4	
	4		4.9	<i>n</i> -C ₁₆₋₂₅	1.0	1.0	1.0	1.0	6.4	5.3	5.4	5.9	
				<i>n</i> -C ₂₅₋₃₅	3.4	3.3	3.3	3.4	2.4	4.2	4.6	1.7	
				<i>n</i> -C ₃₅₋₅₀	0.7	0.7	0.7	0.7	4.9	2.6	2.2	5.3	
	4		9.9	<i>n</i> -C ₁₆₋₂₅	2.0	2.1	2.0	2.1	2.8	4.3	4.6	2.9	
				<i>n</i> -C ₂₅₋₃₅	6.8	6.8	6.8	6.9	3.3	5.3	5.5	2.2	
				<i>n</i> -C ₃₅₋₅₀	1.5	1.5	1.5	1.5	3.9	5.6	5.7	3.3	
EVOO 2	6	Gravex	0.8	<i>n</i> -C ₁₀₋₁₆	0.1	0.1	0.1	0.1	26.6	26.4	26.9	26.9	
				<i>n</i> -C ₁₆₋₂₅	0.7	0.7	0.7	0.7	3.7	2.6	3.0	3.5	
	6		1.4	<i>n</i> -C ₁₀₋₁₆	0.2	0.2	0.2	0.2	2.3	2.8	2.9	3.0	
				<i>n</i> -C ₁₆₋₂₅	1.1	1.1	1.1	1.1	2.2	2.8	2.9	2.6	
	6		2.8	<i>n</i> -C ₁₀₋₁₆	0.4	0.4	0.4	0.4	8.3	6.6	6.5	7.5	
				<i>n</i> -C ₁₆₋₂₅	2.4	2.4	2.4	2.3	6.3	6.4	6.8	4.9	
	18		Pre-existing contamination	0.9	<i>n</i> -C ₂₅₋₃₅	0.3	0.3	0.3	0.3	6.4	5.9	5.5	5.9
					<i>n</i> -C ₃₅₋₅₀	0.6	0.6	0.6	0.6	4.0	4.2	5.0	4.4

*Data corrected for recovery.

3.3.3.3 Limit of quantification

Regarding the sample fortified with the motor oil, the lowest tested concentration for the MOAH (6 replicates) was 0.5 mg/kg which, as visible in Table 3.2, well satisfied the required method performance criteria (recovery within 70-120%, RSD <20%). Since no indication about the evaluation of the total LOQ are given by the JRC guidance (Bratinova & Hoekstra, 2019), it was calculated on the total hump detected in the spiked samples, rather than expressed as the sum of the LOQ of each C-fraction. We are aware that defining a LOQ for a signal given by a hump is hard, and that the LOQ is intrinsically affected by the distribution of the contamination (hump width), but considering the hump LOQ as a sum of C-fraction LOQs does not solve the problem, adds uncertainty to the final measurement and doesn't describe the real situation. Usually, real MOAH contamination doesn't cover the all molecular range from *n*-C₁₀ to *n*-C₅₀. Based on these considerations, total LOQ of the present method was set at 0.5 mg/kg. Nevertheless, according to the JRC guidance (Bratinova & Hoekstra, 2019), the LOQ of each C-fraction, rather than total LOQ, has to be compliant with the required performance criteria. Since Table 10 reports optimal RSD up to a concentration of 0.2 mg/kg, the LOQ of each single C-fraction was set at this value.

3.3.4 MOSH quantification

Although this validation was specifically addressed to MOAH, the method also allowed the quantification of the MOSH fraction, whose recovery was evaluated obtaining the same good performance (see results reported in Table 3.2). Practically quantitative recoveries were achieved for each level tested, with RSD values always lower than 10%. Since under the condition used for MOAH analysis (injection of 100 µL of the final sample extract), the presence of biogenic *n*-alkanes sometimes prevented a reliable quantification of the MOSH hump, a smaller amount of the final sample extract (30 µL) was injected for MOSH quantification. The different amount injected had of course an impact on the LOQ, which increased at value around 0.5 mg/kg for each single C-fraction (still in agreement with the performance criteria required by the JRC guidance (Bratinova & Hoekstra, 2019). To reach lower sensitivity a purification step on an alumina bed could be introduced (Fiselier & Grob, 2009; EN 16995:2017).

In Figure 3.3 it can be appreciated how, differently from when injecting 100 µL, when injecting a smaller volume of the final sample extract (30 µL), the *n*-alkane signal is not overloaded and therefore the quantification is reliable.

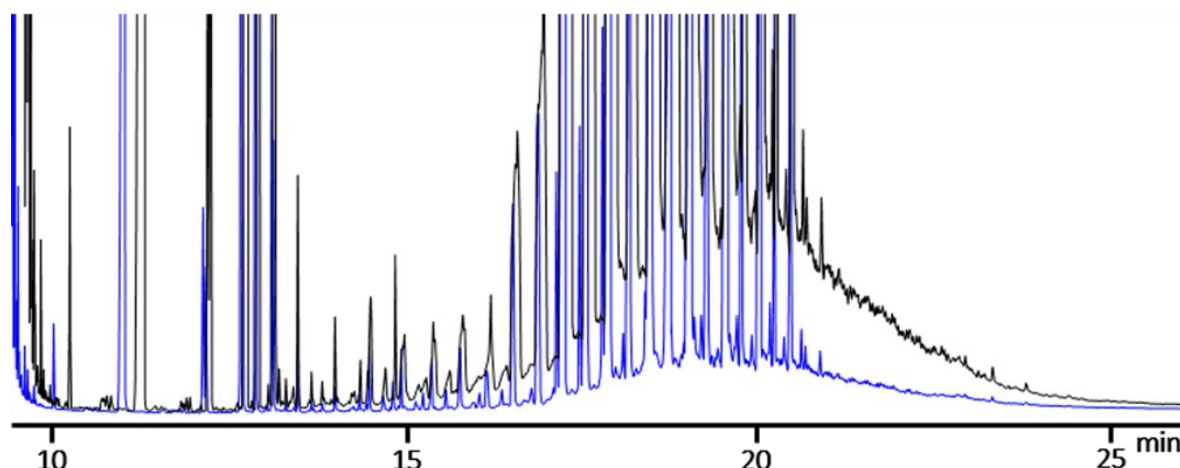


Figure 3.3. Overlay of LC-GC-FID chromatograms of the MOSH fraction of an extra virgin olive oil from the market (EVOO_M1) injected at 30 μ L (blue line) and 100 μ L (black line).

3.3.5 MOH content in EVOO samples

The validated method was used to investigate the presence of MOSH and MOAH in 12 EVOOs purchased from the Italian market, and in two previous points of the supply chain. Specifically, other 10 oils were obtained from the milling of olives from the Friuli-Venezia Giulia region (FVG, Italy) picked directly from the olive trees, and processed with an Abencor system. The remaining 6 oils were sampled directly from the centrifuge drain at the oil mill.

Table 3.4 summarizes the concentrations found in the EVOOs taken from the market. MOSH were quantified using CyCy as internal standard, while MOAH were quantified using all the 4 standards investigated (5B, 1-MN, 2-MN and TTB), and an average value is also reported. In accordance with the JRC Guidance (Bratinova & Hoekstra, 2019), the quantification was carried out for each C-fraction. Total MOSH and MOAH are also reported. In this case, the whole MOSH or MOAH hump present in the sample was integrated, and beside the raw data (n -C₁₀₋₅₀), data corrected for the recovery (n -C₁₀₋₅₀^{*}) were reported too, together with the average value obtained from the four internal standards, corrected for the recovery (n -C₁₀₋₅₀^{**}). Total MOAH quantification, obtained by applying the lower bound (LB) calculation (data not reported in the table), according to which all the C-fraction are summed up by considering each value below the LOQ equal to zero, were in good agreement with those calculated by integrating the whole hump. However, clear rules on how to express the total LOQ and whether to perform the quantification based on the total hump, or on the sum of each C-fraction, using the lower bound approach already employed for the rapid risk assessment of MOAH in the formulas

for infants and follow-on formula (EFSA, 2019), are necessary for better alignment of data among different laboratories.

As we can see from Table 3.4, for all of the internal standards, except for the TBB which gave recovery around 84%, raw data were in good agreement with the data corrected for the recovery (since their recovery ranged from 98 to 106%). Particularly, 5B gave recovery very close to 100% (98%) and could be conveniently used for MOAH quantification, without the need of correcting the data.

None of these oil samples resulted free from MOH contamination. Total MOSH content ranged from 4.8 to 63.1 mg/kg (on average 22.9 mg/kg), while total MOAH content varied between 1.5 and 6.5 mg/kg (on average 3.3 mg/kg).

MOSH data are in agreement with most recent literature data (Zoccali et al., 2016; Gharbi et al., 2017; Liu et al., 2017) and with data reported by Luisi (2019) during a workshop organized by the Italian Society for the Study of Fatty Substances (SISSG) in Bologna in December 2019 (Conte, 2020). Luisi (2019) reported MOSH and MOAH contamination (in the range n -C₁₀₋₃₅) for a large number of samples, among which 850 samples of EVOO from Italy and 107 samples from Greece. MOSH contamination was highlighted in all the samples analyzed, from 1.0 to 64.0 mg/kg (on average 9.7 mg/kg), for EVOO samples from Italy, and from 1.7 to 74.8 mg/kg (on average 17.8 mg/kg) for samples from Greece. Regarding the MOAH, most of the published works reported levels below the LOQ, while Luisi (2019) reported MOAH above the quantification limit (1.0 mg/kg) in 40% of the EVOO samples from Italy (from 1.0 to 13.5 mg/kg, on average 2.5 mg/kg) and in 50% of the samples from Greece (from 1.1 to 12.9 mg/kg, on average 3.9 mg/kg).

When considering the same molecular range (n -C₁₀₋₃₅), our data (MOSH on average 14.2 mg/kg, and MOAH on average 2.1 mg/kg) were in good agreement with those reported by Luisi (2019) for a larger set of samples from the Italian market.

It is interesting to observe that, the higher is the LOQ of the C-fraction, the lower is the quantified MOAH. For example, by applying a LOQ value of 2.0 mg/kg to our dataset, as could be the case of method not applying a pre-enrichment step, but complying with the performance criteria reported in the JRC guidance (Bratinova & Hoekstra, 2019), most of the samples would result contaminated with MOAH amounts lower than the LOQ.

Almost all the EVOOs presented contaminations centred between n -C₂₅ and n -C₃₄, a typical range for lubricating, hydraulic and motor oils (Wagner et al., 2001a), and sometimes the profile made up multiple humps suggesting different sources of contaminations.

Table 3.4. MOSH and MOAH data of the oils sampled from the market.

Sample code	IS MOSH	MOSH (mg/kg)								IS MOAH	MOAH (mg/kg)						
		<i>n</i> -C ₁₀₋₁₆	<i>n</i> -C ₁₆₋₂₀	<i>n</i> -C ₂₀₋₂₅	<i>n</i> -C ₂₅₋₃₅	<i>n</i> -C ₃₅₋₄₀	<i>n</i> -C ₄₀₋₅₀	<i>n</i> -C ₁₀₋₅₀	<i>n</i> -C ₁₀₋₅₀ *		<i>n</i> -C ₁₀₋₁₆	<i>n</i> -C ₁₆₋₂₅	<i>n</i> -C ₂₅₋₃₅	<i>n</i> -C ₃₅₋₅₀	<i>n</i> -C ₁₀₋₅₀	<i>n</i> -C ₁₀₋₅₀ *	<i>n</i> -C ₁₀₋₅₀ **
EVOO_M1	CyCy	<0.5	<0.5	1.0	5.1	1.8	1.6	9.8	9.7	5B	<0.2	0.2	0.9	0.7	1.8	1.9	1.9
										1-MN	<0.2	0.2	1.0	0.8	2.0	1.9	
										2-MN	<0.2	0.2	1.0	0.8	2.0	1.9	
										TBB	<0.2	0.2	0.8	0.6	1.5	1.8	
EVOO_M2	CyCy	<0.5	1.4	3.3	14.5	8.9	7.4	35.7	35.4	5B	<0.2	0.4	1.7	1.1	3.3	3.3	3.3
										1-MN	<0.2	0.5	1.8	1.2	3.5	3.4	
										2-MN	<0.2	0.5	1.9	1.2	3.6	3.4	
										TBB	<0.2	0.4	1.4	0.9	2.8	3.3	
EVOO_M3	CyCy	<0.5	1.0	2.4	8.2	3.1	2.6	17.7	17.6	5B	<0.2	0.3	1.3	1.3	2.8	2.8	2.8
										1-MN	<0.2	0.3	1.3	1.3	3.0	2.8	
										2-MN	<0.2	0.3	1.4	1.4	3.0	2.8	
										TBB	<0.2	0.2	1.1	1.1	2.4	2.8	
EVOO_M4	CyCy	1.8	3.4	5.0	23.1	16.1	14.0	63.5	63.1	5B	<0.2	0.3	1.3	0.7	2.2	2.3	2.2
										1-MN	<0.2	0.3	1.3	0.7	2.3	2.2	
										2-MN	<0.2	0.3	1.4	0.7	2.3	2.2	
										TBB	<0.2	0.2	1.1	0.6	1.8	2.2	
EVOO_M5	CyCy	<0.5	1.3	3.5	16.7	8.4	7.7	38.0	37.7	5B	<0.2	0.7	2.3	1.5	4.5	4.6	4.5
										1-MN	<0.2	0.8	2.4	1.6	4.7	4.5	
										2-MN	<0.2	0.8	2.4	1.6	4.7	4.5	
										TBB	<0.2	0.6	1.9	1.3	3.8	4.5	

Table 3.4. Continued.

Sample code	IS MOSH	MOSH (mg/kg)								IS MOAH	MOAH (mg/kg)						
		<i>n</i> -C ₁₀₋₁₆	<i>n</i> -C ₁₆₋₂₀	<i>n</i> -C ₂₀₋₂₅	<i>n</i> -C ₂₅₋₃₅	<i>n</i> -C ₃₅₋₄₀	<i>n</i> -C ₄₀₋₅₀	<i>n</i> -C ₁₀₋₅₀	<i>n</i> -C ₁₀₋₅₀ *		<i>n</i> -C ₁₀₋₁₆	<i>n</i> -C ₁₆₋₂₅	<i>n</i> -C ₂₅₋₃₅	<i>n</i> -C ₃₅₋₅₀	<i>n</i> -C ₁₀₋₅₀	<i>n</i> -C ₁₀₋₅₀ *	<i>n</i> -C ₁₀₋₅₀ **
EVOO_M6	CyCy	<0.5	0.6	3.3	12.9	6.7	4.8	28.4	28.2	5B	<0.2	0.2	1.2	0.7	2.1	2.2	2.2
										1-MN	<0.2	0.3	1.3	0.7	2.3	2.2	
										2-MN	<0.2	0.3	1.3	0.8	2.3	2.2	
										TBB	<0.2	0.2	1.0	0.6	1.8	2.2	
EVOO_M7	CyCy	<0.5	<0.5	1.9	8.5	1.9	1.2	13.6	13.5	5B	<0.2	0.6	2.2	1.3	4.1	4.2	4.2
										1-MN	<0.2	0.6	2.4	1.4	4.5	4.3	
										2-MN	<0.2	0.6	2.5	1.5	4.6	4.3	
										TBB	<0.2	0.5	1.9	1.1	3.4	4.1	
EVOO_M8	CyCy	<0.5	<0.5	1.1	5.5	1.4	1.0	8.9	8.9	5B	<0.2	0.3	1.3	0.8	2.4	2.5	2.4
										1-MN	<0.2	0.4	1.4	0.8	2.6	2.5	
										2-MN	<0.2	0.4	1.4	0.8	2.6	2.4	
										TBB	<0.2	0.3	1.1	0.7	2.0	2.4	
EVOO_M9	CyCy	<0.5	<0.5	0.5	3.0	0.7	0.5	4.8	4.8	5B	<0.2	<0.2	0.8	0.5	1.5	1.5	1.5
										1-MN	<0.2	0.2	0.9	0.5	1.6	1.5	
										2-MN	<0.2	0.2	0.9	0.5	1.6	1.5	
										TBB	<0.2	<0.2	0.7	0.4	1.3	1.5	
EVOO_M10	CyCy	<0.5	<0.5	2.5	11.0	3.8	2.5	20.1	19.9	5B	<0.2	0.7	2.4	1.6	4.7	4.8	4.9
										1-MN	<0.2	0.8	2.7	1.7	5.1	4.9	
										2-MN	<0.2	0.8	2.7	1.8	5.2	4.9	
										TBB	<0.2	0.6	2.1	1.4	4.1	4.9	

Table 3.4. Continued.

Sample code	IS MOSH	MOSH (mg/kg)								IS MOAH	MOAH (mg/kg)						
		<i>n</i> -C ₁₀₋₁₆	<i>n</i> -C ₁₆₋₂₀	<i>n</i> -C ₂₀₋₂₅	<i>n</i> -C ₂₅₋₃₅	<i>n</i> -C ₃₅₋₄₀	<i>n</i> -C ₄₀₋₅₀	<i>n</i> -C ₁₀₋₅₀	<i>n</i> -C ₁₀₋₅₀ *		<i>n</i> -C ₁₀₋₁₆	<i>n</i> -C ₁₆₋₂₅	<i>n</i> -C ₂₅₋₃₅	<i>n</i> -C ₃₅₋₅₀	<i>n</i> -C ₁₀₋₅₀	<i>n</i> -C ₁₀₋₅₀ *	<i>n</i> -C ₁₀₋₅₀ **
EVOO_M11	CyCy	<0.5	<0.5	2.1	7.7	2.6	1.1	13.5	13.5	5B	<0.2	0.2	1.3	1.3	2.7	2.8	2.8
										1-MN	<0.2	0.2	1.4	1.4	3.0	2.9	
										2-MN	<0.2	0.2	1.4	1.5	3.0	2.9	
										TBB	<0.2	<0.2	1.1	1.1	2.3	2.8	
EVOO_M12	CyCy	<0.5	<0.5	2.9	14.1	3.6	1.6	22.5	22.3	5B	<0.2	1.0	3.4	2.1	6.4	6.6	6.5
										1-MN	<0.2	1.0	3.5	2.2	6.7	6.4	
										2-MN	<0.2	1.0	3.6	2.2	6.8	6.4	
										TBB	<0.2	0.8	2.9	1.8	5.5	6.6	

*Data corrected for recovery **Average obtained with the four internal standards.

Table 3.5 reports the data obtained by the oil extracted by physical means in the laboratory (Abencor apparatus) from hand-picked olives (HPO) collected in different areas in the Friuli-Venezia Giulia region, as well as data obtained by 6 EVOOs sampled at the mill. The physical extraction with this system was intended to resemble the extraction that takes place at the real oil mill, to allow a better comparison of results. In this case MOSH were quantified using CyCy, while MOAH were quantified using the average value obtained from the 4 IS (5B, 1-MN, 2-MN, TBB), all corrected for the recovery.

Oil extracted in the laboratory with the Abencor apparatus included samples from areas close to potential sources of contamination, such as a highway (EVOO_T2, EVOO_T3, EVOO_T9, EVOO_T10), or a steel mill (EVOO_T9, EVOO_T10) or a large industrial area (EVOO_T2, EVOO_T3), as well as others located in areas with no particular sources of pollution and not very urbanized (EVOO_T1, EVOO_T4, EVOO_T5, EVOO_T6, EVOO_T7, EVOO_T8). Regardless of the different exposure to possible environmental pollution, MOSH contamination was detectable in all the samples, while MOAH were not detectable. Except for EVOO_T10, which contained 4.3 mg/kg of MOSH, other samples had similar contamination ranging from 1.3 to 2.1 mg/kg. This data are in agreement with those reported by Gharbi et al. (2016).

EVOOs sampled at the mill showed MOSH contamination ranging from 3.6 to 35.9 mg/kg (on average 11.2 mg/kg), while MOAH ranged from <0.5 to 2.7 mg/kg (on average 1.1 mg/kg).

Table 3.5. MOSH and MOAH data of the oils obtained from olives picked from the trees and sampled at the mill.

Sample code	MOSH (mg/kg)							MOAH (mg/kg)				
	<i>n</i> -C ₁₀₋₁₆	<i>n</i> -C ₁₆₋₂₀	<i>n</i> -C ₂₀₋₂₅	<i>n</i> -C ₂₅₋₃₅	<i>n</i> -C ₃₅₋₄₀	<i>n</i> -C ₄₀₋₅₀	<i>n</i> -C ₁₀₋₅₀ *	<i>n</i> -C ₁₀₋₁₆	<i>n</i> -C ₁₆₋₂₅	<i>n</i> -C ₂₅₋₃₅	<i>n</i> -C ₃₅₋₅₀	<i>n</i> -C ₁₀₋₅₀ *
<i>Oils obtained from olives sampled directly from the trees</i>												
EVOO_T1	<0.5	<0.5	0.5	0.7	<0.5	<0.5	1.3	<0.2	<0.2	<0.2	<0.2	< 0.5
EVOO_T2	<0.5	<0.5	0.7	1.3	<0.5	<0.5	2.1	<0.2	<0.2	<0.2	<0.2	< 0.5
EVOO_T3	<0.5	<0.5	0.5	1.0	<0.5	<0.5	1.5	<0.2	<0.2	<0.2	<0.2	< 0.5
EVOO_T4	<0.5	<0.5	<0.5	0.7	<0.5	<0.5	1.2	<0.2	<0.2	<0.2	<0.2	< 0.5
EVOO_T5	<0.5	<0.5	<0.5	0.9	<0.5	<0.5	1.4	<0.2	<0.2	<0.2	<0.2	< 0.5
EVOO_T6	<0.5	<0.5	0.5	0.7	<0.5	<0.5	1.2	<0.2	<0.2	<0.2	<0.2	< 0.5
EVOO_T7	<0.5	<0.5	0.6	0.9	<0.5	<0.5	1.5	<0.2	<0.2	<0.2	<0.2	< 0.5
EVOO_T8	<0.5	<0.5	0.5	0.9	<0.5	<0.5	1.5	<0.2	<0.2	<0.2	<0.2	< 0.5
EVOO_T9	<0.5	<0.5	0.6	1.1	<0.5	<0.5	1.8	<0.2	<0.2	<0.2	<0.2	< 0.5
EVOO_T10	<0.5	<0.5	0.9	3.1	<0.5	<0.5	4.3	<0.2	<0.2	<0.2	<0.2	< 0.5
<i>Oils sampled at the oil mill leaving the centrifuge</i>												
EVOO_C1	<0.5	<0.5	0.8	4.7	1.7	0.8	8.1	<0.2	<0.2	1.2	1.4	2.7
EVOO_C2	<0.5	<0.5	0.7	2.7	0.6	0.4	4.9	<0.2	<0.2	0.4	0.2	0.7
EVOO_C3	<0.5	<0.5	<0.5	1.4	1.0	0.5	3.4	<0.2	<0.2	0.3	0.5	0.9
EVOO_C4	<0.5	1.2	3.6	5.7	0.5	<0.5	11.2	<0.2	0.5	0.5	<0.2	1.0
EVOO_C5	<0.5	1.2	1.1	1.1	<0.5	<0.5	3.6	<0.2	<0.2	<0.2	<0.2	< 0.5
EVOO_C6	<0.5	<0.5	2.2	21.3	8.4	3.7	35.9	<0.2	<0.2	0.7	0.2	1.0

*Data corrected for recovery.

3.4 Conclusions

A highly sensitive method for the determination of MOAH in extra virgin olive oils, based on a fast, solvent-saving and low sample handling procedure, was optimized and successfully validated. The performance of the method (in terms of recovery, repeatability and LOQ) was found to be fully in line with the requirements of the recent JRC guidance. A LOQ of 0.5 mg/kg was obtained for total MOAH in fortified and real sample. Nevertheless, it was evidenced how a reference approach for its calculation is lacking, and clear rules are needed to standardize the way to express it and to give total contamination from *n*-C₁₀ to *n*-C₅₀. Finally, by reducing the amount of sample to inject, in order to avoid signal overload due to natural *n*-alkanes, the method also allowed a reliable quantification of the MOSH fraction, with a 2.5-fold loss of sensitivity, which led the LOQ on the C-fractions to be assessed at 0.5 mg/kg.

Oils obtained by olives directly picked from the tree showed low MOSH background contamination, regardless of the different provenience. EVOO samples taken from the oil mill showed lower contamination with respect to EVOOs from the market. This may

suggest that filtration (when applied), storage and bottling may be responsible for the increased contamination observed in these oils. However, the small number of oils analyzed does not allow to draw this type of conclusions and further investigation is needed to individuate all possible contamination sources along the production chain, from the field to the bottled oil.

This is currently under evaluation as part of a PhD project and will be the subject of a forthcoming paper.

4 A study on the impact of harvesting operations on the mineral oil contamination of olive oils

This chapter has already been published in: Menegoz Ursol, L., Conchione, C., Peroni, D., Carretta, A., & Moret, S. (2023). A study on the impact of harvesting operations on the mineral oil contamination of olive oils. *Food Chemistry*, 406, 135032.

4.1 Introduction

Mineral oil hydrocarbons (MOH) are petroleum distillation products consisting of complex mixtures of saturated (MOSH) and aromatic (MOAH) hydrocarbons which may be present in various food matrices as the result of environmental and processing contamination, including packaging migration. MOSH include linear, branched and cyclic compounds, whereas MOAH contain single or multiple aromatic ring systems, alkylated to more than 98% (EFSA, 2012a; Bratinova & Hoekstra, 2019). MOSH accumulate in tissues and organs based on their structure and molecular weight, while MOAH show carcinogenic and genotoxic character, particularly evident for species with 3 or more aromatic rings (Grob, 2018a). Starting from 2011, in the absence of legal limits, BMEL has published a series of draft ordinances, the latest of which (BMEL, 2020) suggested a limit of 0.5 mg/kg for MOAH in food (as a result of migration from recycled cardboard packaging). This limit has become a reference for large-scale retail trade of different food, included vegetable oils. In the same context, benchmark levels of 13 mg/kg for MOSH and below the limit of quantification (LOQ) for MOAH in vegetable oils (excluding those of tropical origin), were introduced in 2019 by LAV & BLL, and confirmed in the latest update (LAV & BLL, 2022). More recently, during a meeting of the SCoPAFF, EU Member States agreed on a limit of 2 mg/kg (EC, 2022), equal to the LOQ established by the JRC for fats and oils (Bratinova & Hoekstra, 2019). Even though this limit is not yet legally binding *stricto sensu*, as its enforcement is delegated to individual Member States, food business operators are required to withdraw or recall food products exceeding this limit from the market, according to articles 14 and 19 of Regulation (EC) No 178/2002 on general principles of food safety.

The current official method for MOSH/MOAH determination in edible oils and fats is the EN16995:2017 standard, based on on-line HPLC-GC-FID. Due to high inter-laboratory variability, this method, which does not include an enrichment step, is unable to achieve LOQ lower than 10 mg/kg. To reach lower LOQ, it is necessary to perform sample pre-enrichment to eliminate the bulk of triglycerides before analysis (Biedermann et al., 2009; Bratinova & Hoekstra, 2019; Menegoz Ursol et al., 2022). Removal of interfering

components (olefins and when necessary endogenous *n*-alkanes) is a prerequisite for obtaining interpretable chromatograms and reliable data (Fiselier et al., 2009a; EN 16995:2017; Nestola & Schmidt, 2017; Biedermann et al., 2020).

GC coupled to mass spectrometry (MS) can provide important qualitative information through the identification of markers confirming the petrogenic origin of the contamination, such as steranes and hopanes (Populin et al., 2004), or for searching target aromatics (Jaén et al., 2021). Comprehensive two-dimensional gas chromatography (GC×GC-FID/MS) represents a useful tool for an in-depth characterization of hydrocarbon profiles and identification of contamination sources (Biedermann & Grob, 2009a, 2015, 2019). GC×GC has been proven to increase chromatographic resolution and provide a more detailed characterization of complex matrices by exploiting two different analytical columns independently within one analysis. Furthermore, the informative and highly structured 2D profiles are a powerful tool for visual fingerprinting, which can hereby be used for user-friendly yet effective identification of contamination sources.

Mineral oils are easy to find in fatty matrices even at quite high levels because of their lipophilic nature and their widespread use in processes' mechanization. Vegetable oils are among the most contaminated food matrices (EFSA, 2012a) and various vegetable oils present different levels of contamination, with differences even within the various olive oil categories (Moret et al., 2003). Luisi (2019) reported MOSH and MOAH average levels of 9.7 and 2.5 mg/kg, respectively, in 850 extra virgin olive oils (EVOO) from the Italian market (Conte, 2020). Considering the same molecular range (*n*-C₁₀₋₃₅), Menegoz Ursol et al. (2022) reported comparable average values for MOSH (14.2 mg/kg) and MOAH (2.1 mg/kg). In olive pomace oils, 10-fold higher values were found for both MOSH (Moret et al., 2003) and MOAH (Zoccali et al., 2016; Ruiz et al., 2021).

Oils extracted from olives hand-picked directly from trees usually have background contamination (Menegoz Ursol et al., 2022), while commercial EVOOs have much higher contamination levels. This suggests that processing operations have a very significant impact. Although potential sources of MOH contamination in vegetable oils are already known (Moret et al., 2009), to the best of our knowledge a systematic study along the olive oil production chain is not yet available. Therefore, as part of a PhD project aimed at filling this gap, this work focused on the harvesting phase to assess its incidence/impact in different Italian production realities. The ultimate goal was identifying main contamination sources to enable the implementation of mitigation strategies.

4.2 Materials and methods

4.2.1 Samples

Pre-harvested olive samples were collected directly from the trees in 15 olive groves located in different regions of Italy (5 from Central Italy and 10 from Southern Italy) during oil campaign 2020-21 and sent to our laboratory, where they were stored at -20 °C until the analysis. In each olive grove, olives were hand-picked from at least 10 trees, depending on the size of the olive grove. These incremental samples (200-300 g each) were combined and mixed to obtain an aggregate sample of 2-3 kg from which the laboratory sample to be extracted with the Abencor system (about 1 kg) was derived. Other 17 samples from the same olive groves (in two of which olives were harvested using 2 different methods) were taken after harvesting operations from different containers used for their transport to the mill (e.g. plastic bins, trailers etc.). Again, an aggregate sample of 2-3 kg was obtained combining incremental samples taken from different containers.

Table 4.1 summarizes available sample information. Sample codes indicate the type of culture: traditional (T), intensive (I) or super-intensive (S), and whether the cultivation was biological (B). Olive groves with a maximum of 300 trees/ha are considered traditional, with 300-1000 trees/ha are considered intensive and with more than 1000 trees/ha, up to 2500 trees/ha, are considered super-intensive, even if the plantation density is not the only parameter to be considered (Famiani & Gucci, 2011; Lo Bianco et al., 2021). Information on the proximity to urban areas (distance from urban centers of over 20000 inhabitants within a radius of 10 km from the sampling site) or other possible sources of pollution (distances from main or secondary road and intensity of the vehicular traffic), are also provided. None of the sites were located close to important industrial areas or other potential/evident sources of contamination, except for samples S1, TB5 and TB2, which were about 10-13 km from an airport. TB2 was also located 4 km from a thermoelectric power station. Information about phytosanitary/fertilizing treatments, as well as the harvesting mode, are also reported.

Table 4.1. Characteristics of the sampling sites.

Sample code	Distance from roads/traffic	Distance from urban areas (population)	Phytosanitary (P) or fertilizing (F) treatments	Type of harvesting
TB1	50 m/very low	>10 km	None	(a) Mechanized vibrating comb (b) Pneumatic hand-held comb
TB2	1 km/very low	>10 km	None	Electric hand-held comb
TB3	200 m/very low 800 m/low	8 km (40000)	None	Electric hand-held comb 2T motorized branch shaker
TB4	50 m/very low	>10 km	Zeolite (P)	Pneumatic hand-held comb
TB5	50 m/very low 700 m/medium	2.5 km (380000)	Organic foliar fertilizer (F), Kaolin (P), Copper (P)	Electric hand-held comb
TB6	1 km/low 2.5 km/high	6 km (40000)	Biolivo (F), Oasi Bio (F), Veltery (F), Boroplus (F), Kendal (P), Neoram Blu WG (P)	Electric hand-held comb Trunk shaker with collection cloth
T1	50 m/very low 700 m/low 400 m/medium	>10 km	Copper (P), Deltamethrin (P), Rogor L40 ST 2020 (P)*	Trunk shaker
T2	150 m/low 350 m/medium 1.5 km/high	1 km (50000) 7 km (25000) 10 km (100000)	Biosin Energy (F), Cifo (F), Decis Evo (P), Rame Caffaro Blu WG (P)	Trunk shaker
IB1	300 m/very low 300 m/medium	9 km (25000)	None	Straddle harvester
IB2	100 m/very low 200 m/low 500 m/high	7 km (50000)	None	Pneumatic hand-held comb
IB3	150 m/low 200 m/medium	1.5 km (23000)	Lysodin Boron Express (F), Manisol (F), Coprantol 30 WG (P), Spintor Fly (P)	Pneumatic hand-held comb
IB4	5 km/low	>10 km	Coptrel 500 (F), Dentamet (F), Abyss (F), Idrox (P)	Straddle harvester
I1	50 m/low 400 m/low	2 km (40000)	Manisol (F), Spintor Fly (P)	Pneumatic hand-held comb
I2	150 m/low 400 m/high 1.8 km/high	>10 km	Lysodin Boron Express (F), Manisol (F), Coprantol 30 WG (P), Rogor L40 ST 2020 (P)*	Pneumatic hand-held comb
S1	50 m/low 2 km/medium 2 km/high	10 km (150000)	Kaolin (P), Poltiglia Disperss (P)	(a) Straddle harvester using MOH-based hydraulic oil (b) Straddle harvester using vegetable oil as hydraulic oil

For some of the samplings also lubricants used during harvesting operation were collected and analyzed (Table 4.1). Figure 4.1 shows some photos of the machinery/equipments used for the harvesting.



Figure 4.1. Olive harvesting carried out by hand-held comb (A), trunk shaker (B), mechanized vibrating comb (C) and straddle harvester (D).

4.2.2 Chemicals and standards

n-Hexane, dichloromethane (both distilled before use and check for purity), methanol, *m*-chloroperbenzoic acid (*m*CPBA), potassium hydroxide, sodium thiosulfate and sodium sulfate were purchased from Sigma-Aldrich (St. Louis, Missouri, USA). Ethanol was from Supelco (Bellefonte, Pennsylvania, USA). Water was purified using a MilliQ System from Millipore (Bedford, Massachusetts, USA).

The evaluation of MOSH/MOAH separation performance and their quantification (Biedermann & Grob, 2012a) was performed using the internal standards solution (IS) from Restek (Bellefonte, Pennsylvania, USA), containing *n*-C₁₃ at 0.15 mg/mL, 1,3,5-tritert-butylbenzene (TBB), *n*-C₁₁, cyclohexylcyclohexane (CyCy), pentyl benzene (5B), 1-methyl naphthalene (1-MN), 2-methyl naphthalene (2-MN) at 0.30 mg/mL and 5- α -cholestane (Cho) and perylene (Per) at 0.60 mg/mL. The *n*-C₁₀₋₄₀ *n*-alkane standard mixture (added with *n*-C₅₀), containing even-numbered *n*-alkanes in the specified range, each at 0.05 mg/mL, used to verify the GC performance (both for the LC-GC and the GC \times GC) and the retention time standard mixture, containing *n*-C₁₀, *n*-C₁₁, *n*-C₁₃, *n*-C₁₆, *n*-

C₂₀, *n*-C₂₄, *n*-C₂₅, *n*-C₃₅, *n*-C₄₀ and *n*-C₅₀, used to facilitate integration of the chromatograms according to the given C-fractions (Bratinova & Hoekstra, 2019), were also from Restek.

4.2.3 Instrumentation and chromatographic conditions

Glassware and all the materials intended to come in contact with the sample were rinsed with acetone and distilled *n*-hexane prior use. The Abencor system was from MC2 Ingenieria Y Sistemas (Seville, Spain) and consisted of a hammer mill M-100 and a centrifuge CF-100. The cooking machine HF807 Companion XL was from Moulinex (Ecully, France). The microwave extraction apparatus (MARS5) was from CEM Corporation (Matthews, North Carolina, USA). Sample concentration was performed with a Univapo 100 H centrifuge connected to a V-700 vacuum pump from Büchi AG (Flawil, Switzerland).

4.2.3.1 HPLC-GC-FID

The HPLC-GC-FID system (LC-GC 9000) was from Brechbühler (Zurich, Switzerland) and consisted of an HPLC pump (Phoenix 9000) and a GC (Trace 1310 series) by Thermo Fisher Scientific (Waltham, Massachusetts, USA), with a double channel configuration to have the possibility to perform MOSH and MOAH analysis within the same run. The connection between the two instruments occurred through a Y-interface (Biedermann & Grob, 2009c; Biedermann et al., 2009). The HPLC column was a 250 × 2.1 mm ID by Sepachrom (Milano, Italy), packed with Lichrospher Si-60, 5 µm particle size, while in both the GC channels a 10 m × 0.53 mm ID uncoated/deactivated retention gap, to exploit the retention gap technique (Biedermann & Grob, 2012a), was connected with a 10 m × 0.25 mm ID GC column by Mega (Legnano, Milan, Italy), coated with a 0.15 µm film of PS-255 (1% vinyl, 99% methyl polysiloxane). A steel T-piece, which connected the retention gap to the separation column and a solvent vapour exit (SVE) heated at 140 °C, largely prevented the solvent, which evaporated during partially concurrent eluent evaporation (Boselli et al., 1999), from reaching the FID.

The HPLC flow started with 100% *n*-hexane kept for 0.1 min, subsequently reaching a *n*-hexane/dichloromethane ratio of 70:30 after 0.5 min. The elution occurred at 300 µL/min; MOSH and MOAH fractions were transferred to the GC between 2.1 and 2.6 min, and between 3.8 and 5.3 min, respectively. After 9 minutes of backflush at 500 µL/min, it followed *n*-hexane reconditioning (700 µL/min at 6.5 min, and then 1.5 min at 300 µL/min) prior to the following injection. The carrier (H₂) was set at constant pressure (60

kPa) and 8.5 min after the start of the transfer of the MOSH fraction (which occurred at 51 °C), the temperature gradient reached 350 °C at a rate of 20 °C/min. The FID was heated at 350 °C and set to a data collection rate of 10 Hz. Data were acquired and processed by Chromeleon software (Thermo Fisher Scientific, Waltham, Massachusetts, USA).

4.2.3.2 GC×GC-FID/QTOF

The GC×GC system consisted of an 8890 gas chromatograph equipped with liquid autosampler, cold on-column inlet, FID detector and a 7250 QTOF Mass Spectrometer (Agilent Technologies, Santa Clara, California, USA). The GC transfer line temperature was set at 340 °C, QTOF's ion source and quadrupole were set at 300 and 150 °C, respectively. Ionization was performed in conventional electron ionization (EI) at 70 eV. Collision and quench gas, namely nitrogen and helium, were set 1 and 4 mL/min. Acquisition was performed in full spectra from 50 to 600 m/z at a frequency of 50 spectra/second. The FID employed for parallel detection was set with temperature 320 °C; H₂ flow 30 mL/min, air flow 400 mL/min, makeup flow (N₂) at 25 mL/min and sampling frequency set at 200 Hz.

The column configuration included an uncoated retention gap (10 m x 0.53 mm ID) coupled to a J&W DB-17ms column (15 m x 0.25 mm ID; 0.15 µm of film thickness) by Agilent Technologies as first dimension and a PS-255 (2.45 m x 0.15 mm ID; 0.055 µm of film thickness) by Mega (Legnano, Milan, Italy) as modulation loop and second dimension. The secondary analytical column was connected to deactivated silica capillaries toward QTOF (1 m x 0.1 mm ID) and FID (1 m x 0.18 mm ID) with an unpurged three-way splitter based on Agilent Capillary Flow Technology. Resulting FID/MS split ratio was calculated to be approximately 70:30. 25 µL were injected at 150 µL/min into the on-column injector port set to track-oven mode. The carrier gas was helium, nominal flow was set to 4.5 mL/min for 5.7 min, reduced to 1.5 mL/min over 9 sec (flow ramp change: 20 mL/min); this value was kept constant until the end of the run. The oven temperature program was set as follows: from 45 °C (1 min) to 65°C (4.5 min) at 30 °C/min, to 340 °C (5 min) at 4°C/min.

The system was equipped with a loop-type ZX2 thermal modulator with closed-cycle refrigeration (Zoex Corporation, Houston, Texas, USA) controlled by an Optimode™ v2.0 (SRA Instruments, Cernusco sul Naviglio, Milan, Italy). Hot jet pulse time was set at 350 ms and modulation period was 9 s. Hot jet temperature was programmed from 250 °C (5.1 min) to 400 °C at 4 °C/min. Cold-jet flow, expressed as Mass Flow Controller

(MFC) flow capacity, was programmed through linear regressions as follows: initial value 50%, reduce to 40% during the first 700 seconds, reduce to 5% at 35 minutes then constant until the end of the run.

Data were acquired by MassHunter software (Agilent Technologies, Santa Clara, California, USA). 2D data were processed by GC Image® GC×GC Edition Software, Release 2020r1 (Zoex Corporation, Houston, Texas, USA).

4.2.4 Oil extraction from the olives

To simulate a real extraction system, oil extraction from olives was performed in the laboratory using an Abencor system. Its malaxation unit was replaced by a cooking machine. The milling was carried out on about 800 g of olives, using a 5.5 mm screen, then the malaxation was performed at 40 °C for 45 min with slow continuous mixing (program 3), using the mixing blade, and finally the centrifugation occurred at 3500 rpm for 60 s. Occasionally, it was necessary to add water (milliQ, in the order of 50-100 mL) to perform malaxation and subsequent centrifugation in an optimal way. In presence of slight emulsion, the sample was allowed to separate autonomously from the water overnight, before transferring it to the final container. After completing oil extraction, all components of the pilot plant were washed thoroughly with soap and water in order to avoid cross-contamination between different samples.

4.2.5 MOH analysis

Sample preparation was performed following the protocol from Menegoz Ursol et al. (2022). Briefly, 1 g of oil, added with the IS and dissolved in 10 mL of *n*-hexane, was saponified with 10 mL of a 1.5 N methanolic KOH using MAS. The *n*-hexane phase, separated from methanol by addition of 40 mL of water and cooling at -20°C, was recovered, concentrated and further washed with 3 mL of a 2/1 methanol/water mixture. Finally, the organic phase was concentrated to 700 µL and subjected to epoxidation following the protocol proposed by Nestola & Schmidt (2017).

For MOAH analysis, 100 µL of the sample extract so obtained was injected into the HPLC-GC-FID apparatus, achieving a LOQ of 0.5 mg/kg. Due to overloading by endogenous *n*-alkanes (when injecting 100 µL of the sample extract), a separate run for MOSH analysis was necessary. A lower sample volume (50 µL) was injected in this case (LOQ around 1.0 mg/kg). When this was not sufficient to avoid overloading by *n*-alkanes, or when the sample was subjected to GC×GC-FID/QTOF, an additional purification step, aimed at eliminating this interference, was applied. In brief, 100 µL of saponified and epoxidized

sample was loaded into a glass cartridge (10 mm ID) containing 2.5 g of activated Alox, previously conditioned with 5 mL of *n*-hexane. The elution of the MOSH fraction was carried out with further 5 mL of *n*-hexane, which were recovered and reconcentrated before HPLC-GC-FID analysis.

GC×GC-FID/QTOF analysis was preceded by MOSH and MOAH fractionation. For this purpose, 100 µL of the sample was injected into the HPLC, from which the transfer capillaries towards the GC were disconnected to allow the separate collection of the two outgoing fractions. 25 µL of the latter were then injected for GC×GC characterization.

4.3 Results and discussion

As reported in paragraph 4.2.1, olive samples from different Italian production realities were collected before and after harvesting operations. In some cases, it was also possible to obtain samples of lubricants/greases and hydraulic oils used during harvesting. Detailed instructions were provided to the operators in order to make the sampling as representative as possible.

All the concentrations reported below refer to the extracted oil. The choice to use an Abencor system rather than performing a solvent extraction was based on previous evaluations demonstrating that solvent extraction leads to higher MOH extraction, probably due to faster mass transfer (lower viscosity) and higher solvating power, and therefore does not adequately represent the contamination found in the physically extracted oil (Moret et al., 2003; Gharbi et al., 2017). Extraction yields obtained with the Abencor system were in line with those obtained in the actual mill, and ranged between 10 and 20%, depending on the variety of olives and their degree of ripeness.

4.3.1 Olives sampled from the olive trees (before harvesting)

Based on previous literature (Moret et al., 2003; Gharbi et al., 2017; Menegoz Ursol et al., 2022), olives hand-picked directly from the tree usually have background contamination: around 1-2 mg/kg of MOSH and MOAH below the LOQ (0.5 mg/kg). According to some authors (Gómez-Coca et al., 2016b; Pineda et al., 2017), part of the contamination attributed to mineral oils is the result of biosynthetic mechanisms intrinsic to the plant. However, other authors find it difficult to ascribe the formation of such complex mixtures of hydrocarbons to enzymatic processes (Grob, 2018b).

It is also reported that environmental contamination (Neukom et al. 2002), as well as phytosanitary/fertilizing treatments, can be potential sources of contamination with mineral oils (EFSA, 2012a). According to Regulation (EC) No 889/2008 laying down

rules for the implementation of Regulation (EC) No 834/2007, paraffin and mineral oils can also be used as pesticides on olive trees for organic cultivation.

Olive groves are usually located in countryside areas, therefore high risk of environmental pollution is considered unlikely. Indeed, based on the information collected through the sampling sheets, none of the sampled sites resulted particularly exposed to environmental contamination (urban areas, vehicular traffic, industrial sites, etc.), although slight differences may be present (Table 4.1).

Based on available information, only one of the products used for plant protection/fertilization treatments declared containing MOH. This does not exclude the possible presence of MOH as co-formulants since current regulations do not require a label declaration and there might be leakages of mineral oil from the atomizer pump used to spread the product.

Figure 4.2 shows MOSH and MOAH levels of samples collected directly from the tree. Except for samples TB4 and I2 (that will be discussed separately), 13 out of the 15 hand-picked olives samples contained MOSH from <LOQ to 2.7 mg/kg, in line with the background levels generally found in olives collected at this point of the supply chain. Only in one case (S1), a MOAH contamination of 1.1 mg/kg, whose origin remains unknown, was highlighted. More in detail, 6 out of 7 different samples collected near medium-to-high traffic roads (<700 m) or urban areas (<2 km) (TB5, T1, IB1, IB2, IB3 and I1) contained MOSH levels below the LOQ. Only T2, which was the most exposed to potential sources of environmental pollution, had detectable MOSH (1.6 mg/kg). On the contrary, 3 out of 6 remaining samples from olive groves located more distant from potential contamination sources (TB1, IB4 and S1), had MOSH contamination between 1.6 and 2.7 mg/kg. Again, the other 3 samples (TB2, TB3, TB1) had contamination below the LOQ. In conclusion, no clear correlation was found between the levels of contamination and the position of olive groves with respect to potential environmental sources of contamination.

Phytosanitary/fertilizing treatments also seemed to have a negligible effect on contamination level. No substantial differences were highlighted among samples from olive groves treated and untreated, or between samples from conventional and biological cultivars. Based on available technical sheets, the presence of mineral oils was confirmed only for the phytosanitary called “Rogor L40 ST 2020” (which was declared to contain 8% of hydrocarbons, C₉-aromatics, having CE number 918-668-5 corresponding to isomers of benzene substituted either with methyl groups, or with methyl and ethyl groups or with a propyl group). This product was used in olive groves I2 and T1, but in

neither case visible contamination was observed, probably due to the high volatility of C₉-aromatic hydrocarbons (boiling point: 165-180 °C), comparable to that of *n*-C₁₀.

In samples TB4 (15.5 mg/kg MOSH) and I2 (5.8 mg/kg MOSH), exceptionally high contamination, which cannot be explained by environmental contamination, was highlighted. While contamination of sample I2 was no longer present after harvesting operation (it will be discussed in the next paragraph), the high contamination level found in sample TB4 was confirmed also in the post-harvest olives. The only phytosanitary treatment performed on this olive grove was with zeolite (a material of volcanic origin used to protect the olives from fungi and oil fly), that was found to be free of MOH. The unconfirmed hypothesis is that contamination was due to the addition of mineral oil-based products into the atomizer to allow a better dispersion/adhesion of the active principle to the plants (a not declared practice), or to a leak of lubricating oil from its mechanical components (e.g. the pump).

4.3.2 Harvesting operations and lubricants used

The choice of the harvesting method, although dependent on several factors, is strictly linked to the type of olive grove (age of the plants, planting density, farming and pruning method, etc.), as well as to economic aspects (Famiani & Gucci, 2011; Tous, 2011). Traditional olive groves are the least profitable since they show a limited productivity, mainly linked to the low cultivation density, and their trees are of such age and size that they do not allow automated harvesting but rather manual or semi-mechanized. These are the most widespread in Italy as well as worldwide. However, as the result of technological advances in olive cultivation (mainly regarding harvesting and irrigation) and in virtue of the highest profit margin, higher-densities olive groves are currently spreading. In these cases, harvesting is totally mechanized.

In general, the use of any equipment/machinery implies the use of greases, lubricants and hydraulic oils that may have a mineral oil base and can accidentally end up into the food matrix. Since accidental leaks of lubricants, engine oil and hydraulic oil, as well as contact with lubricated mechanical parts, are probably the most important source of contamination during harvesting operations, lubricants used in the machinery were analyzed and compared with contamination found in olives whenever possible. Contamination from exhaust gases emitted from harvesting machinery and from contact material (bags, bins, nets, etc.) represent other possible sources of contamination. These were not investigated in this study and are believed to have a minor impact with respect to lubricants. Table 4.2 summarizes the characteristics of some lubricants used during

harvesting operation. These were quantified by HPLC-GC-FID. GC×GC-FID data showed good agreement.

Table 4.2. Sampled lubricants and their characteristics. The % of MOAH in brackets (when available), refers to data obtained from the integration of the 2D plot deriving from GC×GC-FID analysis.

Sample code	Equipment/ machinery	Product type (name)	gMOH/ 100g product	% MOAH	MOH distribution [range(s) / center(s)]
TB1	mechanized comb	hydraulic oil	85.9	23.2 (27.3)	<i>n</i> -C ₁₆₋₅₀ / <i>n</i> -C ₂₉ and <i>n</i> -C ₃₅
		lubricating oil (Greenoil Agritecno Flu)	0.0	-	-
TB3	branch shaker	2T oil (Echo PowerMix+ 2T)	52.4	10.2	<i>n</i> -C ₁₀₋₁₆ / <i>n</i> -C ₁₃ and <i>n</i> -C ₁₆₋₅₀ / <i>n</i> -C ₂₈
TB4	pneumatic hand-held comb	lubricating oil (Greenoil Agritecno Flu)	0.0	-	-
TB6	trunk shaker	hydraulic oil	81.6	18.8 (21.9)	<i>n</i> -C ₁₇₋₅₀ / <i>n</i> -C ₃₀
		lubricating grease	66.5	32.2 (34.6)	<i>n</i> -C _{16->50} / <i>n</i> -C ₃₀
IB3	pneumatic hand-held comb	lubricating oil (Zanon Fluid 32)	0.0	-	-
		lubricating oil (Campagnola Big Flu)	93.3	15.5	<i>n</i> -C ₁₂₋₃₂ / <i>n</i> -C ₁₈ and <i>n</i> -C ₂₂
IB4	straddle harvester	hydraulic oil (Ambra Hydrosystem 68HV)	78.6	21.9 (25.4)	<i>n</i> -C ₁₆₋₅₀ / <i>n</i> -C ₂₈
		lubricating grease (New Holland 2001228A)	86.3	1.7 (2.2)	<i>n</i> -C ₂₀₋₅₀ / <i>n</i> -C ₃₃
I1	pneumatic hand-held comb	lubricating oil (Campagnola Fudy Flu)	90.8	24.1	<i>n</i> -C ₁₃₋₃₅ / <i>n</i> -C ₁₈ and <i>n</i> -C ₂₂
I2	pneumatic hand-held comb	lubricating oil (Campagnola Big Flu)	93.3	15.5	<i>n</i> -C ₁₂₋₃₂ / <i>n</i> -C ₁₈ and <i>n</i> -C ₂₂
		lubricating oil (Erg Sinthron 10W40)	78.3	13.3	<i>n</i> -C ₁₆₋₄₈ / <i>n</i> -C ₂₈

4.3.3 Olives sampled after harvesting

As shown in Figure 4.2, for olive oil from 5 out of the 15 olive groves considered (7 traditional, 7 intensive e 1 super-intensive), MOH contamination clearly increased after harvesting operations (red arrow), while it remained practically constant (yellow arrows) for 9 samples and unexpectedly decreased for one (green arrow). When comparing data obtained before and after the harvesting operations, we had to account for inherent variability due to the difficulty to obtain totally representative olive samples. Therefore, small variations in concentration (<30%) for levels above 2.5 mg/kg, or larger ones below

this threshold (as in the case of sample IB1), were not considered significant (high data variability is expected for MOH at low levels).

The decrease in contamination observed for sample I2 can only be explained by assuming that the contamination of the olives in pre-harvest occurred through contact with a dirty material (e.g., the bowl used to mix olives from different trees) and/or was due to a problem of poor representativeness of the olive samples taken before and/or after harvest.

Results of Figure 4.2 highlighted as harvesting operations determined a significant increase of MOSH and MOAH in about 33% of the olive groves considered (in about 40% of the 17 olive samples, if we consider that in 2 groves olives were collected using two different harvesting modes). In all cases, there was a clear correspondence between the HPLC-GC-FID profiles of the olives after harvesting and that of one of the lubricants used during harvesting operations (only for IB2 lubricants were not provided). MOSH/MOAH ratio helped us in identifying the source of contamination, and GC×GC-FID/MS, applied on selected lubricants and olive oil samples, confirmed HPLC-GC-FID data adding some interesting information.

As evident from the bar diagram (Figure 4.2), in 9 samples there was no important increase of the contamination level. These samples were characterized by lower level of mechanization in the harvesting phase. Except for olives from olive groves T1 and T2, which were harvested using a trunk shaker, all other olive samples were harvested using hand-held combs, mainly electric (TB2, TB3, TB5), pneumatic (TB4, IB3, I1, I2) or motor-powered (2T branch shake, in case of TB3). On the contrary, contamination occurred preferably on olives harvested with big machinery, such as trunk shakers equipped with collection cloth (such as TB6), mechanized harvesters (TB1(b) and IB4), and only in one case (IB2), regarded a sample collected with a pneumatic hand-held comb. In most cases the type of cultivation appeared to be a discriminating factor. In fact, groves with high production density are more suitable for mechanized harvesting (Lo Bianco et al., 2021) and therefore more prone to be contaminated by mineral oils. Contamination by mineral oils due to the use of harvesters was already highlighted in the past for the sunflower seeds (Grundböck et al., 2010).

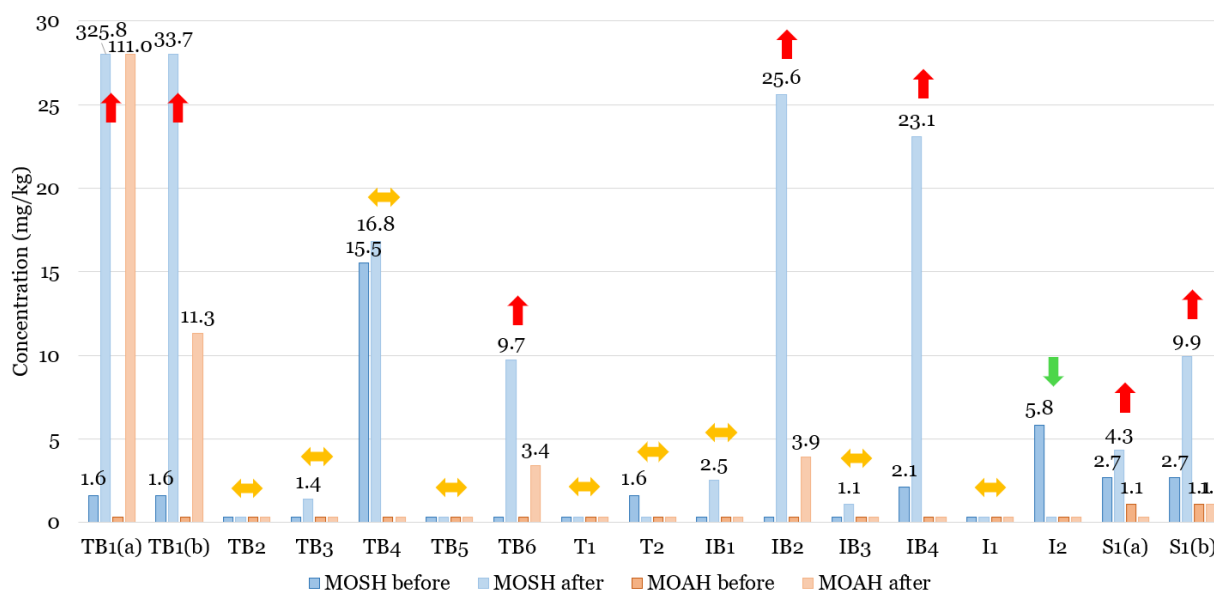


Figure 4.2. MOSH and MOAH concentrations of EVOOs from olives sampled before (hand-picked from the trees) and after harvesting operations. Absence of data labels indicates levels below the LOQ (1.0 mg/kg for MOSH and 0.5 mg/kg for MOAH).

4.3.4 Examples of source identification

The most interesting cases that led to the identification of the source of contamination are discussed below.

Olives from olive grove TB1 represent a very interesting case study. The traditional olive grove was harvested by (a) mechanized vibrating comb (Figure 4.1C) and (b) pneumatic hand-held comb (Figure 4.1A), giving separate olive samples. The producer provided both the hydraulic oil used for the mechanized vibrating comb, a technical oil (85.9 g of MOH per 100 g of product, of which 23.2% were MOAH), and the lubricant used for the hand-held comb (which had no detectable MOH).

As reported previously, EVOO TB1, extracted from olives manually picked from the tree, contained very low MOSH (1.6 mg/kg) and negligible MOAH (<0.5 mg/kg). On the contrary, EVOO TB1(a), extracted in the laboratory from olives harvested with the mechanized vibrating comb, had MOSH and MOAH levels of 325.8 and 111.0 mg/kg, respectively. EVOO TB1(b), obtained from olives from the same olive grove, previously harvested with pneumatic hand-held combs, had instead contamination levels approximately 10 times lower (33.7 mg/kg of MOAH and 11.3 mg/kg of MOAH).

Figure 4.3A shows an overlay of the HPLC-GC-FID traces of MOSH and MOAH fractions of EVOO TB1(a) obtained from olives before and after harvesting operations, as well as of the hydraulic oil used for the mechanized vibrating comb, connected to a tractor by means of a hydraulically operated arm. Both olive oil and hydraulic oil had the same profile

distributed over a wide range of molecular weights from n -C₁₆ to n -C₅₀, probably the result of two different overlapping humps (one centered on n -C₂₉ and another on n -C₃₅). Based on the correspondence of the HPLC-GC-FID profiles and of the MOAH percentage (25.4% for the olive oil and 23.2% for the hydraulic oil), the contamination source of EVOO TB1(a) was uniquely attributed to the hydraulic oil. This very high contamination level was exceptional, and the cause was identified in a leakage from the hydraulic circuit connections of the comb, noticed during sampling. When this happens, harvested olives must be discarded and the machinery must be cleaned to prevent significant contamination.

GC×GC-FID plots of the MOSH fraction (left side of Figure 4.3) of the hydraulic oil of the mechanized vibrating comb (Figure 4.3B) and of EVOO TB1(a) (Figure 4.3C) matched perfectly, confirming that the hydraulic oil was the unique source of contamination for both EVOOs TB1(a) and TB1(b) after harvesting. The red line in B indicates the boundary between MOSH and MOAH areas and demonstrates how HPLC pre-separation of MOSH and MOAH fractions is mandatory in order to avoid co-elution of 4- and 5-ring saturated hydrocarbons (steranes and hopanes) with the highly alkylated two- and three-ring aromatics, as reported by (Biedermann & Grob, 2009a). Surprisingly, EVOO TB1(b) had the same contamination profile found in EVOO TB1(a) (inserts in Figure 4.3C), although at lower levels. This suggested that the use of the mechanized vibrating comb at earlier times had impregnated the harvesting nets with hydraulic oil, which was later transferred to the olives harvested with hand-held combs. For this reason, the use of dirty nets, along with poor machine maintenance, may be critical.

Figure 4.3C refers to samples which underwent a further passage on aluminium oxide to remove interference by endogenous n -alkanes (n -alkanes beyond n -C₂₃ are hardly visible). In agreement with literature data (Biedermann et al., 2015), the 2D MOSH plots showed very orderly patterns with series of homologues clearly visible to indicate the presence of chemical groups with different polarity, such as naphthenes with increasing numbers of cycles or degree of alkylation. MOAH percentage of the hydraulic oil (26.8%) and of EVOO TB1(a) (27.3%), calculated from 2D MOSH and MOAH areas, were in good agreement with HPLC-GC-FID data.

GC×GC-FID plots of the MOAH fraction (right side of Figure 4.3) of the hydraulic oil of the mechanized vibrating comb (Figure 4.3B), as well as that of EVOO TB1(a) (Figure 4.3C), showed a cloud of signal characterized by limited resolution, not dissimilar from the typical mono-dimensional hump. In this case no high degree of structure was observed. Nevertheless, it is possible to draw some interesting conclusions. Elution in the

first dimension indicated high boiling components with a hump centred on $n\text{-C}_{35}$ and well above $n\text{-C}_{40}$. Retention behaviour on the non-polar second dimension, on the other hand, provides information on the chemistry. The MOAH cluster is positioned in the middle of the vertical axis. This excludes elevated polarity, since highly polar compounds such as poly-aromatic hydrocarbons with no or little alkylation would be less retained in the secondary column and would consequently appear in the lower portion of the 2D separation space, similarly to the marker perylene. Since peaks with this elution behaviour are not observed, their presence at significant levels is unlikely.

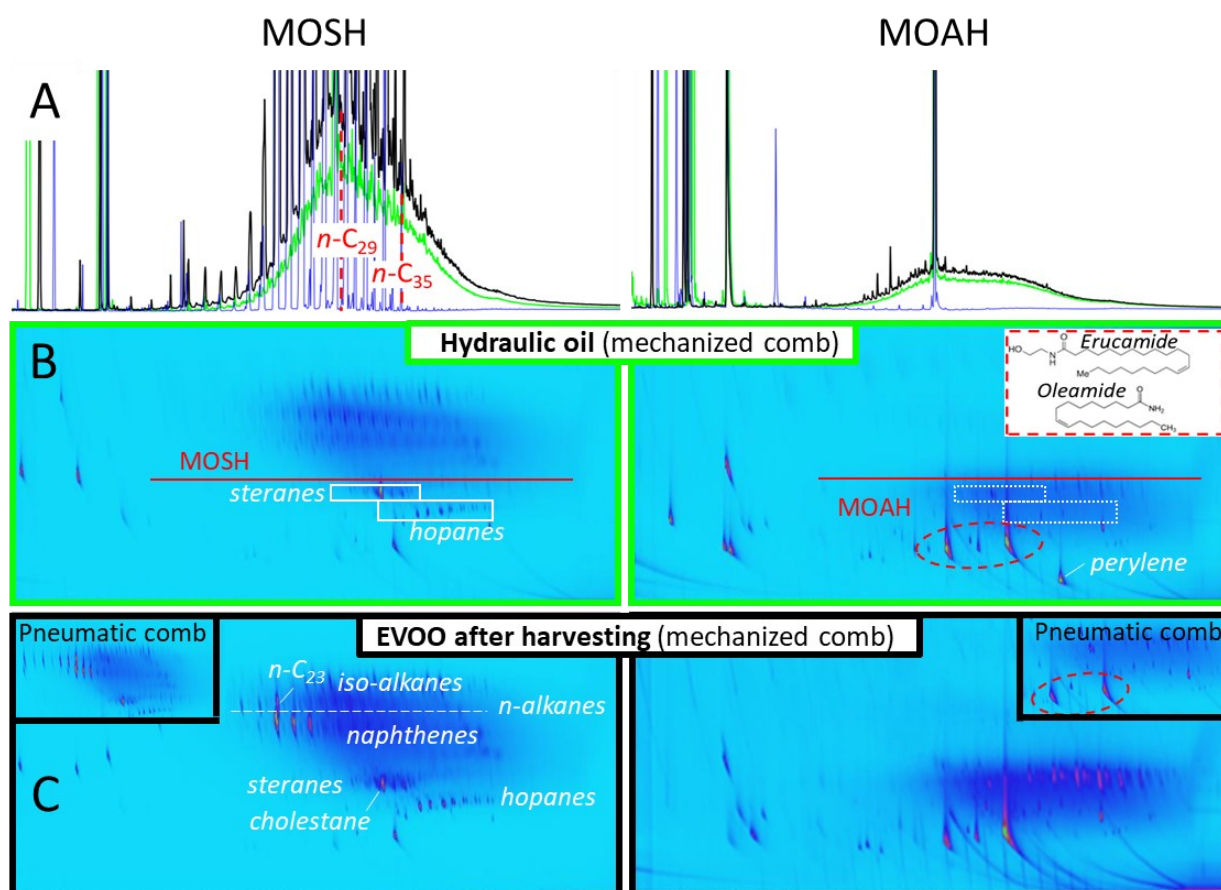


Figure 4.3. Overlay of MOSH and MOAH HPLC-GC-FID chromatograms of samples TB1: EVOO from olives sampled before (blue line) and after harvesting (black line), hydraulic oil of the vibrating comb (green line) (A). Below, from top to bottom: GCxGC-FID plots of the MOSH (left side) and MOAH (right side) fractions of the hydraulic oil of the mechanized vibrating comb (B) and EVOOs from the olives harvested with different equipment (C). Presence of erucamide and oleamide is highlighted (B, C) together with their chemical structure. The red line in B evidences the boundary between MOSH and MOAH areas.

This was supported also by spectral information, which did not highlight such components. MS signal (Figure 4.4) showed complex breakdown patterns, which could be explained by highly alkylated aromatics or multi-unsaturated compounds such as complex polyolefins. This is supported also by the degree of complexity, which suggests an elevated number of isomers not compatible with very low alkylation level. This

information may be valuable for assessing the potential impact of contamination from a customer safety perspective, as these chemical classes are known to have different toxicity compared to polyaromatic hydrocarbons.

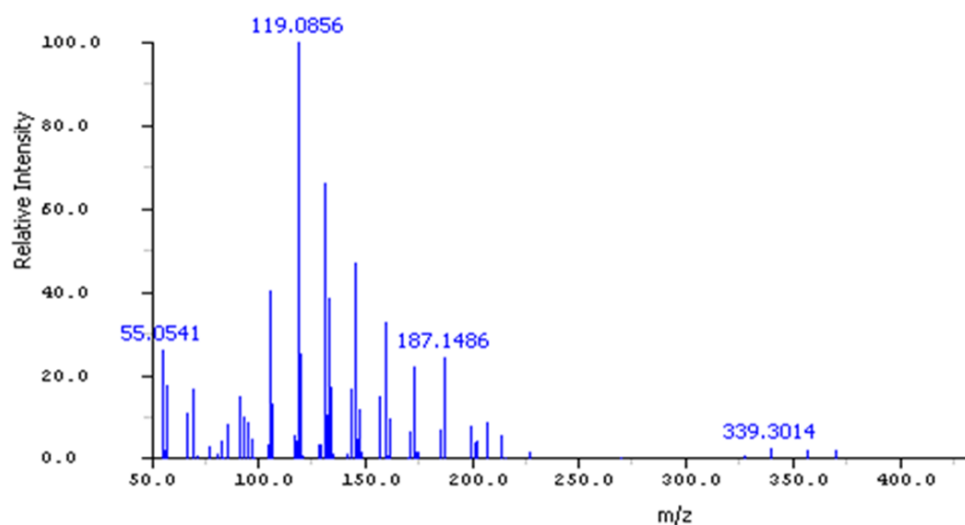


Figure 4.4. MS spectra resulting from an identification attempt performed in a generic point of the MOAH cloud.

In the 2D MOAH plots of Figures 4.3B and 4.3C, two intense spots are highlighted, identified as primary unsaturated amides (erucamide and oleamide). The same spots are also visible in the 2D MOSH plots of Figures 4.5D and 4.5C. Based on the fact that they were occasionally observed in the MOSH and/or MOAH fraction of the 2D plots, but not in the HPLC-GC-FID trace, it was concluded that are artifacts or interferences introduced during sample handling before GC×GC analysis.

Another interesting case was sample IB4, which came from an intensive olive grove where olives were collected using a straddle harvester (Figure 4.1D). After harvesting, MOSH concentration increased from 2.1 to 23.1 mg/kg, while MOAH remained just below the LOQ. This suggested the possible contribution from the food-grade grease (refined to remove the aromatic fraction) used to lubricate the mechanical parts of the harvester. Indeed, the analysis of the grease resulted in a low amount of MOAH (1.7% on the total MOH), perfectly in line with what was found in olive oil (2.2%). In addition, a match was also found in relation to the molecular weight distribution, which for both went from n -C₂₁ to n -C₅₀, centred on n -C₃₃. For confirmation, also the oil from the hydraulic circuit of the same machinery was sampled. However, it showed a molecular weight distribution located at earlier retention times (centred on n -C₂₈ and covering the range n -C₁₇₋₄₄), and 21.9% of MOAH, definitively excluding its contribution to the contamination. Figure 4.5A shows an overlay of the HPLC-GC-FID chromatograms of MOSH and MOAH fractions of

the EVOOs from olives before and after harvesting, together with the traces of the lubricants considered as possible sources of contamination. The good agreement convincingly confirmed the responsibility of the grease.

Starting from a fingerprint approach, and therefore based simply on a comparison of the positions of the clouds of unresolved compounds within the 2D plot, GC×GC-FID confirmed the same hypotheses drawn from the HPLC-GC-FID chromatograms. Indeed, the position of the MOSH cloud of the grease (Figure 4.5B on the left) matched with that of EVOO (Figure 4.5D), and even though the clouds relative to the hydraulic oil (Figure 4.5C) and the grease showed patterns not too dissimilar to each other, their different position within the 2D plot proved to be an element of discrimination. Figure 4.5C' shows how the MS data can be investigated in selective ion chromatogram (SIC) mode to discriminate between different classes of compounds. By extracting m/z of 71 (Carrillo et al., 2022b) and 82 (Biedermann et al., 2015; Carrillo et al., 2022b), which are typical fragments for *n*-alkanes/iso-alkanes and naphthenes respectively, a more in-depth characterization of MOSH is possible.

For the MOAH fraction, the absence of any cloud in the 2D plot of the grease (Figure 4.5B on the right), instead present for the hydraulic oil (not shown), confirmed the absence of aromatic compounds above the limit of quantification.

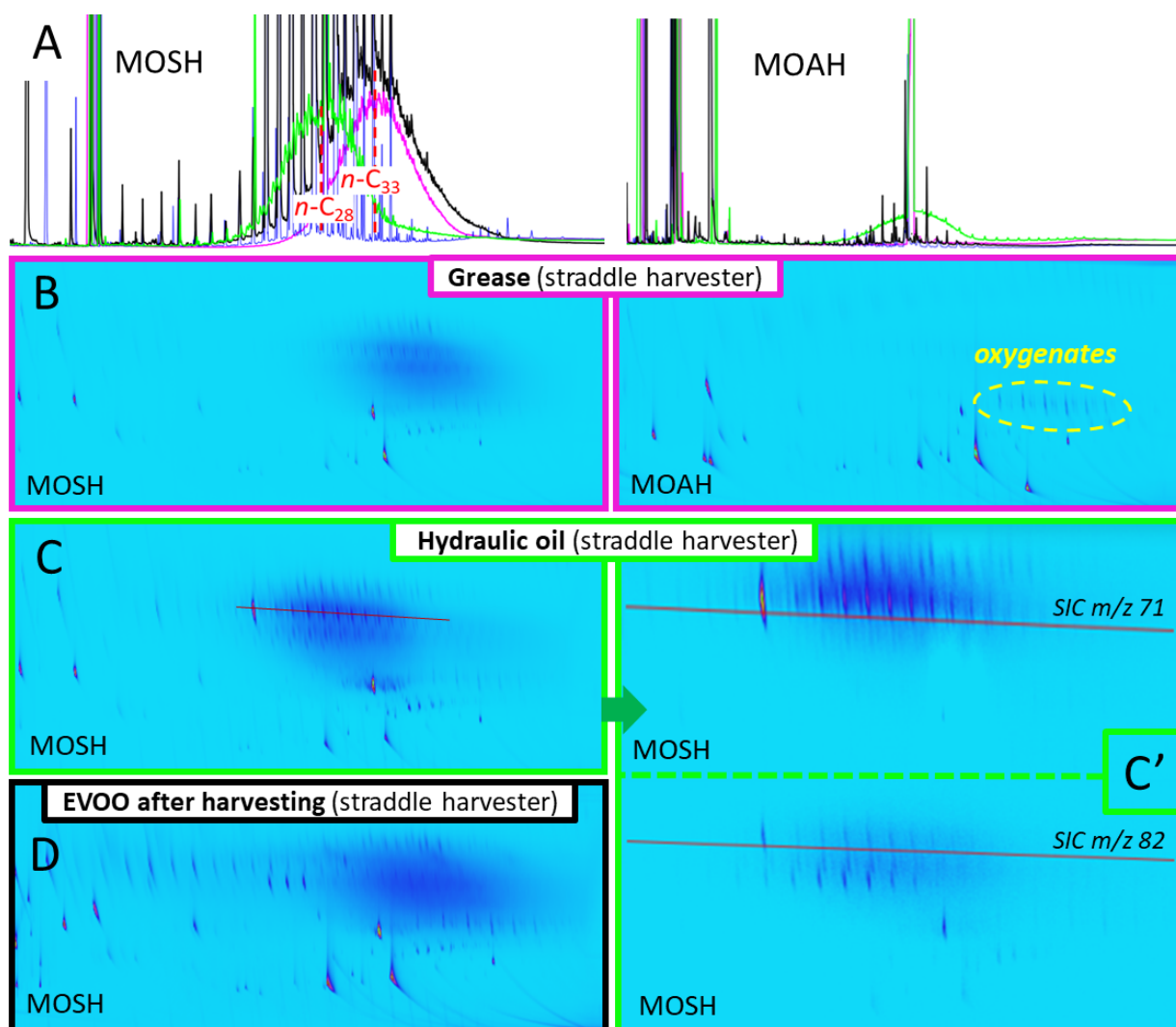


Figure 4.5. Overlay of MOSH and MOAH HPLC-GC-FID chromatograms of samples IB4: EVOO from olives sampled before (blue line) and after harvesting (black line), hydraulic oil (green line) and grease (purple line) of the straddle harvester (A). Below, from top to bottom: GCxGC plots of MOSH and MOAH of the grease (B), MOSH of the hydraulic oil (C), including on the right SIC plots at m/z 71 (alkanes/isoalkanes) and at m/z 82 (naphthenes) (C') and EVOO from olives after harvesting with the straddle harvester (D). In B the presence of oxygenated compounds in the MOAH fraction of the grease is highlighted.

The grease, as well as the EVOO from olives after harvesting (plot not reported), showed the presence of a series of homologues, tentatively identified as esters. While precise labelling may remain challenging, the QTOF confirmed with good confidence that these compounds were oxygenates, in agreement with library search results indicating esters. The exact mass experimentally acquired, which was m/z 257.2475, then exploited for SIC mode (Figure 4.6), was in fact compatible with the formula $C_{16}H_{33}O_2^+$ (m/z 257.2475) with an excellent accuracy of 0.2 ppm, while hydrocarbons could be excluded (m/z $C_{19}H_{29}^+$, 257.2264, m/z , accuracy 80 ppm).

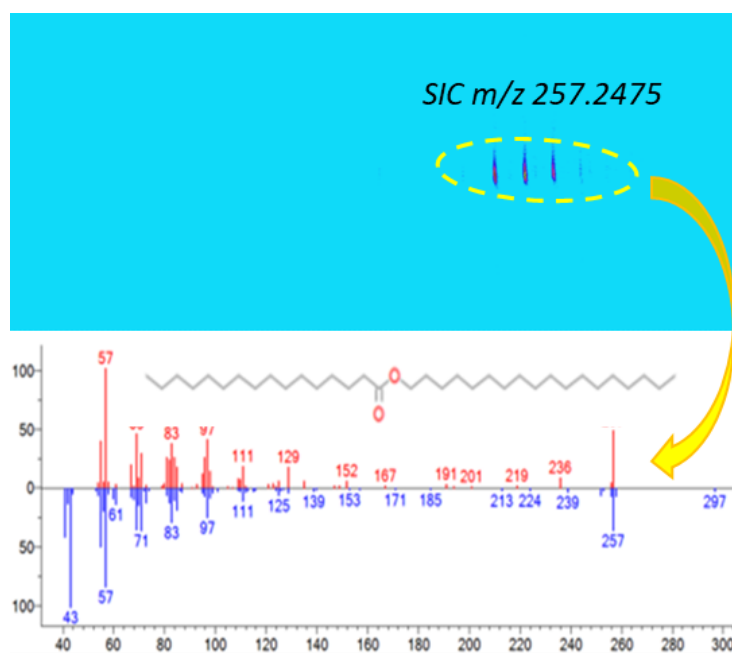


Figure 4.6. Presence of oxygenated compounds in the MOAH fraction of the grease highlighted using SIC mode at m/z 257.2475 (upper figure), together with spectra and hypothesized chemical structure (lower figure). The spectra in red is the experimental one, while the one in blue is the most similar to it from NIST library.

Admittedly, the QTOF is not a requirement for MOSH/MOAH analysis in particular for routine use where low-resolution mass spectrometers may suffice. However, this example showcases the potential added value of high-resolution mass spectrometry for confirming or excluding the presence of interferences containing heteroatoms possibly occurring in matrices or contaminants of various origins, which would lead to unwanted overestimation of the MOAH fraction. In our opinion QTOF detector is thus an interesting additional tool for the development of advanced methodologies and research aimed at in depth characterization thanks to high resolution and other unique identification capabilities such as low-energy ionization and MS/MS mode not explored in the context of this work.

Similarly, correspondence with the grease used to lubricate the mechanical parts was also found for EVOO from olives TB6 after harvesting, where a self-propelled trunk shaker equipped with a collection clot was used. Also in this case, a sample of the hydraulic circuit oil was analysed, but the profile did not match the EVOO sample. Looking at the HPLC-GC-FID traces (Figure 4.7A), both MOSH humps of these two mineral oil products fell under the contamination found in the EVOO and were centred around n -C₃₀. On the other hand, the hydraulic oil had a narrower profile distributed over n -C₁₈₋₅₀, differently from the grease and the EVOO whose profile was broader and reached molecular weights beyond n -C₅₀. MOAH traces (not reported) confirmed the source identification.

The same results were achieved from 2D plots of MOSH fractions reported in Figure 4.7. This was particularly evident by the tailing of the cloud in the GC×GC plots of the grease (Figure 4.7C), present also in the EVOO plot (Figure 4.7E), but not in that of the hydraulic oil (Figure 4.7B). As visible in Figure 4.7D, the olive oil after harvesting had a contamination profile consistent with the presence of poly-alpha-olefins (PAO), absent in the two lubricants used, highlighted also in the GC×GC plot (Figure 4.7E). A profile match was also found with a PAO-based lubricant analysed in the context of another sampling, where three narrow humps related to hexamers, heptamers and octamers deriving from the condensation of 1-hexene units, are evident. This suggested that the final contamination came from multiple sources and that one of these was an undeclared PAO-based lubricant, or a leakage of synthetic motor oil (Grob et al., 2001) from the engine of the trunk shaker used for the harvesting.

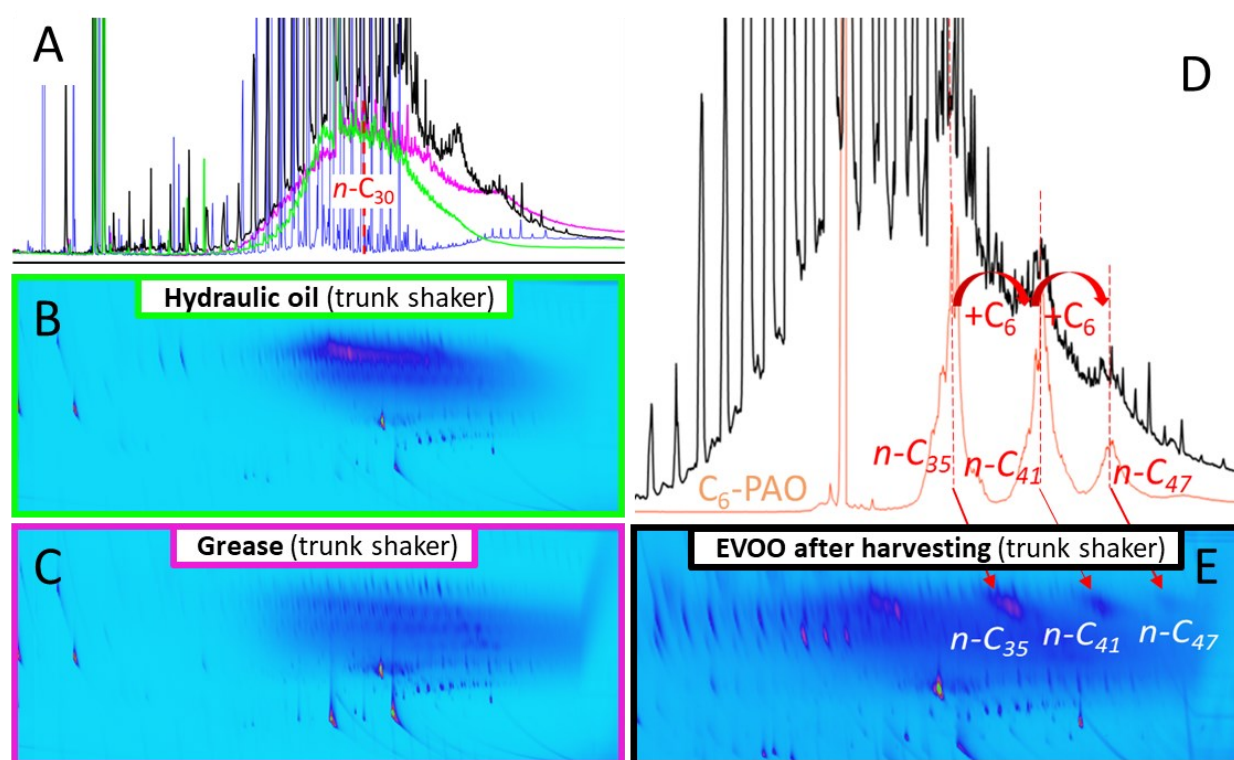


Figure 4.7. Overlay of MOSH HPLC-GC-FID chromatograms of samples TB6: EVOO from olives sampled before (blue line) and after harvesting (black line), hydraulic oil (green line) and grease (purple line) of the trunk shaker (A), as well as EVOO from olives after the harvesting (black line) and a PAO-based lubricant (orange line) (D). Below, GC×GC plots of the MOSH fraction of: hydraulic oil (B), grease (C) and EVOO from olives after harvesting with the trunk shaker (E).

Regarding the use of trunk shakers, it is important to note that such harvesting machine was also used in olive groves T1 and T2, and no increase in contamination levels was observed. In one case, the producer declared that no lubricant was used, while in the other the trunk shaker was not equipped with the collection cloth and the olives fell directly on

the collection nets lying on the ground (Figure 4.1B). This difference, as well as the non-use of lubricants, can explain the different contamination scenarios observed. Indeed, shakers equipped with the collection cloth favour accumulation and permanence of the olives in the central part of the machinery where lubricated mechanical parts are present. The latter samplings support the hypothesis that, if hydraulic circuits are well maintained, there is no possibility of contamination because there is no contact between the lubricating oil and olives. On the contrary, grease on mechanical parts is more exposed to contact with olives.

This was also confirmed by sampling S1, which was carried out in duplicate and separately on olives harvested with two different straddle harvesters, operating either with the use of mineral oil (S1(a)) or vegetable oil (S1(b)) in the hydraulic circuit. Unexpectedly, the highest contamination level was found for the harvester fed with vegetable oil (9.9 mg/kg of MOSH, 1.1 mg/kg of MOAH), instead of mineral oil (4.3 mg/kg of MOSH, <LOQ for MOAH). However, the HPLC-GC-FID profiles of the two samples matched, suggesting a common origin of the contamination, probably attributable to the grease used for the lubrication of the mechanical parts of the two harvesters (not provided), rather than any leak from the hydraulic circuits. The grease, which unlike hydraulic oil is hardly replaceable with a vegetable derivative, was probably the same for both the harvesters, since they belonged to the same company. The GC×GC-FID fingerprint approach also confirmed the common contamination of the two EVOO samples.

Finally, IB2 was the last sample for which an evident MOH increase (from below the quantification limit for both MOSH and MOAH to 25.6 mg/kg for MOSH and 3.9 mg/kg for MOAH), was observed. Since no lubricants were declared/provided, it was not possible to make a comparison as for other samples. The contamination profile (distributed from n -C₁₃ to n -C₄₄) consisted of two humps, one centred on n -C₂₀ and one on n -C₂₇, suggesting a contamination from more than one source (Figure 4.8).

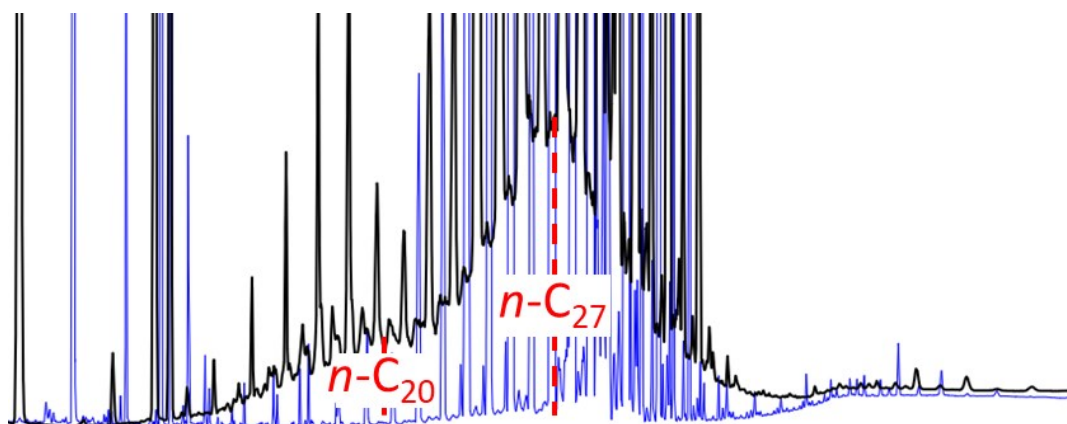


Figure 4.8. HPLC-GC-FID chromatograms of the MOSH fraction of samples IB2 before (blue line) and after harvesting (black line).

None of the other EVOOs from olive harvested using pneumatic held-hand combs underwent a significant MOH increase. However, this does not exclude that contamination may occur during collection with such equipment. During operation, compressed air containing an aerosol of lubricant is pumped through the body of the hand-held comb and finally expelled outside. Use of technical grade lubricants for this purpose, or leakage of lubricating oil at the level of the compressor piston, may possibly result in contamination.

4.4 Conclusions

This work allowed to deepen the knowledge on the contribution of harvesting operations to MOH contamination in the olive oil supply chain. Olives hand-picked from the tree had in general rather low MOSH contamination (ranging from below the LOQ to 2.7 mg/kg) and MOAH below the LOQ (0.5 mg/kg). No clear correlation was found between the contamination level and the proximity to potential sources of environmental contamination. The impact of phytosanitary treatments appeared to be negligible, although it cannot be ruled out that the exceptionally high MOSH level found in sample TB4 before harvesting (15.5 mg/kg) was due to an oil leakage from the sprayer pump (atomizer) or to the addition of mineral oil to the phytosanitary solution (a practice that is unreported, but used by some to improve phytosanitary adhesion to the plant, and which should be avoided).

About 40% of the EVOO samples extracted from olives sampled after the harvesting operations reported an unequivocal MOH increase due to harvesting operations, reaching in one particular case (where an accidental leak of hydraulic oil was observed) 325.8 mg/kg of MOSH and 111.0 mg/kg of MOAH. The remaining samples, for which an

increase due to harvesting operations was found, contained MOSH levels from 4.3 to 33.7 mg/kg (on average 17.7 mg/kg) and MOAH from 1.1 to 11.3 mg/kg (on average 5.1 mg/kg). Of the 7 EVOO samples contaminated during harvesting operations, 4 (TB1(a), TB1(b), IB2 and IB4) exceeded the 2 mg/kg MOAH limit recently recommended by the European Commission (2022), as well as the 13 mg/kg benchmark level for MOSH in vegetable oils recently confirmed by LAV & BLL (2022).

Coupled HPLC-GC-FID resulted to be a good tool for identifying the source of contamination when the process lubricants were available for comparison, allowing to draw conclusions which were then confirmed by the comprehensive approach. Indeed, the GC×GC platform equipped with parallel detection channels (FID/QTOF) allowed an insightful characterization of the hydrocarbon fractions. This methodology offered higher separation power and thus more accurate composition information. In particular, for the highly structured MOSH several chemical classes were successfully separated and identified. Two-dimensional chromatographic fingerprinting allowed for a more straightforward and confident identification of the contamination origin. These findings confirmed the interesting potential of this technique for MOSH/MOAH analysis, supporting the reference methodology for a more insightful investigation of samples positive to contamination.

Based on the results obtained, it is clear that good maintenance of machinery/equipment used during harvesting, their correct use and cleaning are of fundamental importance in reducing the risk of contamination. Despite this, it has been highlighted that for some machinery contamination is the consequence of an unavoidable contact between food matrix and mechanical parts. This is why machinery should start to be designed differently, even though this is a long-term process.

Currently, a reasonable approach is, where machinery characteristics allow it, to replace technical grade lubricants (containing MOSH and MOAH) with refined/food grade lubricants (free of MOAH) or, better, with alternative lubricants free of MOH. Finally, awareness of the problem and adoption of good harvesting practices can help minimizing the risk of incurring high levels of contamination.

5 Evaluation of the impact of olive milling on the mineral oil contamination of extra virgin olive oils

5.1 Introduction

Mineral oil hydrocarbons (MOH) are a class of environmental and processing contaminants. Given their petrogenic origin, together with the large use of petroleum distillation products in many sectors of the food chain, they are widely present in various foodstuffs. Their marked lipophilicity is responsible for their widespread presence in fatty matrices, among which vegetable oils stand out (Brühl, 2016; Gómez-Coca, 2016b; Gharbi et al., 2017). From the chemical point of view, mineral oils are mixtures of thousands of hydrocarbon isomers, classified by chemical structure and for toxicological reasons into mineral oil saturated hydrocarbons (MOSH), comprising paraffins and naphthenes, i.e. linear, branched and cyclic (mainly alkylated) compounds, and mineral oil aromatic hydrocarbons (MOAH), comprising mono- or polyaromatic species, alkylated for more than 98% (EFSA, 2012a; Bratinova & Hoekstra, 2019). Due to the carcinogenic, genotoxic and mutagenic action of compounds with at least 3 aromatic rings, MOAH are of higher concern with respect to MOSH, which instead tend to accumulate in different organs and tissues, mainly those of mass range between n -C₂₀ and n -C₄₀, increasing their volume and leading to formation of microgranulomas and inflammatory states (EFSA, 2012a; Grob, 2018a).

According to the guidance of the Joint Research Centre (Bratinova & Hoekstra, 2019), the reference method for MOH analysis in edible oils and fats involves on-line high performance liquid chromatography HP(LC) - gas chromatography (GC) coupled with flame ionization detection (FID), firstly developed by Biedermann et al., (2009). New methods have been implemented in recent years to overcome limitations of the EN 16995:2017 standard, which does not include sample pre-enrichment, mandatory to reach adequate sensitivity, with particular reference to the DGF C-VI 22 (20) method (Albert et al., 2022) and the updated EN 16995:2017 method, which share the same protocol. A particular attention was also given to improve sample purification methods aimed at removing interference by olefins and, when necessary, by endogenous n -alkanes. Regarding the achievement of low limit of quantification (LOQ) for the MOSH fraction, useful for their evaluation when present at low-level (e.g. background contamination), these methods provide for a saponification step for the removal of the oil matrix, followed by a passage through a column made up of Alox and activated silica, for the removal of the endogenous n -alkanes (n -C₂₁₋₃₅) (Srbínovska et al., 2020) which, when overloading

the chromatogram, can potentially provide unreliable quantifications (Fiselier et al., 2009a). However, proposed methods require some degree of manipulation, as well as the use of significant volumes of adsorbents and solvents. It must be also emphasized that elution through Alox can determine the underestimation of the contamination (around 20%) due to the retention of some isoalkanes (Fiselier et al., 2009a), thus it is considered as an optional tool to be used at the analyst's discretion only when necessary.

Menegoz Ursol et al. (2023) have highlighted how olive harvesting operations, and in particular the use of lubricated machinery, have a significant impact on the mineral oil contamination of olive oils (which increased in 40% of the samples). Nevertheless, according to these data, about 75% of the samples contained a contamination considered acceptable in terms of MOAH if compared to the limit of 2 mg/kg recently recommended by the SCoPAFF (EC, 2022). Data on 12 extra virgin olive oils (EVOOs) from the market, analyzed by the same authors in a previous study (Menegoz Ursol et al., 2022), reported on average higher contamination, suggesting the presence of some criticality in the phases following harvesting, like transportation, extraction and/or following operations. About this, little information is available from the literature. Under certain conditions, contamination was attributed to the containers used to transport the raw material from the field to the extraction plant (Brühl, 2016). Lubricants from machinery used in the extraction plant are considered another important source of contamination (Moret et al., 2009; Brühl, 2016). For example, high MOSH contamination occurring during edible oils extraction was traced back to leaks of lubricants by Neukom et al. (2002). The use of mineral oils as fluids for heat exchangers in processes that require the use of temperature (for example malaxation), which can accidentally come into contact with the food matrix in case of puncture, add another element of risk for older plants (Moh et al., 2002). Packaging materials made up of plastic or metal containers were also considered, as mineral oils can be used in their production (Jickells et al., 1994a; Jickells et al., 1994b; Grob et al., 1997; Moret et al., 2009). On the other hand, other authors have found no significant increase of mineral oils in extra virgin olive oils when investigating a full-process line, albeit with LOQ higher than those achievable now (Moret et al., 2003), thus generating a situation of conflicting information.

For these reasons, the purpose of this work, as part of a PhD project on this topic, was to investigate the incidence of the different processing steps occurring at the olive mill, with a particular focus on the washing step, to provide a more up-to-date and in-depth picture of the situation. In this context, for more accurate MOSH quantification in samples with

low level of contamination, a new Alox protocol to be applied, when necessary, on an aliquot of the sample extracts after saponification/epoxidation, was also optimized.

5.2 Materials and methods

5.2.1 Samples

Samples of olives and related matrices from milling operations (paste and oil) were used to carry out this investigation. Based on availability, samples considered for analysis were olives sampled after transport at the mill (in some cases olives at arrival and olives soon before washing were available), olives after washing operations, olive paste taken after malaxation and, lastly, the finished oil from the vertical centrifuge. Specifically, the investigation involved 14 different milling plants and a total of 25 batches processed (some different batches were processed in the same mill). All mills, whose main information is summarized in Table 5.1, were located in different parts of Italy. Sampling was carried out during the 2020-21 oil campaign and all the samples, after being collected in clean glass containers or in plastic bags shielded with aluminium foil to avoid external contamination, were sent to our laboratory and stored at -18 °C before being processed. In accordance with the instructions provided for sampling, to improve representativeness, olive samples of 200-300 g were taken from at least 10 different points of the entire batch of olives under processing to form an aggregate sample of 2-3 kg, from which the laboratory sample (about 800 or 200 g, according to the study in progress) was derived. For the other matrices (paste, pomace and oil) the sample collected was about 1 kg taken from a generic point of the total mass, assuming a higher homogeneity of the batch following the mixing occurring during malaxation. Of course, because the olives were processed continuously, it was difficult to ensure high sample representativeness from one stage to the next. In some cases, lubricants used in the machinery have also been supplied.

An olive oil extracted from olives hand-picked from the tree, obtained from a previous work (Menegoz Ursol et al., 2023) and containing no detectable MOSH, was used for fortification experiments to evaluate the performance of the Alox protocol. For the same purpose, a sunflower and a rapeseed oil from the second trial of the collaborative study for the revision of the EN16995:2017 method were exploited.

Three samples of olives hand-picked from the tree and the respective olives after harvesting operations from the same previous work were used for a deeper investigation of the impact of the washing step on the final contamination of olive oils.

Similarly, the same 6 samples were also used to evaluate the impact of the presence of olive stones during milling in terms of mineral oil content. This last focus also involved 6 Croatian olive samples (two different varieties, Leccino and Bianchera, from three different locations, Poreč, Vošteni, Buje), which were hand-picked from the trees and sent to our laboratory from the Institute of Agriculture and Tourism of Poreč, as well as an olive sample from South Italy sampled after the harvesting, leftover in our laboratory from a previous project.

Fifteen samples of oil, obtained from the milling of olives of two different varieties (Leccino and Bianchera) together with different amounts of leaves (0%, 2.5% and 5% *w/w*), were provided by the Institute of Agriculture and Tourism of Poreč and used to evaluate the contribution of the latter on the mineral oil contamination found in the finished oil.

Finally, 10 organic EVOOs were purchased from the supermarket and analyzed, to collect occurrence data.

Table 5.1. Characteristics of samples related to the monitoring of the MOH contamination at the mill.

Sample code	Collection container	Transport	Storage (duration)	Lubricant type (brand/name)	Lubricant classification
TB1	Nets	Plastic bins	Plastic bins (1h)	Grease (Zep Prolube Alim Blanche)	Food grade
TB2	Nets	Plastic bins	Plastic bins (3h)	-	-
TB3	Nets	Trailer	Plastic bins (2h)	Grease (Klüberfood NH1 94-402)	Food grade
TB4	Nets	Trailer	Plastic bins (15h)	None	-
TB5	Nets	Trailer	Trailer (2h)	-	-
TB6	Trunk shaker	Trailer	Plastic bins (24h)	Grease (Pieralisi)	Food grade
T1	Nets	Plastic bins	Plastic bins (12h)	Grease (Klüberfood NH1 94-402)	Food grade
T2	Nets	Trailer	Plastic bins (21h)	None	-
IB1	Nets	Plastic bins	Plastic bins (0h)	-	-
IB2	Nets	Plastic bins	Plastic bins (4h)	Separator lubricant oil (Alfa Laval 7098071 55) Grease (Berutox FB 22 - PAO)	Technical grade
IB3	Nets	Plastic bins	Plastic bins (21h)	Separator lubricant oil (Alfa Laval 7098071 55) Grease (Berutox FB 22 - PAO)	Technical grade

Table 5.1. *Continued.*

Sample code	Collection container	Transport	Storage (duration)	Lubricant type (brand/name)	Lubricant classification
IB4	Nets	Plastic bins	Plastic bins (14h)	Grease (Klüberlub NH1 11-222)	Food grade
I2	Nets	Plastic bins	Plastic bins (0.5h)	Separator lubricant oil (Alfa Laval 7098071 55) Grease (Berutox FB 22 - PAO)	Technical grade
S1	Straddle harvester	Trailer	Trailer (0.5h)	-	-
F1A	-	Trailer	Plastic bins (0h)	Grease (Klüberlub NH1 11-222)	Food grade
F1B	-	Trailer	Plastic bins (14h)	Grease (Klüberlub NH1 11-222)	Food grade
F1C	-	Trailer	Plastic bins (14h)	Grease (Klüberlub NH1 11-222)	Food grade
F2A	-	Trailer	Trailer (0.5h)	-	-
F2B	-	Trailer	Trailer (0.5h)	-	-
F3A	-	-	Plastic bins (8h)	Grease (IP)	Technical grade
F3B	-	-	Plastic bins (12h)	Grease (IP)	Technical grade
F3C	-	-	Plastic bins (4h)	Grease (IP)	Technical grade
F4A	-	-	Plastic bins (24h)	Grease (Zep Prolube Alim Blanche)	Food grade
F4B	-	-	Plastic bins (8h)	Grease (Zep Prolube Alim Blanche)	Food grade
F4C	-	-	Plastic bins (20h)	Grease (Zep Prolube Alim Blanche)	Food grade

5.2.2 Reagents and chemicals

n-Hexane and dichloromethane for HPLC (both distilled before use), acetone, methanol, toluene, potassium hydroxide, *m*-chloroperbenzoic acid (*m*CPBA) $\leq 77\%$, sodium thiosulfate, sodium sulfate anhydrous, silica gel (pore size 60Å, particle size 200-425 mesh), aluminium oxide 90 active basic (0.063-0.200 mm, activity stage I), were purchased from Merck (Burlington, Massachusetts, USA). Ethanol absolute was purchased from VWR (Radnor, Pennsylvania, USA). Purified water was obtained with a Milli-Q Advantage A10 system from Millipore (Bedford, Massachusetts, USA).

5.2.3 Standard solutions

A commercial motor oil (80.5% of MOSH, centered on n -C₂₈ and distributed over the range n -C₁₆₋₅₀) was purchased from a local vendor and used to prepare a standard solution at 0.86 mg/mL in toluene. A naphthenic-based process oil called Gravex (73.0% of MOSH, centered on n -C₁₈ and distributed over the range n -C₁₂₋₂₈) was provided by a manufacturer and used to prepare a standard solution at 1.02 mg/mL in toluene.

The MOSH/MOAH retention time standard, containing n -decane (n -C₁₀), n -undecane (n -C₁₁), n -tridecane (n -C₁₃), n -hexadecane (n -C₁₆), n -eicosane (n -C₂₀), n -tetracosane (n -C₂₄), n -pentacosane (n -C₂₅), n -pentatriacontane (n -C₃₅), n -tetracontane (n -C₄₀) and n -pentacontane (n -C₅₀), each at 100 µg/mL in cyclohexane, used to perform the C-fractions cuts and to verify the GC performances (discrimination) (Bratinova & Hoekstra, 2019), was purchased from Restek (Bellefonte, Pennsylvania, USA). From the same supplier was also the MOSH/MOAH standard used to verify the correctness of the transfer windows of MOSH and MOAH fractions from the HPLC to the GC, and as internal standard (ISa) for quantification purposes. The latter contained n -C₁₃ at 150 µg/mL, 1,3,5-tritert-butylbenzene (TBB), n -C₁₁, cyclohexylcyclohexane (CyCy), pentyl benzene (5B), 1-methyl naphthalene (1-MN), 2-methyl naphthalene (2-MN) at 300 µg/mL and 5- α -cholestane (Cho) and perylene (Per) at 600 µg/mL in toluene. An internal standard solution of n -C₁₅, n -C₁₇ and n -C₂₀ (here after called ISb), bought from Merck (Burlington, Massachusetts, USA), was prepared in toluene at concentrations of 583, 634 and 603 µg/mL, respectively. All standard solutions were stored at -18 °C.

5.2.4 Equipment, instrumentation and chromatographic conditions

All labware and materials intended for contact with the matrices under analysis were cleaned with soap and water and/or rinsed with acetone and n -hexane before use.

Whatman Filter Papers Grade 42 were purchased from Whatman products (Cytiva) (Marlborough, Massachusetts, USA).

Two components of the Abencor system, namely the hammer mill M-100, with the 5.5 mm screen, and the centrifugal machine CF-100, were purchased from MC2 Ingenieria Y Sistemas (Seville, Spain). The cooking machine HF807 Companion XL used with the mixing shovel, as replacement for the malaxation unit, was from Moulinex (Ecully, France).

The cutter C 4 VV was obtained from Abacus Systems (Udine, Italy), while the IKA T-18 Basic Ultra Turrax Homogenizer was purchased from IKA-Werke GmbH & Co. KG (Staufen, Germany).

The MARS 5 Digestion Microwave System, equipped with GreenChem Plus Teflon vessels and fiber optic temperature probe, was purchased from CEM Corporation (Matthews, North Carolina, USA).

The Univapo 100 H centrifuge was purchased from UniEquip (Martinsrieder, Munich, Germany) and the Büchi R-II rotary evaporator from Büchi AG (Flawil, Switzerland). Both were connected to a V-700 vacuum pump from Büchi AG (Flawil, Switzerland).

The LC-GC-FID system, commercial name LC-GC 9000, was from Brechbühler (Zurich, Switzerland) and consisted of a HPLC Phoenix 9000 and a GC Trace 1310 series by Thermo Fisher Scientific (Waltham, Massachusetts, USA). The latter had a dual channel configuration to perform MOSH and MOAH analysis within a single GC run. The coupling between LC and GC occurred through a Y-interface (Biedermann et al., 2009; Biedermann & Grob, 2009c) managed by a switching transfer valves system. The LC column was a Lichrospher Si-60 by Sepachrom (Milano, Italy), 25 cm × 2.1 mm ID, packed with 5 µm particle size. GC channels consisted of uncoated/deactivated retention gaps of 10 m × 0.53 mm ID, to exploit the retention gap technique (Biedermann & Grob, 2012a), connected by means of a steel T-piece with GC columns by Mega (Legnano, Milan, Italy), 10 m × 0.25 mm ID and coated with a 0.15 µm film of PS-255 (1% vinyl, 99% methyl polysiloxane). The third exit of the T-piece was connected with the solvent vapour exit (SVE) to exploit partially concurrent eluent evaporation. LC elution occurred at 300 µL/min with *n*-hexane for 0.1 min and turned to *n*-hexane/dichloromethane (DCM) 70:30 within 0.5 min from sample introduction. After 6 min of LC run, 9 min of backflush with DCM at 500 µL/min, followed by reconditioning with *n*-hexane at 700 µL/min for 6.5 min and at 300 µL/min for 1.5 min, were provided. The GC was kept at a constant pressure of 60 kPa, except during fractions transfer from the LC, when the pressure was raised to 90 kPa. The temperature ramp was set as follows: isotherm of 51 °C for 8.5 min after the start of the LC-GC transfer and then a gradient of 20 °C/min up to 350 °C. FID temperature was set at 360 °C.

5.2.5 Oil extraction

Based on the aim of the investigation, the oil was extracted from the olives and the other matrices either physically or chemically.

5.2.5.1 Physical extraction

For physical extraction, about 800 g of olives were crushed with the hammer mill and the relative paste was malaxed in the cooking machine at 40°C for 45 min under slow and continuous mixing (program 3). After that, oil was recovered by centrifugation at 3500 rpm for 60 s. If necessary (based on olive varieties), water was added during malaxation to improve this step and facilitate subsequent centrifugation. Malaxed olives paste was directly subjected to centrifugation. The water-oil mixture obtained was left to separate autonomously overnight and then the physically extracted oil was recovered and available for analysis.

5.2.5.2 Chemical extraction

Based on the purpose, olives were ground using either the Abencor or the cutter. To obtain a more homogeneous olive paste, in the last case, a Politron homogenizer was used after manually removing olive stones which remained intact. Then, for chemical extraction, 7.5 g of the olive paste was weighed inside the Teflon vessel, added with 10 μL of ISb, 15 mL of *n*-hexane and 15 mL of ethanol and positioned, after insertion of a magnetic stir bar to allow sample agitation during the process, inside the microwave apparatus. The microwave cycle included a 5 min pre-heating step to reach 120 °C, then kept for 20 min before cooling. Once reached room temperature, the content was transferred to an Erlenmeyer flask and added with 60 mL of water for phase separation. After a 30 min rest at -18 °C to improve phase separation, the *n*-hexane phase was recovered, transferred into a round-bottomed flask and brought to dryness in the rotary evaporator, thus obtaining the chemically extracted oil for the analysis.

5.2.6 Saponification and epoxidation

Saponification and epoxidation were performed according to (Menegoz Ursol et al., 2022). Briefly, 1 g of oil (the amount could also be lower when extracting with MAE, based on the extraction yields) was subjected to MAS. Oil was weighed inside the Teflon vessel and added with 10 μL of IS, 10 mL of *n*-hexane and 10 mL of 1.5 N methanolic KOH solution. Saponification occurred at 120 °C for 20 min under agitation. Once reached ambient temperature, the sample was added with 40 mL of water, 3 mL of methanol (to break emulsion) and then was left at -18 °C for 30 min. After that, the *n*-hexane phase was collected and evaporated in the Univapo to a volume of 4 mL, subjected to strong stirring after addition of 3 mL of a 2:1 (*v/v*) $\text{CH}_3\text{OH}/\text{H}_2\text{O}$ mixture and centrifuged at 5000

rpm for 5 min. The organic phase was further reconcentrated by evaporation to a volume of 700 μL , to be subjected to epoxidation according to the Nestola & Schmidt (2017) protocol. In particular, 500 μL of a 20% (*m/v*) ethanolic solution of *m*CPBA was added to the *n*-hexane extract and the mixture was then stirred at 500 rpm for 15 min at room temperature. Addition of 2 mL of 10% (*m/v*) aqueous solution of sodium thiosulfate and 500 μL of ethanol, followed by 3 min of stirring, stopped the reaction and improved phase separation. Finally, the organic phase was recovered, added with a spatula tip of sodium sulphate anhydrous, and injected into the LC-GC-FID system or, for samples that required it, subjected to Alox.

5.2.7 Removal of endogenous *n*-alkanes

150 μL of the saponified/epoxidized extract were loaded, in a total volume of 500 μL of *n*-hexane, on a SPE cartridge (10 mm ID) filled with 2.5 g of activated Alox (500 °C overnight) topped by 0.5 g of sodium sulfate, previously conditioned with 5 mL of *n*-hexane. MOSH fraction was then eluted with 5 mL of *n*-hexane and concentrated to 150 μL with the Univapo system, and then gently under a nitrogen stream. Of these, 100 μL were injected into the LC-GC-FID apparatus.

For comparison purpose, the passage on Alox was also applied directly to the oil, with the difference that 150 mg of oil were added with 2 μL of ISa and loaded onto a double bed cartridge formed from bottom to top by 2.5 g of activated Alox, 1 g of activated silica (500 °C overnight) and 0.5 g of sodium sulfate. Conditioning and elution were carried out with 6 mL of *n*-hexane. 100 μL of the extract, reconcentrated to 150 μL , were finally injected into the LC-GC-FID system.

5.2.8 Olive washing in the laboratory

Aliquots of 200 g of olives were transferred into a 500 mL separating funnel, added with 200 mL of milliQ water and strongly shaken for 1 min. Then, water was discarded, and the procedure repeated four more times. After the 5th wash, olives were crushed with the Abencor system and, the paste obtained, extracted with MAE. The oil extracted was saponified with MAS, epoxidized and analyzed. For olive sampled from the tree, given the low contamination level, an additional step involving Alox was performed on saponified/epoxidized samples.

Finally, for selected samples, following the 4th wash, olives were washed according to the same procedure using ethanol, and the oil was extracted and analyzed.

For one of these selected samples, also water and ethanol used for the various washings underwent liquid-liquid extraction with *n*-hexane, and were analyzed. In particular, 20 mL of *n*-hexane were added to the washing medium and, after 1 minute shaking, in case of water the phases were left to separate, while for ethanol phase separation took place by addition of a volume of water four times that of ethanol. The *n*-hexane phase was then recovered and injected.

5.2.9 MOH quantification and analytical sensitivity

Baseline trend was evaluated for each batch of samples thanks to a procedural blank processed simultaneously with them, whose chromatographic trace was overlaid to that of the samples to allow the baseline to be drawn correctly.

The quantification was performed with the internal standard method using CyCy for MOSH and the mean value obtained from 5B, 1-MN, 2-MN and TBB for the MOAH, after their correction for recovery (Menegoz Ursol et al., 2022).

After Alox and saponification/epoxidation, 100 μ L of sample extract, corresponding to approximately 100 mg of the initial sample, were injected into the LC-GC-FID apparatus for MOSH and MOAH quantification, reaching a limit of quantification of 0.5 mg/kg for both. Any peak standing on the top of the humps, and not attributable to mineral oil contamination, was discarded. When Alox was not applied, thus for concentrations of mineral oils that did not require high sensitivities, the injection volume of MOSH was adjusted to 30-50 μ L to avoid overloading by endogenous *n*-alkanes, whose signal was subtracted from the hump, translating in a LOQ of 1 mg/kg.

5.3 Results and discussion

5.3.1 Optimization of MOH extraction from olive paste

To optimize oil extraction from olive paste, different approaches were tested on different aliquots of the same olive paste. The first one was the method proposed by (Biedermann & Grob, 2012a) for wet matrices, which includes a first extraction with ethanol (at amount at least 5 times that of the water) followed by extraction with *n*-hexane and water addition to the combined extracts to separate the *n*-hexane phase. Additional approaches involved microwave assisted extraction (MAE) of wet matrix with 50:50 *n*-hexane/ethanol mixture (Gharbi et al., 2017), and extraction of the dried matrix (60 °C x 60 h) with the same mixture or with *n*-hexane.

Extraction with *n*-hexane/ethanol (30 mL) on wet matrix (7.5 g) resulted to be the method of choice due to the higher oil yield. In fact, in accordance with the order in which the different methods were listed above, yields and corresponding standard deviation, obtained from three replicate analyses, were on average: 9.5 ± 0.9 , 14.7 ± 0.6 , 13.6 ± 0.9 ; 12.2 ± 1.1 . In addition, this method had the advantage of requiring less processing steps, sample handling and execution time.

To have the possibility to refer the MOH content also to the olive weight, 15 μ L of ISb were spiked directly into the olive paste (7.5 g), which was subjected to MAE. Ten out of 15 mL of *n*-hexane introduced in the Teflon vessels were recovered after MAE and left to evaporate until reaching a constant weight. The oil so obtained (around 0.7-1.0 g) was weighted to calculated extraction yield and used for MAS according to the method described in paragraph 5.2.6.

5.3.2 Optimization of the Alox protocol

While first Alox protocols, proposed to remove endogenous *n*-alkanes, were directly applied to the oil sample (Wagner et al., 2001a; Fiselier & Grob, 2009; Zurfluh, 2014; EN16995:2017), later ones were applied on the saponified (Albert et al., 2022) and saponified/epoxidized sample (Nestola, 2022). These more recent protocols have the advantages of requiring less sorbent phase since triglycerides, which engage active sites for their retention, have been removed by saponification.

Starting from the DGF protocol (Albert et al., 2022), which still include a passage on a large amount of sorbent (from the bottom to the top 10 g of activated Alox, 3 g of activated silica and 1 g of anhydrous Na_2SO_4), the amount of sample loaded was reduced six times (to an amount corresponding to 150 mg of oil sample) and the amount of sorbent of about 5 times (the silica layer was omitted). Consequently, also the volume of the solvent used for conditioning the glass cartridge and eluting the MOSH fraction was reduced of about 4-5 times.

Unlike the methods carried out directly on the oil, the application on saponified samples has the advantage of obtaining an increase in sensitivity, as well as to allow their injection for a pre-evaluation, in order to apply this further step on the same sample extract on a case-by-case basis.

For comparison purposes, a low-solvent-consuming protocol, to be directly applied to the oil sample, was also tested by adding 1 g of activated silica on the top of Alox. The activated silica enabled retention of 150 mg of oil, which was verified loading the oil on 1 g of sorbent phase and evaluating its absence after bringing to dryness the fraction collected.

Elution window and quantitative recovery of the MOSH fraction were verified by analyzing successive fractions of 1 mL each and performing recovery tests on olive oil fortified with Gravex and motor oil, respectively, as well as analyzing sunflower and rapeseed oil from the collaborative study (2nd round) for the revision of the EN16995:2017 method. Complete elution was obtained with 5 and 6 mL of *n*-hexane when using Alox and Alox/activated silica respectively. Even when reaching 10 mL of eluate, no significant *n*-alkane breakthrough was observed.

For the fortification experiments, 10 mg/kg of Gravex and motor oil in *n*-hexane and oil (corresponding to 7.4 and 6.9 mg/kg of MOSH respectively) were prepared in triplicate. Spiked solvent was injected directly and after Alox, while spiked oil was injected directly, after saponification/epoxidation, as well as after elution through Alox or Alox/activated silica. Percentage recovery, evaluated comparing the quantified contamination against the expected one (according to fortification), and relative standard deviation (RSD) are shown in Table 5.2.

In the table are also reported quantifications carried out on two sunflower and rapeseed oils with and without added mineral oils, which were compared with estimated content obtained as consensus value from the median of the quantifications provided by the laboratories participating in the collaborative study. Uncertainty of measurement (MU) is also reported.

Table 5.2. Recovery and RSD (3 replicates) of solvent and oil fortified with Gravex and motor oil and data comparison of oils with and without added mineral oils with expected values from a collaborative study.

Matrix	Sample preparation	Gravex		Motor oil	
		Recovery (%)	RSD (%)	Recovery (%)	RSD (%)
Solvent spiked	Direct injection	98.2	1.8	99.2	0.2
	Alox	100.7	3.0	91.6	1.3
Olive oil spiked	Direct injection	102.1	2.3	99.6	3.5
	Alox+Si (on oil sample)	104.0	3.4	90.7	2.2
	MAS/epox	102.2	1.2	105.9	0.8
	MAS/epox/Alox	100.2	0.7	97.1	0.9
		Expected value \pm MU (mg/kg)		Calculated value (mg/kg)	
Sunflower oil		3.1 \pm 1.5		3.3	
Sunflower oil spiked (Base oil T22)	MAS/epox/Alox	5.2 \pm 2.6		5.6	
Rapeseed oil		1.9 \pm 1.0		1.8	
Rapeseed oil spiked (Gravex 913)	MAS/epox/Alox	6.3 \pm 3.1		7.0	

Compared to Gravex, slightly lower recoveries were obtained for motor oil when eluted through Alox, in accordance with previous investigations which verified that Alox can retain part of the contamination, especially for mineral oils with higher molecular mass distribution (Fiselier et al., 2009a; Albert et al., 2022).

Despite this, the Alox protocol showed excellent performance in terms of recovery, associated with a maximum RSD of 3.5%, regardless of its direct application on oil or saponified sample, thus perfectly in line with the requirements of the guidance of the Joint Research Centre (Bratinova & Hoekstra, 2019). Good data agreement was also obtained for two *n*-alkane-rich samples from the inter-collaborative study. For this reason, Alox protocol was confidently applied to samples when needed.

Finally, in Figure 5.1 it can be appreciated how the increase in sensitivity (made possible by the almost complete removal of endogenous *n*-alkanes) obtained with the Alox procedure, and the consequent possibility to inject higher amount of the sample extract (corresponding to about 100 mg of fat) allowed to reach a LOQ of 0.5 mg/kg for the MOSH fraction.

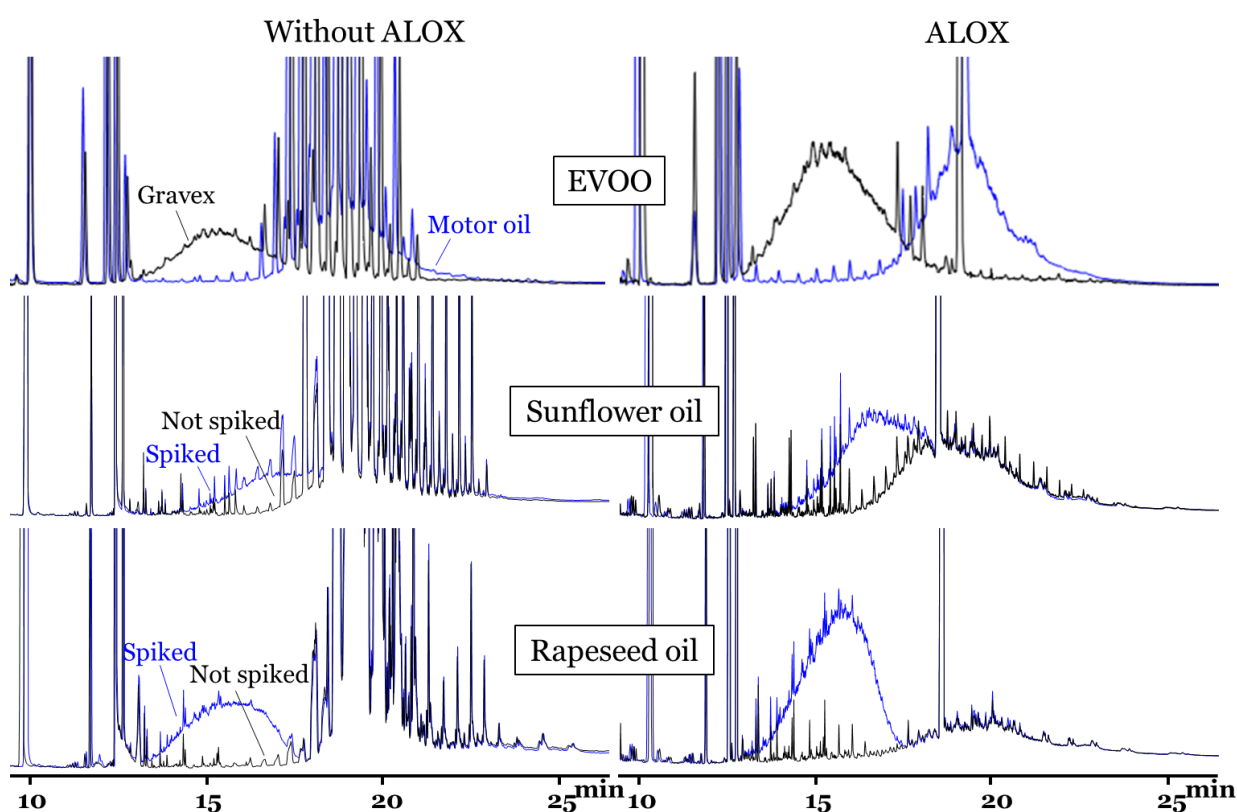


Figure 5.1. Examples of chromatograms relating to different types of vegetable oils before and after Alox applied on the saponified/epoxidized samples.

5.3.3 MOH variations along the processing chain in the mill

MOH contamination of samples taken at different stages of the processing chain was investigated to identify the most critical steps. Extraction yields at the mill were unknown, thus all concentrations were referred to the oil. To obtain comparable data, oil from solid matrices (olives and olive paste) was extracted in the laboratory by physical mean. More in details, olive samples underwent the whole extraction procedure with the Abencor system, while olive paste after malaxation was subjected to centrifugation only.

Samples were taken along the processing line trying to maintain the representativeness of the olive mass entering the mill, but we are aware that such representativeness cannot be guaranteed in a continuous process. To partially address these limitations, we defined a percentage variation threshold of 30%, above which MOH variation were considered significant. Since variability at low concentration could be higher, also variations occurring below 2.5 mg/kg or lower than 1 mg/kg for MOAH and 2 mg/kg for MOSH, were not considered as significant. Furthermore, both the MOAH percentage (for MOAH value above 1 mg/kg) and the chromatographic profiles of the samples were used to confirm significant contribution of new contamination and/or to identify samples with clear problems of poor representativeness. A not coherent change in the chromatographic profile due to e.g. cross contamination along all the processing line, was indicative of this occurrence, as in the example of Figure 5.2C. For the study of the chromatographic profiles, the traces were superimposed after baseline subtraction (to exclude misinterpretations due its drift at the end of the temperature ramp) and the scale modified to make the signals coincide (excluding misinterpretations due to the different levels of contamination of the samples under comparison).

Table 5.3 shows, for each of the samples taken along 25 different processing lines (from the olives entering the mill to the finished oil), the total MOSH and MOAH content (mg/kg) and the MOAH percentage. To obtain information on the transport stage as well, data on olives collected in the olive grove immediately after harvesting operations (from Menegoz Ursol et al., 2023), when available, were also included in the table. Vertical arrows in between two following sampling points indicate significant change in contamination (according to the above criteria) and in which direction. Samples marked in red indicate samples whose profile differed significantly from that of previous and subsequent stages, highlighting a possible problem of poor representativeness or contamination occurred during sampling, and were therefore not taken into account in the calculations.

Table 5.3. MOSH and MOAH concentrations (mg/kg oil) of the samples from the different processing steps, together with the percentage of MOAH, where assessable (values above the LOQ). Arrows indicate significant increase (red arrow) or decrease (green arrow) between one step and the other (in accordance with the established criteria).

Sample code	Olives after harvesting (mg/kg)			Olives after transport (mg/kg)			Olives before washing (mg/kg)			Olives after washing (mg/kg)			Malaxed olive paste (mg/kg)			Olive oil (mg/kg)					
	MOSH	MOAH	%MOAH	MOSH	MOAH	%MOAH	MOSH	MOAH	%MOAH	MOSH	MOAH	%MOAH	MOSH	MOAH	%MOAH	MOSH	MOAH	%MOAH			
TB1	325.8	111.0	25	245.2	94.0	28	↓	143.6	61.1	30	↓	82.5	30.9	27	↑	132.9	50.6	28	115.1	40.2	26
TB2	0.5	0.5		0.5	0.5			n.a.	n.a.			n.a.	n.a.			n.a.	n.a.		14.2	2.2	13
TB3	1.4	0.5		3.3	0.5			2.3	0.5	↓	0.8	0.5			0.5	0.5	↑		3.0	0.5	
TB4	16.8	0.5		17.2	0.5			16.5	0.5		17.8	0.5			22.9	0.5			17.4	0.5	
TB5	0.5	0.5		1.7	0.5			1.4	0.5		1.4	0.5			1.8	0.5			1.8	0.5	
TB6	9.7	3.4	26	↑	15.7	3.7	19	18.0	4.2	19	↓	12.5	2.5	17	16.2	4.1	20	11.7	2.5	18	
T1	0.5	0.5		1.1	0.5			n.a.	n.a.		n.a.	n.a.			12.3	3.8	23	15.9	3.2	17	
T2	1.6	0.5		1.9	0.5			n.a.	n.a.		n.a.	n.a.			4.6	1.4	23	4.8	1.0	18	
IB1	2.5	0.5		↑	n.a.	n.a.		10.5	2.0	16		13.2	1.8	12	↓	6.5	2.3	26	8.3	2.0	20
IB2	25.6	3.9	13	18.4	2.3	11	19.2	2.7	12	↓	10.9	1.5	12	14.1	1.6	10	10.9	1.2	10		
IB3	1.1	0.5		1.9	0.5			0.9	0.5		1.3	0.5		1.4	0.5			2.1	0.5		
IB4	23.1	0.5		26.5	0.7	3	25.2	0.7	3	18.7	0.7	4	52.0	1.0	1.8	32.4	1.0	3			
I2	5.8	0.5		0.9	0.5		↑	3.9	0.5		2.9	0.5		3.1	0.5			3.6	0.5		
S1	n.a.	n.a.		n.a.	n.a.			14.3	0.8	5	2.2	0.5	19	2.2	0.5	19	2.8	0.7	19		
F1A	n.a.	n.a.		n.a.	n.a.			8.8	2.3	21	25.9	8.9	26	9.7	2.8	22	12.3	3.4	22		

Table 5.3. Continued.

Sample code	Olives after harvesting (mg/kg)			Olives after transport (mg/kg)			Olives before washing (mg/kg)				Olives after washing (mg/kg)			Malaxed olive paste (mg/kg)			Olive oil (mg/kg)				
	MOSH	MOAH	%MOAH	MOSH	MOAH	%MOAH	MOSH	MOAH	%MOAH	MOSH	MOAH	%MOAH	MOSH	MOAH	%MOAH	MOSH	MOAH	%MOAH			
F1B	n.a.	n.a.		n.a.	n.a.		26.5	5.0	16	↓	16.6	3.8	19	↑	30.6	8.7	22	37.6	12.0	24	
F1C	n.a.	n.a.		n.a.	n.a.		4.1	0.9	18		9.2	2.8	23	↑	17.9	5.3	23	↓	11.7	3.2	21
F2A	n.a.	n.a.		n.a.	n.a.		1.3	0.5			1.4	0.5			n.a.	n.a.		1.4	0.5		
F2B	n.a.	n.a.		n.a.	n.a.		1.3	0.5			1.4	0.5			n.a.	n.a.		1.3	0.5		
F3A	n.a.	n.a.		n.a.	n.a.		5.3	0.5			1.2	0.5			1.4	0.5	↑	3.6	0.5		
F3B	n.a.	n.a.		n.a.	n.a.		3.4	1.2	26		4.4	1.5	26		3.9	1.1	22	3.7	1.0	21	
F3C	n.a.	n.a.		n.a.	n.a.		4.0	0.5		↓	1.9	0.5			2.5	0.5		2.3	0.5		
F4A	n.a.	n.a.		n.a.	n.a.		1.2	0.5			0.7	0.5			n.a.	n.a.		2.1	0.8	29	
F4B	n.a.	n.a.		n.a.	n.a.		2.0	0.5			0.9	0.5			n.a.	n.a.		0.8	0.5		
F4C	n.a.	n.a.		n.a.	n.a.		0.7	0.5			0.9	0.5			n.a.	n.a.		1.2	0.5		

n.a. not available.

Regarding the transportation stage, according with the information furnished by the operators involved in the sampling, olives were basically moved either inside plastic bins, then loaded on trailers, or loose inside the latter (see Table 5.1). Taking into consideration MOSH data of the first 13 samples reported in Table 5.3, for which data after harvesting operation were available, and based on settled criteria, positive variations of MOH concentration after olive transportation from the olive grove to the mill, also including olive handling at the mill plant that precedes the washing step, was evident in 3 out of the 13 different olive samples analyzed (23% of cases). The increase regarded olives TB6 (+6.0 mg/kg of MOSH) transported inside plastic bins, as well as olives IB1 (+8.0 mg/kg of MOSH, +1.5 mg/kg of MOAH) and I2 (+3.0 mg/kg of MOSH) loose into trailers, and in case of sample IB1 it reached MOAH levels approaching the MOAH limit of 2 mg/kg recently recommended by the SCoPAFF (EC, 2022). However, by comparing the chromatographic profiles of these samples along the processing chain (Figure 5.2), an effective contamination increase due to the transport stage was confirmed only for samples TB6 and I2. In particular, for the former the contamination occurred during transportation from the olive grove to the mill (Figure 5.2A), while for the latter it took place at the mill during the handling of the olives before the washing section (Figure 5.2B). No conclusion can be drawn for sample IB1 (Figure 5.2C), for which chromatogram overlay highlighted poor sample representativeness along the entire processing chain (except for the olives taken before and after washing which showed the same chromatographic profile). The apparent decrease observed for TB1 was attributed to the non-homogenously distributed contamination of this sample, which, as reported by Menegoz Ursol et al. (2023), had an exceptional contamination due to a leakage of lubricant from the harvesting machine.

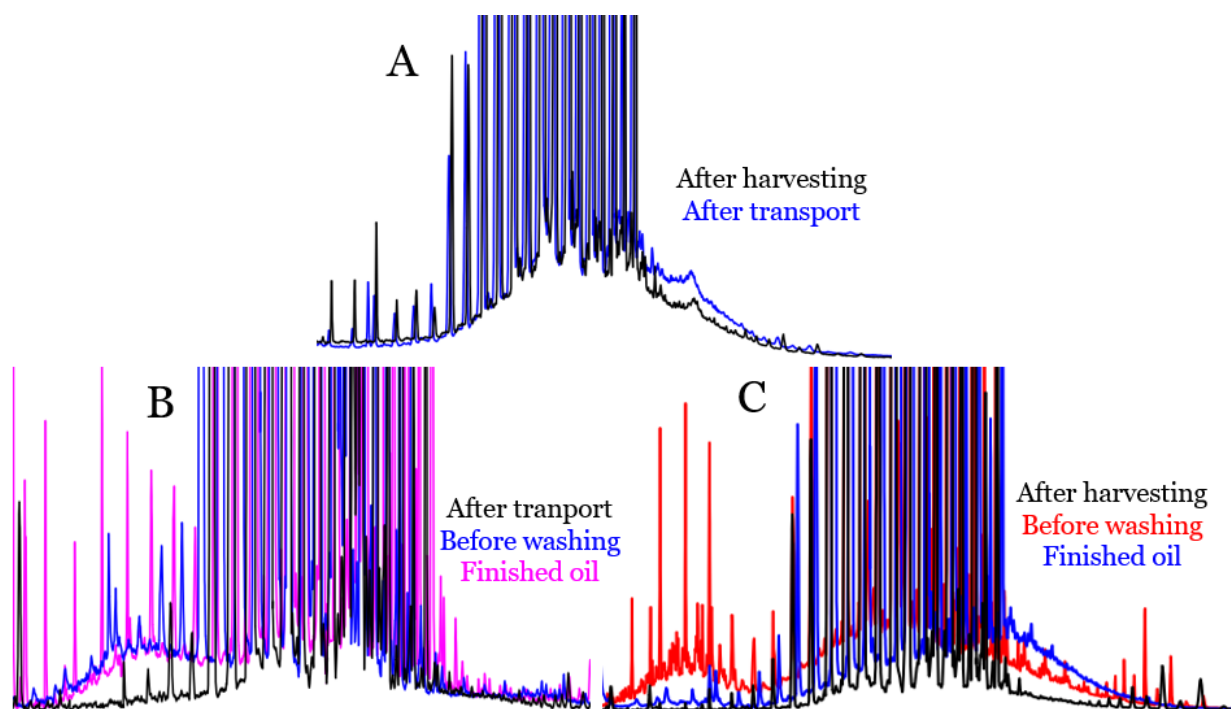


Figure 5.2. Overlay of chromatograms of samples TB6 (A), I2 (B) and IB1 (C) relating to the oil extracted from olives sampled from different processing steps to highlight the effect of transportation.

These results show that transportation rarely represents a critical point. Even when transportation is carried out in open trailers (as often occurs) with possible exposure of olives to the air (exhausts from the tailpipe), due to the relatively short exposure time, expected contamination is low. Higher contamination levels can be expected when olives are transported inside the mill using combustion engine-powered instead of electric-powered forklifts, where exhaust gases can accumulate, but none of the milling operators declared this practice. Leaks from hydraulic circuits of tipper trailers or cross-contamination from previous transportation of contaminated olives or of other goods outside the olive campaign could most probably be responsible of higher contamination. At industrial level, with the purpose to remove soil, dust and other residues, olives are dipped inside a tank full of water (fresh and recycled) where a coarse washing is carried out, possibly with turbulence to increase cleaning efficiency, and after that they are rinsed under water jets (Peri, 2014). Concerning the washing step there are no reportable criticalities (in none of the sample there was an increase in contamination), but rather it clearly had a positive mitigation impact, being able to determine a significant contamination decrease in 24% of the processing lines investigated (6 out of the 25 investigated). In general, this positive impact was more evident on samples with a higher contamination level before the washing step (67% of the sample with MOSH contamination above 10 mg/kg).

After washing, the olives are crushed and the olive paste obtained is malaxed to favor the coalescence of the dispersed and emulsified oil, which is thus more easily separated in the subsequent centrifugation step. After this first coarse centrifugation, a final centrifugation removes the last traces of water and dispersed solids from the oil (Petraakis, 2006; Leone, 2022). Having these machinery mechanical parts in continuous movement, even at high speed, they need to be subjected to lubrication and periodic maintenance. The use of food grade lubricants and the verification of sealing systems is therefore essential, but critical issues may always be present. According with data reported in Table 5.3, crushing/malaxation determined a significant increase in 20% of the processing lines for which data after washing and after malaxation were available, while the following steps (centrifugations) determined a significant but slight MOSH increase (around 3 mg/kg) in only two samples. Nonetheless, Figure 5.3A shows how for sample IB4, for which the increase of the level of contamination after crushing/malaxation was also accompanied by a variation of the chromatographic profile, this contamination was not confirmed in the finished oil, and was then attributed to a dirty container used for sampling or to poor representativeness. On the other hand, for samples F1B and F1C (the former shown in Figure 5.3B as an example), the additional contamination was confirmed in the next step. No difference in profile and MOSH/MOAH ratio was reported for sample TB1, for which this was justified again with the inhomogeneity of the olives. For all these samples, no correspondence was ever found between the contamination in the oil and the profile of the lubricants supplied.

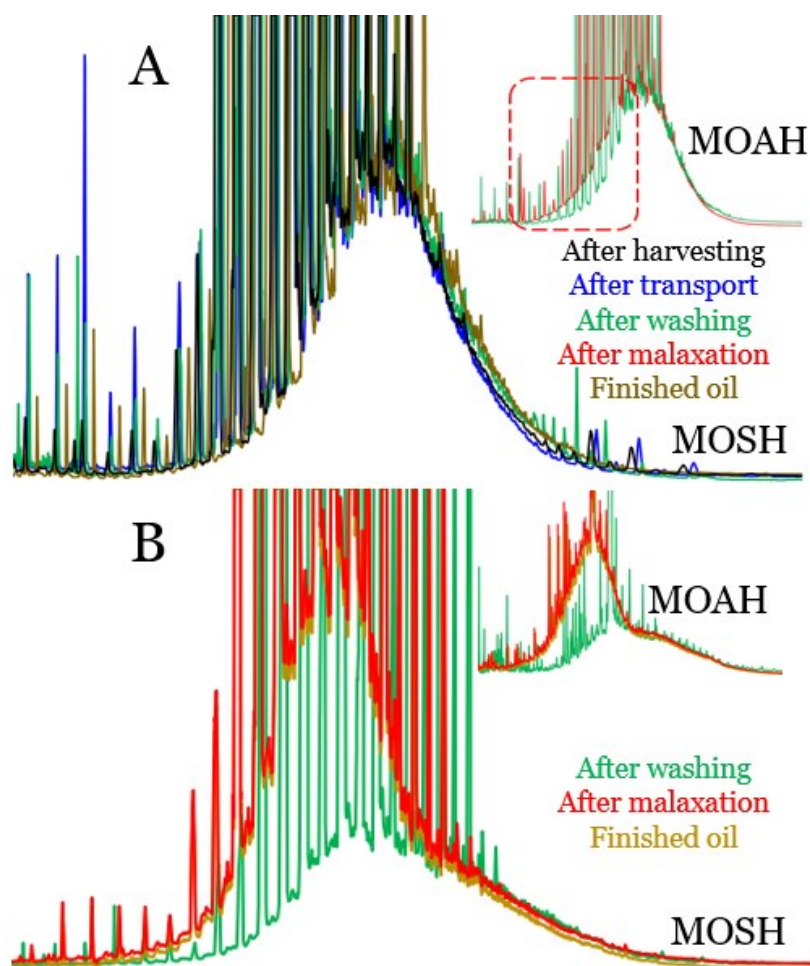


Figure 5.3. Overlay of chromatograms of samples IB4 (A) and F1B (C) relating to the oil extracted from olives sampled from different processing steps to highlight the effect of crushing/malaxation.

Finally, to better highlight the impact of the operations occurring at the mill, where a variation of the contamination was observed, these were divided into two main sections relating to the washing step (the only one capable to determine a reduction of the contamination) and the extraction step, including crushing, malaxation and oil separation. These sections were discussed separately and then compared to the variations occurred relating to the overall milling process.

In accordance with this, starting from data reported in Table 5.3 and after eliminating sample TB1 and all other samples for which, based on the chromatographic profiles, there were doubts about their representativeness, the bar graph in Figure 5.4 was obtained. The bars represent, for each step considered, the differences of MOH concentrations (positive or negative) of the output products compared to corresponding input products, and in particular show, as anticipated, the impact of the overall milling operations (Figure 5.4A), of the washing stage (Figure 5.4B), and of the extraction step (Figure 5.4C).

The overall impact of milling operations was assessed by subtracting MOSH contamination found in the olives entering the mill (before any processing) to that of the

corresponding oil collected from the vertical centrifuge. To obtain more robust data for this comparison, less influenced by the inhomogeneity of the olives (according to sample availability), the value of the olives at the entrance of the olive mill was obtained from the average concentration of the olives after transport and before washing. This was possible because, as visible in Table 5.3, data from these two sampling points were either aligned or directed towards reduction (effect of inhomogeneity) and this, except for sample I2 (already discussed), excluded any possible contribution due to preliminary operations at the mill (defoliation, weighing, handling, etc.).

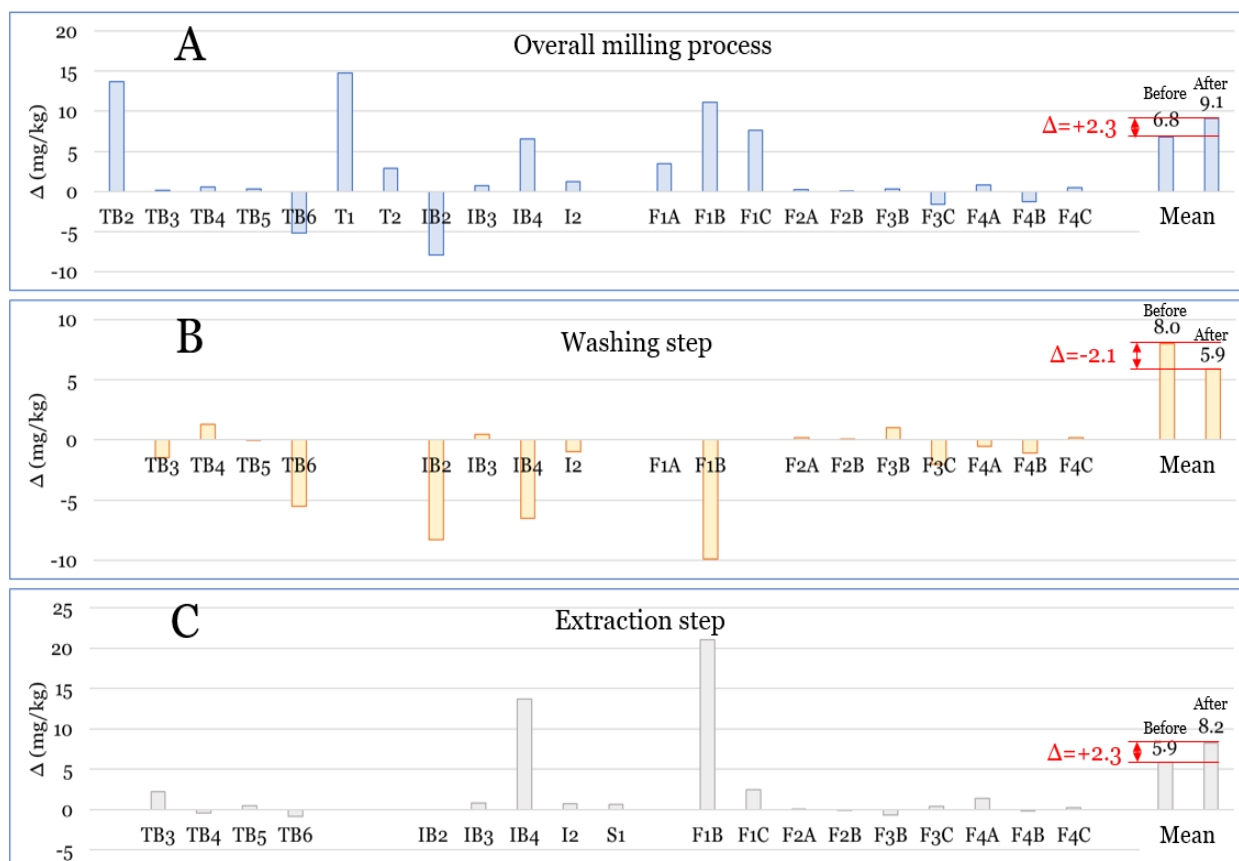


Figure 5.4. Bar plots relating to the variations (in mg/kg) occurring in the various samples in relation to the overall milling process (A), the washing step (B) and the oil extraction step (C). Mean MOSH concentrations of the samples before and after the considered processing step are also reported, together with the average variation.

As can be seen from Figure 5.4A, in about 80% of the samples, the overall processing at the mill led to an increase of the average MOSH contamination of 2.3 mg/kg, which increased from an average of 6.9 mg/kg for the oil obtained from olives at the entrance of the mill to an average of 9.1 mg/kg for the oil exiting from the vertical centrifuge. The percentage of samples for which the variation was significant, in accordance with the established criteria, is equal to 23%. The decreased contamination observed for the remaining 20% of the samples (TB6, IB2, F3C and F4B) was aligned with, and thus clearly

due to, the washing step, which in 60% of the cases proved to be able to remove part of the contamination present on the olive skin (Figure 5.4B). On average washing removed 2.2 mg/kg of MOSH (27% of the contamination present before olive washing). Finally, the extraction step determined an important increase (above the recommended benchmark level of 13 mg/kg by LAV & BLL) in 2 samples (IB4, F1B), which made the decrease due to washing futile, and was responsible of an overall average increase of 2.3 mg/kg (Figure 5.4C).

5.3.3.1 Focus on the washing step

To deepen the knowledge on the potentiality of washing in reducing MOH contamination, different aliquots of olives TB1, TB4 and IB4, collected at the olive grove soon after harvesting operations (they were part of a previous sampling by Menegoz Ursol et al., 2023), were either repeatedly washed in the laboratory or not, and analyzed as described in section 5.2.8. The choice fell on samples TB1 and IB4, because contaminated during harvesting operation (in the former case with an exceptional MOH amount due to a leak from the hydraulic circuit of the vibrating comb used for harvesting, while in the other due to contact of olives with the grease of the harvester), and on TB4, already contaminated at a pre-harvest stage (probably due to a lubricant leak in the atomizer used for phytosanitary treatments). Similarly, washing was carried out also with the corresponding olives hand-picked from the tree before harvesting, which in case of IB4 and TB1 had background contamination. Due to the low amounts of residual olives available, aliquots of 200 g each were processed in duplicate for each sample to mitigate data variability due to possible non-uniform distribution of the contamination.

Table 5.4 reports average total MOSH content of the oil extracted from olives before and after washing (with water only or with water followed by ethanol), and the percentage removal determined by washing performed at the mill and in the laboratory.

Table 5.4. MOSH concentration, expressed on the oil extracted from the olives, following their washing under different conditions.

Sample		% of MOSH variation at the mill	mg/kg of MOSH before washing	After washing with water [mg/kg] (variation %)	After washing with water and ethanol [mg/kg] (variation %)
Olives from the tree	IB4		2.1	2.3	-
	TB4		14.2	8.8 (-38)	7.1 (-50)
	TB1		1.6	2.1	1.8
Olives after harvesting	IB4	-23	23.2	13.3 (-43)	-
	TB4	+8	14.9	8.6 (-42)	-
	TB1	-43	266.0	125.4 (-53)	14.7 (95)

As previously reported, washing at the mill resulted in an appreciable MOH removal corresponding to 23% and 43% of the initial contamination for samples IB4 and TB1, respectively, not confirmed for sample TB4, for which a contamination increase (not significant taking into account data variability) was observed. This variable effect probably depends on the initial contamination level, its distribution, but also on the washing efficiency. Indeed, washing machines, depending on their design and operational characteristics, could remove the dirt and hence particulate matter, to which MOH are easily adsorbed, with different efficiency. This is mostly a mechanical removal, in fact, being poorly soluble in water, mineral oils are unlikely to partition from the olive skin into the aqueous medium. The removal obtained by repeated washes with water in the laboratory was also variable and on average higher. This was probably determined by a more vigorous washing, carried out with 5 successive aliquots of water, in the limited space of the separating funnel, and thus with a high degree of rubbing among olives. Even higher removal percentages were obtained when using ethanol, as later reported.

To better understand the effect of washing with water, taking as an example sample TB1, water discharged after each single washing was extracted with *n*-hexane following the procedure described above. A sample of water from a first wash was also extracted after filtration.

The first wash was able to remove about 70% of the total contamination removed with the sum of all five washes, while for the second wash this percentage already dropped to 15%. However, from the third wash onwards MOH removal almost reached a plateau (visible in Figure 5.5A), around 5%. Probably, while the first two washings removed large part of the coarse particulate on which MOH were adsorbed, then removal probably was affected

by MOH more difficult to take away due to their adherence to the waxy layer that surrounds the olive surface (Bianchi et al., 1992a; Boskou, 2006a).

Nevertheless, MOSH concentration in the extracted oil, after this process, dropped from 266.0 mg/kg to 125.4 mg/kg (47% of the residual contamination compared to the starting value). Although not reported, MOAH underwent the same variation. Thus, to summarize, it was just easier to remove what was present as a mere deposit, rather than what was more strongly bound or dissolved into waxes.

Partial confirmation of these hypotheses came by merging different tests: water filtration, washes with ethanol and physical extraction of the oil from unwashed olives. Starting with the first one, water extracted after filtration did not report any presence of mineral oils, confirming that the decontamination by this medium was the consequence of a physical removal of particulate, rather than a dissolution of mineral oil from the surface of the olives into water.

Going forward, the physically extracted oil was found to be 30% less contaminated than the oil extracted with solvent, confirming that part of the contamination was hardly removable, and remained inside the pomace, despite continuous contact with lipophilic substances such as triglycerides, even under agitation during malaxation. Since it was already verified that waxes are rarely extracted from the skin of the olives during the production of extra virgin olive oil, it did not seem a coincidence that this also happened to the contamination (Grob, 2018b).

Finally, ethanol, which probably solubilize superficial waxes, extensively removed the residual contamination for sample TB1. In particular, the fifth wash carried out with ethanol was able to remove additional 110.7 mg/kg, bringing the contamination level in the oil chemically extracted from the relative olives to about 5% of their starting value (Table 5.4 and Figure 5.5B). A second wash with ethanol, on the other hand, was no longer able to significantly remove contamination. This meant that part of the contamination present was hardly accessible, probably due to its penetration into deeper layers of the olives, with no further possibility of being removed in this way.

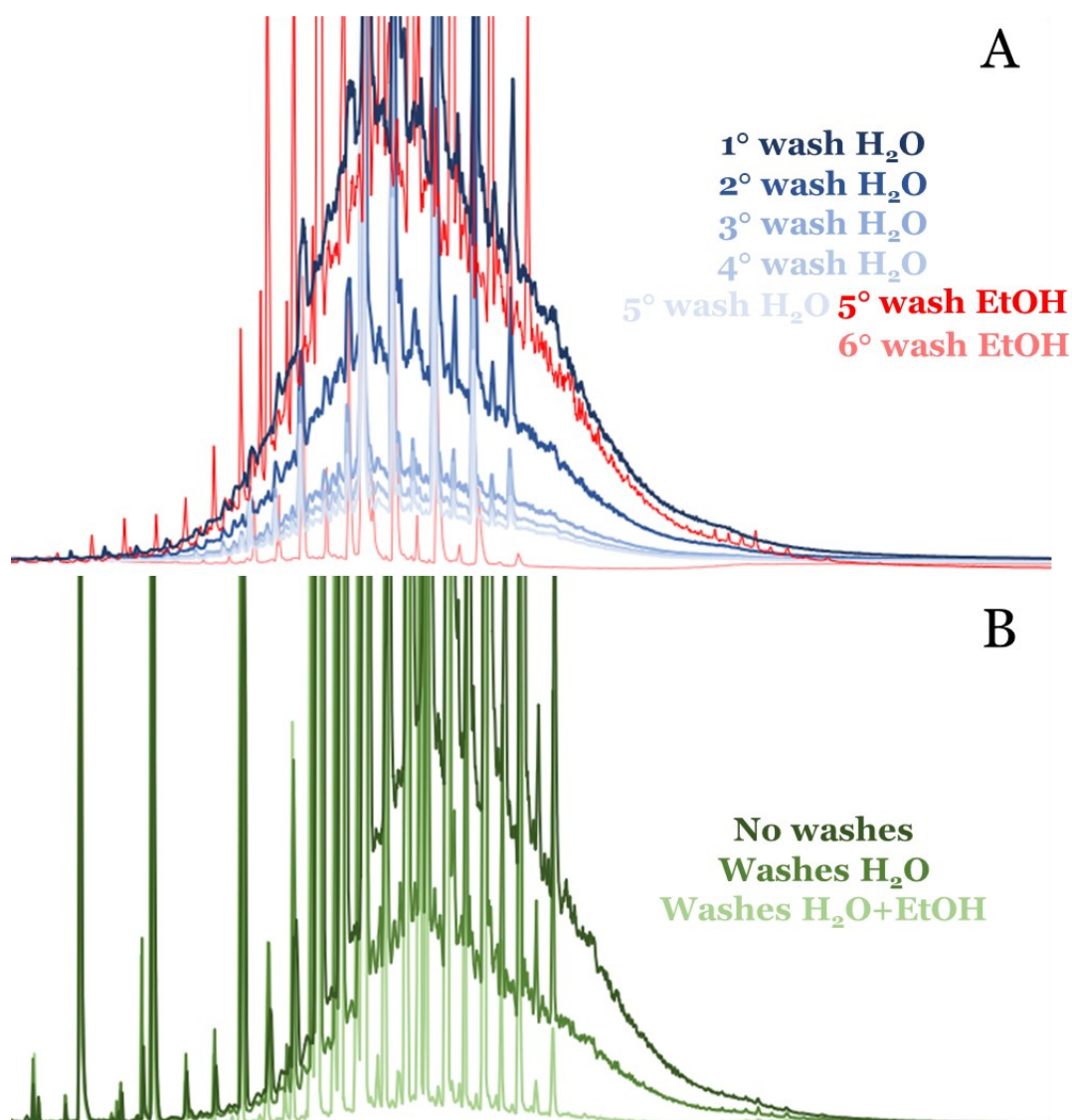


Figure 5.5. Overlay of chromatograms of the *n*-hexane extracts from liquid-liquid extraction of water and ethanol used for washings (A) and of olive oils extracted from the olives before and after these washings (B).

This last assumption was corroborated by olives TB4 and TB1 hand-picked from the tree, having a significant contamination (11.3 mg/kg, already on tree) and background levels (1.6 mg/kg) respectively. As shown in Table 5.4, for sample TB1 ethanol could not remove nothing. For the other sample, something more was perhaps removed with respect to water (or could just be the consequence of the inhomogeneity of the olives), but certainly the variation was not as significant as for olives TB1 sampled after harvesting operations. Thus, excluding endogenous origin, these contaminations probably had the time to penetrate deeper into the fruit. Indeed, background contamination, like that found in olives TB1 from the tree, is likely the result of the continuous uptake from environmental pollution during all stages of fruit development over different months (albeit with a minimal contribution). On the other hand, the contamination in TB4 was hypothesized

to originate from a leak of the atomizer used to carry out phytosanitary treatments (Menegoz Ursol et al., 2023), which were carried out two and three months before the olive oil campaign, giving time to the contamination to migrate. This is probably a process that takes some time, also because olives contain water up to 70% (Boskou, 2006a) which can exert a barrier effect against migration of lipophilic substances, and this would be the reason why the removal was much more extensive for olives contaminated during harvesting.

Thus, this investigation highlighted how, when olives are contaminated during harvesting, a significant part of the contamination remained on the olive surface can be removed by washing. As a consequence, the development of more efficient cleaning methods can play a role in mitigating, at least in part, mineral oils presence in olive oils. Clearly the use of ethanol is not applicable, first of all for an economic reason. However, research could aim to the development of food grade detergents exhibiting a comparable effect.

5.3.3.2 Focus on the olives stones

In light of the previous results, which suggested that part of the contamination was located within the fruit, it was decided to verify if the latter, including background levels found in the olives from the tree, could derive from olive stones. For this purpose, a different aliquot of the same olives used for the washing experiments were crushed with the cutter (able to separate the pulp from the stones, leaving the latter intact), the stones were discarded, and the oil, chemically extracted from the olive paste obtained after further grinding with the homogenizer, was analyzed. The contamination was then compared with that obtained from whole olives. This was performed also on six samples of Croatian olives hand-picked from the tree (BL, BB, VL, VB, PL, PB), as well as on one sample from South Italy (GA). Data are summarized in Table 5.5.

Table 5.5. MOSH concentration in the oil extracted from olives before and after pitting.

Sample	Oil extracted (mg/kg)	
	Whole olive	Without stone
IB4	2.1	2.7
TB4	14.2	16.0
TB1	1.6	1.6
IB4*	23.2	26.2
TB4*	14.9	15.4
TB1*	266.0	289.4
GA*	6.4	6.8
BL	0.9	0.9
BB	1.8	0.9
VL	0.6	0.8
VB	0.5	0.6
PL	1.0	1.9
PB	1.1	1.3

*Olives sampled after harvesting.

With the exception of sample BB (which had very low contamination, most affected by data variability), all samples extracted from olives without olive stones had slightly higher contamination, which can be explained by the fact that the small aliquot of oil from the seed included in the kernel is free of contamination and thus, not being present in the oil obtained from the pulp alone, does not dilute the MOH present. However, this effect should be small given the small amount of oil from the kernel. In any case, contrary to the findings of Gómez-Coca et al. (2016b), these results seem to rule out a contribution to contamination from the olive stone.

5.3.3.3 The impact of olive leaves

During harvesting, the operations carried out to favor the detachment of the olives can also determine the fall of a significant amount of leaves, whose entity can vary according to the harvesting method used (Servili et al., 2022). These, if the preliminary cleaning operations carried out at the milling plant do not remove them adequately, enter the milling process together with the olives (Mihailova et al., 2015). Just like olives, olive leaves are also covered by a waxy layer (Bianchi et al., 1992b) which, combined with the high surface/volume ratio, causes them to act as environmental absorbers. Not surprisingly, leaves have already been used in other works as indicators of environmental contamination towards some lipophilic contaminants, like pesticides and polychlorinated biphenyls (PCB) (Sofuoglu et al., 2013; Taştan et al., 2022), but also mineral oils have been found in concentrations of 15 mg/kg (Gómez-Coca et al., 2016b).

Thus, the impact of the presence of olive leaves during olive milling on the final mineral oil contamination found into the oil was investigated. For this purpose, olives and olive leaves from two different olive varieties, Leccino and Bianchera, were sampled by hand from the same olive grove, where no phytosanitary treatments were carried out. Samples of 1 kg of olives were then milled with the Abencor system to obtain the physically extracted oil, either without (control samples) or with the addition of increasing amounts of leaves (2.5% and 5% *w/w*). In particular, Leccino olives underwent the addition of 2.5% leaves, while both additions were performed on Bianchera ones. Each sample was milled in triplicate and the average values obtained for each sample type, together with its relative range of variation (standard deviation), are shown in Figure 5.6.

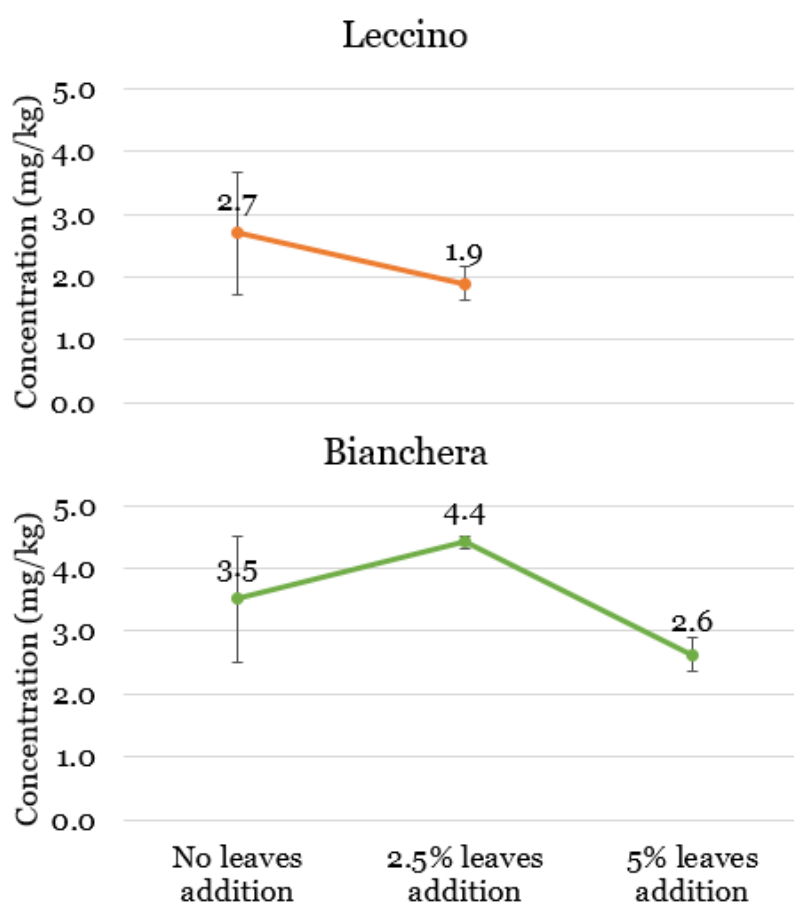


Figure 5.6. Average concentrations of MOSH in two different oil varieties following addition of different percentages of leaves during olive milling.

As visible in the figure, there was no significant increase together with leaves addition, as all concentrations fell within the standard deviation relating to the content of the control olives. However, even not taking into account the standard deviation, the trend turned out to be negative for Leccino olives, while an increase for Bianchera olives with 2.5% leaves was then disavowed by the concentration value in the oil obtained with 5% of them.

Therefore, overall, at least for these amounts of leaves, their presence during milling did not lead to an increase in the concentration of mineral oils, which could be appreciated in the finished oil.

Moreover, even though the olives were sampled in an olive grove with no proximity to particular source of contamination, the contamination of the starting olives fluctuated between slightly higher values than the average level previously found in the olives hand-picked from the tree (Menegoz Ursol et al., 2022; Menegoz Ursol et al., 2023), suggesting however the existence of a certain degree of environmental pollution. According to this, the fact that the presence of leaves did not affect the starting concentrations brought us to the conclusions that either they did not contain mineral oils, which seems unlikely considering their presence in the olives, or that these were difficult to extract during the physical extraction of the oil from the olives, under the standard processing conditions (malaxation at 25 ± 1 °C for 30 min). In fact, if a contamination was present or accessible, based on the fact that leaves do not contain oil and thus do not contribute to the oil yield, this would have determine a reconcentration effect of MOH into the oil, similar to the effect verified for pomace (Moret et al., 2003), albeit with an obviously lower incidence. Nevertheless, it should be emphasized that these olives did not undergo any treatment and were harvested by hand. Therefore, in case of contamination deriving from the harvesting phase, which based on the previous results is mainly distributed on the surface of the olives, the entry of leaves, having the same contamination, into the milling process could most likely have an impact and determine this effect. Future developments should concern an in-depth study of this occurrence.

5.3.4 Extra virgin olive oils from the market

Ten organic EVOOs were bought at the supermarket and analyzed. Data were merged with those of 12 traditional EVOOs, whose quantifications have already been reported by Menegoz Ursol et al. (2022), and compared with data of the oils sampled from the centrifuge at the milling plant.

Starting with EVOOs from the market, oils from traditional agriculture reported an average contamination of 23.0 mg/kg of MOSH and 3.3 mg/kg of MOAH. Similarly, oils from organic agriculture had an average level of 15.0 mg/kg and 3.5 mg/kg, respectively. This alignment was not surprising as it was already verified that the execution of phytosanitary or fertilizing treatments, which is the only discriminating factor between the two categories of oils, did not have a significant impact on mineral oil contamination. On the contrary, harvesting and milling operations, which machinery is common,

resulted to be the main source (Menegoz Ursol et al., 2023). A confirmation of this was also obtained by comparing the chromatographic profiles of these EVOOs, as it was found that indeed all the contaminations could be related to two main ranges of molecular weights, typical of lubricating/motor oils, centered around $n\text{-C}_{29}$, and greases, centered around $n\text{-C}_{33}$ (Figure 5.7).

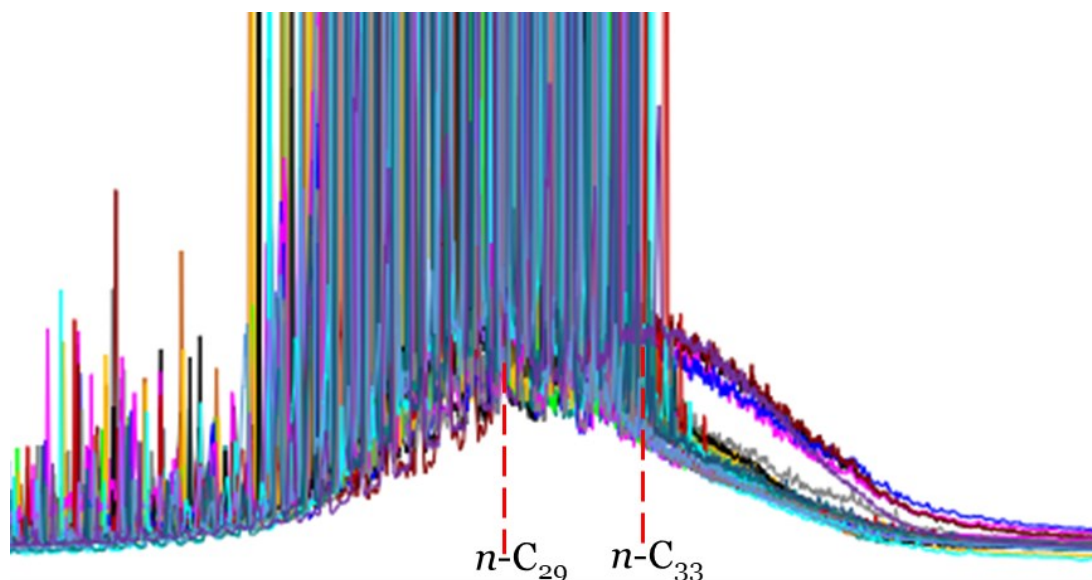


Figure 5.7. Overlay of all 22 MOSH chromatograms of the EVOOs sampled from the market, where the presence of two main molecular weight distributions is highlighted. For better comparison, the scale of the signals has been changed to make them overlap.

On the other hand, the divergence between these oils (total average 19.4 mg/kg for MOSH and 3.4 mg/kg for MOAH) and the oils taken at the exit of the centrifuge at the mill, the latter containing on average 8.6 mg/kg of MOSH and 1.7 mg/kg of MOAH (the upper bound approach was used for calculation and TB1 was excluded, as it was an exceptional and isolated case), seemed to be anomalous. In particular, of the 28 samples considered, 21% exceeded the threshold of 13 mg/kg of MOSH reported in the benchmark levels of LAV & BLL (2022), while 32% exceeded the threshold of 2 mg/kg of MOAH reported in the latter and also imposed by the Commission European (2022). For oils on the market, these percentages rose to 68% and 82% respectively (Figure 5.8).

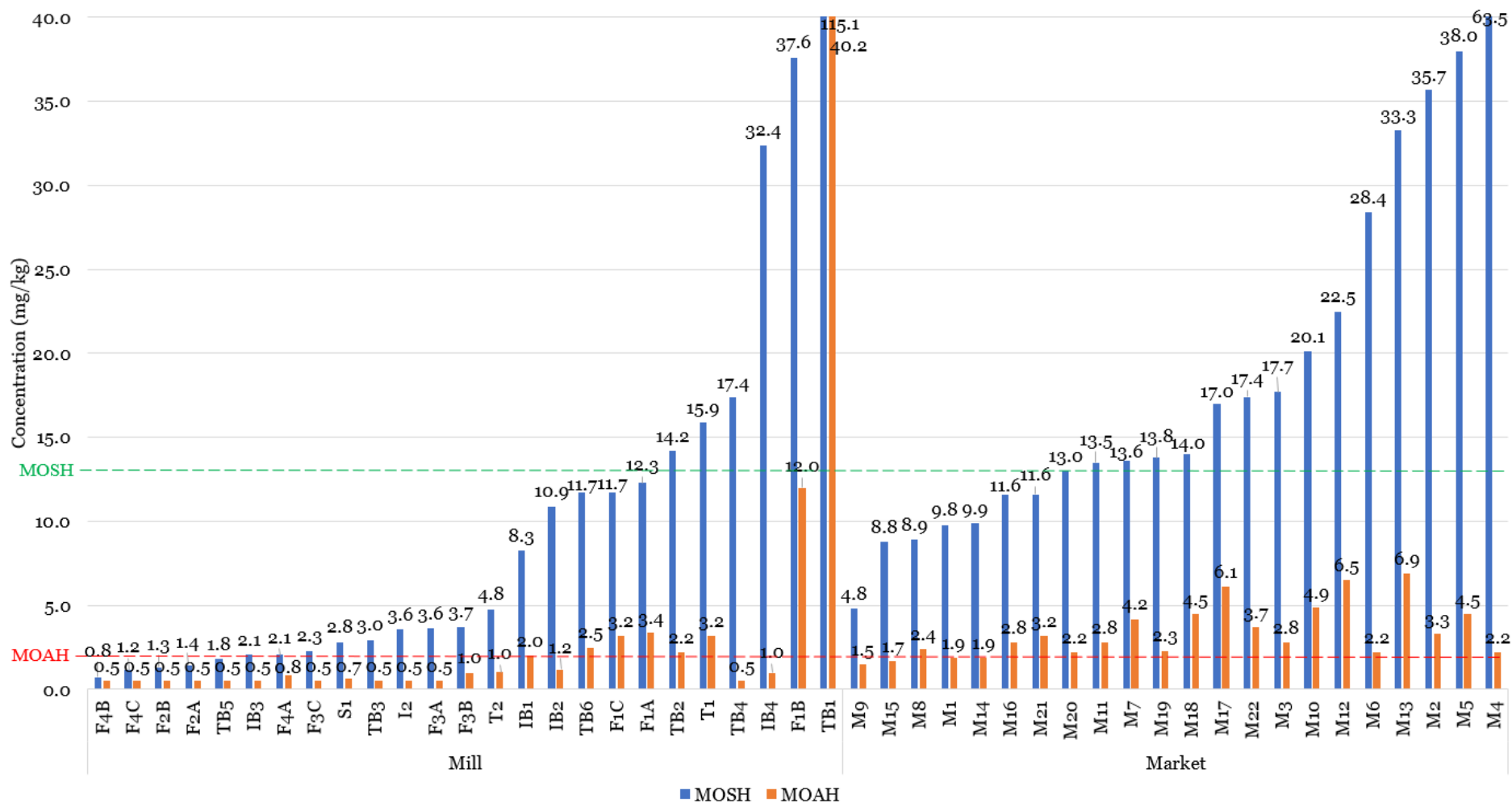


Figure 5.8. Quantifications relating to EVOOs taken from the centrifuge at the milling plant and bought at the supermarket. EVOOs encoded from M1 to M12 were taken from Menegoz Ursol et al. (2022) and derived from traditional agriculture, while from M13 to M22 derived from organic agriculture. Oils were sorted in ascending order based on MOSH content, and concentrations below the LOQ (0.5 mg/kg) were reported with this value. Green and red lines indicate the threshold of 13 mg/kg of MOSH and 2 mg/kg of MOAH respectively, in accordance with the benchmark levels of LAV & BLL (2022) and the limit imposed by the SCoPAFF (EC, 2022).

Although there is no direct correlation between the oils collected at the mill and those bought at the supermarket, the number of samples is high enough to hypothesize that they may be representative of the population from which they were sampled. This would indicate the presence of some criticality in the phases following centrifugation, such as storage, transportation, filtration and bottling.

However, further investigation will be required to precisely identify these last possible sources of contamination prior to marketing, and this will possibly be the subject of further study.

5.4 Conclusions

Mill processing does not seem critical in terms of contamination contribution. Significant MOH increase occurred sporadically, and moreover with a low average incidence (the average increase that a generic sample can undergo due to the milling process was found to be equal to 2.3 mg/kg). In particular, comparing the levels of contamination in the samples before and after processing at the mill, of the 22 batches of olives for which this comparison was possible, only 5 reported a significant increase (23%). On the other hand, an efficient olive washing with water (high turbulence) turned out to be an important step for a partial reduction of the mineral oil content found in the finished oil. The remaining contamination is either partly dissolved in the waxy layer that surrounds the olives or located into its deeper layers. For this reason, research should move in this direction, looking for food grade detergents that can be added to the washing water during this step to efficiently remove MOH. In addition, the oil obtained from pitted and whole olives did not report significant variations in the levels of contamination, excluding that the deeper contamination could originate from olive stones. Even the presence of leaves together with the olives during the milling, in case of samples only subjected to environmental contamination, does not seem to have an impact on the final levels of MOH.

The oils sampled from the centrifuge directly at the mill reported levels of MOSH and MOAH that were 50% lower than those found in oils purchased from the market. This suggests that storage, transportation and bottling operations could play a role in the contribution of mineral oil contamination to finished oils. Future developments aimed at investigating these steps are needed to verify the validity of this assumption.

Finally, in the context of this study, two rapid and solvent saving protocols were optimized, one aimed at the chemical extraction of oil from the olive paste, and the other at the removal of interference by endogenous *n*-alkanes from the MOSH fraction. MAE was chosen for oil extraction, resulting in good extraction yields using a 1:1 *n*-

hexane/ethanol mixture directly on the wet matrix. Also the Alox protocol for *n*-alkane removal, exploiting a small SPE cartridge (reduced use of solvent and adsorbent) and applicable on saponified and epoxidized samples, reported optimal performance that allowed to reach a LOQ of 0.5 mg/kg, useful for the evaluation of background contamination.

6 The impact of the refining process on the mineral oil contamination of olive oils and olive pomace oils

6.1 Introduction

Mineral oil hydrocarbons are food contaminants of petrogenic origin conveniently divided into two main classes, according to their common chemical structure and toxicity: the mineral oil saturated hydrocarbons (MOSH) and the mineral oil aromatic hydrocarbons (MOAH). MOSH include linear (*n*-alkanes), branched (isoalkanes) or cyclic (naphthenes) saturated hydrocarbons, while MOAH comprise aromatic hydrocarbons with a different number of condensed rings, having an alkylation degree higher than 98%, that distinguish them from non-alkylated polycyclic aromatic hydrocarbons (PAH) (EFSA, 2012a).

MOSH are considered less problematic for human health, even though they can accumulate inside the human body increasing the weight of specific organs, whose consequences are still unknown (Barp et al., 2014; Biedermann et al., 2015; Grob, 2018a). Of greater concern are MOAH, mainly when suspected of including 3-5 ring little alkylated compounds with toxicity similar to that of PAH having the same ring number, which are recognized genotoxic and carcinogenic compounds (EFSA, 2012a; Grob, 2018a).

Very recently, EU Member States, in a meeting of the Standing Committee on Plants, Animals, Food and Feed (SCoPAFF) (EC, 2022), agreed to issue a limit of 2 mg/kg for MOAH in fats and oils, corresponding to the maximum acceptable LOQ reported by the guidance of the Joint Research Centre (JRC) (Bratinova & Hoekstra, 2019). The application of this limit is currently delegated to individual Member States. For MOSH, on the other hand, there is no limit, but reference is made to the benchmark level of 13 mg/kg published by the Consumer Protection Consortium of the Federal States (LAV) and Food Federation Germany (former German Federation of Food Law and Food Science, BLL) in 2019, and recently reconfirmed in 2022.

The official method for mineral oil determination in vegetable oils (EN 16995:2017), based on the method firstly introduced by Biedermann et al. (2009), involves the use of high performance liquid chromatography HP(LC) coupled to gas chromatography (GC) and flame ionization detection (FID) (Biedermann et al., 2009; Bratinova & Hoekstra, 2019). However, since this method, when applied without sample pre-enrichment aimed at removing triglycerides, does not allow to reach adequate sensitivity for the MOAH fraction, later a saponification step was included in the revised EN standard as

mandatory, in addition to the epoxidation step for olefin removal. This approach was indeed already used also in other works (Albert et al., 2022; Menegoz Ursol et al., 2022; Nestola, 2022).

It is well known that vegetable oils, due to their apolar nature, are particularly prone to mineral oil contamination and that there are several contamination sources along the entire processing chain (Brühl, 2016; Grob, 2018b). As reported by (Menegoz Ursol et al., 2023), contamination in extra virgin olive oils (EVOOs) derives mainly from harvesting operation, but can also be determined by the other steps along the entire processing chain (see the previous chapters).

While there is an established literature on the removal of PAH during edible oil refining (particularly during the bleaching step where activated carbon is involved) (Gong et al., 2007; Yap et al., 2010; Ma et al., 2017; Kiralan et al., 2019; Ab Razak et al., 2021), to date the impact of refining on the final mineral oil content in olive oils (OOs) and olive pomace oils (OPOs) has been little investigated, and no information at all is available on the fate of low-alkylated MOAH with more than 3 benzene rings (of major toxicological concern). Some authors highlighted a decrease in mineral oil levels during refining, as the consequence of the deodorization phase carried out by vacuum steam distillation of the oil, capable of stripping away the most volatile hydrocarbon fractions. This, for example, was verified for cocoa butter, as well as for grape seed, peanut and lampante olive oil, for which removal of hydrocarbons up to $n\text{-C}_{25-30}$ was witnessed (Wagner et al., 2001b; Moret et al., 2003; Fiorini et al., 2008; Stauff et al., 2020). This was also corroborated by the analysis of the steam distillation condensates, which reported chromatographic profiles in line with that of the contaminations stripped away (Wagner et al., 2001b; Stauff et al., 2020). However, these works mainly concerned fatty matrices other than olive oil except one.

Thus, the aim of this work was, within the scope of a PhD project aimed at investigating mineral oil contamination in the olive oil supply chain, to fill this gap and share some more information in this context.

6.2 Materials and methods

6.2.1 Samples

Six lampante olive oils (LOOs) and 2 crude olive pomace oils (COPOs), together with the relative oils taken in the following refining steps, were supplied by two different plants located in Central and South Italy. In particular, the first plant provided samples from 4

lampante oil refining lines, encoded from LOO1 to LOO4, while the other from 2 lampante oil refining lines, LOO5 and LOO6, and 2 crude pomace oil refining lines, COPO1 and COPO2. More detailed information about the samples and the refining process are provided in Table 6.1.

Finally, 5 OOs and 3 OPOs of different brands were purchased from the Italian market.

Table 6.1. Information relating to the samples of lampante and pomace oils in terms of distribution of the MOH contamination, together with the process conditions capable of having an influence in the removal of the most volatile fractions.

Sample	Origin	Samples analyzed	Deodorization		Time (h)	Additional steps involving distillation
			Vacuum (mbar)	Temperature (°C)		
LOO1	Tunisia	Crude Neutralized Bleached Deodorized	2	227	3	Distillation 227 °C for 10-15 min
LOO2	Italy	Crude Deacidified Neutralized Bleached Deodorized	2	227	3	Deacidification 227 °C for 10-15 min Distillation 227 °C for 10-15 min
LOO3	Italy	Crude Neutralized Bleached Deodorized	2	227	3	Distillation 227 °C for 10-15 min
LOO4	Spain	Crude Neutralized Bleached Deodorized	2	227	3	Distillation 227 °C for 10-15 min
LOO5	Spain	Crude Bleached Deodorized	1	180	2.5	Distillation 180 °C for 10-15 min
LOO6	Spain/Italy	Crude Neutralized Bleached Deodorized	0.8	210	3	Distillation 245 °C for 10-15 min
COPO1	Greece	Crude Bleached Deodorized	0.8	220	5	-
COPO2	Greece	Crude Bleached Deodorized	0.8	210	5	Distillation 235 °C for 10-15 min

6.2.2 Chemicals and standards

n-Hexane, dichloromethane and methanol (all distilled and subsequently subjected to purity check), ethanol, *m*-chloroperbenzoic acid (*m*CPBA), potassium hydroxide, sodium thiosulfate and sodium sulfate were obtained from Sigma-Aldrich (St. Louis, Missouri, USA). Water was purified to milliQ grade using a MilliQ Advantage A10 system from Millipore (Bedford, Massachusetts, USA).

HPLC separation performance was evaluated using the MOSH/MOAH standard (9 components) purchased from Restek (Bellefonte, Pennsylvania, USA), containing *n*-C₁₃ at 0.15 mg/mL, 1,3,5-tritert-butylbenzene (TBB), *n*-C₁₁, cyclohexylcyclohexane (CyCy), pentyl benzene (5B), 1-methyl naphthalene (1-MN), 2-methyl naphthalene (2-MN) at 0.30 mg/mL and 5- α -cholestane (Cho) and perylene (Per) at 0.60 mg/mL, all in toluene. This mixture was also used as internal standard (IS) to carry out quantifications. The MOSH/MOAH retention time standard mixture, containing *n*-C₁₀, *n*-C₁₁, *n*-C₁₃, *n*-C₁₆, *n*-C₂₀, *n*-C₂₄, *n*-C₂₅, *n*-C₃₅, *n*-C₄₀ and *n*-C₅₀, each at 100 μ g/mL in cyclohexane, used to verify GC and GC \times GC performance in terms of discrimination, and to define the cuts relating to C-fractions (Bratinova & Hoekstra, 2019) during integration of chromatograms, was also from the same supplier.

6.2.3 Equipments and instrumentation

Glassware and all the materials intended for contact with samples were washed thoroughly with acetone and *n*-hexane before use. The microwave extraction system (MARS5) used for microwave assisted saponification (MAS), equipped with optical fiber temperature probe RTP-300 Plus, was from CEM Corporation (Matthews, North Carolina, USA). Solvent evaporation was carried out using a Univapo 100 H centrifuge from UniEquip (Martinsrieder, Munich, Germany) connected to a V-700 vacuum pump from Büchi AG (Flawil, Switzerland).

6.2.3.1 HPLC-GC-FID

The on-line HPLC-GC-FID system (LC-GC 9000) from Brechbühler (Zurich, Switzerland), consisted of an HPLC Phoenix 9000 pump and a GC Trace 1310 series from Thermo Fisher Scientific (Waltham, Massachusetts, USA), and had the possibility to process both MOSH and MOAH analysis within the same GC run. Fraction transfer from HPLC to GC occurred by exploiting partially concurrent eluent evaporation through the Y-interface (Biedermann and Grob 2009). The HPLC column was a 25 cm \times 2.1 mm ID, 5 μ m particle size, packed with Lichrospher Si-60 column by DGB (Schlossboeckelheim, Germany). The feeding of the two GC channels was managed by a switching valves system. GC channels included a 10 m \times 0.53 mm ID deactivated retention gap, to allow large volume injection (LVI) (Biedermann & Grob, 2012a), followed by a steel T-piece, connected in turn with a solvent vapour exit (SVE) heated at 140 °C for vapour discharge, and with a 10 m \times 0.25 mm ID GC column by Mega (Legnano, Milan, Italy) with a stationary phase of PS-255 (1% vinyl, 99% methyl polysiloxane), 0.15 μ m film thickness.

MOSH and MOAH separation by the HPLC was accomplished setting a gradient starting with 100% *n*-hexane, kept for 0.1 min, and reaching a 70:30 dichloromethane/*n*-hexane (*v/v*) ratio after 0.5 min, while using an eluent flow of 300 $\mu\text{L}/\text{min}$. The MOSH fraction was eluted from 2.1 to 3.6 min, while the MOAH from 3.8 to 5.3. After 6 min, a backflush with 100% dichloromethane at a flow rate of 500 $\mu\text{L}/\text{min}$ was performed for 9 min, and then the column was reconditioned with *n*-hexane for 6.5 min at flow rate of 700 $\mu\text{L}/\text{min}$, followed by 1.5 min at the initial flow. During the fraction transfer, the GC worked at a constant pressure of 90 kPa, lowered to 60 kPa for the GC run. The temperature gradient, starting from 51 °C and beginning 8.5 min after the transfer of the MOSH from the HPLC started, provided for a 20 °C/min rate, reaching the final temperature of 350 °C, which was kept constant for 5 min. The FID was heated at 360 °C. Data were acquired and processed with Chromeleon 7 Chromatography Data System (CDS) from Thermo Fisher Scientific (Waltham, Massachusetts, USA).

6.2.3.2 GC×GC-MS

The GC×GC system included a GC 8890 from Agilent Technologies (Santa Clara, California, USA) equipped with a QTOF 7250 Mass Spectrometer. Column configuration included a 10 m × 0.53 mm ID uncoated retention gap, allowing for LVI. The column set included a J&W DB-17ms column (15 m × 0.25 mm ID × 0.15 μm film thickness) by Agilent Technologies (Santa Clara, California, USA) as first dimension and a 2.45 m × 0.15 mm ID (0.055 μm of film thickness PS-255) by Mega (Legnano, Milan, Italy) as second dimension. The first part of the secondary column was used as modulation loop. Coupling to the QTOF was achieved through a deactivated fused silica capillary (1 m × 0.1 mm ID). Carrier gas was helium used at a constant flow of 1.5 mL/min. The GC temperature ramp started from 40 °C and, after 2 min, the temperature was increased to 340 °C at 4 °C/min, and kept constant for 5 min. The GC transfer line, the ion source and the quadrupole were set at 340 °C, 300 °C and 150 °C, respectively. Electron impact ionization (EI) was carried out at 70 eV. Nitrogen and helium, used as collision and quenching gas respectively, were set at 1 and 4 mL/min. Acquisition frequency was 50 spectra/second, in full spectra mode from 50 to 600 *m/z*. Modulation (9 s) occurred using a loop-type ZX2 thermal modulator with closed-cycle refrigeration (Zoex Corporation, Houston, Texas, USA), managed by an Optimode™ v2.0 (SRA Instruments, Cernusco sul Naviglio, Milan, Italy). Hot jet ramp started from 250 °C, kept for 2 min, and increased to 400 °C at 4 °C/min, kept until the end of the run. Cold-jet flow, expressed as Mass Flow Controller (MFC) flow capacity, was programmed through linear regressions: starting

value of 50%, was reduced to 40% during the first 700 s, and further reduced to 5% at 35 min (then kept constant until the end of the run). Data were acquired by MassHunter software (Agilent Technologies, Santa Clara, California, USA). 2D data were processed by GC Image® GC×GC Edition Software, Release 2020r1 (Zoex Corporation, Houston, Texas, USA).

6.2.4 Sample preparation

Samples from the lampante oil refining lines were analyzed according to our internally validated method (Menegoz Ursol et al., 2022). Briefly, 1 g oil, following the addition of 10 µL of IS, 10 mL of *n*-hexane and 10 mL of methanolic KOH 1.5 N, was subjected to MAS at 120 °C for 20 min. *n*-Hexane phase was recovered after phase separation, achieved with the addition of 40 mL of milliQ water and 30 min rest at -18 °C, and after addition of few mL of methanol to avoid possible emulsion formation. The *n*-hexane extract was quantitatively recovered, transferred into a test tube, evaporated down to 4 mL and washed with 3 mL of a 2:1 methanol/water (*v/v*) mixture. Operationally, the test tube was vortexed and then centrifuged at 5000 rpm for 5 min. At this point, the extract recovered was evaporated to 700 µL and subjected to epoxidation according to (Nestola & Schmidt, 2017). In particular, the latter was performed with 500 µL of 20% (*m/v*) ethanolic *m*CPBA for 15 min, at ambient temperature and under agitation. The reaction was stopped with 2 mL of 10% (*m/v*) aqueous sodium thiosulfate, and phase separation was improved by the addition of 500 µL of ethanol. The sample extract was then recovered and transferred into an autosampler vial containing a spatula tip of sodium sulfate anhydrous.

Pomace oils usually contains 10-fold higher concentration of mineral oils, thus this type of oil was epoxidized without previous saponification. 300 mg of oil were weighed, added with 10 µL of IS and dissolved in *n*-hexane to a final volume of 1 mL. Then, epoxidation was performed as already described.

6.2.5 Analytical determination

After sample preparation, samples were injected into the HPLC-GC-FID apparatus. For one refining line of pomace oil (COPO2), the HPLC was used to collect the MOAH fractions to be submitted to GC×GC-MS analysis.

For HPLC-GC-FID analysis of the extracts of the lampante oil refining lines, 50 µL and 100 µL were injected for MOSH and MOAH, achieving a limit of quantification (LOQ) on the total hump of 1.0 and 0.5 mg/kg (0.5mg/kg and 0.2 mg/kg on the C-fractions),

respectively. For pomace oil extracts, 50 μL were injected (in order not to exceed the maximum capacity of the LC column towards fat), achieving a LOQ around 4.0 mg/kg on the total hump (2 mg/kg on the C-fractions).

For GC \times GC-MS analysis, the HPLC was disconnected from the GC and used to collect the MOAH fractions of the pomace oil samples. The injection volume was set at 50 μL also in this case. Of the collected fraction, 4 μL of the reconcentrated fraction were injected into the GC \times GC-MS apparatus.

6.3 Results and discussion

To better understand the effect of refining steps, it follows a brief description of the process, which in case of LOOs and COPOs is substantially the same: in a first step, the oil is neutralized removing free fatty acids. This can be performed chemically, by adding a base like NaOH, or physically, by distilling them, even though a combination of the two approaches is feasible. Soaps formed are washed away with water. After that, the oil is bleached by addition of a mix of decolorizing earths and activated carbon and, after removal of these solids by filtration, oil is ready for the last step, which is a deodorization carried out by vacuum steam distillation. At this point, the refined olive oils (ROOs) and refined olive pomace oils (ROPOs) are ready to be blended with small percentages of virgin (VOO) and EVOOs to be sold as OOs and OPOs respectively (Morchio, 2022).

6.3.1 Removal of mineral oil contamination

A total of 8 refining lines were investigated to assess the incidence of the refining process on the mineral oil contamination in ROOs and ROPOs. Table 6.2 shows the distribution of the MOSH contamination present in the oil samples before refining (LOOs and COPOs), in terms of molecular weight distribution and percentage ratio of the fractions $n\text{-C}_{10-25}$ and $n\text{-C}_{10-35}$ with respect to the total $n\text{-C}_{10-50}$ MOSH hump. These evaluations were not reported for MOAH which in general had the same distribution of MOSH.

Table 6.2. MOSH distribution in lampante olive oils and crude olive pomace oils.

Sample	MOSH distribution		% on total $n\text{-C}_{10-50}$	
	Range	Center(s)	$n\text{-C}_{10-25}$	$n\text{-C}_{10-35}$
LOO1	$n\text{-C}_{15} - n\text{-C}_{50}$	$n\text{-C}_{29}$	19.1	66.1
LOO2	$n\text{-C}_{13} - n\text{-C}_{50}$	$n\text{-C}_{29}$	24.2	73.0
LOO3	$n\text{-C}_{16} - n\text{-C}_{50}$	$n\text{-C}_{29}$	14.9	77.3
LOO4	$n\text{-C}_{16} - n\text{-C}_{50}$	$n\text{-C}_{23}/n\text{-C}_{33}$	21.3	68.3
LOO5	$n\text{-C}_{17} - n\text{-C}_{50}$	$n\text{-C}_{28}$	18.6	73.3
LOO6	$n\text{-C}_{14} - n\text{-C}_{50}$	$n\text{-C}_{29}$	20.1	72.4
COPO1	$n\text{-C}_{13} - >n\text{-C}_{50}$	$n\text{-C}_{29}$	21.7	78.0
COPO2	$n\text{-C}_{14} - >n\text{-C}_{50}$	$n\text{-C}_{31}$	10.4	69.6

All the contaminations present into the starting oils were distributed over a similar range of molecular weights, which is typical for contaminations with lubricating oils (Grob, 2018b), such as those encountered by Menegoz Ursol et al. (2023) as a consequence of the harvesting operations. Only in one case the presence of two humps in the chromatogram, centered on lower and higher retention times, was registered (sample LOO4). The percentage of the $n\text{-C}_{10-25}$ and $n\text{-C}_{10-35}$ fractions, with respect to total MOSH contamination in the $n\text{-C}_{10-50}$ range, was in general rather constant.

Chromatogram overlay of the different refining stages (two examples are shown in Figure 6.1) highlighted as the contamination remained constant until before deodorization, and then was completely removed below $n\text{-C}_{20}$, with signal at baseline level, removed consistently between $n\text{-C}_{20-25}$, and partially removed in the next C-fraction ($n\text{-C}_{25-35}$), in the finished oil.

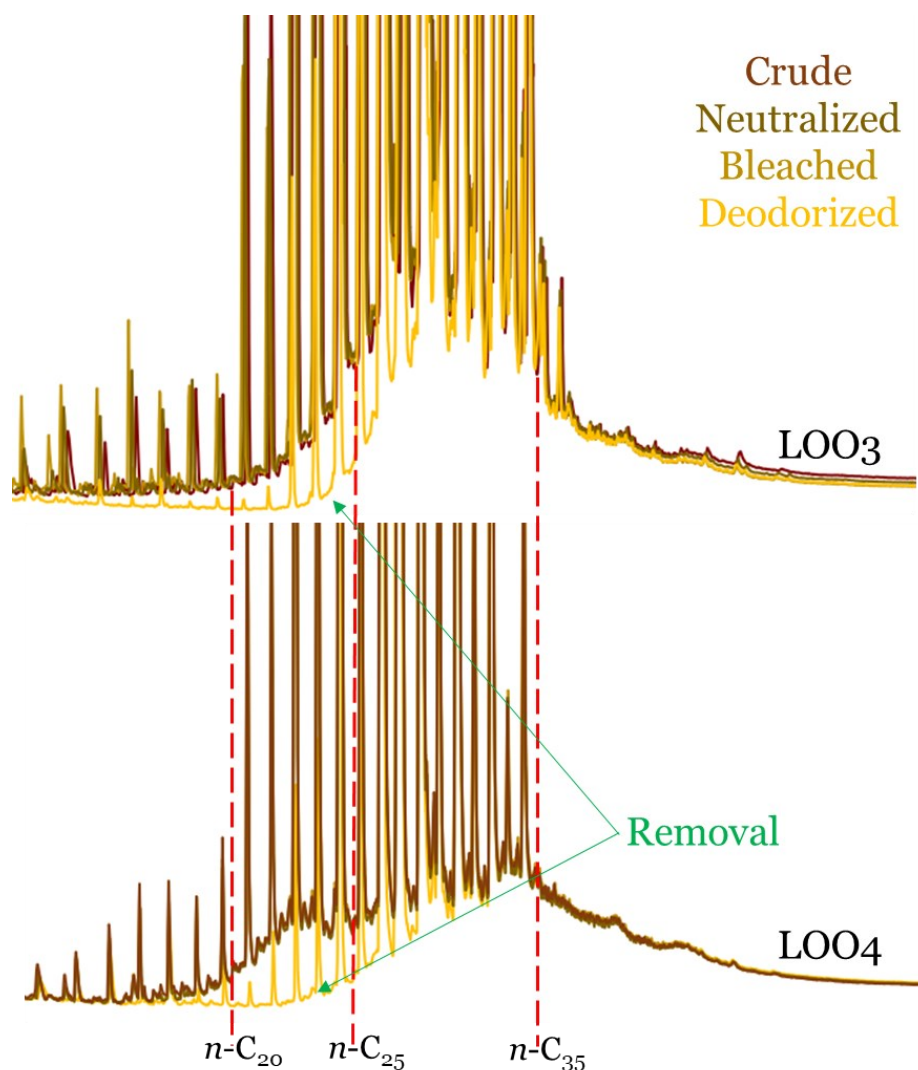


Figure 6.1. Overlay of chromatograms related to the MOSH fractions of samples LOO3 and LOO4, highlighting the loss of the most volatile fraction ($<n-C_{35}$) in the deodorization step of oil refining.

In Table 6.3 are instead reported the quantifications performed on the different samples from each refining step and for each single C-fraction, for both MOSH and MOAH. Along with these, the percentage removals experienced for specific molecular weight ranges ($n-C_{10-25}$, $n-C_{10-35}$ and $n-C_{10-50}$) are also reported. These values, with the exceptions later discussed for samples for which cross-contamination along the processing line was suspected, were obtained as the percentage ratio between the average concentrations from all the steps prior to deodorization (where no variation was found), and that after deodorization.

Table 6.3. MOSH and MOAH concentrations for each refining step, expressed for single C-fractions and as total contamination, and related percentage of removal (%) for fractions $n\text{-C}_{10-25}$, $n\text{-C}_{10-35}$ and $n\text{-C}_{10-50}$ due to deodorization.

Sample	Refining step	MOSH (mg/kg)								Removal (%)			MOAH (mg/kg)					Removal (%)		
		$n\text{-C}_{10-16}$	$n\text{-C}_{16-20}$	$n\text{-C}_{20-25}$	$n\text{-C}_{25-35}$	$n\text{-C}_{35-40}$	$n\text{-C}_{40-50}$	$n\text{-C}_{10-50}$	% ratio $n\text{-C}_{10-35}/n\text{-C}_{10-50}$	$n\text{-C}_{10-25}$	$n\text{-C}_{10-35}$	$n\text{-C}_{10-50}$	$n\text{-C}_{10-16}$	$n\text{-C}_{16-25}$	$n\text{-C}_{25-35}$	$n\text{-C}_{35-50}$	$n\text{-C}_{10-50}$	$n\text{-C}_{10-25}$	$n\text{-C}_{10-35}$	$n\text{-C}_{10-50}$
LOO1	Crude	0.04	0.56	1.4	5.0	1.7	1.9	10.7	66.1				0.06	0.82	0.96	1.1	3.0			
	Neutralized	0.04	0.58	1.5	4.9	1.6	1.9	10.5	67.1	89.9	47.0	33.6	0.13	0.98	0.86	1.2	3.2	91.9	51.9	31.1
	Bleached	0.03	0.57	1.5	5.2	1.7	1.9	11.0	67.0				0.16	0.98	0.98	1.3	3.4			
	Deodorized	-	-	0.21	3.6	1.5	1.8	7.1	53.3				-	0.08	0.87	1.2	2.2			
LOO2	Crude	0.27	0.41	1.4	4.3	1.3	1.1	8.8	73.0	53.6*	18.3*	9.7*	-	0.08	0.62	0.49	1.2	77.7*	15.5*	12.0*
	Deacidified	0.04	0.20	0.74	4.2	1.4	1.3	7.9	66.0				-	0.02	0.58	0.46	1.0			
	Neutralized	0.17	0.37	3.5	21.8	5.0	3.4	34.2	75.4				-	0.22	3.2	3.2	6.6			
	Bleached	0.28	0.60	2.3	9.7	2.9	2.4	18.1	71.0	n.q.	n.q.	n.q.	-	0.09	0.83	0.83	1.8	n.q.	n.q.	n.q.
	Deodorized	-	-	0.55	5.4	2.0	1.7	9.7	61.2				-	-	0.53	1.0	1.5			
LOO3	Crude	-	0.32	2.2	10.5	2.2	1.6	16.8	77.3				0.25	1.2	2.0	1.4	4.9			
	Neutralized	-	0.43	2.5	11.2	2.2	1.6	17.9	78.8	89.5	36.3	27.5	0.30	1.4	2.2	1.6	5.5	90.6	45.7	31.6
	Bleached	-	0.45	2.7	11.2	2.1	1.4	17.8	80.3				0.30	1.5	2.3	1.5	5.7			
	Deodorized	-	-	0.30	8.5	2.3	1.6	12.7	69.3				-	0.16	1.9	1.6	3.7			
LOO4	Crude	-	0.36	2.7	6.7	2.6	1.9	14.2	68.3				-	0.25	0.65	0.39	1.3			
	Neutralized	-	0.34	2.7	7.1	2.8	1.9	14.8	68.4	89.9	43.9	33.1	-	0.28	0.68	0.41	1.4	81.2	28.4	20.9
	Bleached	-	0.41	2.8	6.9	2.7	1.9	14.6	69.0				-	0.32	0.75	0.44	1.5			
	Deodorized	-	-	0.31	5.3	2.3	1.8	9.7	57.5				-	0.05	0.65	0.40	1.1			

Table 6.3. Continued.

Sample	Refining step	MOSH (mg/kg)							% ratio $n\text{-C}_{10-35}/n\text{-C}_{10-50}$	Removal (%)			MOAH (mg/kg)					Removal (%)		
		$n\text{-C}_{10-16}$	$n\text{-C}_{16-20}$	$n\text{-C}_{20-25}$	$n\text{-C}_{25-35}$	$n\text{-C}_{35-40}$	$n\text{-C}_{40-50}$	$n\text{-C}_{10-50}$		$n\text{-C}_{10-25}$	$n\text{-C}_{10-35}$	$n\text{-C}_{10-50}$	$n\text{-C}_{10-16}$	$n\text{-C}_{16-25}$	$n\text{-C}_{25-35}$	$n\text{-C}_{35-50}$	$n\text{-C}_{10-50}$	$n\text{-C}_{10-25}$	$n\text{-C}_{10-35}$	$n\text{-C}_{10-50}$
LOO5	Crude	-	0.09	1.0	3.2	0.85	0.71	5.9	73.3				-	0.44	0.84	0.52	1.8			
	Bleached	-	0.17	1.1	3.5	1.1	0.88	6.8	71.0	n.q.	n.q.	n.q.	-	0.31	0.80	0.41	1.5	n.q.	n.q.	n.q.
	Deodorized	-	0.10	2.6	6.1	1.1	0.83	10.8	81.6				n.q.	n.q.	n.q.	n.q.	n.q.			
LOO6	Crude	0.08	0.33	1.2	4.3	1.1	1.1	8.2	72.4				-	0.59	0.79	0.57	1.9			
	Neutralized	0.17	0.58	1.5	4.9	1.3	1.3	9.8	72.7				-	0.64	0.79	0.61	2.0			
	Bleached	0.08	0.39	1.4	6.1	2.2	2.0	12.2	65.3	92.6	45.8	31.9	-	0.70	1.1	0.73	2.6	89.1	32.8	18.1
	Deodorized	-	-	0.14	3.4	1.3	1.3	6.1	57.7				-	0.07	0.88	0.69	1.6			
COPO1	Crude	0.65	2.4	12.7	40.8	8.9	7.1	72.6	78.0				0.76	2.5	11.2	7.6	22.1			
	Bleached	0.77	2.6	12.9	40.4	9.9	6.9	73.4	77.3	72.3	25.0	16.6	0.70	2.8	12.5	8.3	24.3	87.4	24.8	12.3
	Deodorized	-	-	4.4	38.1	10.1	8.3	60.9	69.8				-	0.43	11.1	8.7	20.2			
COPO2	Crude	0.52	3.1	18.2	124.0	36.4	27.2	209.5	69.6				2.2	15.0	32.4	32.8	82.4			
	Bleached	0.15	3.0	18.0	124.1	39.0	30.7	215.0	67.6	94.5	36.4	21.7	2.2	14.0	33.4	35.2	84.9	98.6	45.7	24.6
	Deodorized	-	-	1.2	91.5	39.4	34.1	166.1	55.8				-	0.23	26.7	36.2	63.1			

*Removal referred to the deacidification step performed by distillation; n.q. not quantifiable.; - not detectable.

To identify problems of poor representativeness along the refining lines, due to possible cross-contamination occurred during sampling (i.e. contact with dirty containers, mixtures with other oils, etc.), the percentage MOSH ratio of the n -C₁₀₋₃₅ fraction on total n -C₁₀₋₅₀ was calculated for each sample, and reported in Table 6.3. This ratio allowed to normalize data within each refining line and to promptly identify suspicious samples. In fact, regardless of the absolute concentration of the contamination, this percentage ratio should remain rather constant along each refining line, except for the steps involving a contamination reduction (deacidification and deodorization). This approach allowed to confirm possible problems of cross-contamination for samples LOO2, LOO5 and LOO6 (data are reported in red in the table).

As shown in the table, of the 6 refining lines for which the contamination decreased, in 5 of them this ratio changed only during the deodorization step (data in green), confirming the removal effect described so far. For the remaining one (sample LOO6), despite the decrease in contamination, a lower ratio before any distillation treatment highlighted a contamination, falling into the heavier C-fractions (visible in the overlay of chromatograms in Figure 6.2B), that was probably introduced during sampling as this additional profile was not confirmed in the deodorized oil. Thus, this problem regarded only the bleached oil. For sample LOO5, for which the MOSH concentration doubled in the finished oil compared to the crude one, the n -C₁₀₋₃₅/ n -C₁₀₋₅₀ percentage ratio increased after deodorization together with the appearance of a new MOSH hump centered on n -C₂₆ (Figure 6.2A). The possible presence of the same contamination in the MOAH fraction could not be evaluated due to the presence of olefins which completely hindered the interpretation of the chromatogram. Anyway, it was not possible to define whether this contamination was introduced during or after the deodorization treatment, even though the fact that the most volatile fraction ($<n$ -C₂₅) was still significantly present would suggest a contamination introduced after this distillation step. Finally, for LOO2, after the initial decrease experienced during the physical deacidification, which in fact was confirmed by a lower n -C₁₀₋₃₅/ n -C₁₀₋₅₀ ratio as happened for the deodorized oils, the latter increased again as the result of the contribution of a significantly high MOSH contamination, which appeared in the neutralized oil and was still visible in bleached oil (Figure 6.2C'), but seemed to be not confirmed from the profile of the finished oil (moreover, the ratio decreased again following deodorization, as expected) (Figure 6.2C''). This seems to indicate cross contamination problems for both neutralized and bleached oil. Anyway, all these specific samples, whose results are reported in red in Table

6.3, were not further taken into consideration for calculations, as well as LOO2 deodorized oil as a precaution.

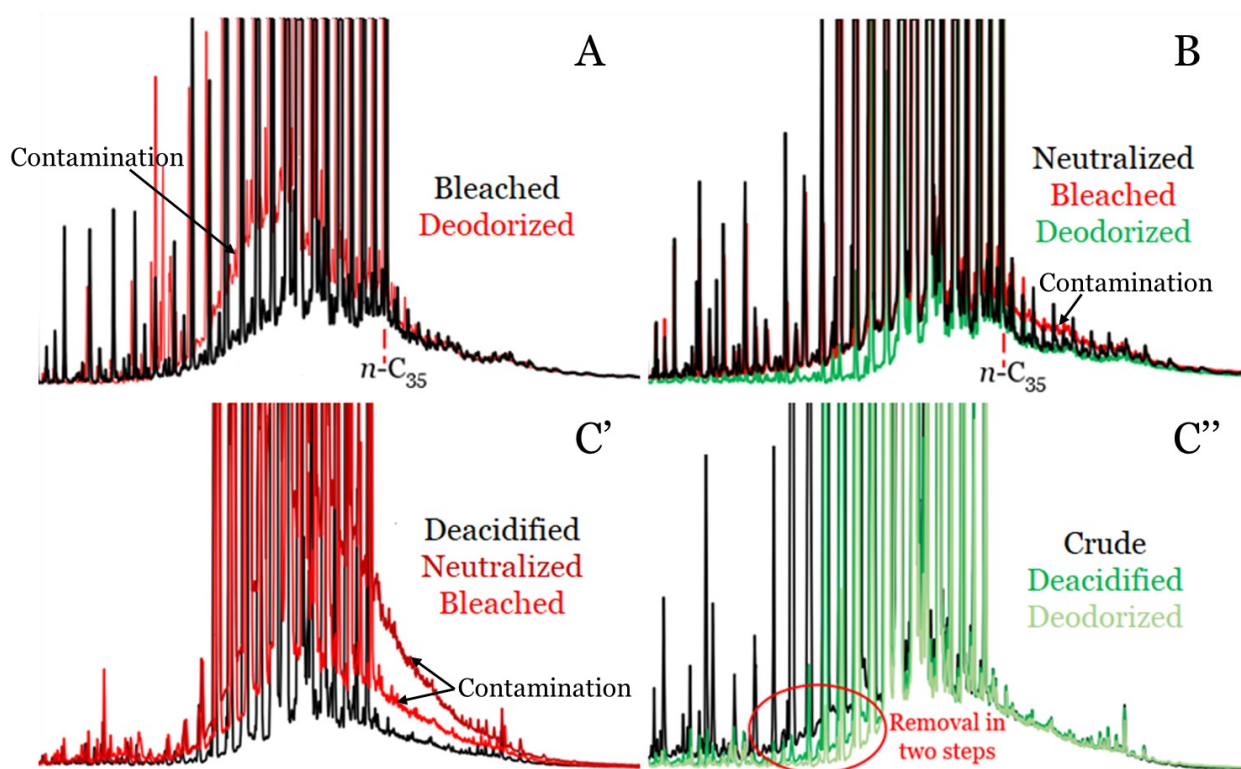


Figure 6.2. Overlay of the chromatograms of LOO5 (A), LOO6 (B) and LOO2 (C' and C''), related to samples coming from different refining steps. In A, B and C, different profiles probably due to cross-contamination occurred during sampling are visible. In C'', removal of the most volatile compounds is already visible during deacidification, and further improved during deodorization.

Of the 6 lampante oils analysed, only LOO3 and LOO4 had a starting MOSH concentration above the benchmark levels (LAV & BLL, 2022), but the refining had a positive impact and allowed them to fall back within the acceptability range (<13.0 mg/kg). The same did not happen for the 2 samples containing MOAH over the SCoPAFF limit (LOO1 and LOO3), even if LOO1 after refining contained 2.1 mg/kg of total MOAH, very close to the recommended limit of 2.0 mg/kg. However, it should be emphasized that, for oils that have undergone refining, olefins are less susceptible to epoxidation and are difficult to remove completely (Biedermann et al., 2020; Nestola, 2022). Therefore, as described later, MOAH data has a certain degree of uncertainty due to residual olefins which make the interpretation of the chromatogram more difficult, adding variability introducing the possibility of overestimations.

In general, for the refining lines where there was a contamination decrease, this was estimated around 10% to 30% of the total MOSH and MOAH concentration (n -C₁₀₋₅₀ range). Actually, not taking into account COPO1 whose behaviour was inexplicably

anomalous, this range narrows to 20-30%. This quite low variability in the removal rate, considering the similar molecular range distributions of the various samples which made it possible to keep this parameter constant and to evaluate only the incidence of the process (see MOSH composition in Table 6.2), underlines how under the deodorization conditions normally adopted (220 ± 10 °C at 1-2 mbar), the removal takes place almost with the same entity, regardless of the duration of the process or the execution of additional distillation steps prior to deodorization. Anyway, to provide an indication, for sample LOO2 which removal due to deacidification by distillation could be evaluated, the total contamination was removed by 10% already during this step.

Looking at the quantifications on the C-fractions for the various samples, the decrease of the MOH generally affected the contamination present up to the C-fraction delimited by n -C₃₅. More specifically, when referring to the most volatile fraction of the MOSH hump considered, i.e. for hydrocarbons with a boiling point lower than or comparable to that of n -C₂₅, the extent of removal was around 90%. Thus, the removal for this fraction was almost complete. This value dropped to around 40% when considering a wider range, thus including heavier hydrocarbons (hydrocarbons below n -C₃₅). Again, for COPO1 these percentages were slightly lower in both cases, without a plausible explanation.

Therefore, to summarize, no critical issues related to the oil refining process, different than possible cross-contamination, have been highlighted in view of the contribution on the final mineral oil contamination. On the contrary, the deodorization step had a positive mitigation impact.

Going into detail regarding the MOAH, the removal was generally in good agreement with that reported for MOSH, except for minor variations affecting low-level contaminations. This was attributed to the presence of isomerized olefins which, albeit partially removed by stripping, remained after epoxidation and co-eluted with the aromatic fraction. Thus, the integration then took place according to an estimate of what was believed to be the profile of the MOAH hump, adding variability to the data (Biedermann et al., 2020), which clearly has a more greater incidence when the level of contamination is low, close to the 2 mg/kg limit recently suggested by the SCoPAFF.

This was particularly evident for samples LOO2, LOO4 and LOO6 (Table 6.3), which were the samples with the lowest MOAH concentration, and thus for which MOSH and MOAH removal percentage data were more misaligned. In the box of Figure 6.3A it is possible to notice the incomplete removal of olefins falling between n -C₂₅ and n -C₃₅ by epoxidation after bleaching, unlike crude oil. Part of them were removed during deodorization (Figure 6.3A), but were still significantly present at the end of the process.

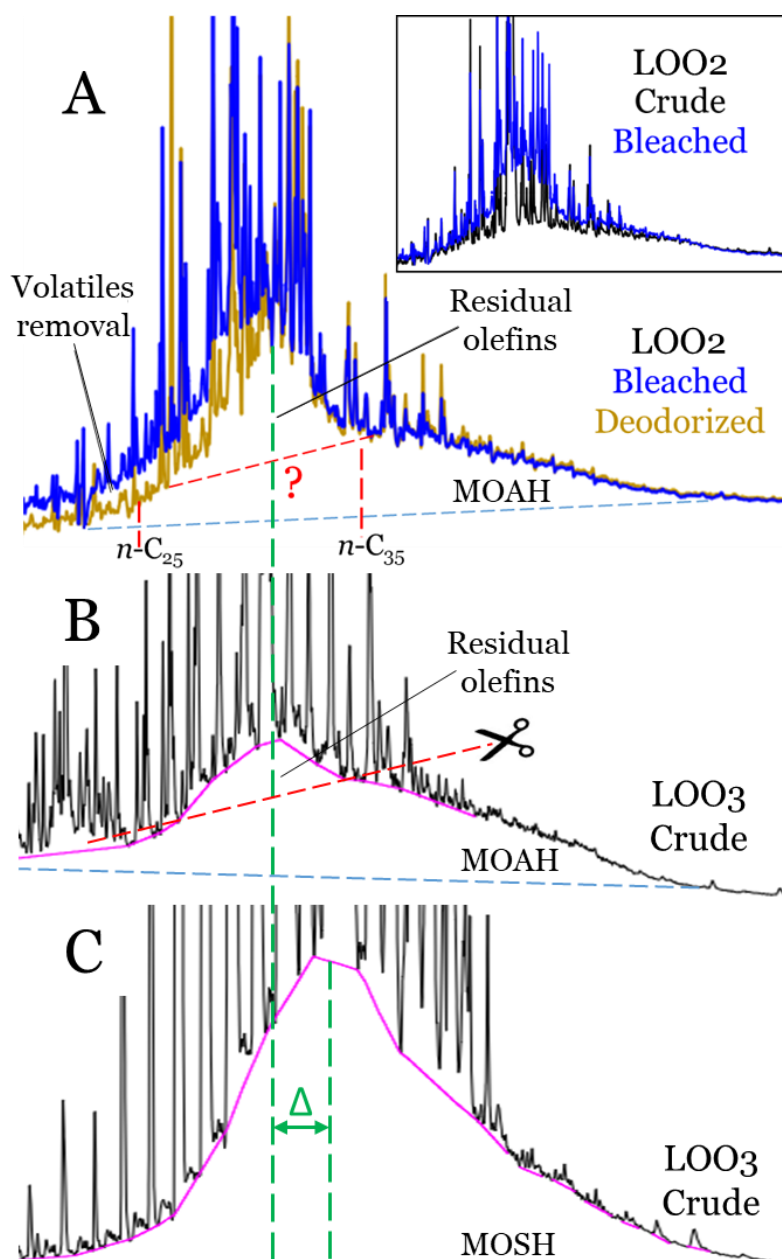


Figure 6.3. Overlay of chromatograms of LOO2 in the different refining steps (A), and example of integration discarding residual olefins for sample LOO2 and LOO3 (A and B). Although the MOAH profile of LOO3 (B) resembles that of its MOSH fraction (C), the retention times of the apexes of the two humps are shifted, and it matches better to that of the residual olefins.

This occurrence is typical for refined oils, not found in virgin ones, and is the result of the isomerization of squalene (i.e. an endogenous compound present at high concentration in olive oils) attributable to the contact of the oil with bleaching earths (Grob et al., 1992b). However, since for some samples even crude oil reported residues of isomerized squalene, this was an indication of the possible cross-contamination due to lampante oil transportation or storage in tanks previously used for refined oils (Grob et al., 1992b). These residues could be mistaken for MOAH due to a similarity with the MOSH profile. However, in most of the cases, as visible in Figure 6.3, the apex of the MOAH hump

(Figure 6.3B), not perfectly centered on the same retention time of the MOSH hump (Figure 6.3C), and the correspondence with the elution zone of the isomerized squalene (Figure 6.3A), disproved this and required these signals to be discarded.

Together with isomerized squalene, also clustered peaks were highlighted in the bleached oil, even if eluted at lower retention times (Figure 6.4). According to the literature, these compounds are mixtures of unsaturated straight-chain hydrocarbons formed during the bleaching step, and tentatively identified as octadecene, octadecadiene, neophytadiene or their isomers (Lanzon et al., 1994). Epoxidation is not able to remove them in the same proportion as it removes isomerized squalene. In fact, as reported by (Biedermann et al., 2020; Nestola, 2022), interfering olefins with a single double bond, or without a saturated carbon atom between double bonds, which is preferentially attacked during epoxidation (as it results in a stabilized radical), are unlikely to be removed in this way. Nevertheless, due to their molecular weight (they elute together with n -C₂₀), they were completely removed by deodorization (Figure 6.4).

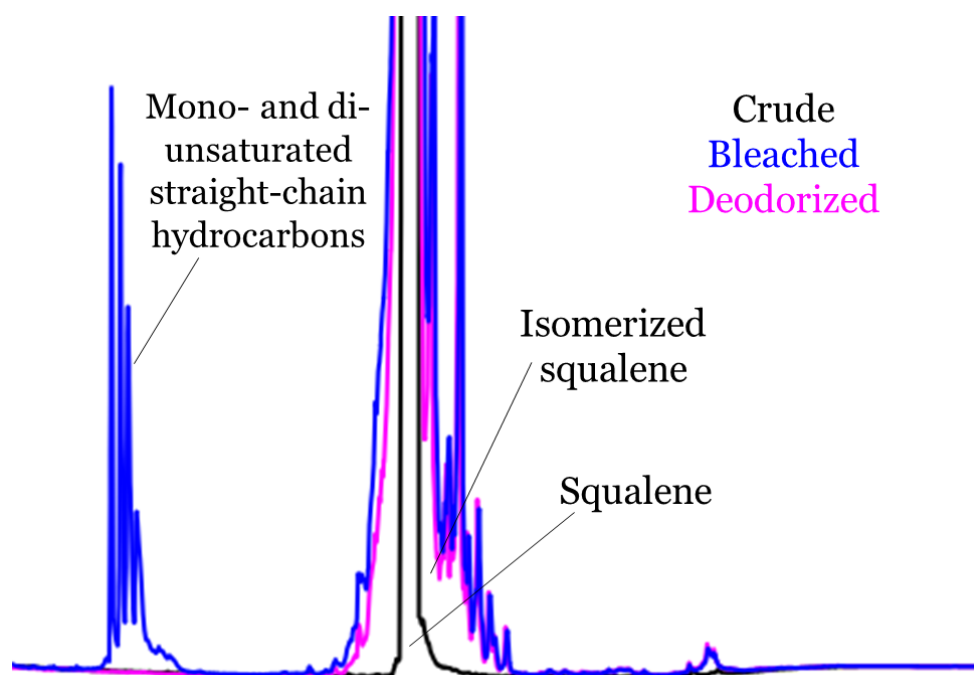


Figure 6.4. Overlay of chromatograms referring to the crude, bleached and deodorized lampante oil of the refining line LOO3, not subjected to epoxidation. Endogenous compounds, interfering with the MOAH fraction, are highlighted.

6.3.2 n -Alkane removal

To better evaluate the entity of the removal, endogenous n -alkanes were exploited. n -Alkanes in olive oils are distributed between n -C₂₁ and n -C₃₅, appear as single and resolved peaks above the mineral oil hump (when present), and are easy recognizable for

the prevalence of odd terms over even ones. Their concentration, as well as their relative ratio, is quite constant for a specific oil, constituting a sort of fingerprint that allows to distinguish it from other oils (Srbinovska et al., 2020). For this reason, they were quantified and then the average concentrations obtained from the steps prior to deodorization, where no variation was expected, were compared with the final concentration of the deodorized oil. Only odd *n*-alkanes were considered, being present at significantly higher concentrations and therefore less influenced by possibly co-eluting signals. This allowed us to verify the impact of deodorization, in the range of interest, for hydrocarbons with a difference in boiling point equal to two carbon atoms. To evaluate whether *n*-alkanes concentration in the refined oil were significantly different from the average value of *n*-alkanes in the previous steps, a t-test (significance level $\alpha=0.05$) was performed. Example of quantifications, for some specific samples, are provided in Table 6.4, where significant variations due to deodorization are highlighted in blue. This evaluation was performed on *n*-alkanes, rather than on the C-fractions related to mineral oil contamination, as variability due to the integration of the chromatogram was significantly lower for isolated peaks. In fact, the variability due to the integration of the C-fractions translated into significant differences also in the *n*-C₄₀₋₅₀ fraction, which is certainly not affected by deodorization.

Table 6.4. Concentrations of endogenous *n*-alkanes in the different steps of the refining process for some selected samples. Significantly different concentrations due to deodorization, with respect to data from the previous steps, are highlighted in blue.

Sample	Refining step	<i>n</i> -alkanes (mg/kg)							
		<i>n</i> -C ₂₁	<i>n</i> -C ₂₃	<i>n</i> -C ₂₅	<i>n</i> -C ₂₇	<i>n</i> -C ₂₉	<i>n</i> -C ₃₁	<i>n</i> -C ₃₃	<i>n</i> -C ₃₅
LOO1	Crude	0.41	5.9	22.2	37.4	21.6	10.4	4.8	1.1
	Neutralized	0.41	5.9	22.3	37.7	21.9	10.7	5.0	1.2
	Bleached	0.42	6.1	22.9	38.7	22.5	10.9	5.0	1.2
	Deodorized	-	0.37	6.0	20.6	17.1	9.9	4.9	1.2
LOO2	Crude	1.1	6.7	16.9	23.8	11.3	5.0	2.4	0.6
	Deacidified	0.03	1.3	9.2	18.4	10.3	5.0	2.5	0.7
	Neutralized	0.09	2.6	11.2	21.3	12.8	7.2	3.4	0.9
	Bleached	0.08	1.9	9.9	19.6	11.2	5.7	2.8	0.8
	Deodorized	-	0.08	2.2	9.6	7.9	4.7	2.5	0.7
LOO5	Crude	0.26	1.4	3.4	5.2	5.7	4.1	1.9	0.5
	Bleached	0.26	1.3	3.2	5.1	5.6	4.0	1.9	0.5
	Deodorized	0.18	1.2	3.3	5.0	5.4	3.9	1.8	0.5
OPO1	Crude	1.12	18.1	25.6	38.7	19.0	13.8	5.9	1.3
	Bleached	1.12	17.9	24.7	36.2	18.3	12.6	5.3	1.1
	Deodorized	-	3.4	13.2	28.2	16.1	12.5	5.4	1.2

In Table 6.5, percentage removals for each *n*-alkane are reported, always calculated as the ratio between the concentration in the finished oil and the average of those of the previous steps. According to data in this table, samples from the first refining plant (LOO1-4) reported a significant removal of *n*-alkanes up to *n*-C₃₃ (LOO4) even though, for the other 3 samples, *n*-alkane removal was reported up to *n*-C₃₁. However, the decrease of these *n*-alkanes, which delimit the boundary between removal and non-removal, was on average around 10%. Regardless of the little differences, for almost all these samples the extent of *n*-alkanes removal was higher than 90% only for the lighter *n*-C₂₁ (removed completely, or nearly so) and *n*-C₂₃, and dropped to about 50% when moving towards *n*-C₂₇. At *n*-C₂₅, the removal was still on average around 80%. All this is in line with what was verified for mineral oil contamination, for which the removal occurred up to the C-fraction *n*-C₂₅₋₃₅, but was significant below *n*-C₂₅. LOO2, which underwent a previous deacidification step by distillation, reported a partial *n*-alkane reduction already at this point, even though to a lesser extent probably due to the rapidity of the process. However, there was no evidence of increased removal of *n*-alkane in the finished oil due to this additional step if compared to all other oils considered. For this sample, an unjustified increase of the *n*-alkanes content in the neutralized and bleached oils, with respect to the expected concentration based on that of the crude and deacidified oils, was highlighted (both are marked in red in Table 6.4). This could somehow confirm the possible cross-contamination hypothesized in the previous paragraph for this sample.

Except for small deviations, a similar decreasing trend after the deodorization step was found for samples LOO6 and OPO2 from the other refining plant. Sample OPO2 reported a slightly higher removal than all the other oils, perhaps due to a significantly longer treatment time (5 h versus 3 h) (although not appreciable for MOH contamination). Despite the additional distillation step at 245 °C before deodorization, LOO6 did not show higher *n*-alkane removal. Probably, this distillation step was too short to have a significant impact on volatiles removal, with respect to the deodorization step. For OPO1, even though it was treated under similar processing conditions with respect to all the other samples, *n*-alkane removal was inexplicably lower, as for MOH. Instead, interesting was sample LOO5, since it was the only one deviating from the standard operating conditions, as it was deodorized at a significantly lower temperature than the other oils (180 °C), and for which it was not possible to assess the impact on mineral oil contamination due to the presence of an additional contamination. For this sample, only *n*-alkane *n*-C₂₁ could be partially removed under these conditions, still remaining for 70%. However, if the MOH

contamination was caused by mixing this sample with another oil, the presence of the lighter *n*-alkanes could also be due to this occurrence.

Thus, according to these data, *n*-alkane removal resulted to be quite constant for small variations in processing conditions. For deodorization processes that take place at 220 ± 10 °C, removal can still be considered quite significant for *n*-alkanes up to *n*-C₂₉ (25%), while those up to *n*-C₂₃ are almost completely removed. Only the duration of the process can slightly improve *n*-alkanes removal. On the other hand, already 40 °C below this temperature, thus for contaminations mainly distributed beyond *n*-C₂₁, as those typically encountered in this food matrix (Menegoz Ursol et al., 2022; Menegoz et al., 2023), *n*-alkanes removal determined by the refining process becomes irrelevant.

Table 6.5. Percentage removal of *n*-alkanes which underwent a significant change in deodorization. Where the removal was not significant, a dash is present.

Sample	<i>n</i> -alkanes removal (%)						
	<i>n</i> -C ₂₁	<i>n</i> -C ₂₃	<i>n</i> -C ₂₅	<i>n</i> -C ₂₇	<i>n</i> -C ₂₉	<i>n</i> -C ₃₁	<i>n</i> -C ₃₃
LOO1	100.0	93.8	73.5	45.6	22.1	7.4	-
LOO2	100.0	98.8	87.1	59.7	30.2	6.3	-
LOO3	98.5	96.1	78.5	50.9	27.2	12.5	-
LOO4	96.3	93.8	75.5	49.6	28.8	16.0	9.3
LOO5	31.1	-	-	-	-	-	-
LOO6	100.0	100.0	82.7	49.2	21.8	5.7	-
OPO1	98.4	82.5	51.3	29.6	17.4	-	-
OPO2	100.0	99.6	91.1	63.9	38.0	20.9	-

6.3.3 Evaluation of the MOAH fraction by GC×GC

Sample COPO2, and the related oils in the subsequent steps of refining, was selected to be subjected to qualitative evaluation by GC×GC-MS. This sample was chosen because in its HPLC-GC-FID chromatogram (as in that of some other oils) was present, in addition to the classic MOAH hump (dotted yellow box in Figure 6.5A), a series of peaks, over a background made up of unresolved signals (dotted red box in Figure 6.5A), for which we attempted an identification.

Although the cloud referring to MOAH was just slightly visible in the total ion chromatogram (TIC) background, probably due to the reduced injection volume and the difference in signal intensity compared to other isolated peaks, the selected ion chromatogram (SIC), for mass-to-charge ratio (*m/z*) of 119, typical of alkylated monoaromatic compounds (Albert et al., 2022), together with its position within the 2D plot, confirmed their presence (Figure 6.5B”). Furthermore, its position in the upper part of the plot, in line with the retention time in the second dimension of the internal standard

TBB (rather alkylated mono-aromatic compound), together with a strong retention in the first dimension, suggested that the contamination included heavily alkylated compounds (also the presence of polyaromatic species could not be excluded a priori), less relevant from the toxicological point of view (Carrillo et al., 2022a).

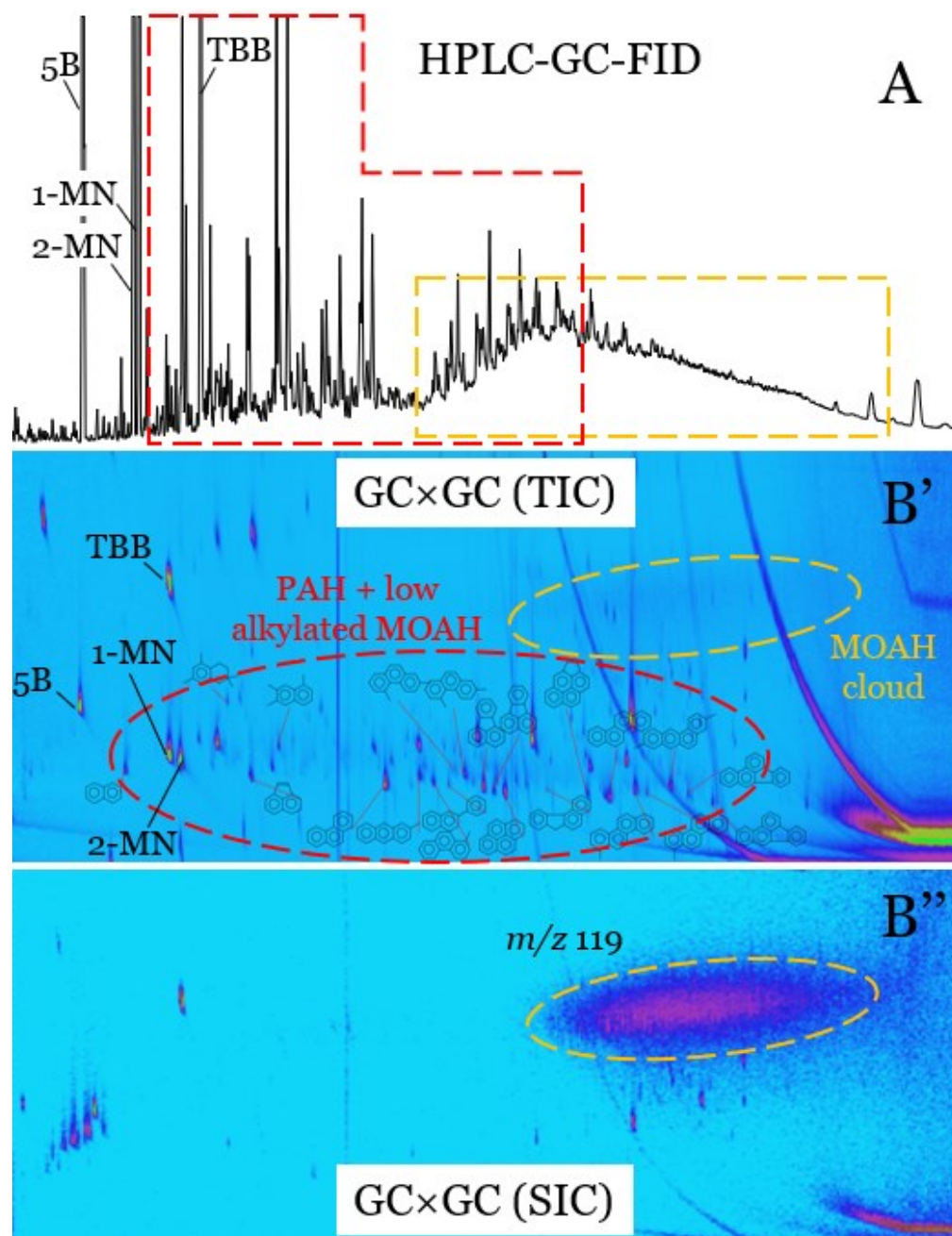


Figure 6.5. HPLC-GC-FID chromatogram of crude pomace oil COPO₂, where the MOAH hump and the series of unresolved peaks and signals for which an identification was attempted are boxed in yellow and red respectively (A). PAH and low alkylated MOAH are encircled in red in the GCxGC plot, while highly alkylated MOAH are encircled in yellow (B). The latter, always encircled in yellow, are better highlighted in the SIC plot (B'').

On the other hand, dozens of isolated spots were present in the lower part of the plot (rather low retention time in the second dimension), distributed over a wide range of

retention times in the first dimension, suggesting that they were relatively polar compounds characterized by a quite wide range of molecular weights (dotted red circle in Figure 6.5B'). Indeed, while some of them were eluted around or just after 1-MN and 2-MN in the first dimension, others also overlapped the highly alkylated MOAH cloud. MS identified such peaks as light and heavy PAH, e.g. naphthalene, pyrene, chrysene, phenanthrene, benzo[b]fluoranthene etc., as well as low alkylated MOAH (methyl substituted) with a similar aromatic core to PAH, having from two to five aromatic rings. These compounds are of high concern due to their genotoxic, mutagenic and carcinogenic character, and are not new for this matrix (Grob, 2018a; Bertoz et al., 2021). Although the GC column used for HPLC-GC-FID and the first dimension of GC×GC had different polarity, elution was primarily governed by the boiling point of the compounds. Therefore, in theory, there could be a reasonable consistency, in terms of the relative position of the different analytes eluted from the two different GC columns. This, for example, was already experienced before also by (Biedermann et al., 2020), using a similar instrumental setup. For this reason, although it is known that peaks of components related to interferents present in the peracid (Nestola, 2022), as well as side products of the epoxidation, also elute in this area of the LC-GC (dotted red box of Figure 6.5A), it cannot be completely ruled out that part of them could relate to the classes of compounds identified.

Fortunately, as visible in Figure 6.6 within the area highlighted by the red dotted circle, correspondent to that in the previous figure, most of these highly toxic compounds were removed or significantly reduced during bleaching. Although in this specific case aromatics had a limited number of rings (1-4) and a low degree of alkylation, removal affected PAH and low alkylated MOAH indiscriminately, regardless of the number of rings, the number of alkylations or their configuration. As highlighted in the literature, activated carbon, which is used in the bleaching step to remove compounds that give color to the oil (Morchio, 2022), is also capable of adsorbing these aromatic compounds. This feature was already verified for the decontamination of vegetable oils from PAH (Gong et al., 2007; Ma et al., 2017), but no reference was ever made to little alkylated MOAH with 3 and more benzene rings, whose decrease cannot be appreciated when analyzing total MOAH (due to the large predominance of the mono- and diaromatic compounds).

In addition, from the GC×GC-MS plot of Figure 6.6, it was possible to confirm the presence of mono- or di-unsaturated straight-chain hydrocarbons forming clustered peaks (already identified before, based on the literature, and shown in Figure 6.4). Artifacts, or external interferences identified as amides (palmitamide, erucamide and

oleamide), already highlighted in one of our previous work, were also present (Menegoz et al. 2023).

Finally, although the bleaching had already removed a large part of these compounds, the residual ones, with the highest degree of volatility, were further stripped away during deodorization (not shown).

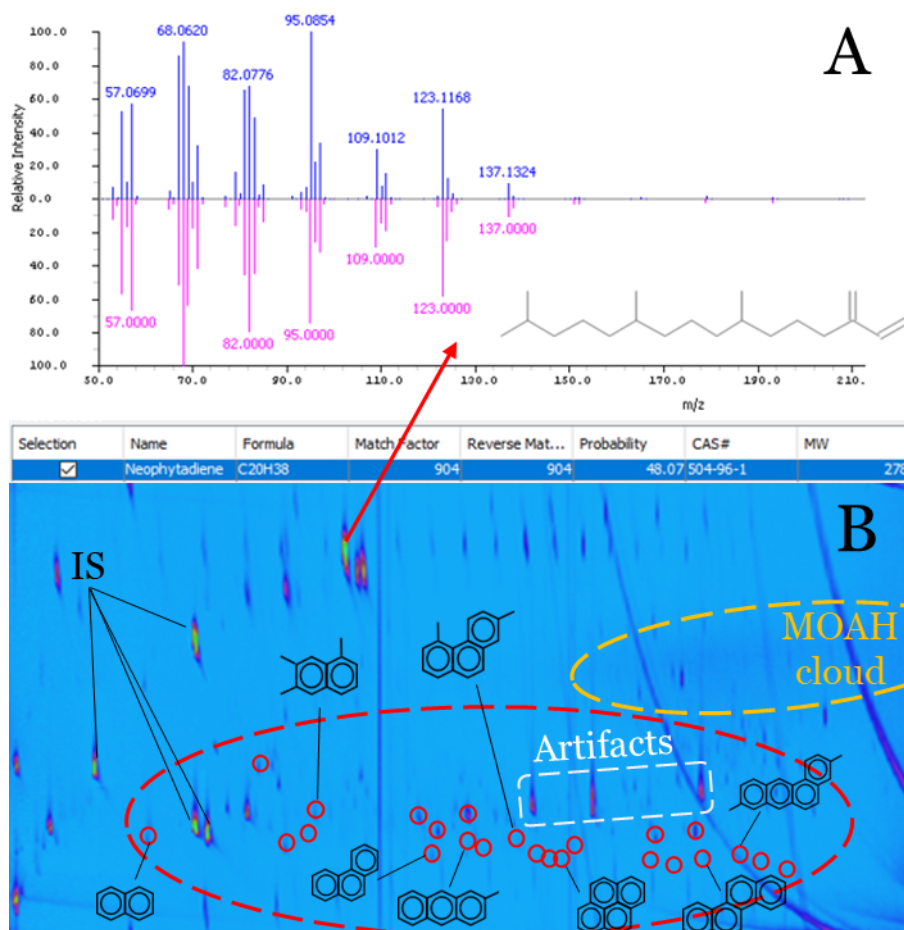


Figure 6.6. (B) shows the GC×GC plot of olive pomace oil COPO2 after bleaching. Most of the signals referable to low alkylated MOAH and PAH, previously present in the area inside the dotted red circle, were removed or reduced in concentration, Their position is highlighted by small red circles. Location of the MOAH cloud, as well as the presence of amides, justified as artifacts or interferences, are highlighted. In (A), MS spectra related to the identification of neophytadiene.

6.3.4 Refined olive oils and refined olive pomace oils from the market

Five refined olive oils (sample codes OO1-5) and 3 refined olive pomace oils (sample codes OPO1-3) were purchased from the market and analyzed. Quantification of total hump, as well of each C-fraction, are provided in Table 6.6. Although concentrations below the LOQ for the C-fractions have been reported in the table, the quantification in the range n -C₁₀₋₅₀ was obtained by integrating the whole hump, in agreement with the latest SCoPAFF summary report, which laid the foundations for the removal of C-fractions (EC, 2022).

Table 6.6. MOSH and MOAH data of olive oils and olive pomace oils from the market. Dash indicates that no signal was detectable.

Sample code	MOSH (mg/kg)						MOAH (mg/kg)					
	<i>n</i> -C ₁₀₋₁₆	<i>n</i> -C ₁₆₋₂₀	<i>n</i> -C ₂₀₋₂₅	<i>n</i> -C ₂₅₋₃₅	<i>n</i> -C ₃₅₋₄₀	<i>n</i> -C ₄₀₋₅₀	<i>n</i> -C ₁₀₋₅₀	<i>n</i> -C ₁₀₋₁₆	<i>n</i> -C ₁₆₋₂₅	<i>n</i> -C ₂₅₋₃₅	<i>n</i> -C ₃₅₋₄₀	<i>n</i> -C ₁₀₋₅₀
OO1	-	-	0.86	14.6	6.8	4.9	27.1	-	<LOQ	1.6	1.5	3.2
OO2	-	-	1.4	33.2	27.7	25.2	87.5	-	<LOQ	1.2	1.3	2.6
OO3	-	<LOQ	0.78	7.9	3.3	2.9	15.1	-	<LOQ	1.7	1.9	3.6
OO4	-	-	1.1	14.1	5.3	3.7	24.2	-	0.29	3.4	2.9	6.6
OO5	-	-	<LOQ	11.8	5.2	4.1	21.5	-	<LOQ	2.0	2.2	4.3
OPO1	-	-	4.9	78.0	31.7	23.9	138.6	-	3.0	20.8	20.4	44.2
OPO2	-	-	12.1	112.9	42.6	30.9	198.6	-	5.4	29.6	32.4	67.4
OPO3	-	-	19.1	156.5	41.4	29.9	246.8	-	7.1	30.5	27.6	65.2

The effect of the deodorization process on these oils was immediately noticeable based on the complete absence of the *n*-C₁₀₋₁₆ and *n*-C₁₆₋₂₀ fractions, removed during this step both for OOs and OPOs. Moreover, the low average percentage of the *n*-C₂₀₋₂₅ fraction for OOs (with respect to the total contamination in the *n*-C₁₀₋₅₀ range), which was around 3%, was perfectly aligned with that of the refined oil samples involved in this study (this comparison was also valid among pomace oils, even if the number of samples was undoubtedly more limited), and clearly differed from that calculated on the EVOO samples from the Italian market reported in the previous chapter (on average around 10%). OOs and OPOs from the market also had a similar distribution of the contaminations with respect to that of the oils considered in this study, mainly centered between *n*-C₂₉ and *n*-C₃₁, typical of lubricating oils (again like EVOOs). Only OO2 oil was centered on slightly heavier molecular weights (*n*-C₃₅), more common for greases, but was something already seen previously also for EVOOs (Menegoz Ursol et al., 2023). Although part of the contamination was surely stripped away, none of the olive oils reported MOSH data below the 13 mg/kg proposed as benchmark level (LAV & BLL, 2022), as well as MOAH data that fulfilled the legal limit of 2 mg/kg (EC, 2022).

Total concentrations of MOSH in OPOs were 10 times higher than those of OOs, and were distributed over a wide range (138.6-246.8 mg/kg), exactly as for data available from the literature (Gómez-Coca et al., 2016b; Zoccali et al., 2016; Ruiz et al., 2021), with a MOAH percentage between 21% and 25%. OOs had instead MOSH generally distributed between 15.1 and 27.1 mg/kg, with only one exception at 87.5 mg/kg which, however, had the lowest MOAH concentration (sample OO2). It cannot be excluded that this additional contamination was already present in the crude oil as result of processing from harvesting

to bottling, rather than due to a criticality during the refining. However, since this oil was packed in an aluminium can and the MOAH contamination was less than 3%, a contamination from a food grade lubricant used during the production of the container cannot be excluded. Anyway, the mean concentration of MOSH and MOAH in the olive oils, in the range $n\text{-C}_{10-35}$, was 17.2 and 2.1 mg/kg respectively, in perfect alignment with data reported by Luisi (2019) related to 97 olive oils considering the same range of molecular weights, having an average concentration of 16.2 mg/kg and 2.3 mg/kg for MOSH and MOAH. The average $n\text{-C}_{10-35}$ MOSH and MOAH content of EVOOs from the market (reported in the previous chapter of this thesis), which until oil extraction share the supply chain with OOs, were also aligned with the latter, with concentrations of 12.7 and 2.3 mg/kg, respectively. This provided an indication that the refining process is not critical in terms contribution to the final contamination.

Instead, even considering the full range of molecular weights ($n\text{-C}_{10-50}$), the EVOOs taken from the vertical centrifuge at the mill plant (see previous chapter) reported significantly lower average values than those just mentioned (8.3 mg/kg of MOSH and 1.6 mg/kg of MOAH). Thus, considering that the refining process did not report significant criticality, it can therefore be assumed that the contribution of contamination can occur in steps like transportation and bottling. For this reason, as future developments, it would be important to investigate these steps and assess their impact on the overall contamination.

6.4 Conclusions

The impact of oil refining on LOOs and COPOs has been reported in this work for the first time. Refining has proven to be capable of lowering their levels of contamination by 10-30%. However, this assumption is applicable to contaminations that are in the typical range of lubricating oils (centered around $n\text{-C}_{29}$) as those found in this work, as for contaminations with a higher boiling point this percentage would certainly decrease. Nevertheless, since based on the studies previously reported in this thesis the contamination derives mainly from olive handling during the harvesting phase, it generally involves precisely this type of source. As further evidence, EVOOs, LOOs and COPOs constantly reported contaminations distributed over this common range of molecular weights.

To provide a precise indication of the molecular weights involved in the removal by distillation, n -alkanes up to $n\text{-C}_{27}$ were removed up to around 50% of their initial content, and this percentage dropped well below 20% when reaching $n\text{-C}_{31}$. This, when translated to mineral oil contamination, resulted in a removal around 90% for the $n\text{-C}_{10-25}$ fraction

and 40% when calculated on the n -C₁₀₋₃₅ fraction, which on the starting oils accounted for an average of 20% and 70% of the total concentration respectively. The behavior of MOAH was in line with that of MOSH, even if part of the data variability encountered was probably due to the presence of olefinic residues that disturbed the integration of the chromatograms.

Finally, perhaps even more important, bleaching, together with subsequent deodorization, seems to be able to remove, in addition to PAH, also 1-4 ring MOAH little alkylated, for which concern from a toxicological point of view is high. This preliminary result needs to be confirmed by further investigations.

CONCLUSIONS AND FUTURE PERSPECTIVES

This PhD project made it possible to provide support both to the scientific community, through the optimization and validation of highly sensitive methods for the analysis of both MOSH and MOAH, as well as to the agricultural and processing sector related to olive oils, by sharing useful information, coming from a comprehensive sampling along the entire supply chain, about its critical points and the sources of mineral oil contamination, to allow the implementation of minimization strategies.

The first part of the work involved the validation of a MAS protocol (enrichment) followed by epoxidation (olefins removal) for highly sensitive determination of MOAH in olive oils. The method reported optimal performance in terms of recovery, repeatability and LOQ (0.5 mg/kg on the total hump), fully in line with the requirements of the JRC guidance. Later on, also an Alox protocol targeting the MOSH fraction, for *n*-alkanes removal, was optimized reaching the same LOQ as for MOAH.

These methods were then used for the analysis of the samples from the monitoring, which represented the second part of the project. What emerged from the first focus on the harvesting phase is that oils obtained by olives directly hand-picked from the tree have in general background MOSH contamination, usually below 2.7 mg/kg, and MOAH below the LOQ (0.5 mg/kg), without clear correlation between the contamination level and the surrounding potential sources of environmental contamination. Also the impact of phytosanitary treatments appeared to be negligible. On the contrary, about 40% of the samples experienced an increase in MOH levels after the harvesting operations, whose origin has been traced back by qualitative assessment of contamination with HPLC-GC-FID and GC×GC-FID/MS to lubricants used in harvesting machinery. For these samples, MOSH and MOAH concentrations were on average 17.7 mg/kg and 5.1 mg/kg respectively. As a consequence, good maintenance of harvesting machinery/equipment is of fundamental importance in reducing the risk of contamination, even though for some machinery the contamination is the consequence of their construction characteristics. Nevertheless, before machinery start to be designed differently, at least refined/food grade lubricants should be used.

Another scenario has instead emerged in relation to the following operations, meaning olive transportation and milling, which was the third part of the work. Transportation, as well as handling at the mill, rarely represent a critical point. Contamination was sporadically introduced during the last steps of the supply chain (crushing, malaxation and centrifugation), with an incidence of 5 processing lines out of 22. Instead, olive washing did not reported any criticality, but indeed, if correctly implemented and made more efficient, it is able to significantly remove the contamination present on the surface

of the olives. Studies aimed at its optimization should therefore be taken into consideration.

Finally, the impact of oil refining on LOOs and COPOs concerned the last part of the work. Refining was not found to be critical in terms of MOH contribution, but rather the deodorization step helped to lower the initial levels of contamination (having a distribution typical of lubricants) by 10-30%, albeit with a greater impact on MOH below n -C₂₅ (90% removed). Nevertheless, the removal also concerned the following fraction (n -C₂₅₋₃₅). In particular, n -alkanes up to n -C₂₇ were removed up to around 50% of their initial content, and this percentage dropped below 20% when reaching n -C₃₁, which was generally considered the upper limit. The behavior of MOAH was in line with that of MOSH, even if more data variability was present due to olefinic residues requiring subjective interpretation of the chromatogram. Bleaching, together with the deodorization, were also able to remove PAH and low alkylated MOAH, which are of major concern from the toxicological point of view.

To summarize, the most critical step of the whole supply chain turned out to be the olive harvesting, even if the use of lubricants also in the other following processes (extraction and refining of olive oil) can always be a potential source of contamination, as demonstrated in some sporadic cases. Refining can partially reduce the contamination. However, the average concentrations of MOH were found to be higher for the EVOOs and OOs sampled from the market (EVOOs: 19.4 mg/kg of MOSH and 3.4 mg/kg of MOAH; OOs: 35.1 mg/kg of MOSH and 4.1 mg/kg of MOAH), compared to those found in the oils sampled at the outlet of the vertical centrifuge directly at the mill (8.6 mg/kg of MOSH and 1.7 mg/kg of MOAH). This suggests that part of the contamination found in the finished oils may concern other phases prior to marketing, such as storage, filtration and bottling. For this reason, future studies should also be extended to these final steps of the supply chain, to evaluate their impact on the overall contamination.

REFERENCES

- Ab Razak, N. A., Mohd Hanafi, M. H., Razak, N. H., Ibrahim, A., & Omar, A. A. (2021). Effective Polycyclic Aromatic Hydrocarbons Removal from Waste Cooking Oils: The Best Evidence Review. *Chemical Engineering Transaction*, 89, 475-480. <https://doi.org/10.3303/CET2189080>
- AFSCA (2017). *Advice 19-2017 action thresholds for mineral oil hydrocarbons in food*.
- Albert, C., Humpf, H. U., & Brühl, L. (2022). Determining MOSH and MOAH with High Sensitivity in Vegetable Oil A New, Reliable, and Comparable Approach Using Online LC-GC-FID Evaluation of Method Precision Data. *Journal of Agricultural and Food Chemistry*, 70, 10337-10348. <https://doi.org/10.1021/acs.jafc.2c01189>
- Baccioni, L., & Peri, C. (2014). Centrifugal separation. in Peri, C. (2014), *The Extra-Virgin Olive Oil Handbook* (pp. 139-153). Wiley Blackwell.
- Barp, L., Biedermann, M., Grob, K., Blas-Y-Estrada, F., Nygaard, U. C., Alexander, J., & Cravedi, J. (2017a). Accumulation of mineral oil saturated hydrocarbons (MOSH) in female Fischer 344 rats: Comparison with human data and consequences for risk assessment. *Science of the Total Environment*, 575, 1263-1278. <https://doi.org/10.1016/j.scitotenv.2016.09.203>
- Barp, L., Biedermann, M., Grob, K., Blas-y-estrada, F., Nygaard, U. C., Alexander, J., & Cravedi, J. (2017b). Mineral oil saturated hydrocarbons (MOSH) in female Fischer 344 rats; accumulation of wax components; implications for risk assessment. *Science of the Total Environment*, 583, 319-333. <https://doi.org/10.1016/j.scitotenv.2017.01.071>
- Barp, L., Kornauth, C., Wuerger, T., Rudas, M., Biedermann, M., Reiner, A., Concin, N., & Grob, K. (2014). Mineral oil in human tissues, Part I: Concentrations and molecular mass distributions. *Food and Chemical Toxicology*, 72, 312-321. <https://doi.org/10.1016/j.fct.2014.04.029>
- Bauwens, G., Barp, L., & Purcaro, G. (2023). Validation of the liquid chromatography-comprehensive multidimensional gas chromatography-time-of-flight mass spectrometer/flame ionization detector platform for mineral oil analysis exploiting interlaboratory comparison data. *Green Analytical Chemistry*, 4, 100047. <https://doi.org/10.1016/j.greeac.2022.100047>
- Bauwens, G., Conchione, C., Sdrigotti, N., Moret, S., & Purcaro, G. (2022). Quantification

- and characterization of mineral oil in fish feed by liquid chromatography-gas chromatography-flame ionization detector and liquid chromatography-comprehensive multidimensional gas chromatography-time-of-flight mass spectrometer/flame ionization detector. *Journal of Chromatography A*, 1677, 463208. <https://doi.org/10.1016/j.chroma.2022.463208>
- Bauwens, G., Pantó, S., & Purcaro, G. (2021). Mineral oil saturated and aromatic hydrocarbons quantification: Mono- and two-dimensional approaches. *Journal of Chromatography A*, 1643, 462044. <https://doi.org/10.1016/j.chroma.2021.462044>
- Bertoz, V., Purcaro, G., Conchione, C., & Moret, S. (2021). A review on the occurrence and analytical determination of PAHs in olive oils. *Foods*, 10(2), 324. <https://doi.org/10.3390/foods10020324>
- BfR (2011). 7. Sitzung der BfR-Kommission für Bedarfsgegenstände. *Protokoll vom 14 April 2011*.
- BfR (2012a). 10. Sitzung der BfR-Kommission für Bedarfsgegenstände. *Protokoll vom 29 November 2012*.
- BfR (2012b). *Determination of hydrocarbons from mineral oil (MOSH & MOAH) or plastics (POSH & PAO) in packaging materials and dry foodstuffs by solid phase extraction and GC-FID*.
- BfR (2021). 27. Sitzung der BfR Kommission für Bedarfsgegenstände. *Protokoll vom 10 November 2021*.
- Bianchi, G., Murelli, C., & Vlahov, G. (1992a). Surface waxes from olive fruits. *Phytochemistry*, 31(10), 3503–3506. [https://doi.org/10.1016/0031-9422\(92\)83716-C](https://doi.org/10.1016/0031-9422(92)83716-C)
- Bianchi, G., Vlahov, G., Anglani, C., & Murelli, C. (1992b). Epicuticular wax of olive leaves. *Phytochemistry*, 32(1), 49-52. [https://doi.org/10.1016/0031-9422\(92\)80104-M](https://doi.org/10.1016/0031-9422(92)80104-M)
- Biedermann-Brem, S., Kasprick, N., Simat, T., & Grob, K. (2012). Migration of polyolefin oligomeric saturated hydrocarbons (POSH) into food. *Food Additives & Contaminants: Part A*, 29(3), 449–460. <https://doi.org/10.1080/19440049.2011.641164>
- Biedermann, M., Barp, L., Kornauth, C., Würger, T., Rudas, M., Reiner, A., Concin, N., & Grob, K. (2015). Mineral oil in human tissues, Part II: Characterization of the

- accumulated hydrocarbons by comprehensive two-dimensional gas chromatography. *Science of the Total Environment*, 506–507, 644–655. <https://doi.org/10.1016/j.scitotenv.2014.07.038>
- Biedermann, M., Fiselier, K., & Grob, K. (2009). Aromatic hydrocarbons of mineral oil origin in foods: method for determining the total concentration and first result. *Journal of Agricultural and Food Chemistry*, 57(19), 8711–8721. <https://doi.org/10.1021/jf901375e>
- Biedermann, M., & Grob, K. (2009a). Comprehensive two-dimensional GC after HPLC pre-separation for the characterization of aromatic hydrocarbons of mineral oil origin in contaminated sunflower oil. *Journal of Separation Science*, 32(21), 3726–3737. <https://doi.org/10.1002/jssc.200900366>
- Biedermann, M., & Grob, K. (2009b). How “white” was the mineral oil in the contaminated Ukrainian sunflower oils? *European Journal of Lipid Science and Technology*, 111(4), 313–319. <https://doi.org/10.1002/ejlt.200900007>
- Biedermann, M., & Grob, K. (2009c). Memory effects with the on-column interface for on-line coupled high performance liquid chromatography-gas chromatography: The Y-interface. *Journal of Chromatography A*, 1216(49), 8652–8658. <https://doi.org/10.1016/j.chroma.2009.10.039>
- Biedermann, M., & Grob, K. (2010). Is recycled newspaper suitable for food contact materials? Technical grade mineral oils from printing inks. *European Food Research and Technology*, 230(5), 785–796. <https://doi.org/10.1007/s00217-010-1223-9>
- Biedermann, M., & Grob, K. (2012a). On-line coupled high performance liquid chromatography-gas chromatography for the analysis of contamination by mineral oil. Part 1: Method of analysis. *Journal of Chromatography A*, 1255, 56–75. <https://doi.org/10.1016/j.chroma.2012.05.095>
- Biedermann, M., & Grob, K. (2012b). On-line coupled high performance liquid chromatography-gas chromatography for the analysis of contamination by mineral oil. Part 2: Migration from paperboard into dry foods: Interpretation of chromatograms. *Journal of Chromatography A*, 1255, 76–99. <https://doi.org/10.1016/j.chroma.2012.05.096>
- Biedermann, M., & Grob, K. (2013). Programmed temperature vaporizing injector to filter

- off disturbing high boiling and involatile material for on-line high performance liquid chromatography gas chromatography with on-column transfer. *Journal of Chromatography A*, *1281*, 106–114. <https://doi.org/10.1016/j.chroma.2013.01.070>
- Biedermann, M., & Grob, K. (2015). Comprehensive two-dimensional gas chromatography for characterizing mineral oils in foods and distinguishing them from synthetic hydrocarbons. *Journal of Chromatography A*, *1375*, 146–153. <https://doi.org/10.1016/j.chroma.2014.11.064>
- Biedermann, M., & Grob, K. (2019). Advantages of comprehensive two-dimensional gas chromatography for comprehensive analysis of potential migrants from food contact materials. *Analytica Chimica Acta*, *1057*, 11–17. <https://doi.org/10.1016/j.aca.2018.10.046>
- Biedermann, M., McCombie, G., Grob, K., Kappenstein, O., Hutzler, C., Pfaff, K., & Luch, A. (2017a). FID or MS for mineral oil analysis? *Journal of Consumer Protection and Food Safety*, *12*(1255), 363–365. <https://doi.org/10.1007/s00003-017-1127-8>
- Biedermann, M., Munoz, C., & Grob, K. (2017b). Update of on-line coupled liquid chromatography – gas chromatography for the analysis of mineral oil hydrocarbons in foods and cosmetics. *Journal of Chromatography A*, *1521*, 140–149. <https://doi.org/10.1016/j.chroma.2017.09.028>
- Biedermann, M., Munoz, C., & Grob, K. (2020). Epoxidation for the analysis of the mineral oil aromatic hydrocarbons in food. An update. *Journal of Chromatography A*, *1624*, 461236. <https://doi.org/10.1016/j.chroma.2020.461236>
- BMEL (2017). *Twenty-Second Ordinance amending the Consumer Goods Ordinance*.
- BMEL (2020). *Twenty-Second Ordinance amending the Consumer Goods Ordinance*.
- Bognar, A. L., Paliyath, G., Rogers, L., & Kolattukudy, P. E. (1984). Biosynthesis of alkanes by particulate and solubilized enzyme preparations from pea leaves (*Pisum sativum*). *Archives of Biochemistry and Biophysics*, *235*(1), 8–17. [https://doi.org/10.1016/0003-9861\(84\)90249-2](https://doi.org/10.1016/0003-9861(84)90249-2)
- Bonvehí, J., & Ventura-Coll, F. (2014). Mineral oil paraffins in jute bags and cocoa butter. *Acta Alimentaria*, *43*(1), 40–52. <https://doi.org/10.1556/AAlim.43.2014.1.5>
- Boselli, E., Grob, K., & Lercker, G. (1999). Solvent Trapping during Large Volume Injection with an Early Vapor Exit. Part 3: The Main Cause of Volatile Component

- Loss during Partially Concurrent Evaporation. *Journal of Separation Science*, 22(6), 327–334. [https://doi.org/10.1002/\(SICI\)1521-4168\(19990601\)22:6<327::AID-JHRC327>3.0.CO;2-B](https://doi.org/10.1002/(SICI)1521-4168(19990601)22:6<327::AID-JHRC327>3.0.CO;2-B)
- Boselli, E., Grolimund, B., Grob, K., Lercker, G., & Amadò, R. (1998). Solvent Trapping during Large Volume Injection with an Early Vapor Exit, Part 1 : Description of the Flooding Process. *Journal of High Resolution Chromatography*, 21(6), 355–362. [https://doi.org/10.1002/\(SICI\)1521-4168\(19980601\)21:6<355::AID-JHR355>3.0.CO;2-B](https://doi.org/10.1002/(SICI)1521-4168(19980601)21:6<355::AID-JHR355>3.0.CO;2-B)
- Boskou, D. (2006a). Characteristics of the Olive Tree and Olive Fruit. in Boskou, D. (2006), *Olive Oil Chemistry and Technology* (2nd ed., pp. 13-19). AOCS Press.
- Boskou, D. (2006b). Storage and Packing. in Boskou, D. (2006), *Olive Oil Chemistry and Technology* (2nd ed., pp. 233-241). AOCS Press.
- Boswell, H. A., Edwards, M., & Tadeusz, G. (2020). Comparison of Thermal and Flow-Based Modulation in Comprehensive Two-Dimensional Gas Chromatography — Time-of-Flight Mass Spectrometry (GC×GC-TOFMS) for the Analysis of Base Oils. *Separations*, 7(4), 70. <https://doi.org/10.3390/separations7040070>
- Brandenberger, S., Mohr, M., Grob, K., & Neukom, H. P. (2005). Contribution of unburned lubricating oil and diesel fuel to particulate emission from passenger cars. *Atmospheric Environment*, 39(37), 6985–6994. <https://doi.org/10.1016/j.atmosenv.2005.07.042>
- Bratinova, S., & Hoekstra, E. (2019). Guidance on sampling, analysis and data reporting for the monitoring of mineral oil hydrocarbons in food and food contact materials, EUR 29666 EN. *Publications Office of the European Union*, JRC115694. <https://doi.org/10.2760/208879>
- Brühl, L. (2016). Occurrence, determination, and assessment of mineral oils in oilseeds and vegetable oils. *European Journal of Lipid Science and Technology*, 118(3), 361–372. <https://doi.org/10.1002/ejlt.201400528>
- Carrillo, J. C., Kamelia, L., Romanuka, J., Kral, O., Isola, A., Niemel, H., & Steneholm, A. (2022a). Comparison of PAC and MOAH for understanding the carcinogenic and developmental toxicity potential of mineral oils. *Regulatory Toxicology and Pharmacology*, 132, 105193. <https://doi.org/10.1016/j.yrtph.2022.105193>

- Carrillo, J. C., Shen, H., Momin, F., Kral, O., Schnieder, H., & Kühn, S. (2022b). GTL synthetic paraffin oil shows low liver and tissue retention compared to mineral oil. *Food and Chemical Toxicology*, *159*, 112701. <https://doi.org/10.1016/j.fct.2021.112701>
- Carro, N., Garcia, I., Ignacio, M. C., Llompart, M., Yebra, M. C., & Moureira, A. (2002). Microwave-assisted extraction and mild saponification for determination of organochlorine pesticides in oyster samples. *Analytical and Bioanalytical Chemistry*, *374*(3), 547–553. <https://doi.org/10.1007/s00216-002-1437-1>
- Castle, L., Kelly, M., & Gilbert, J. (1993). Migration of mineral hydrocarbons into foods. 2. Polystyrene, ABS, and waxed paperboard containers for dairy products. *Food Additives and Contaminants*, *10*(2), 167–174. <https://doi.org/10.1080/02652039309374140>
- CEN (2017). *Foodstuffs - Vegetable oils and foodstuff on basis of vegetable oils - Determination of mineral oil saturated hydrocarbons (MOSH) and mineral oil aromatic hydrocarbons (MOAH) with on-line HPLC-GC-FID analysis, EN 16995:2017.*
- CEN (2021). *Animal feeding stuffs: Methods of sampling and analysis - Determination of mineral oil saturated hydrocarbons (MOSH) and mineral oil aromatic hydrocarbons (MOAH) with on-line HPLC-GC-FID analysis, EN 17517:2021.*
- Cert, A., & Moreda, W. (1998). New method of stationary phase preparation for silver ion column chromatography: Application to the isolation of steroidal hydrocarbons in vegetable oils. *Journal of Chromatography A*, *823*(1–2), 291–297. [https://doi.org/10.1016/S0021-9673\(98\)00183-6](https://doi.org/10.1016/S0021-9673(98)00183-6)
- COI (2022). *Trade standard applying to olive oils and olive pomace oils. COI/T.15/NC No 3/Rev.18.*
- Concin, N., Hofstetter, G., Plattner, B., Tomovski, C., Fiselier, K., Gerritzen, K., Fessler, S., Windbichler, G., Zeimet, A., Ulmer, H., Siegl, H., Rieger, K., Concin, H., & Grob, K. (2008). Mineral oil paraffins in human body fat and milk. *Food and Chemical Toxicology*, *46*(2), 544–552. <https://doi.org/10.1016/j.fct.2007.08.036>
- Concin, N., Hofstetter, G., Plattner, B., Tomovski, C., Fiselier, K., Gerritzen, K., Semsroth, S., Zeimet, A. G., Marth, C., Siegl, H., Rieger, K., Ulmer, H., Concin, H., & Grob, K.

- (2011). Evidence for Cosmetics as a Source of Mineral Oil Contamination in Women. *Journal of Women's Health*, 20(11), 1713–1719. <https://doi.org/10.1089/jwh.2011.2829>
- Conte, L. (2020). On the presence of Mineral Oil Hydrocarbons (MOSH and MOAH) in edible fats and oils : a report from the SISSG related Workshop. *La Rivista Italiana Delle Sostanze Grasse*, XCVII, 9–16.
- Cravedi, J., Grob, K., Cecilie, U., & Alexander, J. (2017). Bioaccumulation and toxicity of mineral oil hydrocarbons in rats - specificity of different subclasses of a broad mixture relevant for human dietary exposures. *EFSA Supporting Publications*, 14(2), 1090E. <https://doi.org/10.2903/sp.efsa.2017.EN-1090>
- David, F., Hoffman, A., Sandra, P. (1999). Finding a needle in a haystack: the analysis of pesticides in complex matrices by automated on-line LC-CGC using a new modular system. *LC GC Europe*, 12(9), 50-558.
- De Koning, S., Janssen, H. G., Van Deursen, M., & Brinkman, U. A. T. (2004). Automated on-line comprehensive two-dimensional LC×GC and LC×GC–ToF MS: Instrument design and application to edible oil and fat analysis. *Journal of Separation Science*, 27(5–6), 397–409. <https://doi.org/10.1002/jssc.200301676>
- De Medina, V. S., Priego-Capote, F., & Luque de Castro, M. D. (2013). Comparison of saponification methods for characterization of the nonsaponifiable fraction of virgin olive oil. *European Journal of Lipid Science and Technology*, 115(11), 1325–1333. <https://doi.org/10.1002/ejlt.201300191>
- DGF (2021). *Application and definitions; Standard Method DGF-C-I 1 (08)*. German standard methods for examining fats, fat products, surfactants and related substances (2nd ed.).
- DGF (2021). *Apparatus; Standard Method DGF-C-I 2 (08)*. German standard methods for examining fats, fat products, surfactants and related substances (2nd ed.).
- DGF (2021). *Sample Preparation; Standard Method DGF-C-I 3 (08)*. German standard methods for examining fats, fat products, surfactants and related substances (2nd ed.).
- DGF (2021). *Procedures; Standard Method DGF-C-I 4 (08)*. German standard methods for examining fats, fat products, surfactants and related substances (2nd ed.).

- DGF (2021). *Sampling report and dispatch of samples; Standard Method DGF-C-I 5 (08)*. German standard methods for examining fats, fat products, surfactants and related substances (2nd ed.).
- Di Giovacchino, L. (2013). Technological Aspects. in Aparicio, R., & Harwood, J. (2013), *Handbook of Olive Oil Analysis and Properties* (2nd ed., pp. 57-96). Springer.
- Droz, C., & Grob, K. (1997). Determination of food contamination by mineral oil material from printed cardboard using on-line coupled LC-GC-FID. *European Food Research and Technology*, 205(3), 239–241. <https://doi.org/10.1007/s002170050158>
- Duhamel, C., Cardinael, P., Peulon-Agasse, V., Firor, R., Pascaud, L., Semard-Jousset, G., Giusti, P., & Livadaris, V. (2015). Comparison of cryogenic and differential flow (forward and reverse fill/flush) modulators and applications to the analysis of heavy petroleum cuts by high-temperature comprehensive gas chromatography. *Journal of Chromatography A*, 1387, 95–103. <https://doi.org/10.1016/j.chroma.2015.01.095>
- EC (1994). Commission Regulation (EC) No 656/95 of 28 March 1995 amending Regulation (EEC) No 2568/91 on the characteristics of olive oil and olive-residue oil and on the relevant methods of analysis and Council Regulation (EEC) No 2658/87 on the tariff and statistical nomenclature and on the Common Customs Tariff. *Official Journal of the European Communities*, L69/1.
- EC (2002). Regulation (EC) No 178/2002 of the European Parliament and of the Council of 28 January 2002 laying down the general principles and requirements of food law, establishing the European Food Safety Authority and laying down procedures in matters of food safety. *Official Journal of the European Communities*, L31/1.
- EC (2004). Regulation (EC) No 852/2004 of the European Parliament and of the Council of 29 April 2004 on the hygiene of foodstuffs. *Official Journal of the European Communities*, L139/1.
- EC (2007). Commission Regulation (EC) No 333/2007 of 28 March 2007 laying down the methods of sampling and analysis for the official control of the levels of lead, cadmium, mercury, inorganic tin, 3-MCPD and benzo(a)pyrene in foodstuffs. *Official Journal of the European Union*, L88/29.
- EC (2008). Commission Regulation (EC) No 889/2008 of 5 September 2008 laying down detailed rules for the implementation of Council Regulation (EC) No 834/2007 on

- organic production and labelling of organic products with regard to organic production, labelling and control. *Official Journal of the European Union*, L250/1.
- EC (2008). Regulation (EC) No 1333/2008 of the European Parliament and of the Council of 16 December 2008 on food additives. *Official Journal of the European Union*, L354/16.
- EC (2009). Regulation (EC) No 1107/2009 of the European Parliament and of the Council of 21 October 2009 concerning the placing of plant protection products on the market and repealing Council Directives 79/117/EEC and 91/414/EEC. *Official Journal of the European Union*, L309/1.
- EC (2009). Commission Regulation (EC) No. 1151/2009 of 27 November 2009 imposing special conditions governing the import of sunflower oil originating in or consigned from Ukraine due to contamination risks by mineral oil and repealing Decision 2008/433/EC. *Official Journal of the European Union*, L313/36.
- EC (2022). Draft joint statement of the Member States regarding the presence of Mineral Oil Aromatic Hydrocarbons (MOAH) in food, including food for infants and young children. *SCoPAFF Summary Report*, 21 April 2022.
- EEC (1966). Regulation No 136/66/EEC of the Council of 22 September 1966 on the establishment of a common organisation of the market in oils and fats. *Official Journal of the European Communities*, 3025/66, pp. 221-231.
- EEC (1991). Commission Regulation (EEC) No 2568/91 of 11 July 1991 on the characteristics of olive oil and olive-residue oil and on the relevant methods of analysis. *Official Journal of the European Communities*, L248/1.
- EFSA (2004). Opinion of the Scientific Panel on food additives, flavourings, processing aids and materials in contact with food (AFC) on mineral oils in jute and sisal bags. *EFSA Journal*, 162, 1–6. <https://doi.org/10.2903/j.efsa.2005.162>
- EFSA (2006). Opinion of the Scientific Panel on food additives , flavourings , processing aids and materials in contact with food (AFC) on a request related to a 13th list of substances for food contact materials. *EFSA Journal*, 4(12), 1–25. <https://doi.org/10.2903/j.efsa.2006.418>
- EFSA (2008). EFSA statement on the contamination of sunflower oil with mineral oil exported from Ukraine. *EFSA Journal*, 6(5), 1–3.

<https://doi.org/10.2903/j.efsa.2008.1049>

- EFSA (2009a). Scientific Opinion on the use of high viscosity white mineral oils as a food additive. *EFSA Journal*, 7(11), 1-39. <https://doi.org/10.2903/j.efsa.2009.1387>
- EFSA (2009b). Review of the criteria for acceptable previous cargoes for edible fats and oils. *EFSA Journal*, 7(5), 1-21. <https://doi.org/10.2903/j.efsa.2009.1110>
- EFSA (2011). Scientific Opinion on the evaluation of the substances currently on the list in the Annex to Commission Directive 96/3/EC as acceptable previous cargoes for edible fats and oils – Part I of III. *EFSA Journal*, 9(12), 1–61. <https://doi.org/10.2903/j.efsa.2011.2482>
- EFSA (2012a). Scientific Opinion on Mineral Oil Hydrocarbons in Food. *EFSA Journal*, 10(6), 1-185. <https://doi.org/10.2903/j.efsa.2012.2704>
- EFSA (2012b). Scientific Opinion on the evaluation of the substances currently on the list in the annex to Commission Directive 96/3/EC as acceptable previous cargoes for edible fats and oils – Part II of III. *EFSA Journal*, 10(5), 1–151. <https://doi.org/10.2903/j.efsa.2012.2703>
- EFSA (2012c). Scientific Opinion on the evaluation of the substances currently on the list in the annex to Commission Directive 96/3/EC as acceptable previous cargoes for edible fats and oils – Part III of III. *EFSA Journal*, 10(12), 1–82. <https://doi.org/10.2903/j.efsa.2012.2984>
- EFSA (2013). Scientific opinion on the safety assessment of medium viscosity white mineral oils with a kinematic viscosity between 8.5 – 11 mm²/s at 100 °C for the proposed uses as a food additive. *EFSA Journal*, 11(1), 1–21. <https://doi.org/10.2903/j.efsa.2013.3073>.
- EFSA (2019). Rapid risk assessment on the possible risk for public health due to the contamination of infant formula and follow-on formula by mineral oil aromatic hydrocarbons (MOAH). *EFSA Supporting Publications*, 16(11), 1-18. <https://doi.org/10.2903/sp.efsa.2019.en-1741>
- Eneh, O. C. (2011). A review on petroleum: Source, uses, processing, products and the environment. *Journal of Applied Sciences*, 11(12), 2084–2091. <https://doi.org/10.3923/jas.2011.2084.2091>

- EU (2011). Commission Regulation (EU) No 10/2011 of 14 January 2011 on plastic materials and articles intended to come into contact with food. *Official Journal of the European Union*, L12/1.
- EU (2011). Commission Implementing Regulation (EU) No 540/2011 of 25 May 2011 implementing Regulation (EC) No 1107/2009 of the European Parliament and of the Council as regards the list of approved active substances. *Official Journal of the European Union*, L153/1.
- EU (2011). Commission Regulation (EU) No 835/2011 of 19 August 2011 amending Regulation (EC) No 1881/2006 as regards maximum levels for polycyclic aromatic hydrocarbons in foodstuffs. *Official Journal of the European Union*, L215/4.
- EU (2012). Commission Regulation (EU) No 231/2012 of 9 March 2012 laying down specifications for food additives listed in Annexes II and III to Regulation (EC) No 1333/2008 of the European Parliament and of the Council. *Official Journal of the European Union*, L83/1.
- EU (2014). Commission Regulation (EU) No 579/2014 of 28 May 2014 granting derogation from certain provisions of Annex II to Regulation (EC) No 852/2004 of the European Parliament and of the Council as regards the transport of liquid oils and fats by sea. *Official Journal of the European Union*, L160/14.
- EU (2014). Commission implementing Regulation (EU) No 853/2014 of 5 August 2014 repealing Regulation (EC) No 1151/2009 imposing special conditions governing the import of sunflower oil originating in or consigned from Ukraine. *Official Journal of the European Union*, L233/25.
- EU (2015). Commission Regulation (EU) 2015/1608 of 24 September 2015 amending Annex IV to Regulation (EC) No 396/2005 of the European Parliament and of the Council as regards maximum residue levels for capric acid, paraffin oil (CAS 64742-46-7), paraffin oil (CAS 72623-86-0), paraffin oil (CAS 8042-47-5), paraffin oil (CAS 97862-82-3), lime sulphur and urea in or on certain products. *Official Journal of the European Union*, L249/14.
- EU (2017). Commission Recommendation (EU) 2017/84 of 16 January 2017 on the monitoring of mineral oil hydrocarbons in food and in materials and articles intended to come into contact with food. *Official Journal of the European Union*, L12/95.

- Famiani, F., & Gucci, R. (2011). Moderni modelli olivicoli. In *Collana divulgativa dell'Accademia (Vol. VII)*. Accademia Nazionale dell'Olio e dell'Olio.
- FAO & WHO (1981). Standard for olive oils and olive pomace oils. *Codex Alimentarius*, CXS 33-1981.
- FEDIOL (2014). *FEDIOL Code of Practice for the transport in bulk of oils into or within the European Union (Oils and fats which are to be (or likely to be) used for human consumption)*, Ref. 14COD152.
- FEDIOL (2018). *FEDIOL code of practice for the management of mineral oil hydrocarbons presence in vegetable oils and fats intended for food uses*, Ref. 14COD341Rev.1.
- Fiorini, D., Fiselier, K., Biedermann, M., Ballini, R., Coni, E., & Grob, K. (2008). Contamination of Grape Seed Oil with Mineral Oil Paraffins. *Journal of Agricultural and Food Chemistry*, 56(23), 11245–11250. <https://doi.org/10.1021/jf802244r>
- Fiorini, D., Paciaroni, A., Gigli, F., & Ballini, R. (2010). A versatile splitless injection GC-FID method for the determination of mineral oil paraffins in vegetable oils and dried fruit. *Food Control*, 21(8), 1155–1160. <https://doi.org/10.1016/j.foodcont.2010.01.011>
- Firestone, D. (2005). Olive oil. in Shahidi, F. (2005), *Bailey's Industrial Oil and Fat Products* (6th ed., pp. 2:303-331). Wiley-Interscience.
- Fiselier, K., Fiorini, D., & Grob, K. (2009a). Activated aluminum oxide selectively retaining long chain *n*-alkanes. Part I, description of the retention properties. *Analytica Chimica Acta*, 634(1), 96–101. <https://doi.org/10.1016/j.aca.2008.12.007>
- Fiselier, K., Fiorini, D., & Grob, K. (2009b). Activated aluminum oxide selectively retaining long chain *n*-alkanes: Part II. Integration into an on-line high performance liquid chromatography-liquid chromatography-gas chromatography-flame ionization detection method to remove plant paraffins for the determination of mineral paraffins in foods and environmental samples. *Analytica Chimica Acta*, 634(1), 102–109. <https://doi.org/10.1016/j.aca.2008.12.011>
- Fiselier, K., & Grob, K. (2009). Determination of mineral oil paraffins in foods by on-line HPLC-GC-FID: Lowered detection limit; contamination of sunflower seeds and oils. *European Food Research and Technology*, 229(4), 679–688.

<https://doi.org/10.1007/s00217-009-1099-8>

- Fiselier, K., Grundböck, F., Schön, K., Kappenstein, O., Pfaff, K., Hutzler, C., Luch, A., & Grob, K. (2013). Development of a manual method for the determination of mineral oil in foods and paperboard. *Journal of Chromatography A*, *1271*(1), 192–200. <https://doi.org/10.1016/j.chroma.2012.11.034>
- Fuchs, B., Süß, R., Teuber, K., Eibisch, M., & Schiller, J. (2011). Lipid analysis by thin-layer chromatography — A review of the current state. *Journal of Chromatography A*, *1218*(19), 2754–2774. <https://doi.org/10.1016/j.chroma.2010.11.066>
- Fujita, H., Honda, K., Hamada, N., Yasunaga, G., & Fujise, Y. (2009). Chemosphere Validation of high-throughput measurement system with microwave-assisted extraction , fully automated sample preparation device , and gas chromatography-electron capture detector for determination of polychlorinated biphenyls in whale blubber. *Chemosphere*, *74*(8), 1069–1078. <https://doi.org/10.1016/j.chemosphere.2008.10.053>
- Gagni, S., & Cam, D. (2007). Stigmastane and hopanes as conserved biomarkers for estimating oil biodegradation in a former refinery plant-contaminated soil. *Chemosphere*, *67*(10), 1975–1981. <https://doi.org/10.1016/j.chemosphere.2006.11.062>
- Gharbi, I., Moret, S., Chaari, O., Issaoui, M., Conte, L. S., Lucci, P., & Hammami, M. (2017). Evaluation of hydrocarbon contaminants in olives and virgin olive oils from Tunisia. *Food Control*, *75*, 160–166. <https://doi.org/10.1016/j.foodcont.2016.12.003>
- Gómez-Coca, R. B., Cert, R., Pérez-Camino, M. C., & Moreda, W. (2016a). Determination of saturated aliphatic hydrocarbons in vegetable oils. *Grasas y Aceites*, *67*(2). <https://doi.org/10.3989/gya.0627152>
- Gómez-Coca, R. B., Pérez-Camino, M. C., & Moreda, W. (2016b). Saturated hydrocarbon content in olive fruits and crude olive pomace oils. *Food Additives and Contaminants*, *33*(3), 391–402. <https://doi.org/https://doi.org/10.1080/19440049.2015.1133934>
- Gong, Z., Alef, K., Wilke, B., & Li, P. (2007). Activated carbon adsorption of PAHs from vegetable oil used in soil remediation. *Journal of Hazardous Materials*, *143*(1-2), 372–378. <https://doi.org/10.1016/j.jhazmat.2006.09.037>

- Graham, S. F., Haughey, S. A., Ervin, R. M., Cancouët, E., Bell, S., & Elliot, C. T. (2012). The application of near-infrared (NIR) and Raman spectroscopy to detect adulteration of oil used in animal feed production. *Food Chemistry*, *132*(3), 1614–1619. <https://doi.org/10.1016/j.foodchem.2011.11.136>
- Griffis, L. C., Twerdok, L. E., Francke-carroll, S., Biles, R. W., Schroeder, R. E., Bolte, H., Faust, H., Hall, W. C., & Rojko, J. (2010). Comparative 90-day dietary study of paraffin wax in Fischer-344 and Sprague – Dawley rats. *Food and Chemical Toxicology*, *48*(1), 363–372. <https://doi.org/10.1016/j.fct.2009.10.024>
- Grob, K. (1987). *On-column Injection in Capillary Gas Chromatography: Basic Technique, Retention Gaps, Solvent Effects*. Huthig GmbH & Company.
- Grob, K. (1991). *On-line coupled LC-GC*. Huthig GmbH & Company.
- Grob, K. (2000). Efficiency through combining high-performance liquid chromatography and high resolution gas chromatography: Progress 1995-1999. *Journal of Chromatography A*, *892*(1–2), 407–420. [https://doi.org/10.1016/S0021-9673\(00\)00048-0](https://doi.org/10.1016/S0021-9673(00)00048-0)
- Grob, K. (2018a). Toxicological Assessment of Mineral Hydrocarbons in Foods: State of Present Discussions. *Journal of Agricultural and Food Chemistry*, *66*(27), 6968–6974. <https://doi.org/10.1021/acs.jafc.8b02225>
- Grob, K. (2018b). Mineral oil hydrocarbons in food - a review. *Food Additives & Contaminants: Part A*, *35*(9), 1845-1860. <https://doi.org/10.1080/19440049.2018.1488185>
- Grob, K., Artho, A., Biedermann, M., Caramaschi, A., & Mikle, H. (1992a). Batching Oils on Sisal Bags Used for Packaging Foods: Analysis by Coupled LC/GC. *Journal of AOAC INTERNATIONAL*, *75*(2), 283–287. <https://doi.org/10.1093/jaoac/75.2.283>
- Grob, K., Artho, A., Biedermann, M., & Egli, J. (1991a). Food contamination by hydrocarbons from lubricating oils and release agents: Determination by coupled LC-GC. *Food Additives and Contaminants*, *8*(4), 437–446. <https://doi.org/10.1080/02652039109373993>
- Grob, K., Artho, A., & Mariani, C. (1992b). Determination of Raffination of Edible Oils and Fats by Olefinic Degradation Products of Sterols and Squalene , Using Coupled LC-GC. *European Journal of Lipid Science and Technology*, *94*(10), 394–400.

- Grob, K., & Biedermann, M. (1996). Vaporising systems for large volume injection or on-line transfer into gas chromatography: Classification, critical remarks and suggestions. *750*(1-2), 11–23. [https://doi.org/10.1016/0021-9673\(96\)00345-7](https://doi.org/10.1016/0021-9673(96)00345-7)
- Grob, K., Biedermann, M., Artho, A., & Egli, J. (1991b). Food contamination by hydrocarbons from packaging materials determined by coupled LC-GC. *Zeitschrift Für Lebensmittel-Untersuchung Und Forschung*, *193*(3), 213–219. <https://doi.org/10.1007/BF01199968>
- Grob, K., & Bronz, M. (1995). On-line LC-GC transfer via a hot vaporizing chamber and vapor discharge by overflow; increased sensitivity for the determination of mineral oil in foods. *Journal of Microcolumn Separations*, *7*(4), 421–427. <https://doi.org/10.1002/mcs.1220070415>
- Grob, K., Huber, M., Boderius, U., & Bronz, M. (1997). Mineral oil material in canned foods. *Food Additives and Contaminants*, *14*(1), 83–88. <https://doi.org/10.1080/02652039709374500>
- Grob, K., Lanfranchi, M., Egli, J., & Artho, A. (1991c). Determination of food contamination by mineral oil from jute sacks using coupled LC-GC. *Journal - Association of Official Analytical Chemists*, *74*(3), 506–512. <https://doi.org/10.1093/jaoac/74.3.506>
- Grob, K., Vass, M., Biedermann, M., & Neukom, H. (2001). Contamination of animal feed and food from animal origin with mineral oil hydrocarbons. *Food Additives & Contaminants*, *18*(1), 1–10. <https://doi.org/10.1080/02652030010000350>
- Grolimund, B., Boselli, E., Grob, K., & Lercker, G. (1998). Solvent Trapping during Large Volume Injection with an Early Vapor Exit, Part 2: Chromatographic Results and Conclusions. *Journal of High Resolution Chromatography*, *21*(7), 378–382.
- Grundböck, F., Fiselier, K., Schmid, F., & Grob, K. (2010). Mineral oil in sunflower seeds: The sources. *European Food Research and Technology*, *231*(2), 209–213. <https://doi.org/10.1007/s00217-010-1264-0>
- Guinda, A., Lanzón, A., & Albi, T. (1996). Differences in hydrocarbons of virgin olive oils obtained from several olive varieties. *Journal of Agricultural and Food Chemistry*, *44*(7), 1723–1726. <https://doi.org/10.1021/jf9505710>
- Helmy, E. I., Kwaiz, F. A., & El-Sahn, O. M. N. (2012). The usage of mineral oils to control

- insects. *Egyptian Academic Journal of Biological Sciences*, 5(3), 167–174.
<https://doi.org/10.21608/eajbsa.2012.14277>
- Henry, J. A. (1998). Composition and toxicity of petroleum products and their additives. *Human & Experimental Toxicology*, 17(2), 111–123.
<https://doi.org/10.1177/096032719801700206>.
- Hochegger, A., Moret, S., Geurts, L., Gude, T., Leitner, E., Mertens, B., O'Hagan, S., Pocas, F., Simat, T. J., & Purcaro, G. (2021). Mineral oil risk assessment: Knowledge gaps and roadmap. Outcome of a multi-stakeholders workshop. *Trends in Food Science & Technology*, 113, 151–166. <https://doi.org/10.1016/j.tifs.2021.03.021>
- Hoh, E., & Mastovska, K. (2008). Large volume injection techniques in capillary gas chromatography. *Journal of Chromatography A*, 1186(1–2), 2–15.
<https://doi.org/10.1016/j.chroma.2007.12.001>
- IARC (1987). Mineral oils: untreated and mildly-treated oils (group 1) highly-refined oils (group 3). *IARC monographs on the evaluation of carcinogenic risks to humans*, 7, 252-254.
- IJO (2005). *IJO Standard 98/01*.
- ISO (2015). *Animal and vegetable fats and oils – Determination of aliphatic hydrocarbons in vegetable oils, ISO 17780:2015*.
- IUPAC Commission on Oils (1992). *Standard Methods for the Analysis of Oils, Fats and Derivatives. 1st Supplement to the 7th Edition*. Blackwell Scientific Publications.
- Jaén, J., Domeño, C., Alfaro, P., & Nerín, C. (2021). Atmospheric Solids Analysis Probe (ASAP) and Atmospheric Pressure Gas Chromatography (APGC) coupled to Quadrupole Time of Flight Mass Spectrometry (QTOF-MS) as alternative techniques to trace aromatic markers of mineral oils in food packaging. *Talanta*, 227, 122079.
<https://doi.org/10.1016/j.talanta.2020.122079>
- JECFA (1995). *Evaluation of Certain Food Additives and Contaminants (Forty-Fourth Report of the Joint FAO/WHO Expert Committee on Food Additives)*. WHO Technical Report Series 859.
- JECFA (2002). *Evaluation of Certain Food Additives and Contaminants (Fifty-ninth report of the Joint FAO/WHO Expert Committee on Food Additives)*. WHO Technical Report Series 913.

- JEFCA (2012). *Toxicological information and information on specifications (Summary report of the seventy-sixth meeting of JEFCA)*. JEFCA/76/SC.
- JEFCA (2013). *Evaluation of Certain Food Additives and Contaminants (Seventy-seventh report of the Joint FAO/WHO Expert Committee on Food Additives)*. WHO Technical Report Series 983.
- Jickells, S. M., Nichol, J., & Castle, L. (1994a). Migration of mineral hydrocarbons into foods. 5. Miscellaneous applications of mineral hydrocarbons in food contact materials. *Food Additives & Contaminants*, *11*(3), 333-341. <https://doi.org/10.1080/02652039409374232>
- Jickells, S. M., Nichol, J., & Castle, L. (1994b). Migration of mineral hydrocarbons into foods. 6. Press lubricants used in food and beverage cans. *Food Additives & Contaminants*, *11*(5), 595-604. <https://doi.org/10.1080/02652039409374259>
- Karasek, L., Wenzl, T., & Ulberth, F. (2010). Proficiency test on the determination of mineral oil in sunflower oil. *European Journal of Lipid Science and Technology*, *112*(3), 321–332. <https://doi.org/10.1002/ejlt.200900147>
- Kieboom, A. P. G., de Kruyf, N., & van Bekkum, H. (1974). Thin-layer chromatographic determination of the stability of complexes of substituted styrenes on silver nitrate-impregnated silica. *Journal of Chromatography A*, *95*(2), 175–180. [https://doi.org/10.1016/S0021-9673\(00\)84076-5](https://doi.org/10.1016/S0021-9673(00)84076-5)
- Kiralan, S. S., Toptanci, I., & Tekin, A. (2019). Further evidence on the removal of polycyclic aromatic hydrocarbons (PAHs) during refining of olive pomace oil. *European Journal of Lipid Science and Technology*, *121*(4), 1800381. <https://doi.org/10.1002/ejlt.201800381>
- Koning, S. De, Janssen, H., & Th, U. A. (2004). Group-type characterisation of mineral oil samples by two-dimensional comprehensive normal-phase liquid chromatography – gas chromatography with time-of-flight mass spectrometric detection. *Journal of Chromatography A*, *1058*(1-2), 217–221. <https://doi.org/10.1016/j.chroma.2004.08.083>
- Koprivnjak, O., Procida, G., & Favretto, L. (1997). Determination of endogenous aliphatic hydrocarbons of virgin olive oils of four autochthonous cultivars from Krk Island (Croatia). *Food Technology and Biotechnology*, *35*(2), 125–131.

- Koster, S., Varela, J., Stadler, R. H., Moulin, J., Cruz-Hernandez, C., Hielscher, J., Lesueur, C., Roïz, J., & Simian, H. (2020). Mineral oil hydrocarbons in foods: is the data reliable? *Food Additives and Contaminants - Part A Chemistry, Analysis, Control, Exposure and Risk Assessment*, 37(1), 69–83. <https://doi.org/10.1080/19440049.2019.1678770>
- Lacoste, F. (2014). Undesirable substances in vegetable oils: Anything to declare? *OCL - Oilseeds and Fats*, 21(1), 1–9. <https://doi.org/10.1051/ocl/2013060>
- Lacoste, F. (2016). International validation of the determination of saturated hydrocarbon mineral oil in vegetable oils. *European Journal of Lipid Science and Technology*, 118(3), 373–381. <https://doi.org/10.1002/ejlt.201500134>
- Lanzon, A., Cert, A., & Graci, J. (1994). The Hydrocarbon Fraction of Virgin Olive Oil and Changes Resulting from Refining. *Journal of the American Oil Chemists Society*, 71(3), 285–291. <https://doi.org/10.1007/BF02638054>
- LAV & BLL (2020). *UPDATE Benchmark levels for mineral oil hydrocarbons (MOH) in foods*, June 2020.
- LAV & BLL (2021). *UPDATE Benchmark levels for mineral oil hydrocarbons (MOH) in foods*, August 2021.
- LAV & BLL (2022). *UPDATE Benchmark levels for mineral oil hydrocarbons (MOH) in foods*, September 2022.
- Lavee, S. (2010). Integrated mechanical, chemical and horticultural methodologies for harvesting of oil olives and the potential interaction with different growing systems. A general review. *Advances in Horticultural Science*, 24(1), 5–15. <https://doi.org/10.1400/132337>
- Leone, A. (2014). Olive milling and pitting. in Peri, C. (2014), *The Extra-Virgin Olive Oil Handbook* (pp. 117-126). Wiley Blackwell.
- Leone, A. (2022). L'impianto per l'estrazione dell'olio vergine. in Conte, L., & Servili, M. (2022), *OLEUM Qualità, tecnologia e sostenibilità degli oli da olive* (pp. 13-51). Edagricole.
- Li, B., Wu, Y., Liu, L., Ouyang, J., Ren, J., Wang, Y., & Wang, X. (2017). Determination of Mineral Oil-Saturated Hydrocarbons (MOSH) in Vegetable Oils by Large Scale Off-Line SPE Combined with GC-FID. *JAOCs, Journal of the American Oil Chemists'*

- Society*, 94(2), 1-9. <https://doi.org/10.1007/s11746-016-2936-0>
- Limbo, S., Peri, C., & Piergiovanni, L. (2014). Extra-virgin olive oil packaging. in Peri, C. (2014), *The Extra-Virgin Olive Oil Handbook* (pp. 179-199). Wiley Blackwell.
- Liu, L., Huang, H., Wu, Y., Li, B., & Ouyang, J. (2017). Offline solid-phase extraction large-volume injection-gas chromatography for the analysis of mineral oil-saturated hydrocarbons in commercial vegetable oils. *Journal of Oleo Science*, 66(9), 981–990. <https://doi.org/10.5650/jos.ess17081>
- Liu, Z., & Phillips, J. B. (1991). Comprehensive Two-Dimensional Gas Chromatography using an On-Column Thermal Modulator Interface. *Journal of Chromatographic Science*, 29(6), 227–231.
- Lo Bianco, R., Caruso, T., Regni, L., & Proietti, P. (2021). Planting Systems for Modern Olive Growing: Strengths and Weaknesses. *Agriculture*, 11(6), 494. <https://doi.org/10.3390/agriculture11060494>
- Lommatzsch, M., Biedermann, M., Grob, K., & Simat, T. J. (2016). Analysis of saturated and aromatic hydrocarbons migrating from a polyolefin-based hot-melt adhesive into food. *Food Additives and Contaminants - Part A Chemistry, Analysis, Control, Exposure and Risk Assessment*, 33(3), 473–488. <https://doi.org/10.1080/19440049.2015.1130863>
- Lommatzsch, M., Biedermann, M., Simat, T. J., & Grob, K. (2015). Argentation high performance liquid chromatography on-line coupled to gas chromatography for the analysis of monounsaturated polyolefin oligomers in packaging materials and foods. *Journal of Chromatography A*, 1402, 94–101. <https://doi.org/10.1016/j.chroma.2015.05.019>
- Lorenzini, R., Fiselier, K., Biedermann, M., Barbanera, M., Braschi, I., & Grob, K. (2010). Saturated and aromatic mineral oil hydrocarbons from paperboard food packaging: Estimation of long-term migration from contents in the paperboard and data on boxes from the market. *Food Additives and Contaminants - Part A Chemistry, Analysis, Control, Exposure and Risk Assessment*, 27(12), 1765–1774. <https://doi.org/10.1080/19440049.2010.517568>
- Low, L.K., Shymansky, P.M., Kommineni, C., Naro, P.A., & Mackerer, C.R. (1992). Oral absorption and pharmacokinetics studies of radiolabelled normal paraffinic,

- isoparaffinic and cycloparaffinic surrogates in white oil in Fisher 344 rats. In *Transcript of the Toxicology Forum Special Meeting on Mineral Hydrocarbons*, 86-101. Oxford.
- Luisi, A. (2016). MOSH and MOAH mineral oils: validation of the method of analysis and occurrence on real samples. *SISSG Round Table*, 7 June 2016, Udine (Italy).
- Luisi, A. (2019). MOSH and MOAH: validation of the analytical method and occurrence on oils. *Presentation at the SISSG Workshop "MOSH & MOAH negli Olii e Grassi Alimentari: Aspetti Tossicologici e Analitici, Fonti di Contaminazione"*, 12-13 December 2019, Bologna (Italy).
- Ma, Y., Shi, L., Liu, Y., & Lu, Q. (2017). Effects of Neutralization , Decoloration , and Deodorization on Polycyclic Aromatic Hydrocarbons during Laboratory-Scale Oil Refining Process. *Journal of Chemistry*, 2017, 7824761. <https://doi.org/10.1155/2017/7824761>
- Magnusson, B. Örnemark, U. (2014). *Eurachem Guide: The Fitness for Purpose of Analytical Methods – A Laboratory Guide to Method Validation and Related Topics*. (2nd Ed).
- Mander, L. N., & Williams, C. M. (2016). Chromatography with silver nitrate: Part 2. *Tetrahedron*, 72(9), 1133–1150. <https://doi.org/10.1016/j.tet.2016.01.004>
- Mascrez, S., Danthine, S., & Purcaro, G. (2021). Microwave-Assisted Saponification Method Followed by Solid-Phase Extraction for the Characterization of Sterols and Dialkyl Ketones in Fats. *Foods*, 10(2), 445. <https://doi.org/10.3390/foods10020445>
- Mattara, P. (2013). *Mineral oil determination in edible oils with a special focus on the aromatic fraction* [Master's thesis, University of Udine].
- Menegoz Ursol, L. (2019). *Validation of a LC-GC-FID method for the determination of mineral oil in olive oil* [Master's thesis, University of Udine].
- Menegoz Ursol, L., Conchione, C., Peroni, D., Carretta, A., & Moret, S. (2023). A study on the impact of harvesting operations on the mineral oil contamination of olive oils. *Food Chemistry*, 406, 135032. <https://doi.org/10.1016/j.foodchem.2022.135032>
- Menegoz Ursol, L., Conchione, C., Srbinovska, A., & Moret, S. (2022). Optimization and validation of microwave assisted saponification (MAS) followed by epoxidation for high-sensitivity determination of mineral oil aromatic hydrocarbons (MOAH) in

- extra virgin olive oil. *Food Chemistry*, 370, 130966. <https://doi.org/10.1016/j.foodchem.2021.130966>
- Mihailova, A., Abbado, D., & Pedentchouk, N. (2015). Differences in *n*-alkane profiles between olives and olive leaves as potential indicators for the assessment of olive leaf presence in virgin olive oils. *European Food Research and Technology*, 117(9), 1480–1485. <https://doi.org/10.1002/ejlt.201400406>
- Moh, M. H., Tang, T. S., & Tan, G. H. (2001). Quantitative Determination of Diesel Oil in Contaminated Edible Oils Using High-Performance Liquid Chromatography. *Journal of the American Oil Chemists' Society*, 78, 519–525. <https://doi.org/10.1007/s11746-001-0296-x>
- Moh, M. H., Tang, T. S., & Tan, G. H. (2002). GC determination of synthetic hydrocarbon-based thermal heating fluid in vegetable oils. *Journal of the American Oil Chemists' Society*, 79, 1039-1043. <https://doi.org/10.1007/s11746-002-0599-y>
- Momchilova, S., & Nikolova-Damyanova, B. (2003). Stationary phases for silver ion chromatography of lipids: Preparation and properties. *Journal of Separation Science*, 26(3–4), 261–270. <https://doi.org/10.1002/jssc.200390032>
- Morchio, G. (2022). Raffinazione dell'olio vergine e lampante ed estrazione e raffinazione dell'olio di sansa. in Conte, L., & Servili, M. (2022), *OLEUM Qualità, tecnologia e sostenibilità degli oli da olive* (pp. 53-101). Edagricole.
- Moret, S. (2016). Mineral oils (MOSH & MOAH) in vegetable oils: occurrence and analytical methods. Overview of analytical methods. *SISSG Round Table*, 7 June 2016, Udine (Italy)
- Moret, S., Barp, L., Grob, K., & Conte, L. (2011). Optimised off-line SPE-GC-FID method for the determination of mineral oil saturated hydrocarbons (MOSH) in vegetable oils. *Food Chemistry*, 129(4), 1898–1903. <https://doi.org/10.1016/j.foodchem.2011.05.140>
- Moret, S., Conchione, C., Srbinovska, A., & Lucci, P. (2019). Microwave-based technique for fast and reliable extraction of organic contaminants from food, with a special focus on hydrocarbon contaminants. *Foods*, 8(10), 503. <https://doi.org/10.3390/foods8100503>
- Moret, S., & Conte, L. S. (2000). Polycyclic aromatic hydrocarbons in edible fats and oils:

- Occurrence and analytical methods. *Journal of Chromatography A*, 882(1–2), 245–253. [https://doi.org/10.1016/S0021-9673\(00\)00079-0](https://doi.org/10.1016/S0021-9673(00)00079-0)
- Moret, S., Grob, K., & Conte, L. (1996). On-line high-performance liquid chromatography-solvent evaporation-high-performance liquid chromatography-capillary gas chromatography-flame ionisation detection for the analysis of mineral oil polyaromatic hydrocarbons in fatty foods. *Journal of Chromatography A*, 750(1–2), 361–368. [https://doi.org/10.1016/0021-9673\(96\)00453-0](https://doi.org/10.1016/0021-9673(96)00453-0)
- Moret, S., Grob, K., & Conte, L. (1997). Mineral oil polyaromatic hydrocarbons in foods, e.g. from jute bags, by on-line LC-solvent evaporation (SE)-LC-GC-FID. *Zeitschrift für Lebensmitteluntersuchung und Forschung A*, 204, 241–246. <https://doi.org/10.1007/s002170050071>
- Moret, S., Marega, M., Conte, L. S., & Purcaro, G. (2012). Sample Preparation Techniques for the Determination of Some Food Contaminants (Polycyclic aromatic hydrocarbons, Mineral oils and Phthalates). In Pawliszyn, J., Bayona, J., Dugo, P., Chris Le, X., Kee Lee, H., Li, X., & Lord, H. (2012), *Comprehensive Sampling and Sample Preparation* (pp. 313-356). Elsevier.
- Moret, S., Populin, T., & Conte, L. S. (2009). La contaminazione degli oli vegetali con oli minerali. *La Rivista Italiana Delle Sostanze Grasse*, LXXXVI, 3–14.
- Moret, S., Populin, T., & Conte, L. S. (2010). Chapter 55 - Mineral Paraffins in Olives and Olive Oils. In Preedy, V. R., & Watson, R. R. (2010), *Olives and Olive Oil in Health and Disease Prevention* (pp. 499-506). Elsevier. <https://doi.org/10.1016/B978-0-12-374420-3.00055-3>
- Moret, S., Populin, T., Conte, L. S., Grob, K., & Neukom, H. P. (2003). Occurrence of C15–45 mineral paraffins in olives and olive oils. *Food Additives and Contaminants*, 20(5), 417–426. <https://doi.org/10.1080/0265203031000098687>
- Moret, S., Purcaro, G., & Conte, L. (2014a). *Il campione per l'analisi chimica*. Springer-Verlag Italia.
- Moret, S., Sander, M., Purcaro, G., Scolaro, M., Barp, L., & Conte, L. (2013). Optimization of pressurized liquid extraction (PLE) for rapid determination of mineral oil saturated (MOSH) and aromatic hydrocarbons (MOAH) in cardboard and paper intended for food contact. *Talanta*, 115, 246–252.

- <https://doi.org/10.1016/j.talanta.2013.04.061>
- Moret, S., Scolaro, M., Barp, L., Purcaro, G., & Conte, L. S. (2016). Microwave assisted saponification (MAS) followed by on-line liquid chromatography (LC)-gas chromatography (GC) for high-throughput and high-sensitivity determination of mineral oil in different cereal-based foodstuffs. *Food Chemistry*, *196*, 50–57. <https://doi.org/10.1016/j.foodchem.2015.09.032>
- Moret, S., Scolaro, M., Barp, L., Purcaro, G., Sander, M., & Conte, L. (2014b). Optimisation of pressurised liquid extraction (PLE) for rapid and efficient extraction of superficial and total mineral oil contamination from dry foods. *Food Chemistry*, *157*, 470–475. <https://doi.org/10.1016/j.foodchem.2014.02.071>
- Nartea, A. (2017). *A study on possible sources of mineral oil contamination in olive and extra virgin olive oil* [Master's thesis, University of Udine].
- Nash, J. F., Gettings, S. D., Diembeck, W., Chudowski, M., & Kraus, A. L. (1996). A Toxicological Review of Topical Exposure to White Mineral Oils. *Food and Chemical Toxicology*, *34*(2), 213–225. [https://doi.org/10.1016/0278-6915\(95\)00106-9](https://doi.org/10.1016/0278-6915(95)00106-9)
- Nasini, L., & Proietti, P. (2014). Olive harvesting. in Peri, C. (2014), *The Extra-Virgin Olive Oil Handbook* (pp. 89-106). Wiley Blackwell.
- Nestola, M. (2022). Automated workflow utilizing saponification and improved epoxidation for the sensitive determination of mineral oil saturated and aromatic hydrocarbons in edible oils and fats. *Journal of Chromatography A*, *1682*, 463523. <https://doi.org/10.1016/j.chroma.2022.463523>
- Nestola, M., & Schmidt, T. C. (2017). Determination of mineral oil aromatic hydrocarbons in edible oils and fats by online liquid chromatography–gas chromatography–flame ionization detection – Evaluation of automated removal strategies for biogenic olefins. *Journal of Chromatography A*, *1505*, 69–76. <https://doi.org/10.1016/j.chroma.2017.05.035>
- Neukom, H. P., Grob, K., Biedermann, M., & Noti, A. (2002). Food contamination by C20-C50 mineral paraffins from the atmosphere. *Atmospheric Environment*, *36*(30), 4839–4847. [https://doi.org/10.1016/S1352-2310\(02\)00358-8](https://doi.org/10.1016/S1352-2310(02)00358-8)
- Niyonsaba, E., Manheim, J. M., Yerabolu, R., & Kenttamaa, H. I. (2019). Recent Advances in Petroleum Analysis by Mass Spectrometry Recent Advances in Petroleum Analysis

- by Mass Spectrometry. *Analytical Chemistry*, 91(1), 156–177. <https://doi.org/10.1021/acs.analchem.8b05258>
- Nocun, M., & Andersson, J. T. (2012). Argentation chromatography for the separation of polycyclic aromatic compounds according to ring number. *Journal of Chromatography A*, 1219, 47–53. <https://doi.org/10.1016/j.chroma.2011.11.006>
- Nolvachai, Y., Kulsing, C., & Marriott, P. J. (2017). Multidimensional gas chromatography in food analysis. *Trends in Analytical Chemistry*, 97, 124–137. <https://doi.org/10.1016/j.trac.2017.05.001>
- Noti, A., Grob, K., Biedermann, M., & Deiss, U. (2003). Exposure of babies to C15 – C45 mineral paraffins from human milk and breast salves. *Regulatory Toxicology and Pharmacology*, 38(3), 317–325. [https://doi.org/10.1016/S0273-2300\(03\)00098-9](https://doi.org/10.1016/S0273-2300(03)00098-9)
- Paré, J. R. J., Belanger, M. R., & Stafford, S. S. (1994). Microwave-Assisted Process (MAP™): a new tool for the analytical laboratory. *Trends in Analytical Chemistry*, 13(4), 176–184. [https://doi.org/10.1016/0165-9936\(94\)87033-0](https://doi.org/10.1016/0165-9936(94)87033-0)
- Peri, C. (2014a). Olive cleaning. in Peri, C. (2014), *The Extra-Virgin Olive Oil Handbook* (pp. 113-116). Wiley Blackwell.
- Peri, C. (2014b). Filtration of extra-virgin olive oil. in Peri, C. (2014), *The Extra-Virgin Olive Oil Handbook* (pp. 155-164). Wiley Blackwell.
- Peri, C. (2014c). Extra-virgin olive oil storage and handling. in Peri, C. (2014), *The Extra-Virgin Olive Oil Handbook* (pp. 165-178). Wiley Blackwell.
- Peri, C. (2014d). The olive oil refining process. in Peri, C. (2014), *The Extra-Virgin Olive Oil Handbook* (pp. 201-210). Wiley Blackwell.
- Petrakis, C. (2006). Olive Oil Extraction. in Boskou, D. (2006), *Olive Oil Chemistry and Technology* (2nd ed., pp. 191-223). AOCS Press.
- Pfister, M. K., Horn, B., Riedl, J., & Esslinger, S. (2018). Vibrational spectroscopy in practice: Detection of mineral oil in sunflower oil with near- and mid-infrared spectroscopy. *NIR News*, 29(3), 6–11. <https://doi.org/10.1177/0960336018763196>
- Picouet, P. A., Gou, P., Hyypiö, R., & Castellari, M. (2018). Implementation of NIR technology for at-line rapid detection of sunflower oil adulterated with mineral oil. *Journal of Food Engineering*, 230, 18–27.

- <https://doi.org/10.1016/j.jfoodeng.2018.01.011>
- Pineda, M., Rojas, M., Gálvez-Valdivieso, G., & Aguilar, M. (2017). The origin of aliphatic hydrocarbons in olive oil. *Journal of the Science of Food and Agriculture*, *97*(14), 4827–4834. <https://doi.org/10.1002/jsfa.8353>
- Pirow, R., Blume, A., Hellwig, N., Herzler, M., Huhse, B., Hutzler, C., Pfaff, K., Thierse, H. J., Tralau, T., Vieth, B., & Luch, A. (2019). Mineral oil in food, cosmetic products, and in products regulated by other legislations. *Critical Reviews in Toxicology*, *49*(9), 742–789. <https://doi.org/10.1080/10408444.2019.1694862>
- Polyakova, A., Van Leeuwen, S. , & Peters, R. (2022). Review on chromatographic and specific detection methodologies for unravelling the complexity of MOAH in foods. *Analytica Chimica Acta*, *2022*, *1234*, 340098. <https://doi.org/10.1016/j.aca.2022.340098>
- Populin, T., Biedermann, M., Grob, K., Moret, S., & Conte, L. (2004). Relative hopane content confirming the mineral origin of hydrocarbons contaminating foods and human milk. *Food Additives and Contaminants*, *21*(9), 893–904. <https://doi.org/10.1080/02652030400001164>
- Purcaro, G., Barp, L., & Moret, S. (2016). Determination of hydrocarbon contamination in foods. A review. *Analytical Methods*, *8*(29), 5755–5772. <https://doi.org/10.1039/c6ay00655h>
- Purcaro, G., Moret, S., & Conte, L. (2009). Optimisation of microwave assisted extraction (MAE) for polycyclic aromatic hydrocarbon (PAH) determination in smoked meat. *Meat Science*, *81*(1), 275–280. <https://doi.org/10.1016/j.meatsci.2008.08.002>
- Purcaro, G., Moret, S., & Conte, L. (2012). Hyphenated liquid chromatography-gas chromatography technique: Recent evolution and applications. *Journal of Chromatography A*, *1255*, 100–111. <https://doi.org/10.1016/j.chroma.2012.02.018>
- Purcaro, G., Moret, S., & Conte, L. (2013a). Sample pre-fractionation of environmental and food samples using LC-GC multidimensional techniques. *Trends in Analytical Chemistry*, *43*, 146–160. <https://doi.org/10.1016/j.trac.2012.10.007>
- Purcaro, G., Tranchida, P. Q., Barp, L., Moret, S., Conte, L., & Mondello, L. (2013b). Detailed elucidation of hydrocarbon contamination in food products by using solid-phase extraction and comprehensive gas chromatography with dual detection.

- Analytica Chimica Acta*, 773, 97–104. <https://doi.org/10.1016/j.aca.2013.03.002>
- Purcaro, G., Zoccali, M., Tranchida, P. Q., Barp, L., Moret, S., Conte, L., Dugo, P., & Mondello, L. (2013c). Comparison of two different multidimensional liquid-gas chromatography interfaces for determination of mineral oil saturated hydrocarbons in foodstuffs. *Analytical and Bioanalytical Chemistry*, 405(2–3), 1077–1084. <https://doi.org/10.1007/s00216-012-6535-0>
- Quisillo, C. (2021). *Optimization of ultra-sound assisted saponification for mineral oil determination in olive oil* [Master's thesis, University of Udine].
- Ruiz, J. L. H., Liébanas, J. A., Vidal, J. L. M., Frenich, A. G., & González, R. R. (2021). Offline solid-phase extraction and separation of mineral oil saturated hydrocarbons and mineral oil aromatic hydrocarbons in edible oils, and analysis via gc with a flame ionization detector. *Foods*, 10(9), 2026. <https://doi.org/10.3390/foods10092026>
- Ruiz-Méndez, M. V., & Aguirre-González, M. R. (2013). Olive Oil Refining Process. in Aparicio, R., & Harwood, J. (2013), *Handbook of Olive Oil Analysis and Properties* (2nd ed., pp. 715-738). Springer.
- Samuels, L., Kunst, L., & Jetter, R. (2008). Sealing plant surfaces: Cuticular wax formation by epidermal cells. *Annual Review of Plant Biology*, 59, 683–707. <https://doi.org/10.1146/annurev.arplant.59.103006.093219>
- SANTE (2019). *Guidance on Analytical Quality Control and Method Validation for Pesticide Residues Analysis in Food and Feed*, SANTE/12682/2019.
- SCF (1989). *Minutes of the 67th Meeting of the Scientific Committee for Food*. III/3681/89-EN.
- SCF (1995). *Opinion on mineral and synthetic hydrocarbons*. SCF reports: 37th series. III/5611/95.
- Scotter, M. J., Castle, L., & Massey, R. C. (2003). A study of the toxicity of five mineral hydrocarbon waxes and oils in the F344 rat, with histological examination and tissue-specific chemical characterisation of accumulated hydrocarbon material. *Food and Chemical Toxicology*, 41(4), 489–521. [https://doi.org/10.1016/s0278-6915\(02\)00279-x](https://doi.org/10.1016/s0278-6915(02)00279-x).
- Sdrigotti, N., Collard, M., & Purcaro, G. (2021). Evolution of hyphenated techniques for mineral oil analysis in food. *Journal of Separation Science*, 44(1), 464–482.

<https://doi.org/10.1002/jssc.202000901>

- Servili, M., Esposito, S., Taticchi, A., Veneziani, G., Genovese, A., Sacchi, R. (2022). Estrazione, conservazione, packaging e qualità. in Conte, L., & Servili, M. (2022), *OLEUM Qualità, tecnologia e sostenibilità degli oli da olive* (pp. 103-165). Edagricole.
- Shoda, T., Toyoda, K., Uneyama, C., Takada, K., & Takahashi, M. (1997). Lack of carcinogenicity of mediumviscosity liquid paraffin given in the diet to F344 rats. *Food and Chemical Toxicology*, 35(12), 1181–1190. [https://doi.org/10.1016/s0278-6915\(97\)00105-1](https://doi.org/10.1016/s0278-6915(97)00105-1)
- Sofuoglu, S. C., Yayla, B., Kavcar, P., Ates, D., Turgut, C., & Sofuoglu, A. (2013). Olive tree, *Olea europaea* L., leaves as a bioindicator of atmospheric PCB contamination. *Environmental Science and Pollution Research*, 20(9), 6178–6183. <https://doi.org/10.1007/s11356-013-1640-y>
- Spack, L. W., Leszczyk, G., Varela, J., Simian, H., Gude, T., & Stadler, R. H. (2017). Understanding the contamination of food with mineral oil: the need for a confirmatory analytical and procedural approach. *Food Additives and Contaminants - Part A Chemistry, Analysis, Control, Exposure and Risk Assessment*, 34(6), 1052–1071. <https://doi.org/10.1080/19440049.2017.1306655>
- Srbinska, A., Conchione, C., Lucci, P., & Moret, S. (2020a). On-Line HP(LC)-GC-FID Determination of Hydrocarbon Contaminants in Fresh and Packaged Fish and Fish Products. *Journal of AOAC INTERNATIONAL*, 104(2), 267-273. <https://doi.org/10.1093/jaoacint/qsaa144>
- Srbinska, A., Conchione, C., Menegoz Ursol, L., Lucci, P., & Moret, S. (2020b). Occurrence of *n*-Alkanes in Vegetable Oils and Their Analytical Determination. *Foods*, 9(11), 1546. <https://doi.org/10.3390/foods9111546>
- Stauff, A., Schnapka, J., Heckel, F., & Matissek, R. (2020). Mineral Oil Hydrocarbons (MOSH/MOAH) in Edible Oils and Possible Minimization by Deodorization Through the Example of Cocoa Butter. *European Journal of Lipid Science and Technology*, 122(7), 1900383. <https://doi.org/10.1002/ejlt.201900383>
- Tamborrino, A. (2014). Olive paste malaxation. in Peri, C. (2014), *The Extra-Virgin Olive Oil Handbook* (pp. 127-136). Wiley Blackwell.

- Taştan, P., Taştan, Ö., & Şahyar, B. Y. (2022). Detection of Pesticide Residues in Olive Leaves From İzmir, Turkey. *International Journal of Nature and Life Sciences*, 6(1), 1–11. <https://doi.org/10.47947/ijnls.ijnls.1031087>
- Tous, J. (2011). Olive Production Systems and Mechanization. *Acta Horticulturae*, 924(22), 169–184. <https://doi.org/10.17660/ActaHortic.2011.924.22>
- Tranchida, P. Q., Donato, P., Cacciola, F., Beccaria, M., Dugo, P., & Mondello, L. (2013). Potential of comprehensive chromatography in food analysis. *Trends in Analytical Chemistry*, 52, 186–205. <https://doi.org/10.1016/j.trac.2013.07.008>
- Tranchida, P. Q., Purcaro, G., Dugo, P., Mondello, L., & Purcaro, G., (2011a). Modulators for comprehensive two-dimensional gas chromatography. *Trends in Analytical Chemistry*, 30(9), 1437–1461. <https://doi.org/10.1016/j.trac.2011.06.010>
- Tranchida, P. Q., Zoccali, M., Purcaro, G., Moret, S., Conte, L., Beccaria, M., Dugo, P., & Mondello, L. (2011b). A rapid multidimensional liquid-gas chromatography method for the analysis of mineral oil saturated hydrocarbons in vegetable oils. *Journal of Chromatography A*, 1218(42), 7476–7480. <https://doi.org/10.1016/j.chroma.2011.06.089>
- Van der Westhuizen, R., Ajam, M., Coning, P. De, Beens, J., Villiers, A. De, & Sandra, P. (2011). Comprehensive two-dimensional gas chromatography for the analysis of synthetic and crude-derived jet fuels. *Journal of Chromatography A*, 1218(28), 4478–4486. <https://doi.org/10.1016/j.chroma.2011.05.009>
- Van Heyst, A., Vanlancker, M., Vercammen, J., Van Den Houwe, K., Mertens, B., & Van Hoeck, E. (2018). Analysis of mineral oil in food: results of a Belgian market survey. *Food Additives & Contaminants: Part A*, 35(10), 2062–2075. <https://doi.org/10.1080/19440049.2018.1512758>
- Vendeuvre, C., Bertoncini, F., Duval, L., & Thiébaud, D. (2007). Comprehensive Two-Dimensional Gas Chromatography for Detailed Characterisation of Petroleum Products. *Oil & Gas Science and Technology*, 62(1), 43–55. <https://doi.org/10.2516/ogst:2007004>
- Vollmer, A., Biedermann, M., Grundböck, F., Ingenhoff, J. E., Biedermann-Brem, S., Altkofer, W., & Grob, K. (2011). Migration of mineral oil from printed paperboard into dry foods: Survey of the German market. *European Food Research and*

- Technology*, 232(1), 175–182. <https://doi.org/10.1007/s00217-010-1376-6>
- Wagner, C., Neukom, H. P., Galetti, V., & Grob, K. (2001a). Determination of Mineral Paraffins in Feeds and Foodstuffs by Bromination and Preseparation on Aluminium Oxide: Method and Results of a Ring Test. *Mitteilungen aus Lebensmitteluntersuchung und Hygiene*, 92, 231–249.
- Wagner, C., Neukom, H. P., Grob, K., Moret, S., Populin, T., & Conte, L. (2001b). Mineral paraffins in vegetable oils and refinery by-products. *Mitteilungen aus Lebensmitteluntersuchung und Hygiene*, 92(5), 499–514.
- Wagner, M., & Oellig, C. (2018). Screening for mineral oil saturated and aromatic hydrocarbons in paper and cardboard directly by planar solid phase extraction and by its coupling to gas chromatography. *Journal of Chromatography A*, 1588, 48–57. <https://doi.org/10.1016/j.chroma.2018.12.043>
- Wagner, M., & Oellig, C. (2022). Screening for mineral oil hydrocarbons in vegetable oils by silver ion–planar solid phase extraction. *Journal of Chromatography A*, 1662, 462732. <https://doi.org/10.1016/j.chroma.2021.462732>
- Weber, S., Schrag, K., Mildau, G., Kuballa, T., Walch, S. G., & Lachenmeier, D. W. (2018). Analytical Methods for the Determination of Mineral Oil Saturated Hydrocarbons (MOSH) and Mineral Oil Aromatic Hydrocarbons (MOAH)—A Short Review. *Analytical Chemistry Insights*, 13, 1177390118777757. <https://doi.org/10.1177/1177390118777757>
- Weisman, W. (1998). *Analysis of Petroleum Hydrocarbons in Environmental Media*. Amherst Scientific Publishers.
- Wrona, M., Pezo, D., & Nerin, C. (2013). Rapid analytical procedure for determination of mineral oils in edible oil by GC-FID. *Food Chemistry*, 141(4), 3993–3999. <https://doi.org/10.1016/j.foodchem.2013.06.091>
- Yap, C. L., Gan, S., & Ng, H. K. (2010). Application of vegetable oils in the treatment of polycyclic aromatic hydrocarbons-contaminated soils. *Journal of Hazardous Materials*, 177(1-3), 28-41. <https://doi.org/10.1016/j.jhazmat.2009.11.078>
- Zoccali, M., Barp, L., Beccaria, M., Sciarrone, D., Purcaro, G., & Mondello, L. (2016). Improvement of mineral oil saturated and aromatic hydrocarbons determination in

- edible oil by liquid-liquid-gas chromatography with dual detection. *Journal of Separation Science*, 39(3), 623–631. <https://doi.org/10.1002/jssc.201501247>
- Zoccali, M., Dugo, P., Tranchida, P.Q., Mondello, L. (2012). Rapid Multidimensional Liquid–Gas Chromatography for the Analysis of Saturated Hydrocarbon Contamination in Foods containing Vegetable Oil. *LC GC Europe* 25(1), 20-25.
- Zoccali, M., Salerno, T. M. G., Tranchida, P. Q., & Mondello, L. (2021). Use of a low-cost, lab-made Y-interface for liquid-gas chromatography coupling for the analysis of mineral oils in food samples. *Journal of Chromatography A*, 1648, 462191. <https://doi.org/10.1016/j.chroma.2021.462191>
- Zoccali, M., Schug, K. A., Walsh, P., Smuts, J., & Mondello, L. (2017). Flow-modulated comprehensive two-dimensional gas chromatography combined with a vacuum ultraviolet detector for the analysis of complex mixtures. *Journal of Chromatography A*, 1497, 135-143. <https://doi.org/10.1016/j.chroma.2017.03.073>
- Zoccali, M., Tranchida, P. Q., & Mondello, L. (2015). On-Line Combination of High Performance Liquid Chromatography with Comprehensive Two-Dimensional Gas Chromatography-Triple Quadrupole Mass Spectrometry: A Proof of Principle Study. *Analytical Chemistry*, 87(3), 1911–1918. <https://doi.org/10.1021/ac504162a>
- Zoccali, M., Tranchida, P. Q., & Mondello, L. (2020). A lab-developed interface for liquid-gas chromatography coupling based on the use of a modified programmed-temperature-vaporizing injector. *Journal of Chromatography A*, 1622, 461096. <https://doi.org/10.1016/j.chroma.2020.461096>
- Zurfluh, M., Biedermann, M., & Grob, K. (2014). Enrichment for reducing the detection limits for the analysis of mineral oil in fatty foods. *Journal Fur Verbraucherschutz Und Lebensmittelsicherheit*, 9(1), 61–69. <https://doi.org/10.1007/s00003-013-0848-6>

LIST OF PUBLICATIONS

Publications in international peer reviewed journals

- Menegoz Ursol, L., Conchione, C., Peroni, D., Carretta, A., & Moret, S. (2023). A study on the impact of harvesting operations on the mineral oil contamination of olives oils. *Food Chemistry*, 406, 135032.
- Srbinovska, A., Gasparotto, L., Conchione, C., Menegoz Ursol, L., Lambertini, F., Suman, M., & Moret, S. (2023). Mineral oil contamination in basil pesto from the Italian market: Ingredient contribution and market survey. *Journal of Food Composition and Analysis*, 115, 104914.
- Srbinovska, A., Conchione, C., Celaj, F., Menegoz Ursol, L., & Moret, S. (2022). High sensitivity determination of mineral oils and olefin oligomers in cocoa powder and related packaging: Method validation and market survey. *Food Chemistry*, 396, 133686.
- Menegoz Ursol, L., Conchione, C., Srbinovska, A., & Moret, S. (2022). Optimization and validation of microwave assisted saponification (MAS) followed by epoxidation for high-sensitivity determination of mineral oil aromatic hydrocarbons (MOAH) in extra virgin olive oil. *Food Chemistry*, 370, 130966.
- Srbinovska, A., Conchione, C., Menegoz Ursol, L., Lucci, P., & Moret, S. (2020). Occurrence of *n*-Alkanes in Vegetable Oils and Their Analytical Determination. *Foods*, 9(11).

Manuscripts in progress

- Menegoz Ursol, L., & Moret, S. Evaluation of the impact of olive milling on the mineral oil contamination of extra virgin olive oils. *To be submitted*.
- Menegoz Ursol, L., Conchione, C., Peroni, D., & Moret, S. The impact of the refining process on the mineral oil contamination of olive oils and olive pomace oils. *To be submitted*.

**CONTRIBUTIONS TO
NATIONAL AND
INTERNATIONAL
CONFERENCES AND
SEMINARS**

Oral communications

- Moret, S., & Menegoz Ursol, L. (2022). Mineral oils in vegetable oils: background, analysis and the role of MS. *7th MS Food Day*, Florence (Italy), 5-7 October 2022. Oral communication.
- Peroni, D., Carretta, A., Menegoz Ursol, L., & Moret, S. (2022). Advancing MOSH/MOAH analysis towards speciation and contaminants identification. *7th MS Food Day*, Florence (Italy), 5-7 October 2022. Oral communication.
- Menegoz Ursol, L. (2022). Optimization of rapid analytical protocols for monitoring the contamination with hydrocarbons of petrogenic origin in the olive oil supply chain. *26th Workshop on the Developments in the Italian PhD Research on Food Science, Technology and Biotechnology*, Asti (Italy), 19-21 September 2022. Oral communication.
- Menegoz Ursol, L., Srbinovska, A., Conchione, C., Brkić Bubola, K., Koprivnjak, O., & Moret, S. (2022). On-line HPLC-GC-FID determination of exogenous and endogenous hydrocarbons in olive oils of different cultivars milled under different conditions. *26th International Symposium on Separation Sciences*. Ljubljana (Slovenia), 28 June-1 July 2022. Oral communication.
- Menegoz Ursol, L., & Moret, S. (2022). Solvent-saving sample preparation for high-sensitivity determination of MOSH and MOAH in vegetable oils. *Edible oils and fats: innovation and sustainability in production and control*, Perugia (Italy), 15-17 June 2022. Oral communication.
- Peroni, D., Carretta, A., Menegoz Ursol, L., & Moret, S. (2022). Advancing MOSH/MOAH analysis towards speciation and contaminants identification. *Edible oils and fats: innovation and sustainability in production and control*, Perugia (Italy), 15-17 June 2022. Oral communication.
- Menegoz Ursol, L., Conchione, C., Srbinovska, A., & Moret, S. (2021). Rapid and high-sensitivity determination of mineral oil aromatic hydrocarbons (MOAH) in extra virgin olive oil (EVOO): method validation and first results. *18th Euro Fed Lipid Congress and Expo - Fats, Oils and Lipids: for a Healthy and Sustainable World*, On-line meeting, 18-21 October 2021. Oral communication.
- Menegoz Ursol, L., & Moret, S. (2021). Optimization of rapid analytical protocols for monitoring the contamination with hydrocarbons of petrogenic origin in the olive oil supply chain. *I Giovani e la Chimica in Friuli-Venezia Giulia*, Trieste (Italy), 31 September 2021. Oral communication.

- Menegoz Ursol, L. (2019). The UNIUD PhD Project on monitoring of MOSH and MOAH in the production chain of olive oils: “Optimization of rapid analytical protocols for monitoring the contamination with hydrocarbons of petrogenic origin in the olive oil supply chain”. *MOSH and MOAH in edible oils and fats: toxicologic and analytical issues, sources of contamination*, Bologna (Italy), 12-13 December 2019. Oral communication.

Seminars

- Menegoz Ursol, L., & Moret, S. (2022). MOSH/MOAH analysis: objectives, state of the art and development of advanced methods. *MOSH/MOAH analysis: objectives, state of the art and development of advanced methods*, 27 October 2022. Webinar
- Menegoz Ursol, L., & Moret, S. (2022). Monitoring of mineral oil contamination along the olive oil supply chain: first results with particular focus on the harvesting phase. *Mineral oils in food – Update on the new Summary Report of the European Commission*, 26 July 2022. Webinar.

POSTERS

- Peroni, D., Carretta, A., Menegoz Ursol, L., & Moret, S. (2023). Advancing MOSH/MOAH analysis towards speciation and contaminant identification. *14th Multidimensional Chromatography Workshop*, Liege (Belgium), 30 January-1 February 2023. Poster. *To be submitted*.
- Menegoz Ursol, L., Conchione, C., Peroni, D., Carretta, A., & Moret, S. (2022). A study on the impact of harvesting operations on mineral oil contamination of extra virgin olive oils. *10th International Symposium of Recent Advances in Food Analysis*, Prague (Czech Republic), 6-9 September 2022. Poster.
- Albendea, P., Menegoz Ursol, L., Conchione, C., & Moret, S. (2022). A study on the transfer of mineral oil contaminants from the diets to the pigs. *10th International Symposium of Recent Advances in Food Analysis*, Prague (Czech Republic), 6-9 September 2022. Poster.
- Menegoz Ursol, L. (2021). Optimization of rapid analytical protocols for monitoring the contamination with hydrocarbons of petrogenic origin in the olive oil supply chain. *1st Telematic Workshop on the Developments in the Italian PhD Research on Food Science, Technology, and Biotechnology*, On-line meeting, 14-15 September 2021. Poster.

AWARDS

- Menegoz Ursol, L. (2022). Bronze Prize for Oral Presentation by Young Researcher. *26th International Symposium on Separation Sciences*. Ljubljana (Slovenia), 28 June-1 July 2022.